



**Diversity, taphonomy and palaeoecology in the Ediacaran
of Newfoundland**

by © Giovanni Pasinetti (Manuscript style Thesis) submitted to the
School of Graduate Studies in partial fulfillment of the requirements
for the degree of

Doctoral program in Earth Science
Memorial University of Newfoundland



October 2024

Abstract

Pre-Cambrian outcrops in the Bonavista and Avalon peninsulas of Newfoundland (CA) record a diverse fossiliferous assemblage, dominated by macroscopic organisms presenting extinct Bauplans. In particular, frondose organisms such as the Rangeomorpha and the Arboreomorpha represent the most diverse groups and are typically composed by a number of self-repeating branch orders and sometimes a stalk or a stem. Despite traces of early metazoan life being present, the position of the Ediacaran groups in the tree of life is not always well defined. Moreover, their taxonomy and taphonomy – and in turn their palaeobiology and palaeoecology – are poorly understood. In this work we describe three taxa, two rangeomorphs (*Culmofrons plumosa* and *Charnia ewinoni* gen. et sp. nov.) and one problematic metazoan (*Lydonia jiggamintia* gen. et sp. nov.), with a comprehensive overview of their phylogenetic position, their taphonomy, their auto-ecology and population dynamics. Morphometric analyses allow us to formally separate the three species from other taxa, and to erect two new species endemic to Newfoundland (*C. ewinoni* and *L. jiggamintia*).

For the two rangeomorphs species, we find evidence for a reclining lifestyle and symbiotic relationships with the microbiota of the underlying sediments, supported by taphonomical evidence and palaeoenvironmental considerations, in contrast with traditional reconstructions that would put the rangeomorphs erect in the water column. The exceptional preservational quality of the Bonavista material further allow us to identify never described before reproductive structures, as well as to further our understanding of rangeomorphs developmental models.

Specimens from the Bonavista peninsula, previously identified as the pseudofossil *Blackbrookia*, are here reassigned to *Lydonia jiggamintia* gen. et sp. nov., on the basis of morphometrical analyses and of structures indicating the presence of a metazoan-grade

aquiferous system. The analyses of the specimens of a single fossiliferous surface allow us to propose population and growth dynamics models which are consistent with poriferan-grade organisms.

The resulting picture of the Avalon Assemblage of Newfoundland is that of a dynamic environment, with a large diversity and a complex trophic net, involving micro- and macroscopic organisms. Moreover, we suggest that the presence of metazoans in the Ediacaran is largely underestimated in the literature, potentially due to a taphonomical bias.

General Summary

This thesis focuses on fossils from the Eastern region of Newfoundland (CA), in particular the Bonavista and Avalon peninsulas. Most of the outcrops in the region present sedimentary rocks recording extinct ecosystems that were very different from modern ones. The rocks were deposited during the Ediacaran period, pre-dating the animal diversification event known as the Cambrian explosion.

The Ediacaran of Newfoundland has a large diversity of species, many of which have not yet found a position in the tree of life, due to their peculiar body plans, resembling self-repeating branches that radiate from a central axis. Among those, the Arboreomorpha and, in particular, the Rangeomorpha represent the dominant groups and were traditionally interpreted as immotile organisms anchored to the seafloor and standing upright in the water column. In this manuscript, we describe two Rangeomorpha from Newfoundland (second and third chapter), as well as another organism of unknown affinities (fourth chapter).

The rangeomorphs *Culmofrons plumosa* from the Bonavista Peninsula are amazingly preserved, and the fine details recorded on the MUN Surface locality allow us to produce a new taphonomic model for the species, which calls for a re-interpretation of the organism as a reclining frond laying on the seafloor, potentially gathering nutrients from a symbiotic relationship with bacteria in the sediments.

In the third chapter, using statistical analyses, we describe a new species of the rangeomorph genus *Charnia* from a close by locality. The new species *Charnia ewinoni* is also interpreted as a recliner based on the orientations of some specimens in relation to the inferred palaeocurrent.

In the fourth chapter we describe a new species of unknown affinities, *Lydonia jiggamintia*, which had been previously compared to the form *Blackbrookia* from the Charnian

of the UK. This new genus has a porose surface, which is indicative of an animal-like organism, potentially one of the earliest Porifera.

This thesis work describes a variegated Ediacaran environment, potentially hosting animal-grade organisms and a large variety of forms and life-styles.

Acknowledgements

I would like to thank my supervisor prof. D. McIlroy for the great opportunity and the help throughout the years.

I thank my supervisory committee members Dr. R.S. Taylor and Dr. H. Corlett for their great help and support, Dr. J. Matthews for his useful suggestions and help, Dr. L. Herringshaw for his availability, K. Hiscock for his amazing practical help and P. Thurlow for supporting safety in the field.

I also thank my colleagues J.M. Neville, C. McKean, H.G. Fitzgerald, D. Pérez-Pinedo, N. Chida, P. Olschewski and M. Steele for their help, their great ideas and all of the amazing times in Newfoundland.

Thanks are due to Edith and Nev Samson, whose friendship and support made fieldwork so accessible.

Ringrazio i miei genitori per il loro enorme supporto e per avermi dato la possibilità di seguire le opportunità.

Un ringraziamento speciale va a Cami per il suo enorme supporto e comprensione in ogni momento durante questi anni.

Table of Contents

Title Page	I
Abstract	II
General Summary	IV
Acknowledgements	VI
Table of Contents	VII
List of Figures	X
List of Tables	XII
Chapter 1 : Introduction	1
1. Author contributions	2
2. Introduction to the Ediacaran biota	3
3. Ediacaran of Newfoundland	7
3.1. Geology of Newfoundland.....	7
3.2. Fossil Communities.....	10
3.3. Rangeomorphs.....	12
4. Open research questions	14
4.1. Overall evolutionary and taxonomical framework.....	14
4.2. Modes of life of Ediacaran organisms.....	16
5. Materials and methods	18
5.1. Field methodologies.....	18
5.2. Data analysis methodologies.....	18
6. Summary of original research	19
7. References:	21
Chapter 2 : Palaeobiology and taphonomy of the rangeomorph <i>Culmofrons plumosa</i>	28
1. Author contribution	29
2. Key words	30
3. Abstract	30
4. Introduction	31
5. Geological setting	33
5. Materials and methods	35
5.1. Dataset compilation and statistical analyses.....	35
5.2. Retrodeformation.....	36
6. Results	37
6.1. Morphological description of <i>Culmofrons plumosa</i>	37
6.2. Atypical rangeomorph structures.....	44

6.3.	Morphometric analysis.....	46
6.4.	Taphonomy of the Ediacaran biota of Avalonia.....	53
6.5.	<i>Culmofrons</i> preservation on the MUN Surface.....	55
7.	Discussion	58
7.1.	<i>Culmofrons</i> systematics	58
7.2.	Palaeobiology.....	60
8.	Conclusion	72
9.	Acknowledgements	74
10.	Data archiving statement	75
11.	References.....	76
Chapter 3 : A taxonomic and palaeobiologic consideration of <i>Charnia</i> spp. from the Bonavista Peninsula of Newfoundland (CA)		82
1.	Author contribution.....	83
2.	Key words	84
3.	Abstract.....	84
4.	Introduction.....	85
5.	Geological setting	88
5.	Materials and methods	92
5.1.	Data collection	92
5.2.	Linear models.....	96
5.3.	Backtransform morphospace	97
5.4.	PCA and HCPC.....	98
6.	Results	100
6.1.	Statistical analyses	100
6.2.	Backtransform morphospace	108
6.3.	Hierarchical clustering based on principal components (HCPC)	111
6.4.	Bonavista Peninsula <i>Charnia</i> sp.	114
6.5.	Systematic Palaeontology	116
7.	Discussion	120
7.1.	Bonavista Peninsula specimens	120
7.2.	Other specimens from Newfoundland	122
7.3.	Orientation of the Matthews Surface specimens	124
7.4.	<i>Charnia-Fractofusus</i> life-association	126
7.5.	Mode of Life of <i>Charnia</i> spp.....	129
8.	Conclusion	135
9.	Acknowledgements	137
10.	References.....	138
Chapter 4 : The macrofossil <i>Lydonia jiggamintia</i> gen. et sp. nov. from the Ediacaran of Newfoundland: from pseudofossil to metazoan-grade epibiont .		144
1.	Author contributions	145
3.	Key Words	146

4. Abstract.....	146
5. Introduction.....	147
6. Geological setting	150
7. Materials and Methods.....	152
8. Results	155
8.1. Morphology of the Catalina Dome “ <i>Blackbrookia</i> ”	155
8.2. Population structure of the Johnson Discovery Surface	167
8.3. Other porose-textured taxa from the Mistaken Point biota.....	170
8.4. Competing models for “ <i>Blackbrookia</i> ” morphology	172
9. Discussion	177
9.1. Systematic Palaeontology	179
9.2. Morphological Reconstruction.....	182
9.3. Palaeobiology and development of the Catalina Dome specimens	183
9.4. Population Models	185
9.5. Candidate sponges of Ediacaran age from Newfoundland.....	187
10. Conclusions.....	188
12. References	190
Summary	197
List of References	199

List of Figures

Chapter 1: Introduction

Figure 1.1: diversity of Ediacaran organisms from Eastern region of Newfoundland. ... Error! Bookmark not defined.	
Figure 1.2: map of Newfoundland and detail of the eastern portion of the island.....	8
Figure 1.3: diversity at Mistaken Point.....	11
Figure 1.4: diversity of rangeomorphs from Newfoundland.	12

Chapter 2: Palaeobiology and taphonomy of the rangeomorph *Culmofrons plumosa*

Figure 2.1: map and stratigraphy of the Catalina Dome.....	33
Figure 2.2: <i>Culmofrons plumosa</i> and <i>Beothukis mistakensis</i>	38
Figure 2.3: different preservation types on the MUN Surface.	40
Figure 2.4: <i>Culmofrons plumosa</i> specimens from the MUN Surface, Bonavista Peninsula. .	42
Figure 2.5: <i>Culmofrons plumosa</i> reconstruction.....	43
Figure 2.6: putative reproductive structures.	45
Figure 2.7: linear regressions between variable pairs.....	47
Figure 2.8: PCA scree plots.	49
Figure 2.9: PCA ordinations.	50
Figure 2.10: backtransform projection of the measured morphospace of <i>Culmofrons plumosa</i>	52
Figure 2.11: taphonomic model.	57
Figure 2.12: development and growth of <i>Culmofrons</i>	65

Chapter 3: A taxonomic and palaeobiologic consideration of *Charnia* spp. from the Bonavista Peninsula (CA)

Figure 3.1: diversity of <i>Charnia</i> sp. from Newfoundland.	87
Figure 3.2: map and stratigraphy of the fossiliferous localities.....	89
Figure 3.3: preservation on the Matthews Surface.	91
Figure 3.4: idealized <i>Charnia masoni</i> from the UK explaining how the different variables were collected.	93
Figure 3.5: box plots showing statistical differences for each of the 5 continuous variables between the two main specimen groups.	101
Figure 3.6: size frequency distribution graphs for the first 8 variables.	104
Figure 3.7: size frequency distribution graphs of the ratios of the continuous variables (cm) over the length of the petalodium (V1; cm).....	105
Figure 3.8: linear models for different transformed and untransformed variables.	107
Figure 3.9: backtransform morphospace analyses of the largest first-order branch of each specimen.	110
Figure 3.10: HCPC clusters solutions computed on PCA based on different variables.	112
Figure 3.11: holotype and paratype of <i>Charnia ewinoni</i>	119
Figure 3.12: other <i>Charnia</i> specimens from Newfoundland.	123

Figure 3.13: rose plots showing the orientation of the <i>C. ewinoni</i> specimens on the Matthews Surface.	124
Figure 3.14: in life associations on the Matthews Surface	128

Chapter 4: The macrofossil *Lydonia jiggamintia* gen. et sp. nov from the Ediacaran of Newfoundland: from pseudofossil to metazoan-grade epibiont

Figure 4.1: map and stratigraphy of the fossiliferous localities.....	151
Figure 4.2: diversity of specimens from the JDS.....	155
Figure 4.3: linear models between different variables in the JDS population.	157
Figure 4.4: backtransform morphospace analyses of part of the JDS population (N=33)....	159
Figure 4.5: rose plot and ripples orientation.	160
Figure 4.6: <i>Lydonia</i> upper surface patterns.....	163
Figure 4.7: pores morphology in ‘ <i>Blackbrookia</i> ’.....	164
Figure 4.8: rangeomorph-‘ <i>Blackbrookia</i> ’ associations.	166
Figure 4.9: size frequency distribution graphs and BIC	168
Figure 4.10: other porose-textured taxa.	171
Figure 4.11: holotype of <i>Lydonia</i>	180

List of Tables

Chapter 3: A taxonomic and palaeobiologic consideration of *Charnia* spp. from the Bonavista Peninsula (CA)

Table 3.1: list of measured variables used in this study.94

Chapter 4: The macrofossil *Lydonia jiggamintia* gen. et sp. nov from the Ediacaran of Newfoundland: from pseudofossil to metazoan-grade epibiont

Table 4.1: variables used in this study.....152

Chapter 1 : Introduction

Pasinetti Giovanni^{1*}, gpasinetti@mun.ca, 0000-0003-3104-9758

McIlroy Duncan¹, 0000-0001-9521-499X

¹MUN Palaeobiology Group, Department of Earth Sciences, Memorial University of Newfoundland (CA)

*Corresponding author

1. Author contributions

Conceptualization: G. Pasinetti (GP);

Data Curation Management: GP;

Formal Analysis: GP;

Funding Acquisition: D. McIlroy (DM);

Investigation: GP;

Methodology: GP;

Project Administration: GP;

Resources: GP; Software: GP;

Supervision: DM;

Validation: GP, DM;

Visualization: GP;

Writing – Original Draft Preparation: GP;

Writing – Review & Editing: GP, DM.

2. Introduction to the Ediacaran biota

In “The Origin of Species”, Darwin (1959) interrogated himself about a major inconsistency in his theory of Evolution: “The Cambrian Explosion”. At Darwin’s time there was no known fossiliferous record from the Pre-Cambrian, leaving the scientist wondering how “several of the main divisions of the animal kingdom suddenly appear in the lowest known fossiliferous..., ...and why we do not find rich fossiliferous deposits belonging to these assumed earliest periods before the Cambrian system?”. It would take almost a century after the death of Darwin for geologists to accept fossil evidence as definitive proof of life in Pre-Cambrian strata (Schopf, 2000). A major discovery was made by young English girl, Tina Negus, and successively the student Roger Mason, in the Charnwood Forest in Leicestershire (UK), that led to the identification of some of the first described Pre-Cambrian body fossils, such as *Charnia masoni* and *Charniodiscus concentricus* (Ford, 1958, 1962). The work of Sprigg, Glaessner and Wade (Turner and Vickers-Rich, 2007) revealed a rich biota in the Flinders Ranges of South Australia, in the Ediacara Hills, which became eponymous with the last Proterozoic period before the Cambrian (Knoll et al., 2006). Pre-Cambrian fossiliferous localities have since been discovered worldwide, revealing a large diversity of taxonomic groups, and leading to progressively increasing interest in the Ediacaran Period and improved understanding of early multicellular and metazoan evolution.

The highest abundance of Pre-Cambrian fossils can be found in the Late Ediacaran, in a period spanning from the end Gaskiers Glaciation, 579.88 ± 0.44 Ma (Pu et al., 2016) to the appearance of *Treptichnus pedum*, at the base of the Cambrian Period (Brasier et al., 1994). The Ediacaran biota appears shortly after the Gaskiers glaciation and rapidly diversifies, producing a large variety of forms (**Fig. 1.1**), including numerous extinct Bauplans that have not yet found a defined position in the tree of life (Dunn et al., 2021). The complexity of

Ediacaran organisms largely precedes in time the diversification of the Eumetazoa in the Phanerozoic, raising questions on their phylogenetic relationships with extant taxa, to the point that some authors have proposed that many of them might have belonged to extinct kingdoms (Seilacher, 1989, 1992).

Among the Ediacaran biota are benthic macro-organisms such as the enigmatic Rangeomorpha (**Fig. 1.1 A, C**) and Arboreomorpha (**Fig. 1.1C**), which dominate the Avalon Assemblage, the oldest of the three traditional subdivisions of the Late Ediacaran (Waggoner, 2003), along with the oldest putative metazoan (**Fig. 1.1 B**) and eumetazoan (**Fig. 1.1 D**). The Avalon Assemblage is recorded in rocks formed around the palaeocontinent of Avalonia, the Avalonian Terrane, which now outcrops in renowned localities in the Charnwood Forest (UK) (McIlroy and Horak, 2006), as well as in the eastern regions of Newfoundland, in particular the Avalon and Bonavista peninsulas (CA) (Hofmann et al., 2008). After the appearance of the first recognizable body fossils in the Drook Formation of the Avalon Peninsula 574.14 ± 0.19 Ma in the world famous Mistaken Point Ecological Reserve (MPER) (Matthews et al., 2020), distal continental platforms and slopes surrounding the microcontinent of Avalonia saw a rich diversification in macroscopic life.

With the appearance of the Dickinsoniomorpha (Bobrovskiy et al., 2018) and Erniettomorpha (Hall et al., 2020), as well as other extinct Ediacaran groups, along with the first Bilateria (Ivantsov, 2009, 2010; Parry et al., 2017; Evans et al., 2020), the Avalon Assemblage transitions into the more dynamic White Sea Assemblage, where motility, predation and bioturbation start to play a role in the ecosystems (Ivantsov, 2011, 2013; Ivantsov et al., 2019, 2020).

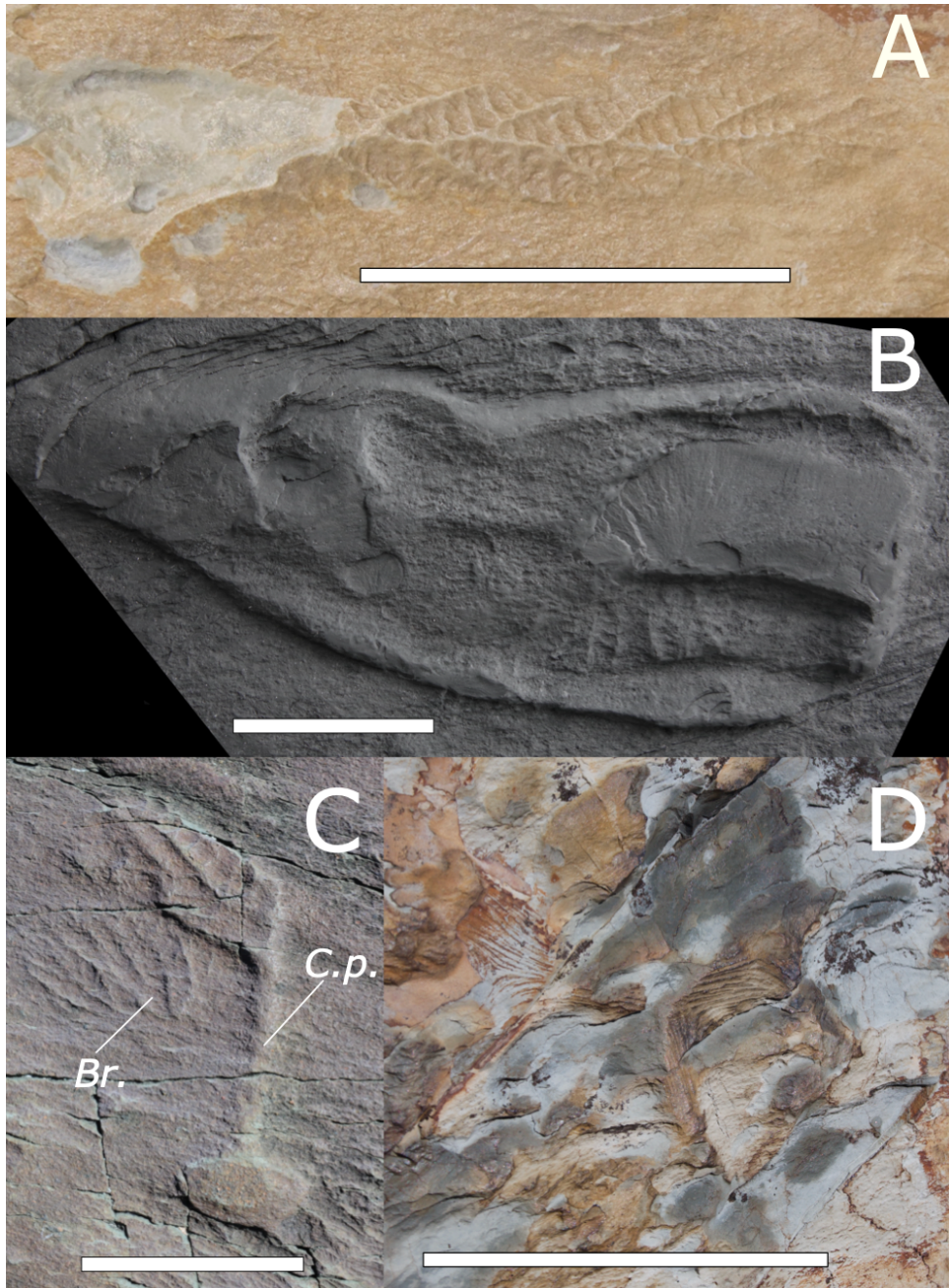


Figure 1.1: diversity of Ediacaran organisms from Eastern region of Newfoundland.

A) *Charnia* sp. from the MUN Surface (Bonavista Peninsula), a typical rangeomorph; **B)** *Lydonia jiggamintia* sp. nov. from the Discovery Surface (Bonavista Peninsula), a putative Porifera; **C)** *Charniodiscus procerus* (“C.p.”), a reclining arboreomorph and a small *Bradgatia linfordensis* (“Br.”), a multibranched-rangeomorph from the E Surface in the Mistaken Point Ecological Reserve (Avalon Peninsula); **D)** *Haootia* sp. from the MUN Surface (Bonavista Peninsula), a putative cnidarian. Scale bars = 5 cm.

The youngest Late Ediacaran faunal subdivision, the Nama Assemblage, sees the drastic reduction in number and diversity of the typical Ediacaran elements, in favor of increasing bilaterian activity and the subsequent lengthening of the marine carbon cycle creation and occupation of new ecological niches, such as the planktonic and the infaunal realms, made possible by the appearance of a mixed layer in seafloor sediments (Seilacher and Pflüger, 1994; McIlroy and Logan, 1999; Bottjer et al., 2000; Bottjer, 2010; Budd and Jensen, 2017; Mangano and Buatois, 2017).

Causes for the extinction of the Ediacaran biota are still debated. Even though typically Ediacaran taxa see a reduction in diversity and abundance in progressively younger strata, in favor of increasing diversification of eumetazoans and Phanerozoic taxa, it is not clear whether the disappearance of the Ediacaran biota is to be attributed to an abrupt extinction (Amthor et al., 2003), a progressive replacement (Seilacher, 1989, 1992; Seilacher and Pflüger, 1994; Butterfield, 2007), or a “Cheshire-Cat” disappearance (Laflamme et al., 2013). This last hypothesis proposes that some Ediacaran taxa might have survived major environmental changes - such as the agronomic revolution of the Cambrian, which displaced the microbial matgrounds thought to be involved with Ediacaran preservations (Gehling, 1999) - but could have been excluded from the taphonomic window (Briggs, 2003; Laflamme et al., 2011, 2013).

3. Ediacaran of Newfoundland

3.1. Geology of Newfoundland

The eastern regions of Newfoundland (the Bonavista and Avalon peninsulas, **Fig. 1.2**), corresponding to the western portions of the Avalon Terrane (Nance et al., 2002), are characterized by a predominance of sedimentary rocks deposited in offshore, distal shelf and continental slope settings, in what have been interpreted in a basin and sub-basin system on the side of a volcanic arc, and separated by a topological height, the Harbour Main (Wood et al., 2003). The main magmatic and orogenic activity in the area show crystallization dates between 635 and 570 Ma (Nance et al., 1991; Murphy et al., 1999), preceding and slightly overlapping the first appearance of the Ediacaran Biota 574.14 ± 0.19 Ma (Matthews et al., 2020). The Harbour Main Group is directly overlain by the Conception Group, which is characterized by turbiditic successions and abundant volcanic ash, indicative of arc-related basin deposition, either intra-arc (Dec et al., 1992), back-arc (Murphy et al., 1999) or fore-arc (Wood et al., 2003), with the latter being the most likely hypothesis. The overlying St. John's and Signal Hill groups record a transition to shallower depositional environments, with alluvial fan and delta deposits, and a substantially scarcer fossiliferous record. Rocks outcropping in the Bonavista Peninsula (**Fig. 1.2**) are broadly coeval to the Mistaken Point Ecological Reserve fossiliferous successions (**Fig. 1.2**) and have been lithostratigraphically correlated with the Conception and the St. John's Groups (O'Brien and King, 2002, 2005). Fossiliferous outcrops are known from the East portion of the Bonavista Peninsula, which presents turbiditic successions thought to have been deposited in a sub-basin of the Harbour Main system (Mason et al., 2013). The western portion of the peninsula is separated from the easterly deep-marine successions by the Spillars Cove/English Harbour Fault and represents Late Ediacaran rocks deposited in shallow waters and subaerial environments (O'Brien and King, 2002, 2005).

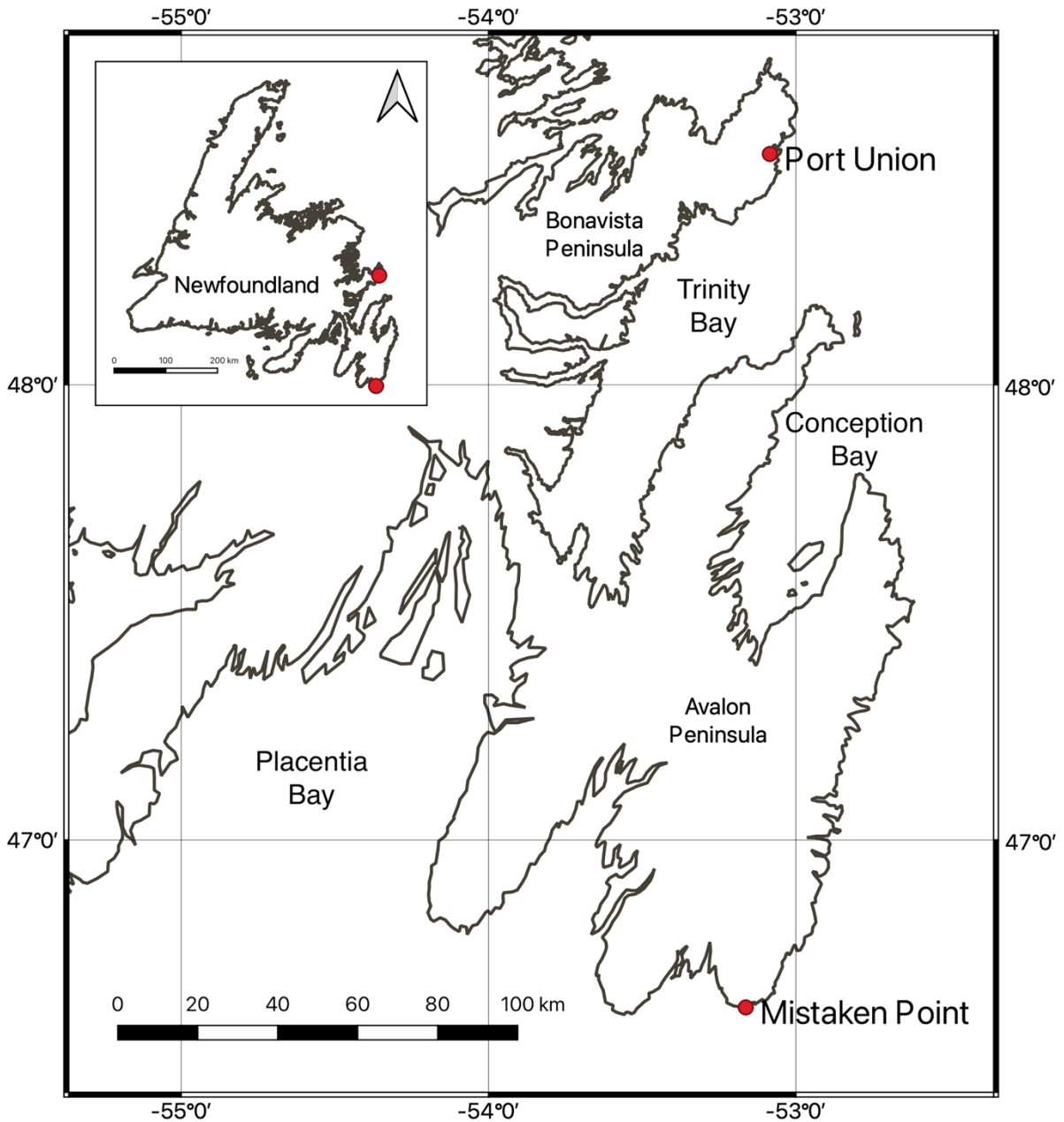


Figure 1.2: map of Newfoundland and detail of the eastern portion of the island.

The two main fossiliferous areas, the Mistaken Point Ecological Reserve in the Avalon Peninsula and the Discovery UNESCO Global Geopark in the proximity of the town of Port Union in the Bonavista Peninsula are indicated by red dots.

Ediacaran fossils in the Conception and St. John's groups are typically preserved *in situ* (Fig. 1.3), with no transport, often buried by turbiditic currents or tuffs deposited from the

water column. Different taphonomic models have been proposed for the peculiar preservation of Ediacaran organisms, which are often found as both positive and negative. Narbonne (2005) initially proposed the so-called “Conception-style” taphonomic model, which involves burial and casting of the organisms under a rapidly solidifying volcanic ash, which Seilacher 1999 considered to be an “Ediacaran Pompei”. Differences in tissue strength and decomposition rates allow for the differential preservation of positive and negative features, with sturdier structures (e.g., the stems and basal discs of rangeomorphs and arboreomorphs, **Fig. 1.1 C**) persisting longer after burial by the ash than the more labile portions of organisms such as the fronds portion. The lithifying ash would therefore cast the top of persisting structures, but more delicate structures would rapidly disappear prior to ash lithification, only leaving an impression on the seafloor sediments. However, this model underestimates the role of microbial activity on the seafloor, which is thought to have been extensively covered in microbial mats during the Ediacaran (Pfluger, 1999). Extensive microbial mats, which would have not been affected by metazoan bioturbation, could have played a role in rapid biomineralization of the sediments surrounding the bodies of the Ediacaran biota, by depositing framboidal pyrite and effectively producing a “microbial death mask”. In turn, this would have allowed for detailed preservations (Gehling, 1999; Liu, 2016) and effaced preservation of necro-mass (Liu et al., 2011), or favored silica-cement deposition around the bodies of buried macro-organisms (Slagter et al., 2022), perhaps by smothering of the mat before casting (McIlroy et al., 2009).

3.2. Fossil Communities

A large variety of taxa have been described from the Ediacaran outcrops of the UK and Newfoundland, including pseudofossils such as the ivesheadiomorphs (**Fig. 1.3**), which have been interpreted as microbial buildups on decaying necro-mass (Liu et al., 2011) and body-fossils of macro-organisms *sensu stricto*, with an observable difference between the two preservational end-members (Antcliffe et al., 2015). Notably, the first record of eumetazoan life also come from Newfoundland, with the oldest eumetazoan ichnofossils (Menon et al., 2013; Liu and McIlroy, 2015) as well as the earliest cnidarian body fossils (Liu et al., 2014, 2015) (**Fig. 1.1 D**). Among them, rangeomorphs and arboreomorphs are the first groups that present complex body plans, which could suggest tissue organization and even the presence of functional organs. Both taxa are typically preserved as negative or positive impressions on a fossiliferous surface (**Fig. 1.3**) and true body fossils are extremely rare and problematic: this leads to a scarce understanding of their three-dimensional morphology, as only one side of the organisms can be observed at once.

Since Ediacaran fossiliferous surfaces record a “snapshot” of extinct communities, with most of the taxa being preserved with little to no transport, and possibly even in life position (**Fig. 1.3**), it is possible to conduct community and spatial analyses, and even hypothesize ecological succession models (Seilacher, 1992; Mitchell and Butterfield, 2018; McIlroy et al., 2021; Pasinetti and McIlroy, 2023).

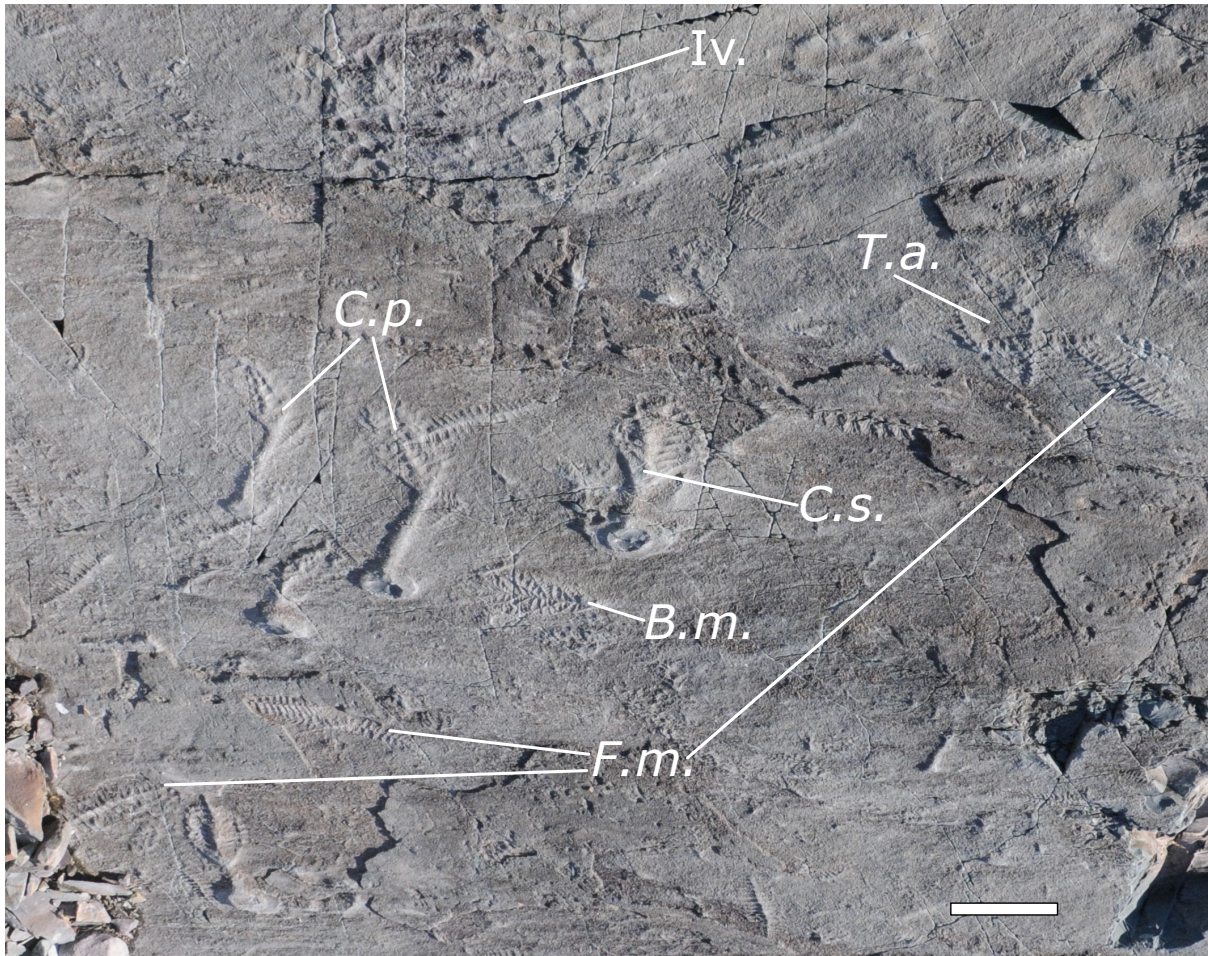


Figure 1.3: diversity at Mistaken Point.

The famous “Seilacher’s Corner” from the E Surface in the Mistaken Point Ecological Reserve, depicting a snapshot of a diverse Ediacaran community. In a small area (Scale bar = 10 cm) several species can be found, including the rangeomorphs *Beothukis mistakensis* (“*B.m.*”) and the super-abundant *Fractofusus misrai* (“*F.m.*”), the arboreomorphs *Charniodiscus procerus* (“*C.p.*”) and *Charniodiscus spinosus* (“*C.s.*”), ivesheadiomorphs (“*Iv.*”) pseudofossils and *Thectardis avalonensis* (“*T.a.*”), which has been interpreted as one of the earliest Porifera (Clapham et al., 2004).

3.3. Rangeomorphs

The Rangeomorpha appear around 570 Ma in the Mistaken Point Ecological Reserve (Liu et al. 2013; Matthews et al., 2020) and show a rapid diversification (Fig. 1.4), followed by a decline in abundance and diversity throughout the rest of the late Ediacaran, till their eventual disappearance before the beginning of the Cambrian (Laflamme et al., 2013). Rangeomorphs are characterized by a frondose portion, the “petalodium”, composed by a variable number of first-order branches (“FOB”) arranged on both sides of an axis (“midline”), which can then subdivide to form up to three further orders (so-called “rangeomorph elements”), and can have an elongated basal structure, traditionally interpreted as a stem, sometimes with a holdfast (“basal disc”).

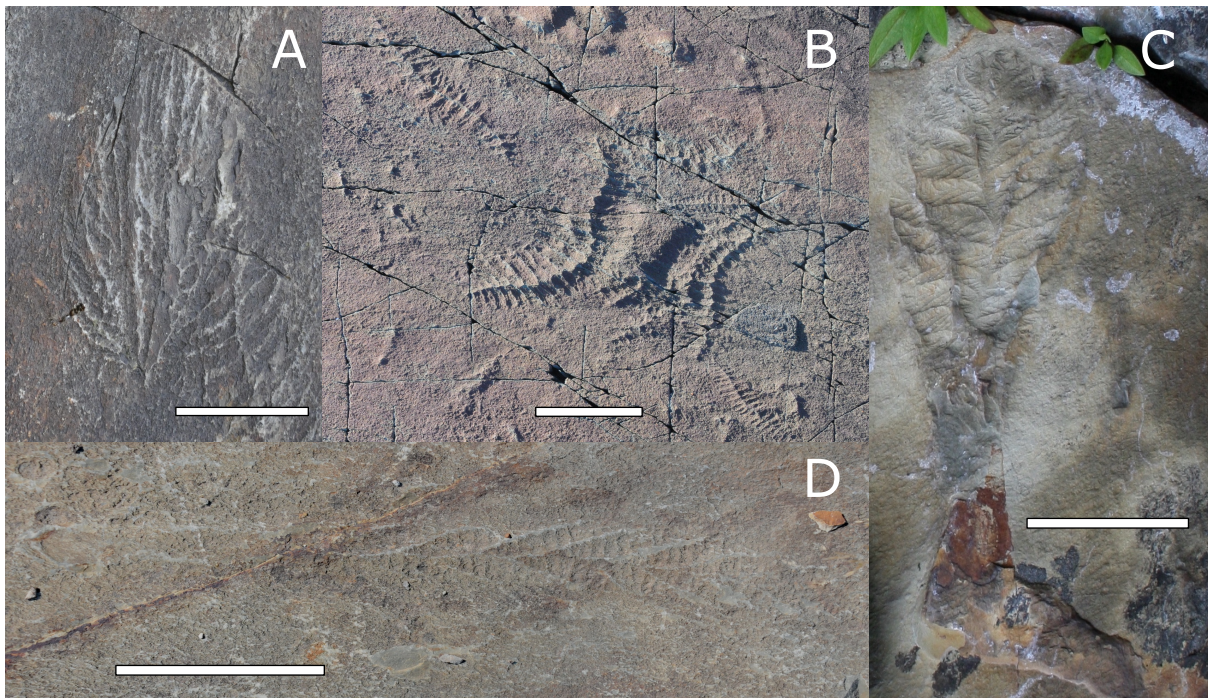


Figure 1.4: diversity of rangeomorphs from Newfoundland.

A) *Bradgatia linfordensis* from Capelin Gulch, Bonavista Peninsula, a multipolar member of the Rangida; **B)** *Fractofusus misrai* from the E Surface at Mistaken Point, a bipolar rangiid; **C)** *Culmofrons plumosa* from the MUN Surface, Bonavista Peninsula, a unipolar member of the

Charnida; **D**) *Charnia ewinoni* from the Matthews Surface, Bonavista Peninsula, a unipolar charniid. Scale bars = 5 cm.

Branch morphologies, orientations and arrangements, as well as the presence or absence of a stem, show a large intra- and inter-specific diversity. This results in the Rangeomorpha being a taxonomic group that encompasses several very different Bauplans, all based upon the presence of the “rangeomorph element” in a number of different orientations (Jenkins, 1985; Brasier et al., 2012). A first morphologic distinction can be made between unipolar and bi- and multi polar fronds: unipolar fronds present first-order branches stemming on both sides of a midline with a baso-apical direction (e.g., *Culmofrons plumosa*, *Charnia masoni*, **Fig. 1.4 C-D**). Typically, only unipolar fronds can have a stem. Bipolar fronds have a single axis, but first-order branches without a preferential growth direction, producing two axes of rough symmetry (**Fig. 1.4 B**): one perpendicular to and one that is both coincident with and parallel to the midline (e.g., *Fractofusus misrai*, *F. anderson*, *Hapsidophyllas flexibilis*). A larger number of midlines, and their respective rows of first-order branches, that converge to a central point are characteristic of multipolar fronds (e.g., *Bradgatia linfordensis*, **Fig. 1.4 A**).

The polarity of the frond is not considered a fundamental taxonomic trait and the Rangeomorphs (Narbonne et al., 2009; Dececchi et al., 2017), which are instead classified in two groups on the basis of the rotation of the first-order branches (Narbonne et al., 2009): 1) the Charnida (**Fig. 1.4 C-D**), which have rotated first-order branches, showing only one row of second-order branches on each FOB and 2) the Rangida (**Fig. 1.4 A-B**), with unrotated first-order branches which show two rows of second-order branches on each FOB.

4. Open research questions

4.1. Overall evolutionary and taxonomical framework

Evolutionary relationships between the different “Ediacaran Fronds” and Phanerozoic macroscopic life are still poorly understood, especially because of the scarcity of proper Precambrian body fossils. It has been proposed that organisms with the “quilted” (Rangeomorph) elements of the Ediacara biota might be reunited in an extinct kingdom, the so called Vendobionta (Buss & Seilacher 1994), forming a monophyletic group. This possibility is supported by the phylogenetic analyses of Dececchi et al. (2017), which find the Rangeomorph and the Arboreomorph as sister groups to the Erniettomorpha. However, the work of Laflamme and Narbonne (2008) emphasizes the body plan differences between the different groups, suggesting that modular Bauplans evolved independently different times in the Ediacaran biota.

It has been suggested that the rangeomorphs might had eumetazoan-grade tissues (Dunn et al., 2021), however, no definitive evidence has been put forth to support this claim and no tissues or organs have been definitely been interpreted as indisputably eumetazoan. The proposition of a placozoan-like common ancestor for the metazoan (Dufour and McIlroy, 2017, 2018), rather than a porifera-like one (Cavalier-Smith, 2017), opens the possibility of Rangeomorpha being an extinct sister group to the animals. Although it is quite likely that the Rangeomorpha and the Arboreomorpha belonged to the Opisthokonta, the only non-photosynthetic multicellular clade, their position within the group will remain problematic till definitive evidence in the form of complete body fossils with metazoan-grade tissue organization can be found.

The taxonomic framework of the Rangeomorpha is also problematic: the low diversity of the assemblages—compared to comparable Phanerozoic communities (Clapham et al.,

2003)—might be due to different organisms being reunited under “waste-bin” taxa, with the resulting genera and species incorporating specimens which are only superficially similar to each other (McIlroy et al., 2022). This might result in ecological models being compromised and the complexity of Ediacaran ecosystems being underestimated.

4.2. Modes of life of Ediacaran organisms

Despite the early work of Seilacher (1989, 1992), which considered different feeding strategies for the so-called Vendobionta (now encompassing the Rangeomorpha and Arboreomorpha), the frondose habitus and the presence of stem in some taxa has led most authors to interpret several rangeomorph and arboreomorph species as being erect in the water column, from which they would gather nutrients from particulate organic matter (i.e. filter-feeding) or direct absorption of dissolved organic matter (i.e. osmotrophy). Under this assumption, the self-repeating branching has been interpreted as an evolutionary strategy to maximize nutrient exchange (Laflamme et al., 2009; Hoyal Cuthill and Conway Morris, 2017) and some population models, proposing ecological successions of tiered organisms which are competing for access to the water column, have been proposed (Clapham and Narbonne, 2002; Clapham et al., 2003; Darroch et al., 2013, 2018).

However, some species, such as *Fractofusus misrai* and *F. andersoni*, have always been interpreted as having lived reclined on the seafloor (Gehling and Narbonne, 2007; Hofmann et al., 2008), even though they present petalodia composed of the same rangeomorph elements as other taxa that are interpreted as having lived erect. This would require an explanation of how homologous rangeomorph elements can be functional in completely different life positions, therefore making the distinction between fronds interpreted as erect or reclining arbitrary and not based on morphological evidence. Moreover, there is scarce direct taphonomical evidence that the Rangeomorphs were erect in the water column, forcing us to assume as a null hypothesis that the reclining position in which we now find them on the fossiliferous surfaces was also the life position (McIlroy et al., 2021). Traditional models in which the fronds are felled by a turbidite (Seilacher, 1999; Clapham and Narbonne, 2002; Wood et al., 2003; Laflamme and Narbonne, 2008; Narbonne et al., 2009; Vixseboxse et al., 2021) invoke

unrealistic fluid-dynamics (McIlroy et al., 2022) and complex taphonomic explanations for tuffite deposition (Wood et al., 2003).

Additionally, taphonomic evidence of a reclining lifestyle for species originally interpreted as erect (e.g., *Rangea schneiderhoehni*, *Charnia masoni*, *Hapsidophyllas flexibilis*, *Charniodiscus* gen., *Culmofrons plumosa*) is ever growing (Grazhdankin and Seilacher, 2005; Grazhdankin et al., 2008; Taylor et al., 2021; Pérez-Pinedo et al., 2022; Pasinetti and McIlroy, 2023). This has been coupled with a re-interpretation of the functional morphology of the rangeomorph elements: a reclining organism would accumulate H₂S at the interface with the seafloor, which could result in toxic conditions. The rangeomorph elements could then be interpreted as an adaptation to these conditions, by creating a suitable environment for sulfur-oxidizing bacteria, which might have had a symbiotic relationship with the Rangeomorpha, reducing the toxicity and providing them with a source of organic carbon in exchange for oxygenation and environmental protection (Dufour and McIlroy, 2017; McIlroy et al., 2020, 2021; Pasinetti and McIlroy, 2023).

5. Materials and methods

5.1. Field methodologies

Ediacaran fossils are protected in Newfoundland and Labrador under Reg. 67/11, of the Historic Resources Act 2011 and their access is only allowed under permission from the Government of Newfoundland and Labrador. Therefore, removal and collection are prohibited: collection of data in the field rely on replication methodologies, including photography of the surfaces, photometry and physical replication of the fossils via latex molds. Latex (or silicone) molds allow to obtain a high-resolution negative of the fossil impression, which can then be photographed as it is or reverted into a positive replica of the fossils by producing a plaster cast of the latex mold.

5.2. Data analysis methodologies

A variety of methodologies for data analysis were involved in this research work, including qualitative assessment of the fossils, photography under controlled lighting, morphometric analyses, morphospace analyses, ordination analyses, clustering analyses and population analyses. Morphometric and orientation data were collected and digitized with the software ImageJ from referenced field photographs or plaster casts photographed under controlled lighting. RStudio was used to perform the different analyses. Details for each methodology are described in the pertaining chapters.

6. Summary of original research

This research work includes three chapters, which address taxonomic and taphonomic problems and discuss the palaeoecology of three different Ediacaran taxa from Newfoundland, respectively two charniid rangeomorphs (*Culmofrons plumosa* and *Charnia* spp.) and one problematic body fossil (*Lydonia* gen. nov.).

Culmofrons plumosa appears to be a typical stemmed rangeomorph frond and has been described from MPER (Laflamme et al., 2012), but it is predominantly known from the MUN Surface in the Discovery Geopark (Bonavista Peninsula; Liu et al., 2016; Hawco et al., 2020), where some exceptionally preserved specimens are found. Our work investigates taxonomic differences between *Culmofrons plumosa* and other charniid rangeomorphs, proposes a new taphonomic model involving extensive microbial activity pre- and post-burial and suggests a reclining lifestyle for the frond. This interpretation further supports the hypothesis of McIlroy et al. (2021), by proving the reclining lifestyle of a stemmed, unipolar rangeomorph frond.

Another stemmed frond from the Bonavista Peninsula is described in the second chapter as a new species of *Charnia* on the base of morphological and developmental differences from the type species *Charnia masoni*. *C. ewinoni* sp. nov. has some crucial differences from *C. masoni*, which have been typically attributed to taphonomic factors (Laflamme et al., 2007), such as the presence of a stem or a straight midline rather than a zig-zagged one. Through the use of hierarchical clustering based on morphometric variables and morphospace analyses of the first-order branches shape, we show that *C. ewinoni* indeed represent a different organism from *C. masoni* rather than its taphomorph. A reclining mode of life is also proposed for *C. ewinoni*, which is often found to be oriented in the opposite direction with respect with the turbidite currents i.e. with the tip in an upslope direction), making it unrealistic to interpret the organism as erect in the water column and felled by the turbiditic currents. As the genus

Charnia is one of the most common Avalonian taxa, as well as one of the model organisms to depict an erect lifestyle for the Ediacaran biota, this new interpretation casts profound doubts on our traditional understanding of Ediacaran ecosystems and calls for a better taphonomic assessment of co-generic species (*C. masoni* and *C. gracilis*).

In the third chapter, we describe *Lydonia jiggamintia* sp. nov., a new non-rangeomorph species from the Bonavista Peninsula and MPER. The species, which was previously interpreted as a pseudofossil of decaying necromass (“Ivesheadiomorphs”; Liu et al., 2011), show higher organizational traits, such as well-defined morphometrical traits, consistent shapes and the presence of what has been interpreted as an aquiferous system. Such traits can be interpreted as metazoan-grade structures (Dunn et al., 2021), adding to the ever growing Pre-Cambrian animals fossil record, which already include undisputable eumetazoans (Ivantsov, 2010; Liu et al., 2014). We propose that the aquiferous system of *Lydonia* might be similar to that of modern encrusting demosponges, reinforcing the contested previous claims of the presence of Pre-Cambrian sponges and extending the fossiliferous record of the phylum.

In conclusion, this research investigates taxonomic and taphonomic aspects of three Ediacaran taxa from Newfoundland: *Culmofrons plumosa* and *Charnia ewinoni* sp. nov. (charniid rangeomorphs) and *Lydonia jiggamintia* sp. nov. The study confirms the taxonomic identity and proposes a reclining lifestyle for *C. plumosa* and *C. ewinoni*, and suggests metazoan-grade structures in *L. jiggamintia*, potentially expanding the porifera fossil record. Overall, these findings reshape our understanding of Ediacaran ecosystems and emphasize the need for re-evaluating traditional interpretations.

7. References:

- Amthor, J. E., Grotzinger, J. P., Schröder, S., Bowring, S. A., Ramezani, J., Martin, M. W., et al. (2003). Extinction of *Cloudina* and *Namacalathus* at the Precambrian-Cambrian boundary in Oman. *Geol* 31, 431. doi: 10.1130/0091-7613(2003)031<0431:EOCANA>2.0.CO;2
- Antcliffe, J. B., Hancy, A. D., and Brasier, M. D. (2015). A new ecological model for the ~565Ma Ediacaran biota of Mistaken Point, Newfoundland. *Precambrian Research* 268, 227–242. doi: 10.1016/j.precamres.2015.06.015
- Bobrovskiy, I., Hope, J. M., Ivantsov, A., Nettersheim, B. J., Hallmann, C., and Brocks, J. J. (2018). Ancient steroids establish the Ediacaran fossil *Dickinsonia* as one of the earliest animals. *Science* 361, 1246–1249. doi: 10.1126/science.aat7228
- Bottjer, D. J. (2010). The Cambrian substrate revolution and early evolution of the phyla. *J. Earth Sci.* 21, 21–24. doi: 10.1007/s12583-010-0160-7
- Bottjer, D. J., Hagadorn, J. W., and Dornbos, S. Q. (2000). The Cambrian substrate revolution. *GSA Today* 10, 32.
- Brasier, M., Cowie, J., and Taylor, M. (1994). Decision on the Precambrian-Cambrian boundary stratotype. *Episodes* 17, 3–8. doi: 10.18814/epiiugs/1994/v17i1.2/002
- Brasier, M. D., Antcliffe, J. B., and Liu, A. G. (2012). The architecture of Ediacaran fronds. *Palaeontology* 55, 1105–1124. doi: 10.1111/j.1475-4983.2012.01164.x
- Briggs, D. E. G. (2003). The Role of Decay and Mineralization in the Preservation of Soft-Bodied Fossils. *Annu. Rev. Earth Planet. Sci.* 31, 275–301. doi: 10.1146/annurev.earth.31.100901.144746
- Budd, G. E., and Jensen, S. (2017). The origin of the animals and a ‘Savannah’ hypothesis for early bilaterian evolution: Early evolution of the animals. *Biol Rev* 92, 446–473. doi: 10.1111/brv.12239
- Butterfield, N. J. (2007). Macroevolution and macroecology through Deep Time. *Palaeontology* 50, 41–55. doi: 10.1111/j.1475-4983.2006.00613.x
- Cavalier-Smith, T. (2017). Origin of animal multicellularity: precursors, causes, consequences—the choanoflagellate/sponge transition, neurogenesis and the Cambrian explosion. *Phil. Trans. R. Soc. B* 372, 20150476. doi: 10.1098/rstb.2015.0476
- Clapham, M. E., and Narbonne, G. M. (2002). Ediacaran epifaunal tiering. *Geology* 30, 627–630. doi: 10.1130/0091-7613(2002)030<0627:EET>2.0.CO;2

- Clapham, M. E., Narbonne, G. M., and Gehling, J. G. (2003). Paleoecology of the oldest known animal communities: Ediacaran assemblages at Mistaken Point, Newfoundland. *Paleobiology* 29, 527–544. doi: 10.1666/0094-8373(2003)029<0527:POTOKA>2.0.CO;2
- Clapham, M. E., Narbonne, G. M., Gehling, J. G., Greentree, C., and Anderson, M. M. (2004). *Thectardis avalonensis*: A new Ediacaran fossil from the Mistaken Point biota, Newfoundland. *Journal of Paleontology* 78, 1031–1036. doi: 10.1666/0022-3360(2004)078<1031:taanef>2.0.co;2
- Darroch, S. A. F., Laflamme, M., and Clapham, M. E. (2013). Population structure of the oldest known macroscopic communities from Mistaken Point, Newfoundland. *Paleobiology* 39, 591–608. doi: 10.1666/12051
- Darroch, S. A. F., Laflamme, M., and Wagner, P. J. (2018). High ecological complexity in benthic Ediacaran communities. *Nat Ecol Evol* 2, 1541–1547. doi: 10.1038/s41559-018-0663-7
- Darwin, C. (1859). *On the origin of species by means of natural selection, or, The preservation of favoured races in the struggle for life*. 6th ed. London: John Murray.
- Dec, T., O'Brien, S. J., and Knight, I. (1992). Late precambrian volcanoclastic deposits of the avalonian eastport basin (newfoundland appalachians): petrofacies, detrital clinopyroxene geochemistry and palaeotectonic implications. *Precambrian Research* 59, 243–262. doi: 10.1016/0301-9268(92)90059-W
- Decechi, T. A., Narbonne, G. M., Greentree, C., and Laflamme, M. (2017). Relating Ediacaran Fronds. *Paleobiology* 43, 171–180. doi: 10.1017/pab.2016.54
- Dufour, S. C., and McIlroy, D. (2017). Ediacaran pre-placozoan diploblasts in the Avalonian biota: the role of chemosynthesis in the evolution of early animal life. *Geological Society, London, Special Publications* 448, 211–219. doi: 10.1144/SP448.5
- Dufour, S. C., and McIlroy, D. (2018). An Ediacaran pre-placozoan alternative to the pre-sponge route towards the Cambrian explosion of animal life: a comment on Cavalier-Smith 2017. *Phil. Trans. R. Soc. B* 373, 20170148. doi: 10.1098/rstb.2017.0148
- Dunn, F. S., Liu, A. G., Grazhdankin, D. V., Vixseboxse, P., Flannery-Sutherland, J., Green, E., et al. (2021). The developmental biology of *Charnia* and the eumetazoan affinity of the Ediacaran rangeomorphs. *Sci. Adv.* 7, eabe0291. doi: 10.1126/sciadv.abe0291
- Evans, S. D., Hughes, I. V., Gehling, J. G., and Droser, M. L. (2020). Discovery of the oldest bilaterian from the Ediacaran of South Australia. *Proc Natl Acad Sci USA* 117, 7845–7850. doi: 10.1073/pnas.2001045117
- Ford, T. D. (1958). Pre-Cambrian fossils from Charnwood Forest. *Proceedings of the Yorkshire Geological Society* 31, 211–217. doi: 10.1144/pygs.31.3.211
- Ford, T. D. (1962). The Pre-Cambrian fossils of Charnwood Forest. *Transactions of the Leicester Literary and Philosophical Society* 56, 57–62.

- Gehling, J. G. (1999). Microbial Mats in terminal Proterozoic siliciclastics: Ediacaran death masks. *PALAIOS* 14, 40. doi: 10.2307/3515360
- Gehling, J. G., and Narbonne, G. M. (2007). Spindle-shaped Ediacara fossils from the Mistaken Point assemblage, Avalon Zone, Newfoundland. *Can. J. Earth Sci.* 44, 367–387. doi: 10.1139/e07-003
- Grazhdankin, D., and Seilacher, A. (2005). A re-examination of the Nama-type Vendian organism *Rangea schneiderhoehni*. *Geol. Mag.* 142, 571–582. doi: 10.1017/S0016756805000920
- Grazhdankin, D. V., Balthasar, U., Nagovitsin, K. E., and Kochnev, B. B. (2008). Carbonate-hosted Avalon-type fossils in arctic Siberia. *Geol* 36, 803. doi: 10.1130/G24946A.1
- Hall, J. G., Smith, E. F., Tamura, N., Fakra, S. C., and Bosak, T. (2020). Preservation of erniettomorph fossils in clay-rich siliciclastic deposits from the Ediacaran Wood Canyon Formation, Nevada. *Interface Focus.* 10, 20200012. doi: 10.1098/rsfs.2020.0012
- Hawco, J. B., Kenchington, C. G., Taylor, R. S., and Mcilroy, D. (2020). A multivariate statistical analysis of the Ediacaran rangeomorph taxa *Beothukis* and *Culmofrons*. *PALAIOS* 35, 495–511. doi: 10.2110/palo.2020.049
- Hofmann, H. J., O'Brien, S. J., and King, A. F. (2008). Ediacaran biota on Bonavista Peninsula, Newfoundland, Canada. *J. Paleontol.* 82, 1–36. doi: 10.1666/06-087.1
- Hoyal Cuthill, J. F., and Conway Morris, S. (2017). Nutrient-dependent growth underpinned the Ediacaran transition to large body size. *Nat Ecol Evol* 1, 1201–1204. doi: 10.1038/s41559-017-0222-7
- Ivantsov, A., Nagovitsyn, A., and Zakrevskaya, M. (2019). Traces of locomotion of Ediacaran macroorganisms. *Geosciences* 9, 395. doi: 10.3390/geosciences9090395
- Ivantsov, A. Yu. (2009). New reconstruction of *Kimberella*, problematic Vendian metazoan. *Paleontol. J.* 43, 601–611. doi: 10.1134/S003103010906001X
- Ivantsov, A. Yu. (2010). Paleontological evidence for the supposed Precambrian occurrence of Mollusks. *Paleontol. J.* 44, 1552–1559. doi: 10.1134/S0031030110120105
- Ivantsov, A. Yu. (2011). Feeding traces of Proarticulata—the Vendian metazoa. *Paleontol. J.* 45, 237–248. doi: 10.1134/S0031030111030063
- Ivantsov, A. Yu. (2013). Trace fossils of Precambrian metazoans “Vendobionta” and “Mollusks.” *Stratigr. Geol. Correl.* 21, 252–264. doi: 10.1134/S0869593813030039
- Ivantsov, A., Zakrevskaya, M., Nagovitsyn, A., Krasnova, A., Bobrovskiy, I., and Luzhnaya (Serezhnikova), E. (2020). Intravital damage to the body of *Dickinsonia* (Metazoa of the late Ediacaran). *J. Paleontol.* 94, 1019–1033. doi: 10.1017/jpa.2020.65

- Jenkins, R. J. F. (1985). The enigmatic Ediacaran (late Precambrian) genus *Rangea* and related forms. *Paleobiology* 11, 336–355. doi: 10.1017/S0094837300011635
- Knoll, A. H., Walter, M. R., Narbonne, G. M., and Christie-Blick, N. (2006). The Ediacaran Period: a new addition to the geologic time scale. *LET* 39, 13–30. doi: 10.1080/00241160500409223
- Laflamme, M., Darroch, S. A. F., Tweedt, S. M., Peterson, K. J., and Erwin, D. H. (2013). The end of the Ediacara biota: Extinction, biotic replacement, or Cheshire Cat? *Gondwana Research* 23, 558–573. doi: 10.1016/j.gr.2012.11.004
- Laflamme, M., Flude, L. I., and Narbonne, G. M. (2012). Ecological tiering and the evolution of a stem: the oldest stemmed frond from the Ediacaran of Newfoundland, Canada. *J. Paleontol.* 86, 193–200. doi: 10.1666/11-044.1
- Laflamme, M., and Narbonne, G. M. (2008). Ediacaran fronds. *Palaeogeography, Palaeoclimatology, Palaeoecology* 258, 162–179. doi: 10.1016/j.palaeo.2007.05.020
- Laflamme, M., Narbonne, G. M., Greentree, C., and Anderson, M. M. (2007). Morphology and taphonomy of an Ediacaran frond: *Charnia* from the Avalon Peninsula of Newfoundland. *SP* 286, 237–257. doi: 10.1144/SP286.17
- Laflamme, M., Schiffbauer, J. D., Narbonne, G. M., and Briggs, D. E. G. (2011). Microbial biofilms and the preservation of the Ediacara biota: Ediacaran preservation. *Lethaia* 44, 203–213. doi: 10.1111/j.1502-3931.2010.00235.x
- Laflamme, M., Xiao, S., and Kowalewski, M. (2009). Osmotrophy in modular Ediacara organisms. *Proceedings of the National Academy of Sciences* 106, 14438–14443. doi: 10.1073/pnas.0904836106
- Liu, A. G. (2016). Framboidal Pyrite Shroud Confirms the “Death Mask” model for moldic preservation of Ediacaran soft-bodied organism. *PALAIOS* 31, 259–274. doi: 10.2110/palo.2015.095
- Liu, A. G., Matthews, J. J., and McIlroy, D. (2016). The *Beothukis* / *Culmofrons* problem and its bearing on Ediacaran macrofossil taxonomy: evidence from an exceptional new fossil locality. *Palaeontology* 59, 45–58. doi: 10.1111/pala.12206
- Liu, A. G., Matthews, J. J., Menon, L. R., McIlroy, D., and Brasier, M. D. (2014). *Haootia quadriformis* n. gen., n. sp., interpreted as a muscular cnidarian impression from the Late Ediacaran period (approx. 560 Ma). *Proc. R. Soc. B.* 281, 20141202. doi: 10.1098/rspb.2014.1202
- Liu, A. G., and McIlroy, D. (2015). Horizontal surface traces from the Fermeuse Formation, Ferryland (Newfoundland, Canada), and their place within the Late Ediacaran ichnological revolution. *Geological Association of Canada, Miscellaneous Publication* 9, 141–156.

- Liu, A. G., McIlroy, D., Antcliffe, J. B., and Brasier, M. D. (2011). Effaced preservation in the Ediacara biota and its implications for the early microfossil record: Ediacaran Taphomorph. *Palaeontology* 54, 607–630. doi: 10.1111/j.1475-4983.2010.01024.x
- Mangano, G. M., and Buatois, L. A. (2017). The Cambrian revolutions: Trace-fossil record, timing, links and geobiological impact. *Earth-Science Reviews* 173, 96–108. doi: 10.1016/j.earscirev.2017.08.009
- Mason, S. J., Narbonne, G. M., Dalrymple, R. W., and O’Brien, S. J. (2013). Paleoenvironmental analysis of Ediacaran strata in the Catalina Dome, Bonavista Peninsula, Newfoundland. *Can. J. Earth Sci.* 50, 197–212. doi: 10.1139/cjes-2012-0099
- Matthews, J. J., Liu, A. G., Yang, C., McIlroy, D., Levell, B., and Condon, D. J. (2020). A chronostratigraphic framework for the rise of the Ediacaran macrobiota: New constraints from Mistaken Point Ecological Reserve, Newfoundland. *Geological Society of America Bulletin* 133, 13. doi: 10.1130/B35646.1
- McIlroy, D., Brasier, M. D., and Lang, A. S. (2009). Smothering of microbial mats by macrobiota: implications for the Ediacara biota. *Journal of the Geological Society* 166, 1117–1121. doi: 10.1144/0016-76492009-073
- McIlroy, D., Dufour, S. C., Taylor, R., and Nicholls, R. (2021). The role of symbiosis in the first colonization of the seafloor by macrobiota: Insights from the oldest Ediacaran biota (Newfoundland, Canada). *Biosystems* 205, 104413. doi: 10.1016/j.biosystems.2021.104413
- McIlroy, D., Hawco, J., McKean, C., Nicholls, R., Pasinetti, G., and Taylor, R. (2020). Palaeobiology of the reclining rangeomorph *Beothukis* from the Ediacaran Mistaken Point Formation of southeastern Newfoundland. *Geol. Mag.*, 1–15. doi: 10.1017/S0016756820000941
- McIlroy, D., and Horak, J. M. (2006). “Neoproterozoic: the late Precambrian terranes that formed Eastern Avalonia,” in *The Geology of England and Wales*, eds. P. J. Brenchley and P. F. Rawson (The Geological Society of London), 9–23. doi: 10.1144/GOEWP.2
- McIlroy, D., and Logan, G. A. (1999). The impact of bioturbation on infaunal ecology and evolution during the Proterozoic-Cambrian transition. *PALAIOS* 14, 58. doi: 10.2307/3515361
- McIlroy, D., Pérez-Pinedo, D., Pasinetti, G., McKean, C., Taylor, R. S., and Hiscott, R. N. (2022). Rheotropic epifaunal growth, not felling by density currents, is responsible for many Ediacaran fossil orientations at Mistaken Point. *Front. Earth Sci.* 10, 849194. doi: 10.3389/feart.2022.849194
- Menon, L. R., McIlroy, D., and Brasier, M. D. (2013). Evidence for Cnidaria-like behavior in ca. 560 Ma Ediacaran *Aspidella*. *Geology* 41, 895–898. doi: 10.1130/G34424.1
- Mitchell, E. G., and Butterfield, N. J. (2018). Spatial analyses of Ediacaran communities at Mistaken Point. *Paleobiology* 44, 40–57. doi: 10.1017/pab.2017.35

- Murphy, J. B., Keppie, J. D., Dostal, J., and Nance, R. D. (1999). “Neoproterozoic-early Paleozoic evolution of Avalonia,” in *Laurentia-Gondwana connections before Pangea* (Geological Society of America). doi: 10.1130/0-8137-2336-1.253
- Nance, R. D., Murphy, J. B., and Keppie, J. D. (2002). A Cordilleran model for the evolution of Avalonia. *Tectonophysics* 352, 11–31. doi: 10.1016/S0040-1951(02)00187-7
- Nance, R. D., Murphy, J. B., Strachan, R. A., D’Lemos, R. S., and Taylor, G. K. (1991). Late Proterozoic tectonostratigraphic evolution of the Avalonian and Cadomian terranes. *Precambrian Research* 53, 41–78. doi: 10.1016/0301-9268(91)90005-U
- Narbonne, G. M. (2005). The Ediacara biota: Neoproterozoic origin of animals and their ecosystems. *Annu. Rev. Earth Planet. Sci.* 33, 421–442. doi: 10.1146/annurev.earth.33.092203.122519
- Narbonne, G. M., Laflamme, M., Greentree, C., and Trusler, P. (2009). Reconstructing a lost world: Ediacaran rangeomorphs from Spaniard’s Bay, Newfoundland. *J. Paleontol.* 83, 503–523. doi: 10.1666/08-072R1.1
- O’Brien, S. J., and King, A. F. (2002). Neoproterozoic Stratigraphy of the Bonavista Peninsula: preliminary results, regional correlations and implication for sediment-hosted stratiform copper exploration in the Newfoundland Avalon Zone. *Geological Survey* 02, 229–244.
- O’Brien, S. J., and King, A. F. (2005). Late Neoproterozoic (Ediacaran) stratigraphy of Avalon Zone sedimentary rocks, Bonavista Peninsula, Newfoundland. *Geological Survey* 05, 13.
- Parry, L. A., Boggiani, P. C., Condon, D. J., Garwood, R. J., Leme, J. de M., McIlroy, D., et al. (2017). Ichnological evidence for meiofaunal bilaterians from the terminal Ediacaran and earliest Cambrian of Brazil. *Nat Ecol Evol* 1, 1455–1464. doi: 10.1038/s41559-017-0301-9
- Pasinetti, G., and McIlroy, D. (2023). Palaeobiology and taphonomy of the rangeomorph *Culmofrons plumosa*. *Palaeontology* 66, e12671. doi: 10.1111/pala.12671
- Pérez-Pinedo, D., McKean, C., Taylor, R., Nicholls, R., and McIlroy, D. (2022). *Charniodiscus* and *Arborea* are separate genera within the Arboreomorpha: Using the holotype of *C. concentricus* to resolve a taphonomic/taxonomic tangle. *Front. Earth Sci.* 9, 785929. doi: 10.3389/feart.2021.785929
- Pfluger, F. (1999). Matground structures and redox facies. *PALAIOS* 14, 25. doi: 10.2307/3515359
- Pu, J. P., Bowring, S. A., Ramezani, J., Myrow, P., Raub, T. D., Landing, E., et al. (2016). Dodging snowballs: Geochronology of the Gaskiers glaciation and the first appearance of the Ediacaran biota. *Geology* 44, 955–958. doi: 10.1130/G38284.1

- Schopf, J. W. (2000). Solution to Darwin's dilemma: Discovery of the missing Precambrian record of life. *PNAS* 97, 6947–6953.
- Seilacher, A. (1989). Vendozoa: Organismic construction in the Proterozoic biosphere. *LET* 22, 229–239. doi: 10.1111/j.1502-3931.1989.tb01332.x
- Seilacher, A. (1992). Vendobionta and Psammocorallia: lost constructions of Precambrian evolution. *Journal of the Geological Society* 149, 607–613. doi: 10.1144/gsjgs.149.4.0607
- Seilacher, A., and Pflüger, F. (1994). “From biomats to benthic agriculture: A biohistoric revolution,” in *Biostabilization of Sediments*, eds. W. E. Krumbein, D. M. Paterson, and L. J. Stal (Bibliotheks Und Infomationssystem Der Carl Von Ossietzky Universität), 97–105.
- Slagter, S., Hao, W., Planavsky, N. J., Konhauser, K. O., and Tarhan, L. G. (2022). Biofilms as agents of Ediacara-style fossilization. *Sci Rep* 12, 8631. doi: 10.1038/s41598-022-12473-1
- Taylor, R. S., Matthews, J. J., Nicholls, R., and McIlroy, D. (2021). A re-assessment of the taxonomy, palaeobiology and taphonomy of the rangeomorph organism *Hapsidophyllas flexibilis* from the Ediacaran of Newfoundland, Canada. *PalZ* 95, 187–207. doi: 10.1007/s12542-020-00537-4
- Turner, S., and Vickers-Rich, P. (2007). Sprigg, Glaessner and Wade and the discovery and international recognition of the Ediacaran fauna. *SP* 286, 443–445. doi: 10.1144/SP286.37
- Vixseboxse, P. B., Kenchington, C. G., Dunn, F. S., and Mitchell, E. G. (2021). Orientations of Mistaken Point Fronds Indicate Morphology Impacted Ability to Survive Turbulence. *Front. Earth Sci.* 9, 762824. doi: 10.3389/feart.2021.762824
- Waggoner, B. (2003). The Ediacaran biotas in space and time. *Integrative and Comparative Biology* 43, 104–113. doi: 10.1093/icb/43.1.104
- Wood, D. A., Dalrymple, R. W., Narbonne, G. M., Gehling, J. G., and Clapham, M. E. (2003). Paleoenvironmental analysis of the late Neoproterozoic Mistaken Point and Trepassay formations, southeastern Newfoundland. *Can. J. Earth Sci.* 40, 1375–1391. doi: 10.1139/e03-048

Chapter 2 : Palaeobiology and taphonomy of the rangeomorph *Culmofrons plumosa*

Pasinetti Giovanni^{1*}, gpasinetti@mun.ca, 0000-0003-3104-9758

McIlroy Duncan¹, 0000-0001-9521-499X

*Corresponding author

Published in *Palaeontology*, 66, e12671

doi: [10.1111/pala.12671](https://doi.org/10.1111/pala.12671) 1

1. Author contribution

Conceptualization: G. Pasinetti (GP), D. McIlroy (DM), R.S. Taylor (RST);

Data Curation Management: GP;

Formal Analysis: GP;

Funding Acquisition: DM;

Investigation: GP, DM;

Methodology: GP, DM;

Project Administration: GP, DM;

Resources: DM;

Software: GP;

Supervision: DM;

Validation: GP, DM, RST, D Pérez-Pinedo (DPP);

Visualization: GP;

Writing – Original Draft Preparation: GP;

Writing – Review & Editing: GP, DM, RST.

2. Key words

RANGEOMORPH, AVALON ASSEMBLAGE, PALAEOBIOLOGY, TAPHONOMY, REPRODUCTION, ONTOGENY

3. Abstract

The deep marine Ediacaran fossil record of Avalonia is dominated by the Rangeomorpha, a clade characterized by up to four orders of fractal-like branching. Despite their abundance, morphological diversity and the recent increase in Ediacaran studies, aspects of their palaeobiology, palaeoecology and phylogenetic position in the tree of life are still hotly debated. The clade has traditionally been interpreted as consisting of organisms that lived erect in the water column and tethered to the seafloor, based on the intuitive interpretation of their frondose body plan.

However, recent work has challenged this view and instead proposes a reclining mode of life for several rangeomorphs, possibly in symbiosis with chemoautotrophic bacteria. Here, we offer a detailed description of exceptionally preserved specimens of *Culmofrons plumosa* from the Discovery UNESCO Global Geopark in Newfoundland, Canada. We suggest that *Culmofrons plumosa* should be reinterpreted as a reclining organism based on taphonomic and morphological evidence. Additionally, reproductive modes and a growth model of the species are here inferred, and they appear to be most consistent with a reclining mode of life, offering a novel palaeobiological reconstruction of the species.

4. Introduction

The Rangeomorpha is an extinct clade (Dececchi et al., 2017) of macro-organisms of debated phylogenetic affinity made up of several orders of self-similar ‘rangeomorph units’ (sensu Narbonne, 2004), which may be: (1) attached to a stem or stolon (e.g., *Culmofrons*, Laflamme et al., 2012; *Pectinifrons*, Bamforth et al., 2008); or (2) arising from other rangeomorph elements (e.g., *Bradgatia*, Brasier et al., 2012); a basal disc may be present (Brasier et al., 2012; Laflamme et al., 2012; Hawco et al., 2020) The clade is named after the genus *Rangea*, first described by Gürich (1929, 1933) in Namibia. Rangeomorphs were later discovered in Charnwood Forest (UK) (Ford, 1958, 1962) and later reported from several localities worldwide, including the famous Mistaken Point Ecological Reserve (MPER), in the Avalon Peninsula in Newfoundland (CA) (Anderson and Misra, 1968; Misra, 1969) and the Catalina Dome in the Discovery UNESCO Global Geopark, in the Bonavista Peninsula (Newfoundland, CA) (O’Brien and King, 2002, 2005; Hofmann et al., 2008). The clade dominates the so-called ‘Avalon biota’ of the Ediacaran (Waggoner, 2003; Boddy et al., 2022). The Rangeomorpha have been divided into: the Rangida, with double-sided first-order branches; and the Charnida, with single-sided first-order branches (Narbonne, 2004; Narbonne et al., 2009). Traditionally the Rangeomorpha have been interpreted as organisms living erect in the water column, filter-feeding or obtaining dissolved organic carbon (DOC) by osmotrophy (Laflamme et al., 2009), with the notable exceptions of the reclining epifaunal taxa *Fractofusus misrai* and *F. andersoni* (Gehling and Narbonne, 2007).

This study focuses on exceptionally preserved specimens of the rangeomorph species *Culmofrons plumosa* from the MUN Surface, Catalina Dome (Liu et al., 2016; **Fig. 2.1**), which has generally been considered to belong to the Charnida (Laflamme et al., 2012). The monospecific genus *Culmofrons* is known only from the Ediacaran of Newfoundland and

consists of a basal disc and stem attached to an oval frond with five or more first-order branches and a zig-zagged midline (Laflamme et al., 2012; **Fig. 2.2 A**). First-order branches of *Culmofrons* are single-sided (sensu Narbonne et al., 2009), and are composed of displayed, sub-parallel second-order branches that in turn have displayed third- and fourth-order branches (Laflamme et al., 2012). The type material comes from the Lower Mistaken Point Surface (LMP) at the MPER but is not as well preserved as specimens from the MUN Surface (Liu et al., 2016a).

In this work, we employ developmental and taxonomic statistical analyses, integrated with a new taphonomic model for the MUN Surface, to describe the palaeobiology, palaeoecology and ontogeny of *Culmofrons plumosa*. Newly discovered impressions beneath exceptionally preserved specimens are also investigated as potential reproductive structures.

5. Geological setting

The Ediacaran successions of the Catalina Dome on the Bonavista Peninsula are correlated on lithostratigraphic grounds with the Conception Group and St. John's Group of the Eastern Avalon Peninsula (O'Brien and King, 2002, 2005; Hofmann et al., 2008) (**Fig. 2.1**).

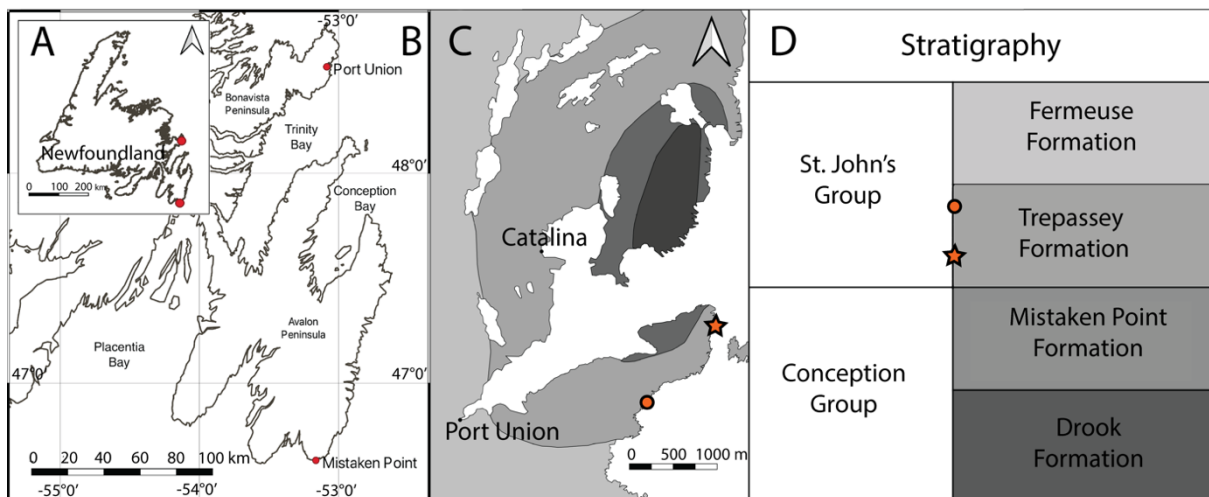


Figure 2.1: map and stratigraphy of the Catalina Dome.

A) Position of MPER and the Catalina Dome in Newfoundland; **B)** map of the Avalon and Bonavista peninsulas; **C)** map of the Catalina Dome showing the MUN Surface locality (star) and the Back Cove locality (circle); **D)** simplified stratigraphy of the Catalina Dome indicating the position of the MUN Surface and the Back Cove.

The holotype and paratypes of *Cu. plumosa* have been described from a fossiliferous surface (LMP) from the Mistaken Point Formation of the St. John's Group in the MPER (Laflamme et al., 2012) (**Fig. 2.2 A**). The specimens described herein, however, are from the MUN Surface, close to the base of the Port Union Member of the Trepassey Formation of the Catalina Dome (**Fig. 2.1**).

Fossils on the MUN Surface are preserved in both negative and positive epirelief (**Fig. 2.3**) atop a siltstone that is overlain by a thin tuffite (Liu et al., 2016a). One additional specimen (NFM F-3972; **Fig. 2.2 B**) from the Back Cove locality in the upper portion of the Port Union Member of the Trepassy Formation in the Catalina Dome was also included in this study. We note that this is a different locality than the Back Cove locality described by Liu et al. (2014), which lies within the Fermeuse Formation.

5. Materials and methods

5.1. Dataset compilation and statistical analyses

Twelve specimens of *Culmofrons* from the Bonavista and Avalon peninsulas (four figured herein), the holotype of *Charnia masoni* from the Charnwood Forest (UK) and the holotype of *Beothukis mistakensis* from the MPER (the only complete specimen of *Beothukis mistakensis* known; McIlroy et al. 2020; 2022) (**Fig. 2.2 C**) have been studied morphometrically. As these taxa are protected and preserved in situ; silicone moulds of the fossils have been used to produce jesmonite replicas for photography under controlled lighting. Both the silicone moulds and the jesmonite casts of the four figured specimens are accessioned at The Rooms Corporation of Newfoundland and Labrador (NFM) (St. John's, NL), under the accession numbers NFM F-3972–3975. Morphometric traits and non-equidistant semi-landmarks outlining the frond outer perimeters were digitized from high quality pictures using imageJ and analysed in R (RStudio v1.2.5019; RStudio Team, 2020). Data are available at Dryad Digital Repository (Pasinetti and McIlroy, 2023).

Relationships between continuous variables were initially explored with regression analyses. A multivariate analysis of principal components (PCA) was run on scaled selected variables and the output was plotted along the major components, using the R packages factoMine v2.4 and FactoMineExtra v1.0.7 (Lê et al., 2008). Equidistant semi landmark coordinates were computed using the package Stereomorph v1.6.4 (Olsen and Westneat, 2015; Olsen, 2017) and Procrustes analyses were run to obtain generalized coordinates. Principal components analyses were run on the coordinate dataset to characterize *Culmofrons* morphospace and were re-plotted in a backtransform morphospace to visually represent shape variations within the taxon (cf. method of Olsen, 2017: fig. 1).

5.2. Retrodeformation

Retrodeformation is typically applied to Ediacaran fossils from the Avalon Assemblage. This technique consists of estimating the degree of metamorphic distortion of the fossiliferous surfaces and subsequently removing the distortion from digital images of the fossils. The degree of distortion is estimated based on direction of cleavage as well as the use of strain ellipses: holdfasts and discs (such as *Aspidella*) are typically assumed to have been originally circular in life, and their observable eccentricity is interpreted as proof of distortion. However, no *Aspidella* are preserved at the LMP locality and on the MUN Surface they are rare and show minimal distortion. Furthermore, there is no direct evidence for *Culmofrons* basal discs having been perfectly circular. As the assumptions necessary for linear models derived from different morphometric traits were largely satisfied, therefore no retrodeformation has been applied to the specimens in this study.

6. Results

6.1. Morphological description of *Culmofrons plumosa*

The type material of *Culmofrons plumosa* is located at LMP locality in the MPER in the southern Avalon Peninsula of Newfoundland (Laflamme et al., 2012). Subsequent discoveries from the Bonavista Peninsula outcrops (here described, some illustrated in **Fig. 2.4**), while initially compared to *Beothukis* (Liu et al., 2016a), were later assigned to *Culmofrons* based on morphometric analysis (Taylor et al., 2019; Hawco et al., 2020; McIlroy et al., 2020).

Culmofrons plumosa typically consists of a sub-elliptical frond that is basally tapered towards a parallel sided, sometimes curved stem that usually ends in a globose structure (sometimes referred as a ‘holdfast’ or ‘basal disc’). Our descriptions follow the descriptive terminology proposed by (Dunn et al., 2021): the terms first-order, second-order, third-order... refer to the hierarchical position of the branch in the fractal organization, while the adjectives primary, secondary, tertiary... refer to the ontogenetical order of branch formation.

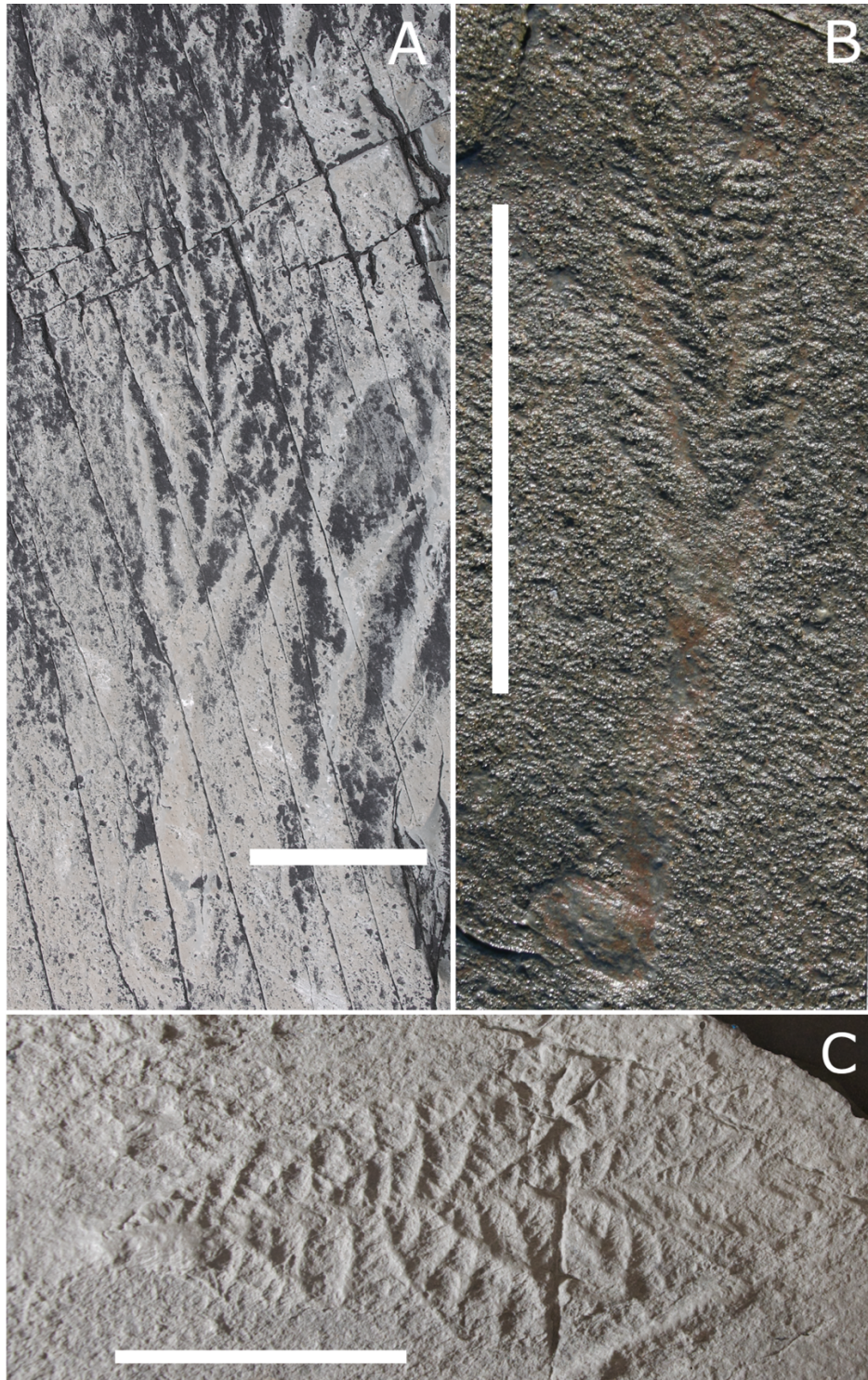


Figure 2.2: *Culmofrons plumosa* and *Beothukis mistakensis*.

A) *Culmofrons plumosa* holotype from Lower Mistaken Point (in situ; plastotype Royal Ontario Museum, Canada: ROM-61522); **B)** *Culmofrons plumosa* from Back Cove, Catalina Dome (NFM F-3972); **C)** *Beothukis mistakensis* holotype from Mistaken Point E Surface (in situ; plastotype: Oxford University Museum, UK: OUMNH A T.410/p). All scale bars represent 5 cm.

The frond is typically preserved as a negative impression here, we describe the branching patterns recorded as impression on the palaeoseafloor, but the three-dimensional body plan of the organism can only be inferred. In the most complete specimens (**Fig. 2.4 B-C**) at least nine first-order branches can be recognized, preserved in negative epirelief, with little to no evidence of branch overlap. The first-order branches are arranged with a glide plane symmetry, with branches alternating between the right ('d', dextral) and left sides ('s', sinistral) of a zig-zagged midline (**Fig. 2.5**). These first-order branches typically share their proximal margins with their respective precedent first-order branch, forming the midline. First-order branches "d1" (the basal-most first-order branch) and s1 are located at the right and left margins of the frond, respectively. First-order branches "d2" and "s2" appear to originate respectively from the basal portion of the first-order branches "s1" and "d2" (**Fig. 2.5 A**).

No clear separation is visible between the impressions of the basal portion of s1 and d1 and the branches that originate from them, suggesting that successive branches were originating in a sympodial fashion (cf. Dunn et al., 2018, 2019). Alternatively, it is possible that first-order branches arise from a central stalk, which could have been above the preservational plane of the fossils. As "s2" inserts immediately after the first second-order branch of "d2" ("d2.1") and shares with it a margin for the length of the first 4 second-order branches ("d2.1"–"d2.4"), "s2" and "d2" show an apparent bilateral symmetry (actually glide-plane symmetry; see **Fig. 2.5 A**), while s1 assumes a more distal position and might lose its connection with "d2" with maturity.

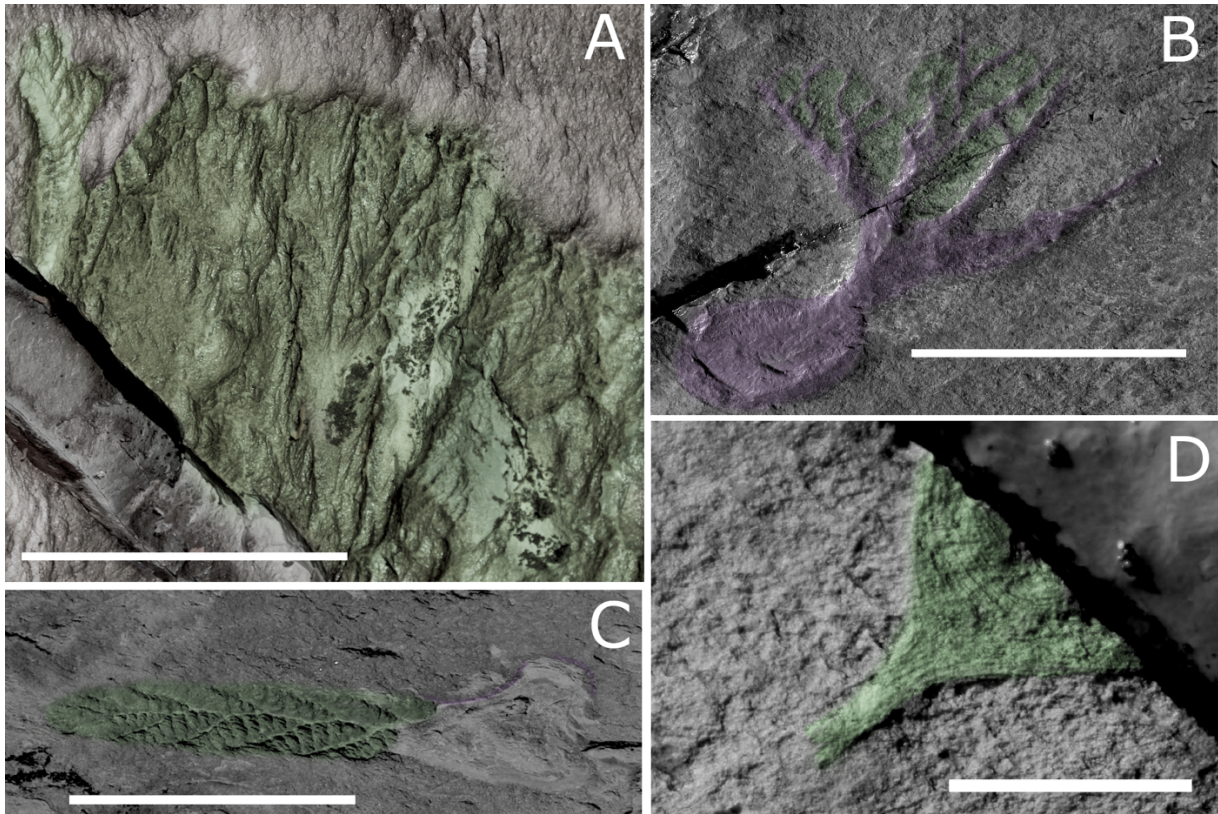


Figure 2.3: different preservation types on the MUN Surface.

Negative epirelief in green, positive epirelief in purple. **A)** *Bradgatia* sp.; **B)** *Primocandelabrum* sp.; **C)** *Charnia* sp.; **D)** *Haootia* sp. Scale bars represent: 5 cm (**A–C**); 1 cm (**D**).

The successive first-order branches (“d3”, “s3”) insert at the proximal margin of the preceding and opposite first-order branch in proximity of, respectively, “s2.7” and “d3.5”, wedging between the two precedent first-order branches and separating them. Branches increase in length towards the base of the frond with the exception of the two basal-most branches (“d1” and “s1”), which are typically slightly shorter than the neighbouring branches. Second-order branches originate from the first-order branches with increasingly more acute angles in the basal-apical direction (cf. branch “s2” in **Fig. 2.5 A**). Second-order branches typically increase in size towards the midpoint of their first-order branch (cf. branches “s2.1”–“s2.10” in **Fig. 2.5 A**). Second-order branches typically have consistent sigmoidal shapes (e.g.,

Fig. 2.4 A–C; 2.5 B) throughout a first-order branch, with little to no evidence of overlapping. The second-order elements of each first-order branch close to the margin are commonly subtriangular (e.g., **Fig. 2.5 A**: “s1.7”, “s2.10”). Most specimens do not preserve second-order branching associated with the basal-most first-order branch on the right-hand side of the fossil (“d1”). Second-order branches of the second first-order right branch (“d2”) may present secondary growth, extending behind the outer margin of the organism and growing above (and leaving an impression on the upper surface of) the most basal first-order branch on the right-hand side (“d1”) (impressions “si” in **Fig. 2.4 B**).

The sigmoidal shape of the second-order branches is dictated by the arrangement of the third-order branches, which are typically arranged in alternating series on the left and right side of the second-order branches (**Fig. 2.5 B**). Proximally the left series is predominant, with the right series presenting increasingly bigger third-order branches distally, resulting in a glide-plane symmetry along the second-order branches axes in the central and distal portion of the second-order branches. The subtriangular apical-most second-order branches present only a radiating left series of third-order branches, with the biggest third-order branches at the centre of the series (e.g., **Fig. 2.5 A**: “s1.7”, “s2.10”).

Fourth-order branching can be observed on both sides of the third-order branches, presenting the typical alternation of left and right series in a glide plane symmetry (**Figs. 2.4; 2.5 B**).

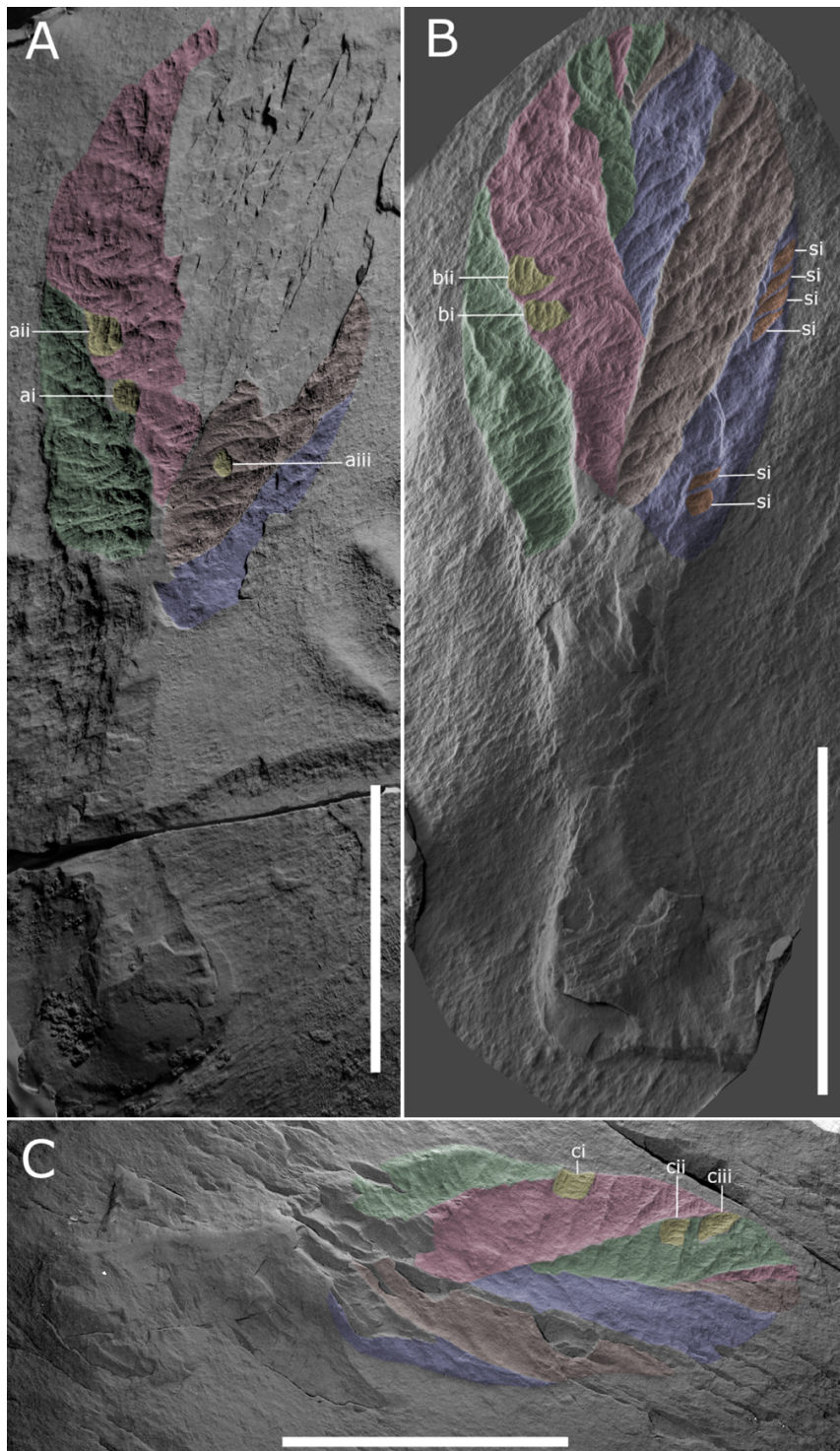


Figure 2.4: *Culmofrons plumosa* specimens from the MUN Surface, Bonavista Peninsula.

Preserved individual first-order branches have been coloured green, pink, blue and brown. Reproductive impressions are coloured in yellow, secondary growth impressions in orange. **A)** NFM F-3973 showing impressions “ai”–“aiii”; **B)** NFM F-3974 showing impressions “bi”–“bii” and secondary growth impressions “si”; **C)** NFM F-3975 showing impressions “ci”–“ciii”. All scale bars represent 5 cm.

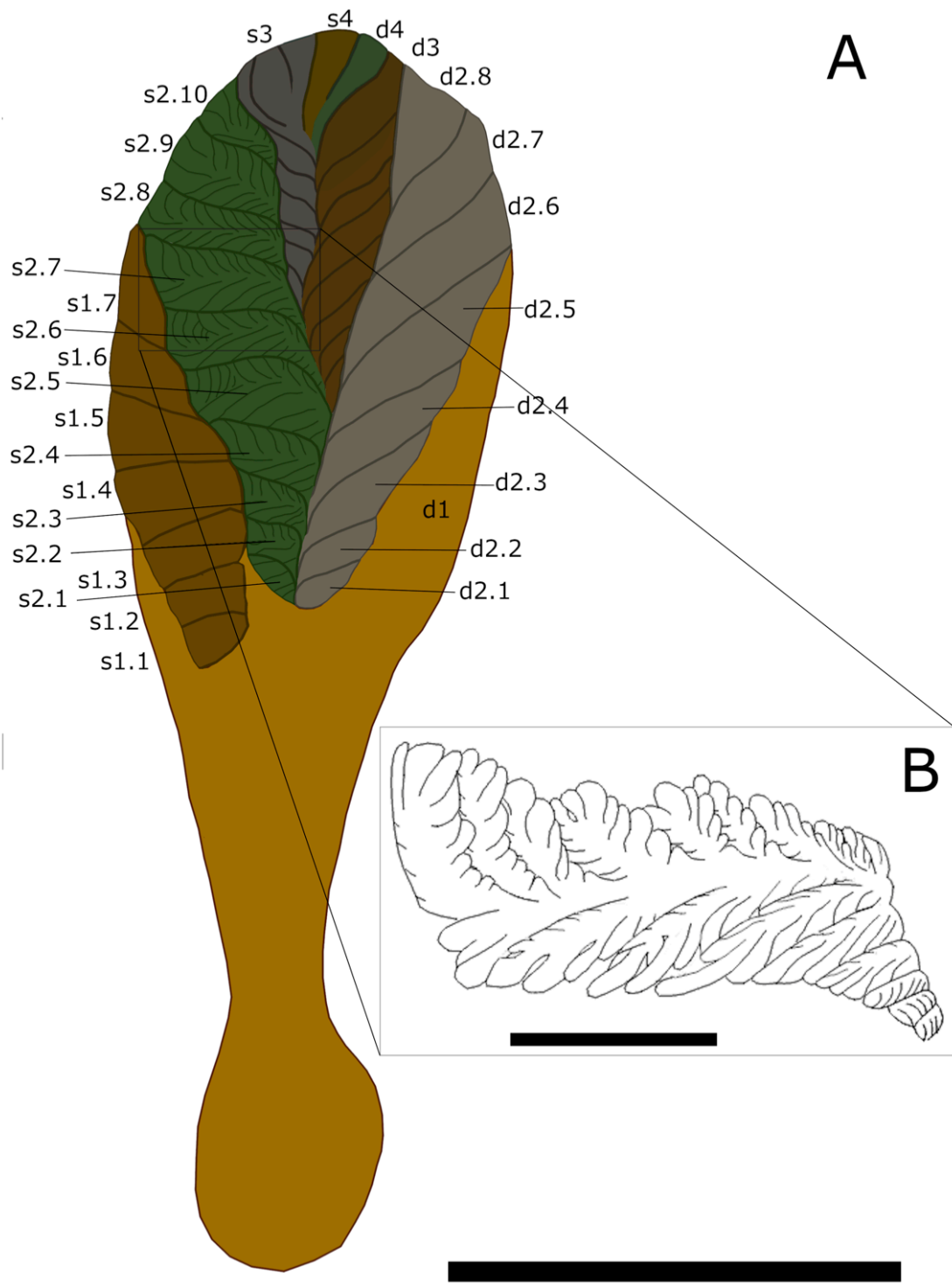


Figure 2.5: *Culmofrons plumosa* reconstruction.

A) interpretative drawing of a complete *Culmofrons plumosa* specimen. First- and second-order branches are labelled; each first-order branch has a different colour; **B)** detail of second-order branch “s2.7”, showing third- and fourth-order branches. Scale bars represent: 5 cm (**A**); 1 cm (**B**).

6.2. Atypical rangeomorph structures

At least six of the best preserved *Culmofrons* (three of which figured herein) possess hitherto undescribed atypical rangeomorph structures below the tips of secondary branches located on first-order branches “s2” and “s3” (**Figs. 2.4; 2.6**). The impressions are all morphologically similar and share a homologous position within the frond (cf. **Fig. 2.4 A–C**), they should thus be interpreted as functional biological structures rather than taphonomic artefacts.

These atypical impressions resemble third-order branches that are rotated towards the tip of the frond and are clustered in a bundle-like arrangement (**Fig. 2.6 C**). Two third-order branches are arranged symmetrically at the centre of the bundle, originating from a common central position (**Fig. 2.6 C**, blue and purple), with supplementary branches overgrowing the central branches on their distal margins (**Fig. 2.6 C**, green). The structures are separated from the rest of the secondary branch via a constriction of the epithelium at the base of the bundle.

Fourth-order branches are recognizable and appear to be rotated towards the centre of the bundles (**Fig. 2.6 C**).

In NFM-F-3973, a third atypical structure can be recognized: impression “aiii” is sub-elliptical and underlies the third-order branches of the second-order branch “d2.4” (**Fig. 2.4 A**). This impression has no recognizable rangeomorph architecture and does not appear to have a developmental relationship with the secondary branch that hosts it, as it is in a central position in the second-order branch “d2.4”, cutting across third-order branches.

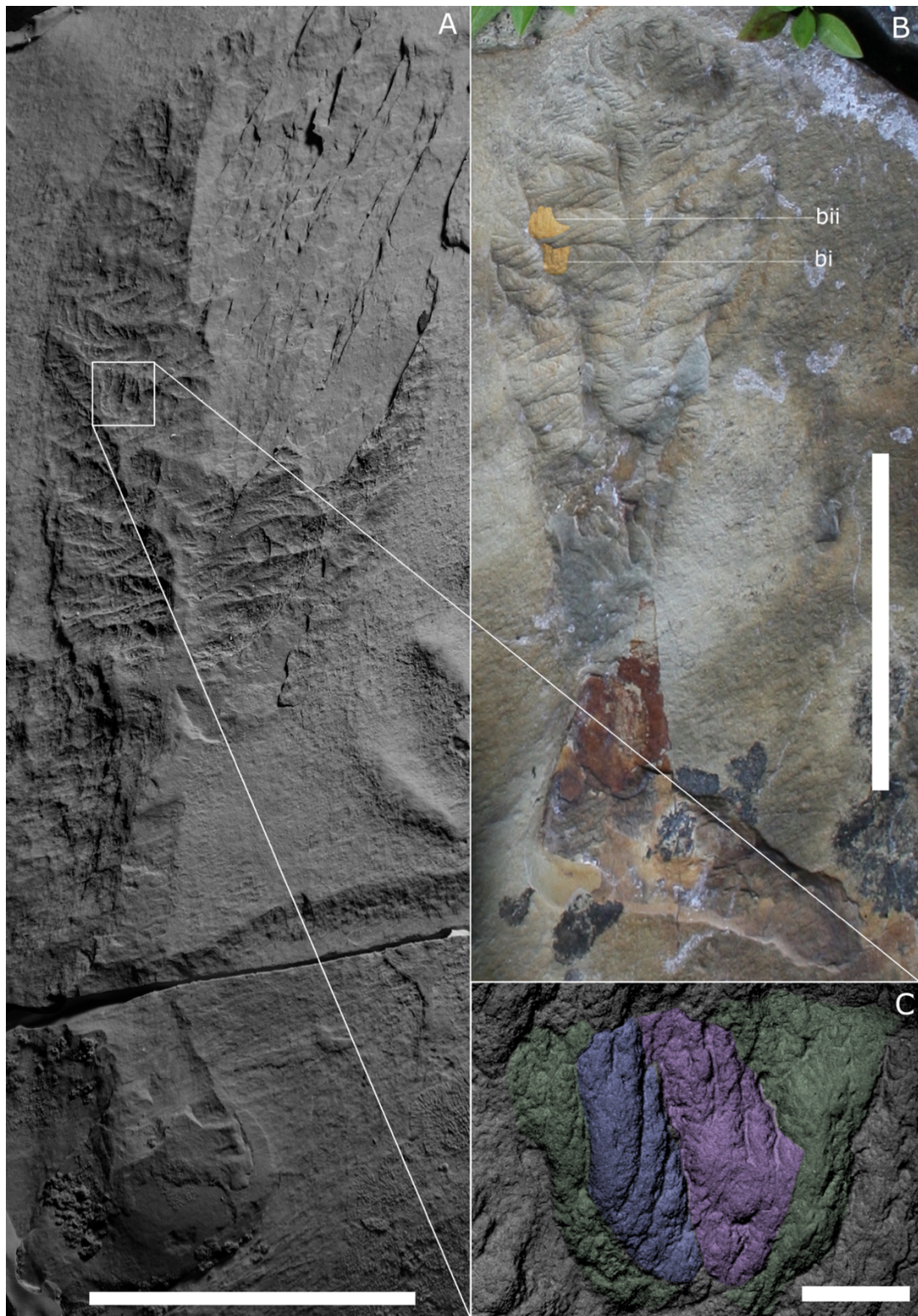


Figure 2.6: putative reproductive structures.

A) position of impression “aai” in NFM F-3973; **B)** position of impressions “bi” and “bii” in MUN2 (in situ; NFM F-3974); **C)** detail of impression “aai”. Different third-order branches are coloured in green, purple and blue. Scale bars represent: 5 cm (**A-B**); 1 cm (**C**).

6.3. Morphometric analysis

6.3.1. Linear models

Explorative linear regressions were performed between selected variables: total length against maximum frond lengths (**Fig. 2.7 A**) and total lengths against maximum frond widths (**Fig. 2.7 B**). Additionally, maximum stem lengths (**Fig. 2.7 C**) were tested against the total length of the specimens, then maximum frond lengths and frond widths were tested against each other (**Fig. 2.7 D**). Morphometric data from the holotype of *Beothukis* were also plotted for comparison (given earlier debate about whether *Beothukis* and *Culmofrons* are congeneric; Brasier et al., 2012; Laflamme et al., 2012; Liu et al., 2016a; Hawco et al., 2020), but not included in the regressions (**Fig. 2.7**). Assumptions of linear relationship, independence, homoscedasticity and normality were satisfied for each of the linear models applied to continuous variables. However, introducing *Beothukis* to the dataset creates an outlier with high leverage: the linear regressions figured were therefore only applied to *Culmofrons* specimens. Higher R² values were recorded in all cases when the regressions did not include *Beothukis mistakensis*. Positive relationships can be observed in each of the computed regressions, suggesting an allometric growth model (all p-values $\ll 0.05$). Lower positive relationships and lower R² values are obtained when comparing widths of the specimens with total lengths (**Fig. 2.7 B**), suggesting either faster growth rates in a basal-apical direction (in the stem and the frond length; **Fig. 2.7 A, C**) than laterally (frond width; **Fig. 2.7 B, D**) or a higher variability in frond length compared to frond width.

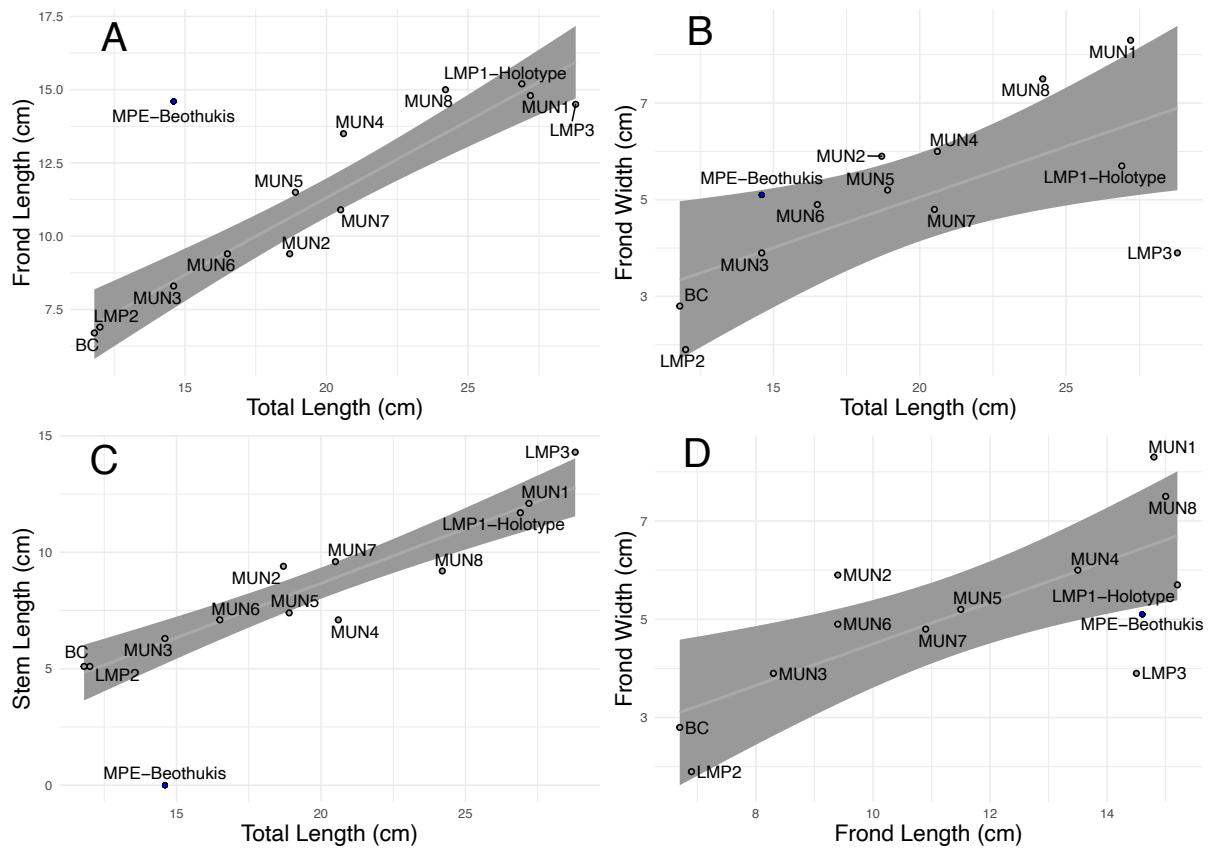


Figure 2.7: linear regressions between variable pairs.

A) Total length of the specimens and length of the fronds ($y = 0.52589x + 0.79318$, $R^2 = 0.9059$; $p = 1.887$); **B)** total length of the specimens and width of the fronds ($y = 0.20937x + 0.86703$; $p = 0.01745$); **C)** total length of the specimens and length of the stems ($y = 0.46796x - 0.68655$, $R^2 = 0.8826$; $p = 5.768$); **D)** length of the fronds and width of the fronds ($y = 0.4228x + 0.2717$, $R^2 = 0.5564$; $p = 0.005341$). **A–D):** morphometric data for the holotype of *Beothukis* (not included in the regression) is indicated with a blue data point; casts of MUN1–3 accessioned as NFM F-3973–5 respectively.

6.3.2. PCA

Multidimensional analysis of principal components allows for reduction of the dimensionality of a dataset comprising several continuous variables by linearly combine them into a new set of variables, called principal components (PCs).

PCA was compiled using the seven following continuous variables, chosen using the Kaiser–Meyer–Olkin test for sampling adequacy (Kaiser, 1970): specimen total length, frond length, frond width, stem length, stem width, discs diameter, and length of the first left and first right first-order branches. For this study, only continuous variables consistently measurable in all the studied specimens were used, as consideration of categorical variables, such as descriptors typically used to describe rangeomorphs (e.g., furled/unfurled, rotated/unrotated; Brasier and Antcliffe, 2009; Brasier et al., 2012), involves more subjective biological and taphonomic inferences, and might therefore be independent of taxonomy. Characters relating to branch organization (e.g., number of second-order branches) are not uniformly preserved across all the specimens, particularly second-order and higher order branches and therefore only well-preserved specimens (12 *Culmofrons plumosa* specimens and the holotypes of *Beothukis mistakensis* and *Charnia masoni*) were included in the analyses. Continuous variables were scaled to have a mean of 0 and standard deviation of 1.

Visual analysis of the scree plot of the eigenvalues of the principal components suggests that the first 3 PCs should be retained, as they explain 93.4% of the total variance (Dim-1: 63.9%; Dim-2: 20.1%; Dim-3: 9.4%; **Fig. 2.8 A**). The major contributions to the first 3 PCs come, respectively, from the original variables: length of the first left first-order branch (Contribution to Dim-1: 18.0%, Fig. 8B), frond length (Contribution to Dim-2: 57.2%; **Fig. 2.8 C**) and frond width (Contribution to Dim-3: 43.7%; **Fig. 2.8 D**).

In both graphs, showing the ordination of the specimens in Dim-1 and Dim-2 (**Fig. 2.9 A**) and Dim-2 and Dim-3 (**Fig. 2.9 B**), *Culmofrons plumosa* specimen from the MUN Surface appear to be grouped together while the LMP and the Back Cove specimens lie at the margins.

The holotypes of *Beothukis mistakensis* and *Charnia masoni* consistently plot far from *Culmofrons* specimens in the ordinations for Dimensions 1 and 2, and 2 and 3 (**Fig. 2.9 A-B**).

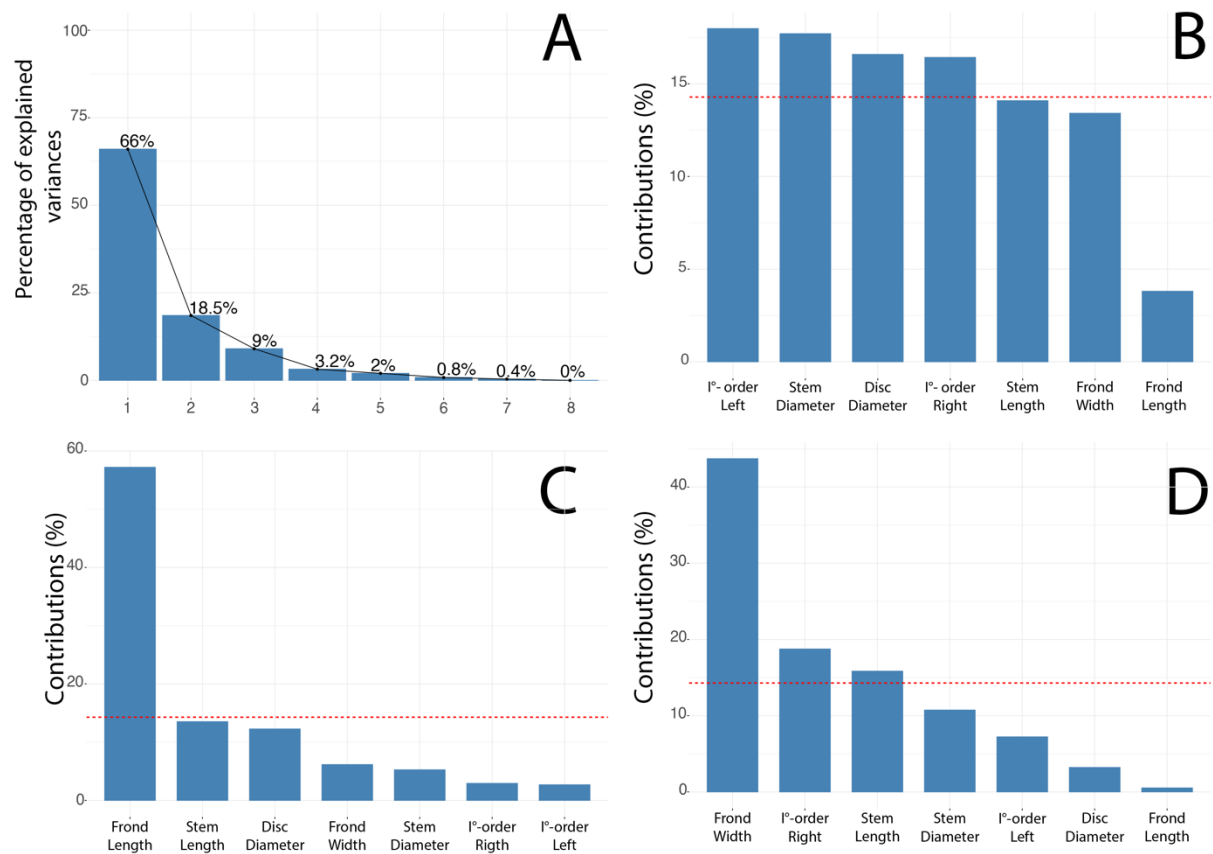


Figure 2.8: PCA scree plots.

A) Scree plot of the percentage of variation described by each computed principal component; **B–D)** contributions of variables to: **B,** Dim-1; **C,** Dim-2; **D,** Dim-3.

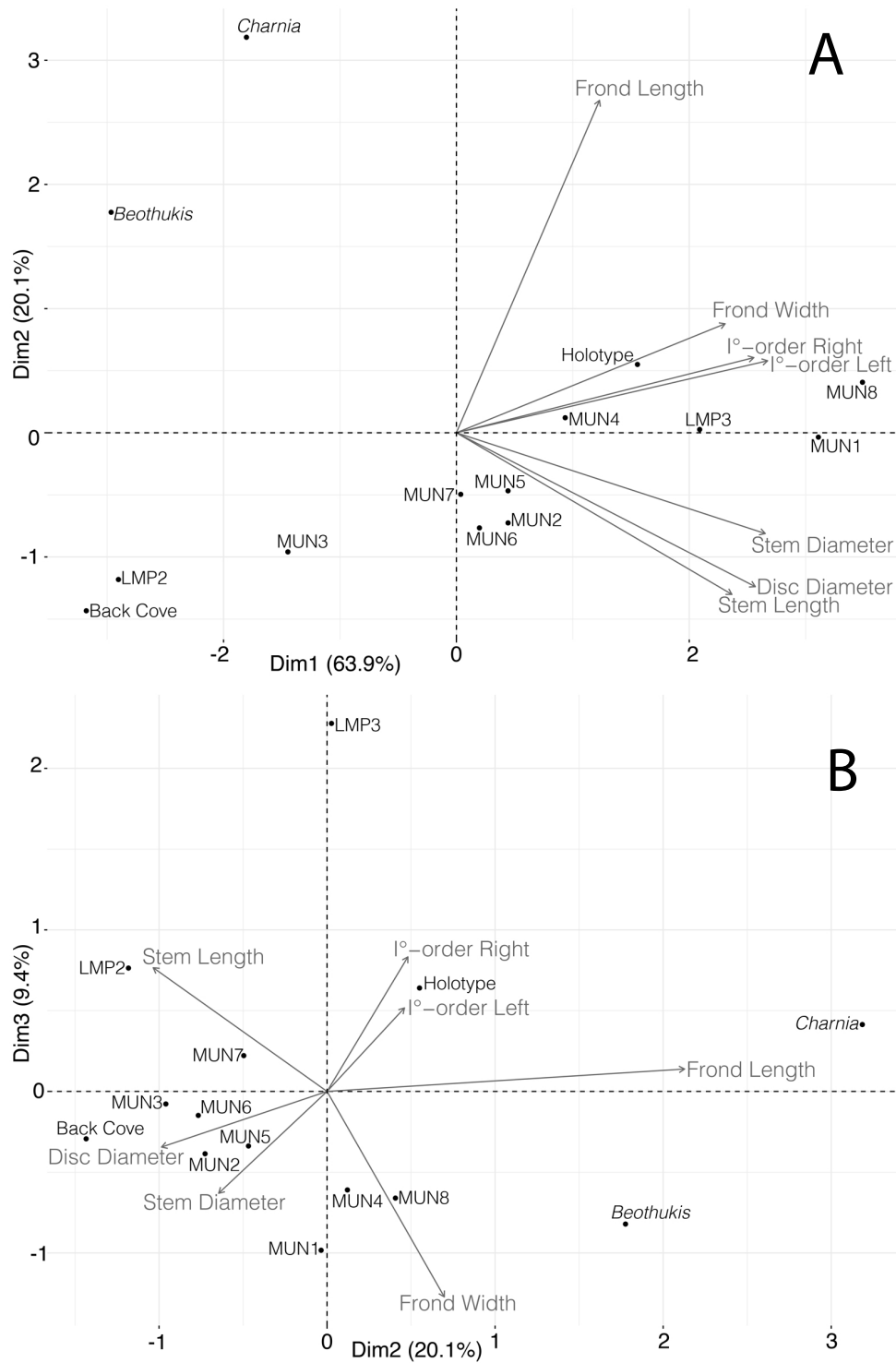


Figure 2.9: PCA ordinations.

A) Biplot showing ordination of the individuals along Dim-1 and Dim-2, and the directions of the variables; **B)** biplot showing ordination of the individuals along Dim-2 and Dim-3, and the directions of the variables. On both plots, the length of each arrow is proportional to the contribution to that PC. Casts of MUN1–3 accessioned as NFM F-3973–5 respectively.

6.3.3. *Backtransform morphospace analyses*

To overcome the limitations of traditional PCA, we propose the use of Generalized Procrustes Analysis (GPA) to create a backtransform morphospace graph within which different specimen shapes can be plotted. A backtransform morphospace graph allows visualization of theoretical shape variability within a group of biological entities. In this study, Procrustes coordinates were obtained performing a GPA on a dataset of *Culmofrons* (traced from digital images) and transformed in a series of equidistant semi-landmarks. This approach (first used in Ediacaran taxonomy by Laflamme et al. (2007) to characterize *Charnia* species from Newfoundland) can be used to perform an ordination of the specimens based on similarity of their shapes scaled to the same centroid size, plotting them against a backtransform graph and disregarding variance due to specimen size, orientation and position.

When GPA is performed on the *Culmofrons* dataset it shows that two components explain 94% of the observed variation in *Culmofrons* shape (PC1: 87%, PC2: 7%; **Fig. 2.10**). The biggest variation can be observed between the MUN Surface specimens, while the holotype and other material from the LMP Surface plot within the morphospace occupied by the MUN Surface specimens (**Fig. 2.10**).

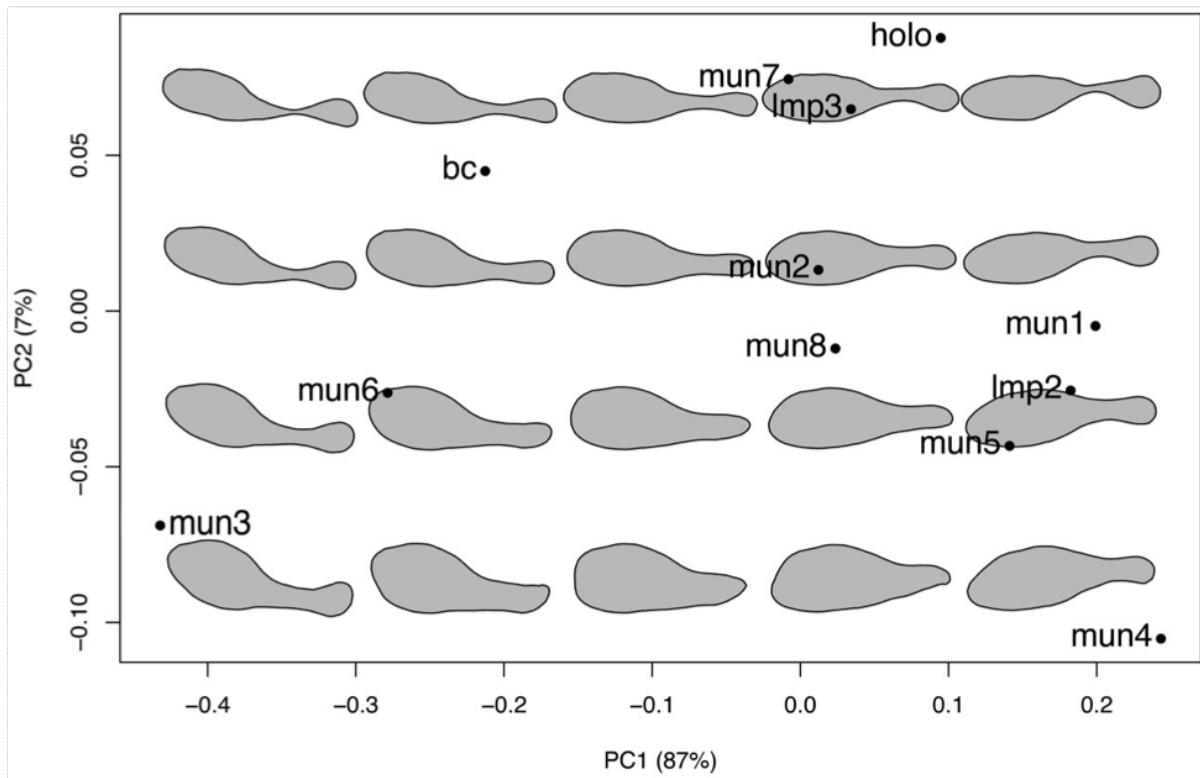


Figure 2.10: backtransform projection of the measured morphospace of *Culmofrons plumosa*.

Specimens are ordinated according to PC1 and PC2, obtained with a GPA. Casts of mun1–3 accessioned as NFM F-3973–5 respectively.

6.4. Taphonomy of the Ediacaran biota of Avalonia

Ediacaran fossils of the Avalonian assemblage have been traditionally interpreted as the result of mouldic preservation of body impressions of the organisms between the seafloor and the smothering sediments ('death mask' model), in what is known as 'Conception-style' preservation (Gehling, 1999; Narbonne, 2005). This preservation style is the norm in the siliciclastic successions of Avalonia (cf. Liu, 2016). To explain the differential preservations as positive (typically stems and basal discs) and negative (fronds) epireliefs often observed in a single specimen, Gehling (1999) initially proposed that some tissues remained intact until early lithification of the overlying ash cast them in positive epirelief. Delicate tissues, prone to faster decomposition, would only leave an impression by smothering the underlying microbial mat (producing negative epireliefs), as the three-dimensional form would decay before the lithification of the ash (Gehling, 1999). Sturdier elements, such as stems, would take more time to decay, allowing the sediments above them to lithify and preserving their external mould. The poorly lithified sediments and the microbial mat underlying the stems of the organisms would have been pushed in the overlying mould after the stem decayed, preserving the mould as a positive epirelief. Authigenic mineralization of a microbial matgrounds growing above dead organisms may have played a crucial role in the death mask preservation of the fossil (Laflamme et al., 2011; Tarhan et al., 2016). The experimental work of Darroch et al. (2012) and Slagter et al. (2022) further highlighted the importance of a microbial mat in the early formation of microbial death masks over decaying soft tissues, having implications concerning fidelity of preservation of the impressions.

The presence of framboidal pyrite associated with Ediacaran fossils from Newfoundland (Liu, 2016) supports the concept that microbial mats could enhance pyritization in a modified death mask model (see Gehling, 1999; Mapstone and McIlroy, 2006). Reduced

sulfur for pyritization of the death mask was likely to have been supplied by chemoautotrophic bacteria living in microbial mats, consistent with the $\delta^{34}\text{S}$ fractionation in pyrite reported by Wacey et al. (2015) from the Fermeuse Formation of the Bonavista Peninsula.

6.5. *Culmofrons* preservation on the MUN Surface

The MUN Surface outcrops in the Trepassey Formation of the Catalina Dome, in an interval dominated by medium to thick bedded sandstones interpreted as turbidites (Liu, 2016; Liu et al., 2016). *Culmofrons* fronds are preserved as impressions on a fine, beige to brown and lustrous mineralized veneer ('3' in **Fig. 2.11 A**), rich in iron oxides. The veneer covers a thin (c. 1 cm) hemipelagite ('2' in **Fig. 2.11 A**), which caps a c. 13 cm thick bed of normally graded siltstone ('1' in **Fig. 2.11 A**) (Liu et al., 2016a). The mineralized veneer is immediately overlain by a normally graded, 6 mm thick, fine-tuff ('4' in **Fig. 2.11 A**) followed by a succession of thickly bedded coarse-grained cross-bedded sandstones.

We interpret that the ferruginous veneer represents the redox boundary separating oxic and anoxic conditions in the seafloor at the time of burial. The position of the redox boundary is controlled by microbial activity and could be found within a microbial matground or at the interface between the matground and the water column.

If it is accepted that the ferruginous veneer reflects the original presence and position of microbial mats/death masks ('2' in **Fig. 2.11 B**), this has potential implications for the taphonomy of *Culmofrons* on the MUN Surface. Akin to the Gehling's death mask model (Gehling, 1999), it is likely that the frondose parts of the organisms decayed early after being buried by the ash (**Fig. 2.11 C**), leaving an impression on the microbial matground, being quickly cast by the lithifying tuff/tuffite (see Matthews et al., 2020). The fine detail in the frondose portions of the organisms suggests that the organisms spent a considerable amount of time in contact with the microbial matground, allowing a deep impression of the fronds to form in the matground (cf. *Fractofusus*, *Beothukis* and *Charnia*).

It is unlikely that the veneer was precipitated on the top of the *Culmofrons* fronds: if that was the case, we would have to assume that there was a period of time during which the

buried frond decomposed, leaving an impression on the underlying silt, which would have been later transferred to the veneer. This would imply a collapse of the veneer into the impressions left on the siltstone and a subsequent loss of resolution. Moreover, we hypothesize that *Culmofrons*, a multicellular opisthokont, probably of metazoan grade, would not have been able to survive entirely below the redox layer, but was more likely to have lived at the interface, with the upper portion of the frond exposed to oxic waters.

Since the ferruginous veneer covers positive features of fossils, such as *Culmofrons* stems on the MUN surface (cf. **Fig. 2.11 B**), and those features are often preserved in great detail, without any evidence for mat tearing or displacement, it is possible that it reflects matground growth over the tissue of the stem during the life of the organism, rather than having been displaced after the decay of the stem as the Gehling (1999) model suggests. Notably, the arboreomorph *Charniodiscus procerus* is also inferred to have lived with the stem buried underneath the matground, sometimes even with *Fractofusus* specimens growing on top of the stem (Pérez-Pinedo et al., 2022). The resulting fossil (**Fig. 2.11 D**), a combination of negative impressions and positive epireliefs, is likely to be the result of the preservation of an organism living partially buried under the matground (stem portion) and partially above it, smothering the matground and exchanging oxygen and nutrients with the water column above and porewater system below (frondose portion). This is consistent with the presence of abundant preserved filaments on the surface (Liu and Dunn, 2020), which are preserved as positive epireliefs on the veneer, but are interrupted where fossil impressions are present. It is therefore unlikely that the fronds fell above the filaments, which would have been otherwise preserved in positive epirelief under Gehling's model, but rather pre-existing fronds would have prevented the filaments from being in contact with the matground, precluding their preservation.

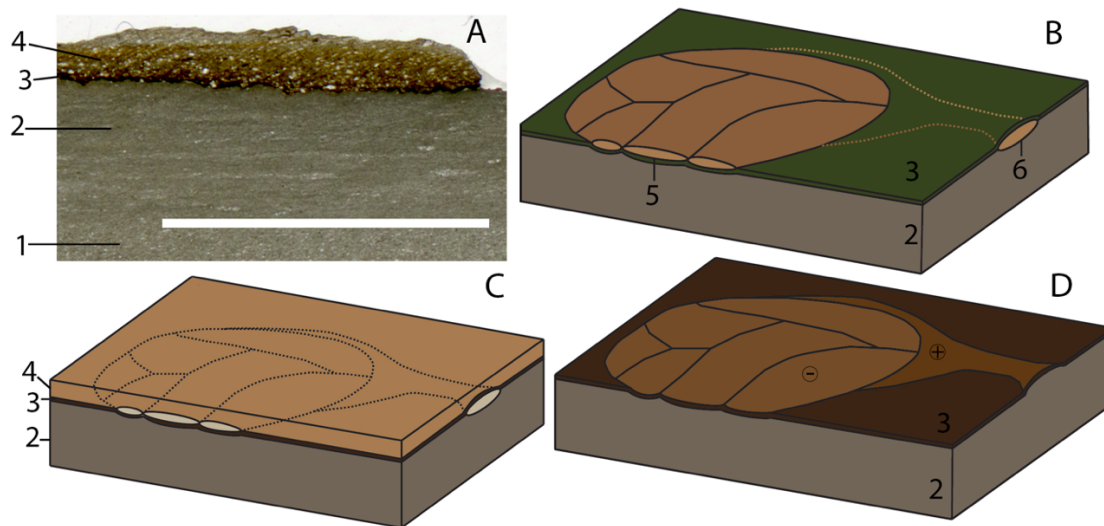


Figure 2.11: taphonomic model.

A) Thin section of the MUN surface; **B)** *Culmofrons plumosa* in life, with the frond (5) reclining of top of the microbial matground and the stem (6) underneath the matground; **C)** *Cu. plumosa* buried underneath ash that would eventually turn into tuff (4); **D)** *Cu. plumosa* preserved as a negative impression (-) and positive epirelief (+) on a mineralized veneer (3). Numbered features: 1, siltstone; 2, hemipelagite; 3, mineralized veneer; 4, normally graded tuff; 5, frond; 6, stem. Scale bar in A represents 1 cm.

7. Discussion

7.1. *Culmofrons* systematics

PCA consistently groups together *Culmofrons* specimens from the MUN Surface, leaving specimens from LMP and Back Cove consistently at the margins of the ordination (**Fig. 2.9**). However, the result of the GPA (shape analysis, **Fig. 2.10**) suggests that all of the *Culmofrons* specimens studied occupy a very similar morphospace and have a similar broad frond profile. We suggest that all the studied specimens could therefore be classified within the same species and the observed variation can be partially explained by ontogeny. As the holotype plots well within the species morphospace yet presents a much greater size than the rest of the specimens, we interpret it to be a super-mature specimen. We hypothesize that the MUN Surface population represented a group of organisms of a similar age class, due to their low size variability, as shown by the PCA ordinations (**Fig. 2.9**).

We note that the absence of proper outgroups and the small size of the database preclude accurate multidimensional analyses, and result in different clustering possibilities for the specimens assigned to *Culmofrons*. Bigger datasets of well-preserved material will be necessary to properly address systematics within the Charnida.

PCA shows that *Beothukis mistakensis* and *Culmofrons plumosa* consistently plot away from each other. Including the holotype of *Charnia masoni* in the PCA ordinations results in *Ch. masoni* plotting even further away from both *Cu. plumosa* and *B. mistakensis*. It is also important to note other major differences between the two Newfoundland species and *Charnia*, such as presence of rotated second-order branches and absence of fourth-order branches in the latter, are not recorded in the ordination.

Even though it is not possible to draw taxonomic conclusions based on a small number of specimens, our results suggest that *B. mistakensis* and *Cu. plumosa* might represent, together

with other yet undescribed stemmed rangeomorphs from the Bonavista Peninsula, a monophyletic group within Charnida.

In our view, this result suggests that the traditional classification of *Cu. plumosa* (Laflamme et al., 2012) and *B. mistakensis* (Narbonne et al., 2009) as belonging the rangeomorph clade Charnida might need review and the possibility of erecting a new rangeomorph clade should be investigated, whilst highlighting the necessity of a taxonomic revision of the major rangeomorph groups.

Contributions to the PCs from variables related to the stems and discs (which are absent in *Charnia* and *Beothukis*) (**Fig. 2.8**) are important but limited. Excluding the variables related to stem and disc (stem length, stem diameter and disc diameter) (not figured) still results in *Charnia* and *Beothukis* plotting outside the *Culmofrons* space, which suggests that the three taxa differ substantially in frond Bauplan.

7.2. Palaeobiology

7.2.1. *Reclining lifestyle*

The Rangeomorpha and the coeval (possibly related) clade Arboreomorpha have been historically interpreted as living erect in the water column and obtaining organic carbon via filter-feeding on particulate organic carbon (POC) or osmotrophically absorbing DOC (Narbonne, 2004; Laflamme and Narbonne, 2008; Laflamme et al., 2009).

This notion had been implied in the reconstruction of the Ediacaran ecosystems and is a precept that underpins ecological and tiering models proposed for the biota (Clapham and Narbonne, 2002; Darroch et al., 2013; Mitchell and Kenchington, 2018). However, based on a lack of direct evidence for rangeomorphs having lived erect in the water column, it is necessary to assume the null hypothesis that they lived in the orientation that we see them preserved for at least part of their life cycle (i.e. reclining on the seafloor; McIlroy et al., 2021). It has also been suggested (Dufour and McIlroy, 2017; McIlroy et al., 2021) that ecto- or endo-symbiotic relationships with chemosynthetic bacteria would have provided the rangeomorphs with a more reliable source of organic carbon than filter-feeding or osmotrophy, questioning whether osmotrophy is a realistic exclusive feeding strategy for large organisms living in seawater (Liu et al., 2015; Butterfield, 2020). McIlroy et al. (2021) further noted that the surface area analogue microbial osmotrophs in Laflamme et al. (2009) are either intestinal parasites of vertebrates or have symbionts (McIlroy et al. 2021).

It has recently been proposed that a sessile, reclining or recumbent, epibenthic lifestyle may have characterized some rangeomorphs (e.g., *Beothukis mistakensis*, McIlroy et al. 2020, 2022; *Hapsidophyllas flexibilis*, Taylor et al. 2021; *Bradgatia linfordensis*, *Fractofusus misrai*, *Pectinifrons abyssalis*, Pérez-Pinedo et al., 2023) and non-rangeomorph taxa including both incertae sedis (e.g., *Gigarimaneta samsoni*; Taylor et al., 2021) and members of the

Arboreomorpha (e.g., *Charniodiscus* spp.; see Pérez-Pinedo et al. 2022). In particular, *Charniodiscus procerus*, an Arboreomorph from MPER which has both positive (stem and holdfast) and negative (frond) epirelief preservation, has been shown to have lived recumbent on the seafloor, with the stem covered by the microbial matground and the frond exposed to the water column (Pérez-Pinedo et al., 2022).

Here, we also propose a reclining lifestyle for the rangeomorph *Culmofrons plumosa*. This can be inferred from the taphonomy of the MUN Surface: as the mineralized veneer is uninterrupted in preserving negative impressions as well as coating positive epirelief features, a certain amount of time would have been required for the microbial growth to colonize the top of positively preserved structures. Laflamme et al. (2011) suggested that organisms can be preserved as positive epireliefs if they were already felled on the seafloor before burial if the overlying layer lithified before the decomposition of the stem. This is also the first step towards the formation of diffuse ivesheadiomorphs (Liu et al., 2011). The classic death mask model (Gehling, 1999) does not fully account for preservation of taxa by a single mineralized veneer that both drapes the stem and underlies the frond as it does in *Culmofrons* from the MUN surface.

Structures observed in positive epirelief typically include the most basal dextral first-order branch of each specimen, which usually does not show evidence of second or higher order branching (**Fig. 2.5**). Since evidence of well-preserved secondary growth from more apical first-order branches can be observed as a negative impression atop the positively preserved basal dextral branches (“si” in **Fig. 2.4B**), it can be inferred that the organisms were still alive when the positively preserved structures were covered by microbial growth (preserves as the ferruginous veneer) and before secondary growth occurred.

The specimens described herein are considered to be thin-bodied reclining organisms with branches at a level slightly below the seafloor, or possibly even living partially buried in

the sediment with furred tips of the branches partially extending into the water column. It is possible that first formed parts of the organism, such as basal discs and stems may have been covered by a microbial mat for much of lifespan of the *Culmofrons* organism.

7.2.2. *Development and growth*

A well supported rangeomorph growth model for *Charnia masoni*, the type species of the Charnida, has been recently proposed (Dunn et al., 2019, 2021). That research suggests that *Charnia* grew by apical addition of first-order sigmoid-shaped branches that are arranged with a glide-plane symmetry, expanding by inflation after the specimen had reached a certain number of branches (see fig. 4 in Dunn et al., 2021). The frond of *Charnia* can thus be interpreted as a series of first-order branches that successively originated from the tip of an axial branch.

First-order branches in *Charnia* typically have the same number of second-order branches, suggesting that they originated early in the growth of new first-order branches and then became larger through ontogeny by a process of inflationary growth (Dunn et al., 2021).

While homologies and phylogenetic relationships between *Charnia* and *Culmofrons* are yet unclear, a similar growth program can be inferred for *Culmofrons*. First-order branches in *Culmofrons* all have similar numbers of second-order branches (10–12) (**Fig. 2.12 B**) but, unlike *Charnia* (Dunn et al., 2021), these second-order branches reach a maximum size near the midpoint of the first-order branches (**Fig. 2.5**). This suggests that second-order branches were added early during the ontogeny and consequently inflationary growth occurred progressively.

However, the most basal (i.e., oldest) first-order branches on both sides of the axis (“d1” and “s1”) are usually slightly smaller than the younger first-order branches (**Fig. 2.12 A**), suggesting an allometric development with increased inflationary growth of the second-order branches at the midpoint along the length of the first-order branches, perhaps once the specimens reach maturity. The most basal first-order branches are consistently on the right side of the specimens (in *Ch. masoni* we note that it is most commonly the left side); they do not

demonstrate higher order rangeomorph branching and they can be overlain by secondary growth structures originating from the adjacent (more apical) branch (**Fig. 2.4 B**). It is therefore possible that the oldest first-order branches of *Culmofrons* were eventually subject to die-off during the life of the organisms and offered a substrate for secondary growth, with potential reabsorption of the disused structures. Alternatively, the basal-most non-rangeomorph branches might represent a support structure or the remainder of a generative region involved in the organism development. The consistency of the first branch being on the dextral side of *Culmofrons* in all of the analysed specimens (and the sinistral side of *Charnia*) supports a reclining mode of life for both taxa (if they were erect taxa that fell to the substrate upon death/burial it seems unlikely that they would always fall the same way up; see McIlroy et al., 2021).

Dunn et al. (2021) found evidence of interconnection between each first-order branch and the branch in an opposite and immediately more basal position. The two most basal first-order branches in *Culmofrons* are separated by the stem and are thus separate from one another (at least at the surface of the organism- they may have been connected within the stem), however, all successive first-order branches appear to be connected at their basal regions with the immediately opposing branch (e.g., **Fig. 2.5**, branches “d1” and “s1”). This suggests that, like *Charnia*, first-order branches in *Culmofrons* originate in succession from a basal and proximal portion of their respectively opposite and immediately more basal first-order branch. This is coincident with the first and second second-order branches, separating and moving distally after the fifth or sixth second-order branches as younger first-order branches develop, inflate and occupy the space between them (e.g., **Fig. 2.6**, “d3” inserting between “s2” and “d2” in proximity of “s2.6”). First-order branches are therefore likely to have originated from a specific ‘generative’ area at the distal apex of the frond, located between the two youngest first-order branches of each specimen.

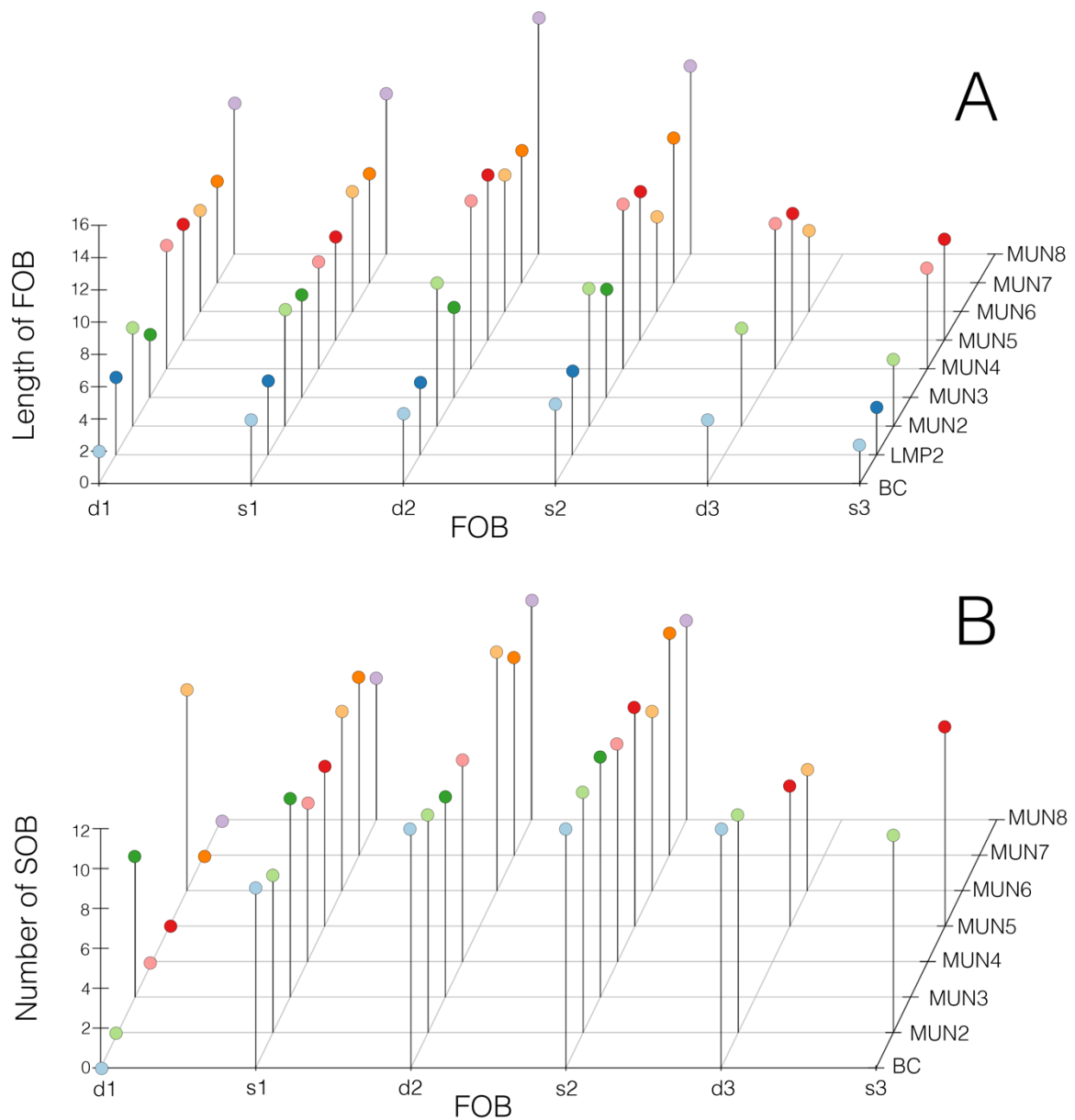


Figure 2.12: development and growth of *Culmofrons*.

A) Lengths (cm) of first-order branches (FOB) according to their ontogenetical position (d1: oldest – s3: youngest) for each specimen. **B)** number of second-order branches (SOB) for each first-order branch according to their ontogenetical position (d1: oldest – s3: youngest) for each specimen. Note that, on both plots, some values are missing as the branches are not preserved in the fossils; d1 typically does not preserve second-order branches. Casts of MUN2–3 accessioned as NFM F-3974–5 respectively.

It is also possible that second-order branches within each first-order branch originated from the apical portion of the respective first-order branches, but due to the preservation of rangeomorph branching as negative impressions, it is not possible to determine three-dimensional morphology to assess interconnectivity between adjacent second-order branches. Second-order branches develop allometrically, with the basal-most second-order branches being smallest, and inflationary growth being most developed in the medial positions along the first-order branch.

Additionally, second-order branches may be triangular rather than sigmoidal, particularly towards the frond margin where the second-order branch morphology appears to be modified to fill any space between adjacent first-order branches.

We suggest here that the position of *Culmofrons* and *Beothukis* within Charnida should be reviewed in future works, as it is difficult to assess branching homologies between the two genera and the type species of the family, *Charnia masoni*. Additionally, secondary growth of the second-order branches can be recognized in some *Culmofrons* specimens (**Fig. 2.4 B**), suggesting that *Culmofrons* was more morphologically variable (similarly to the Rangida *Bradgatia linfordensis*) than even the very large super-mature *Charnia masoni* (“*grandis* type”) in which morphology is strongly conserved throughout growth with no evidence of secondary growth (Dunn et al., 2021).

7.2.3. *Reproduction in Rangeomorpha and reproductive structures in Cu. Plumosa*

The reproductive strategies of the Rangeomorpha are not entirely understood and a consensus has not been reached on the prevalent reproductive strategies adopted within the clade, in part due to the scarcity of fossil evidence of the earliest life stages of the group (Liu et al., 2013). It has been suggested that the Rangeomorpha reproduced seasonally and sexually, based on the size-frequency distributions of specimens of the reclining rangeomorph *Fractofusus misrai* on the D and E surfaces at MPER (Darroch et al., 2013). Based on spatial analyses of the D, E and LMP surfaces at MPER, Mitchell and Kenchington (2018) suggested that efficiency of dispersal of propagules was the main driver in the evolution of Ediacaran ecosystems of stemmed taxa, rather than competition for resources in a tiering model, as previously proposed by Clapham and Narbonne (2002). It has also been hypothesized, based on analysis of spatial distributions, that at least one taxon (*Fractofusus andersoni*) reproduced asexually via stolons, resulting in aggregation of smaller specimens around the parent organism, which may have had a secondary dispersal stage (Mitchell et al., 2015). Liu and Dunn (2020) observed filaments interconnecting different specimens, suggesting that those structures could have been involved in stoloniferous reproduction. However, filaments can sometimes connect specimens of seemingly similar age classes or specimens belonging to different species (Liu and Dunn, 2020), which weakens this hypothesis. The resulting corpus of literature proposes several different possible reproductive strategies, both sexual and asexual, many of which are based on mathematical models, while direct fossil evidence for reproductive strategies remains scarce.

Aberrant structures in the multifoliate rangeomorph *Hylaecullulus fordi* from Charnwood Forest (UK) are interpreted as over-compensatory damage response (Kenchington et al., 2018). Those structures are preserved on the same plane as the rest of the organism, in

continuity with the normal branches and displacing neighbouring branches, suggesting contemporaneity. The structures in *H. fordi* appear to be reverting to lower order branches, demonstrating the truly modular nature of the Rangeomorpha and the ability of individual functional modules to grow independently. In contrast, at least six *Culmofrons* specimens from the MUN Surface, three of which (NFMF 3973–3975) are figured herein (**Fig. 2.4**), show systematically distributed anomalous structures that occupy homologous positions in well-preserved specimens. These structures are continuous with normal branches, do not extend beyond the associated second-order branches (**Fig. 2.6**) and they are inserted within (beneath) second-order branches without displacing the neighbouring third-order branches. It is thus unlikely that the observed structures in *Culmofrons* represent damage repair or over-compensatory secondary growth: the strong morphological resemblance and positioning of “bi” and “bii”, and “ci” and “cii” with their counterparts “aii” and “aii” suggest a functional interpretation rather than an accidental occurrence (**Fig. 2.4**). The exception to this is impression “aiii”, which is not terminally placed (**Fig. 2.4 A**) and does not have rangeomorph branching, meaning that it might either: (1) not be part of the associated *Culmofrons* and could be an unrelated taxon; (2) represent damage repair; or (3) represent a taphonomic artefact.

We suggest that the unusual rangeomorph impressions observed in *Culmofrons* could represent bundles of third-order branches in the process of separating from the organism, in a process akin to asexual reproduction.

7.2.4. Comparison with placozoan reproductive structures

Placozoans have a simple body plan consisting of two epithelia bounded by mesenchyme (some with symbionts; Gruber-Vodicka et al., 2019) and have two reproductive strategies: binary fission and budding. Placozoan binary fission involves creating a division origin followed by separation into two sister organisms (Pearse, 1989; Zuccolotto-Arellano and Cuervo-González, 2020). This differs from *Culmofrons*, in which the structures appear at higher orders of branching; this may represent a true reproductive process, resulting in the production of daughter organisms. Placozoa can also reproduce by budding, resulting in motile larvae with two undifferentiated cell layers (Thiemann and Ruthmann, 1990).

Unlike placozoan modes of reproduction, *Culmofrons* appears to produce complex structures, possessing preestablished rangeomorph architecture differentiated from a single functional unit (second-order branch) rather than by binary fission. The complexity of the structures observed in *Culmofrons* may provide evidence for a life cycle with several morphologically distinct phases (Brasier and Antcliffe, 2004). The generation of a fundamental reproductive module is an effective reproductive strategy for rapid establishment of new growth and reduced genetic requirements in that each reproductive unit, even though composed of third-order branches (and therefore functionally a portion of a second-order branch) has the potential to generate an entire frond. The potential ability of bundles of third-order branches to revert into first-order branches and establish a new organism is consistent with the growth model proposed for *Cu. plumosa* above.

Employment of modular reproductive structures has a further advantage in that each element in a rangeomorph organism could potentially become a new individual, allowing for efficient dispersal.

7.2.5. *Functional palaeobiology of asexual reproduction*

In the Charnida, primary growth developed from the tip towards the base (Dunn et al., 2018; McIlroy et al., 2020), with addition of rangeomorph units being followed by inflation (Brasier et al., 2012; Laflamme et al., 2012). Secondary growth tips have been reported in the multifoliate rangeomorph *Bradgatia* (Brasier and Antcliffe, 2009) and *Beothukis* (McIlroy et al., 2020), resulting in expansion of the lateral/distal margin. In *Culmofrons*, impressions ai–“aii”, “bi”–“bii” and “ci”–“cii” do not form at the margin of the mature frond. If correctly interpreted as reproductive units, the non-marginal position of these impressions reinforces the hypothesis that *Culmofrons* was a recliner, with growth of reproductive bodies originating below the frond and emerging from between primary order units into the overlying seawater.

Hydrozoans can reproduce asexually by developing juvenile organisms as evaginations of the endoderm and the ectoderm (Technau and Steele, 2012). Hydrozoan buds develop from the side of the body of the mother organism and get displaced basally as they mature and start to separate (Bode et al., 1973; Shostak, 2018). Separation of the modular structures (impressions “ai”–“aiii”, “bi”–“bii”, “ci”–“cii”) might have evolved to overcome the anatomical impediment to metazoan-like budding imposed by the inferred thick epithelium of the Rangeomorpha (Butterfield, 2020).

Weak constricted connections between the third-order branches of the observed structures and associated secondary branches might be a convenient way to separate the mature reproductive modules.

The morphology of *Hylaecullulus fordi* has led to the proposal of two means to evolve modularity, either by: (1) greater integration (cf. octocorallian coloniality); or (2) by relaxation of integration (cf. the green algae *Caulerpa prolifera*) (Kenchington et al. 2018) to generate new stems. Our discovery of abnormal structures in *Culmofrons*, if their reproductive function

was confirmed, would suggest that rangeomorphs might have had true modularity and the ability to separate modules as an asexual reproductive strategy (see Brasier and Antcliffe, 2004). This would suggest that multifoliate rangeomorphs should not be interpreted as colonial organisms, and that their modularity was probably achieved by relaxation of integration via the organization in higher order branches of the fundamental functional unit, the second-order branches. The employment of secondary asexual reproductive strategies such as budding and binary fission have been documented as a response to starvation periods in the Cnidaria (Technau and Steele, 2012). It is possible that the seafloor where *Culmofrons* reclined was subject to episodic smothering by thin layers of sediment. In such a setting the generation of upward growing budding structures into the overlying defaunated seafloor would have provided a viable reproductive strategy for repopulation of slowly aggrading seafloors (Kenchington and Wilby, 2014).

Further identification of reproductive structures in well-preserved specimens of *Culmofrons plumosa* and other rangeomorphs will be necessary to positively interpret structures such as the impressions “ai”, “aii”, “aiii”, “bi”, “bii”, “ci” and “cii” as reproductive modules.

8. Conclusion

Recently discovered specimens of *Culmofrons plumosa* from the Bonavista Peninsula reveal exquisite details of rangeomorph branching, revealing hitherto undocumented structures and providing insights into rangeomorph palaeobiology. Taphonomic observations on the Catalina Dome material suggest a reclining lifestyle for *Cu. plumosa*, possibly hosting symbionts as has recently been described for *Beothukis mistakensis* (McIlroy et al., 2020, 2021). A morphological description of the new material and morphometric analyses support the validity of the genus *Culmofrons* and its differentiation from the genera *Beothukis* and *Charnia*. The species *Culmofrons plumosa* reveals a high morphometric variability, but a rather conserved morphology and a deterministic growth plan. Three specimens present a total of seven abnormal structures, six of which have been recognized as potential reproductive structures. These six impressions resemble bundled tertiary order branches and can thus be differentiated from over-compensatory growth or secondary growth as is observed in *Hylaecullulus*, *Beothukis* (Kenchington et al., 2018; McIlroy et al., 2020) and some *Culmofrons* (Fig. 2.2B).

Based on the similarity of the structures with the secondary growth tips observed in *Bradgatia* (Brasier and Antcliffe, 2009) and on the growth models proposed for *Charnia* (Dunn et al., 2018) and *Beothukis* (McIlroy et al., 2020) we suggest that the structures observed in *Culmofrons* might represent modular reproductive structures, possibly as an adaptation to sediment smothering events or nutrient crises. Comparison of the newly described impressions within *Culmofrons* with the reproductive strategies of extant basal metazoans suggests that the Rangeomorpha were non-colonial and did not have a metazoan Bauplan, and that rangeomorph branching might represent true modularity. We also infer a growth model for *Cu. plumosa* and

we suggest that, similar to *Ch. masoni*, the species grew by early addition of first-order, primary branches and later inflation.

9. Acknowledgements

Fossil surfaces in the Bonavista Peninsula are protected under Reg. 67/11, of the Historic Resources Act 2011 and their access is only allowed under permission from the Government of Newfoundland and Labrador. Fieldwork near Port Union was conducted under permit from the Government of Newfoundland and Labrador.

Thanks are due to: Rod S Taylor, for his great contributions in the field, and in the conception and editing of this manuscript; Edith and Neville Samson for their kind support; J Matthews and A Liu for discovery of the MUN Surface. P Thurlow, H Fitzgerald, C McKean, JM Neville, D Pérez-Pinedo, C Locatelli and B Smith for field assistance; and Natural Sciences and Engineering Research Council of Canada (NSERC) for Discovery Grant (individual) and DAG funding to DM. A Liu and an anonymous referee commented on an earlier draft of this manuscript.

10. Data archiving statement

Data for this study are available in the Dryad Digital Repository:

<https://doi.org/10.5061/dryad.ksn02v785>

Editor: Nicholas Butterfield

11. References

- Anderson, M. M., and Misra, S. B. (1968). Fossils found in the Pre-Cambrian Conception Group of South-eastern Newfoundland. *Nature* 220, 680–681. doi: 10.1038/220680a0
- Bamforth, E. L., Narbonne, G. M., and Anderson, M. M. (2008). Growth and ecology of a multi-branched Ediacaran rangeomorph from the Mistaken Point assemblage, Newfoundland. *Journal of Paleontology* 82, 763–777. doi: 10.1666/07-112.1
- Boddy, C. E., Mitchell, E. G., Merdith, A., and Liu, A. G. (2022). Palaeolatitudinal distribution of the Ediacaran macrobiota. *JGS* 179, jgs2021-030. doi: 10.1144/jgs2021-030
- Bode, H., Berking, S., David, C. N., Gierer, A., Schaller, H., and Trenkner, E. (1973). Quantitative analysis of cell types during growth and morphogenesis in *Hydra*. *W. Roux' Archiv f. Entwicklungsmechanik* 171, 269–285. doi: 10.1007/BF00577725
- Brasier, M., and Antcliffe, J. B. (2004). Decoding the Ediacaran enigma. *Science* 305, 1115–1117. doi: 10.1126/science.1102673
- Brasier, M. D., and Antcliffe, J. B. (2009). Evolutionary relationships within the Avalonian Ediacara biota: new insights from laser analysis. *Journal of the Geological Society* 166, 363–384. doi: 10.1144/0016-76492008-011
- Brasier, M. D., Antcliffe, J. B., and Liu, A. G. (2012). The architecture of Ediacaran fronds. *Palaeontology* 55, 1105–1124. doi: 10.1111/j.1475-4983.2012.01164.x
- Butterfield, N. J. (2020). Constructional and functional anatomy of Ediacaran rangeomorphs. *Geol. Mag.*, 1–12. doi: 10.1017/S0016756820000734
- Clapham, M. E., and Narbonne, G. M. (2002). Ediacaran epifaunal tiering. *Geology* 30, 627–630. doi: 10.1130/0091-7613(2002)030<0627:EET>2.0.CO;2
- Darroch, S. A. F., Laflamme, M., and Clapham, M. E. (2013). Population structure of the oldest known macroscopic communities from Mistaken Point, Newfoundland. *Paleobiology* 39, 591–608. doi: 10.1666/12051
- Darroch, S. A. F., Laflamme, M., Schiffbauer, J. D., and Briggs, D. E. G. (2012). Experimental formation of a microbial death mask. *PALAIOS* 27, 293–303. doi: 10.2110/palo.2011.p11-059r
- Decechi, T. A., Narbonne, G. M., Greentree, C., and Laflamme, M. (2017). Relating Ediacaran fronds. *Paleobiology* 43, 171–180. doi: 10.1017/pab.2016.54
- Dufour, S. C., and McIlroy, D. (2017). Ediacaran pre-placozoan diploblasts in the Avalonian biota: the role of chemosynthesis in the evolution of early animal life. *Geological Society, London, Special Publications* 448, 211–219. doi: 10.1144/SP448.5

- Dunn, F. S., Grazhdankin, D. V., Liu, A. G., and Wilby, P. R. (2021). The developmental biology of *Charnia* and the eumetazoan affinity of the Ediacaran rangeomorphs. *Science Advances*, 14.
- Dunn, F. S., Liu, A. G., and Donoghue, P. C. J. (2018). Ediacaran developmental biology: Ediacaran developmental biology. *Biol Rev* 93, 914–932. doi: 10.1111/brv.12379
- Dunn, F. S., Wilby, P. R., Kenchington, C. G., Grazhdankin, D. V., Donoghue, P. C. J., and Liu, A. G. (2019). Anatomy of the Ediacaran rangeomorph *Charnia masoni*. *Pap Palaeontol* 5, 157–176. doi: 10.1002/spp2.1234
- Ford, T. D. (1958). Pre-Cambrian fossils from Charnwood Forest. *Proceedings of the Yorkshire Geological Society* 31, 211–217. doi: 10.1144/pygs.31.3.211
- Ford, T. D. (1962). The Pre-Cambrian fossils of Charnwood Forest. *Transactions of the Leicester Literary and Philosophical Society* 56, 57–62.
- Gehling, J. G. (1999). Microbial mats in terminal Proterozoic siliciclastics: Ediacaran death masks. *PALAIOS* 14, 40. doi: 10.2307/3515360
- Gehling, J. G., and Narbonne, G. M. (2007). Spindle-shaped Ediacara fossils from the Mistaken Point assemblage, Avalon Zone, Newfoundland. *Can. J. Earth Sci.* 44, 367–387. doi: 10.1139/e07-003
- Gruber-Vodicka, H. R., Leisch, N., Kleiner, M., Hinzke, T., Liebeke, M., McFall-Ngai, M., et al. (2019). Two intracellular and cell type-specific bacterial symbionts in the placozoan *Trichoplax* H2. *Nat Microbiol* 4, 1465–1474. doi: 10.1038/s41564-019-0475-9
- Gürich, G. (1929). Die ältesten fossilien Südafrikas. *Zeitschrift für Praktische Geologie* 37.
- Gürich, G. (1933). Die kuibis-fossilien der Namaformation von Südwestafrika. *Paläontologische Zeithschrift* 15, 137–145.
- Hawco, J. B., Kenchington, C. G., Taylor, R. S., and Mcilroy, D. (2020). A multivariate statistical analysis of the Ediacaran rangeomorph taxa *Beothukis* and *Culmofrons*. *PALAIOS* 35, 495–511. doi: 10.2110/palo.2020.049
- Hofmann, H. J., O'Brien, S. J., and King, A. F. (2008). Ediacaran biota on Bonavista Peninsula, Newfoundland, Canada. *J. Paleontol.* 82, 1–36. doi: 10.1666/06-087.1
- Kaiser, H. F. (1970). A second generation little jiffy. *Psychometrika* 35, 401–415. doi: 10.1007/BF02291817
- Kenchington, C. G., Dunn, F. S., and Wilby, P. R. (2018). Modularity and Overcompensatory Growth in Ediacaran Rangeomorphs Demonstrate Early Adaptations for Coping with Environmental Pressures. *Current Biology* 28, 3330-3336.e2. doi: 10.1016/j.cub.2018.08.036

- Kenchington, C. G., and Wilby, P. R. (2014). Of time and taphonomy: preservation in the Ediacaran. *The Paleontological Society Papers* 20, 23. doi: <https://doi.org/10.1017/S1089332600002825>
- Laflamme, M., Flude, L. I., and Narbonne, G. M. (2012). Ecological tiering and the evolution of a stem: the oldest stemmed frond from the Ediacaran of Newfoundland, Canada. *J. Paleontol.* 86, 193–200. doi: 10.1666/11-044.1
- Laflamme, M., and Narbonne, G. M. (2008). Competition in a Precambrian world: palaeoecology of Ediacaran fronds. *Geology Today* 24, 182–187. doi: 10.1111/j.1365-2451.2008.00685.x
- Laflamme, M., Schiffbauer, J. D., Narbonne, G. M., and Briggs, D. E. G. (2011). Microbial biofilms and the preservation of the Ediacara biota: Ediacaran preservation. *Lethaia* 44, 203–213. doi: 10.1111/j.1502-3931.2010.00235.x
- Laflamme, M., Xiao, S., and Kowalewski, M. (2009). Osmotrophy in modular Ediacara organisms. *Proceedings of the National Academy of Sciences* 106, 14438–14443. doi: 10.1073/pnas.0904836106
- Lê, S., Josse, J., and Husson, F. (2008). FactoMineR: An R Package for Multivariate Analysis. *J. Stat. Soft.* 25. doi: 10.18637/jss.v025.i01
- Liu, A. G. (2016). Framboidal pyrite shroud confirms the “Death Mask” model for moldic preservation of Ediacaran soft-bodied organism. *PALAIOS* 31, 259–274. doi: 10.2110/palo.2015.095
- Liu, A. G., and Dunn, F. S. (2020). Filamentous Connections between Ediacaran Fronds. *Current Biology* 30, 1322-1328.e3. doi: 10.1016/j.cub.2020.01.052
- Liu, A. G., Kenchington, C. G., and Mitchell, E. G. (2015). Remarkable insights into the paleoecology of the Avalonian Ediacaran macrobiota. *Gondwana Research* 27, 1355–1380. doi: 10.1016/j.gr.2014.11.002
- Liu, A. G., Matthews, J. J., and McIlroy, D. (2016). The *Beothukis* / *Culmofrons* problem and its bearing on Ediacaran macrofossil taxonomy: evidence from an exceptional new fossil locality. *Palaeontology* 59, 45–58. doi: 10.1111/pala.12206
- Liu, A. G., McIlroy, D., Antcliffe, J. B., and Brasier, M. D. (2011). Effaced preservation in the Ediacara biota and its implications for the early macrofossil record: Ediacaran Taphomorph. *Palaeontology* 54, 607–630. doi: 10.1111/j.1475-4983.2010.01024.x
- Liu, A. G., McIlroy, D., Matthews, J. J., and Brasier, M. D. (2013). Exploring an Ediacaran ‘nursery’: growth, ecology and evolution in a rangeomorph palaeocommunity. *Geology Today* 29, 23–26. doi: 10.1111/j.1365-2451.2013.00860.x
- Liu, A. G., McIlroy, D., Matthews, J. J., and Brasier, M. D. (2014). Confirming the metazoan character of a 565 Ma trace-fossil from Mistaken Point, Newfoundland. *PALAIOS* 29, 420–430. doi: 10.2110/palo.2014.011

- Mapstone, N. B., and McIlroy, D. (2006). Ediacaran fossil preservation: Taphonomy and diagenesis of a discoid biota from the Amadeus Basin, central Australia. *Precambrian Research* 149, 126–148. doi: 10.1016/j.precamres.2006.05.007
- Matthews, J. J., Liu, A. G., Yang, C., McIlroy, D., Levell, B., and Condon, D. J. (2020). A chronostratigraphic framework for the rise of the Ediacaran macrobiota: New constraints from Mistaken Point Ecological Reserve, Newfoundland. *Geological Society of America Bulletin* 133, 13. doi: 10.1130/B35646.1
- McIlroy, D., Dufour, S. C., Taylor, R., and Nicholls, R. (2021). The role of symbiosis in the first colonization of the seafloor by macrobiota: Insights from the oldest Ediacaran biota (Newfoundland, Canada). *Biosystems* 205, 104413. doi: 10.1016/j.biosystems.2021.104413
- McIlroy, D., Hawco, J., McKean, C., Nicholls, R., Pasinetti, G., and Taylor, R. (2020). Palaeobiology of the reclining rangeomorph *Beothukis* from the Ediacaran Mistaken Point Formation of southeastern Newfoundland. *Geol. Mag.*, 1–15. doi: 10.1017/S0016756820000941
- Misra, S. B. (1969). Late Precambrian (?) Fossils from Southeastern Newfoundland. *Geol Soc America Bull* 80, 2133. doi: 10.1130/0016-7606(1969)80[2133:LPFFSN]2.0.CO;2
- Mitchell, E. G., and Kenchington, C. G. (2018). The utility of height for the Ediacaran organisms of Mistaken Point. *Nat Ecol Evol* 2, 1218–1222. doi: 10.1038/s41559-018-0591-6
- Mitchell, E. G., Kenchington, C. G., Liu, A. G., Matthews, J. J., and Butterfield, N. J. (2015). Reconstructing the reproductive mode of an Ediacaran macro-organism. *Nature* 524, 343–346. doi: 10.1038/nature14646
- Narbonne, G. M. (2004). Modular construction of Early Ediacaran complex life forms. *Science* 305, 1141–1144. doi: 10.1126/science.1099727
- Narbonne, G. M. (2005). The Ediacara biota: Neoproterozoic origin of animals and their ecosystems. *Annu. Rev. Earth Planet. Sci.* 33, 421–442. doi: 10.1146/annurev.earth.33.092203.122519
- Narbonne, G. M., Laflamme, M., Greentree, C., and Trusler, P. (2009). Reconstructing a lost world: Ediacaran rangeomorphs from Spaniard’s Bay, Newfoundland. *J. Paleontol.* 83, 503–523. doi: 10.1666/08-072R1.1
- O’Brien, S. J., and King, A. F. (2002). Neoproterozoic Stratigraphy of the Bonavista Peninsula: preliminary results, regional correlations and implication for sediment-hosted stratiform copper exploration in the Newfoundland Avalon Zone. *Geological Survey* 02, 229–244.
- O’Brien, S. J., and King, A. F. (2005). Late Neoproterozoic (Ediacaran) stratigraphy of Avalon Zone sedimentary rocks, Bonavista Peninsula, Newfoundland. *Geological Survey* 05, 13.

- Olsen, A. M. (2017). Feeding ecology is the primary driver of beak shape diversification in waterfowl. *Funct Ecol* 31, 1985–1995. doi: 10.1111/1365-2435.12890
- Olsen, A. M., and Westneat, M. W. (2015). StereoMorph: an R package for the collection of 3D landmarks and curves using a stereo camera set-up. *Methods Ecol Evol* 6, 351–356. doi: 10.1111/2041-210X.12326
- Pasinetti, G., and McIlroy, D. (2023). Data from: Palaeobiology and taphonomy of the rangeomorph *Culmofrons plumosa*. *Dryad Digital Repository*. doi: 10.5061/dryad.ksn02v785
- Pearse, V. B. (1989). Growth and Behavior of *Trichoplax adhaerens*: First Record of the Phylum Placozoa in Hawaii. *Pacific Science* 43, 5.
- Pérez-Pinedo, D., McKean, C., Taylor, R., Nicholls, R., and McIlroy, D. (2022). *Charniodiscus* and *Arborea* are separate genera within the Arboreomorpha: Using the holotype of *C. concentricus* to resolve a taphonomic/taxonomic tangle. *Front. Earth Sci.* 9, 785929. doi: 10.3389/feart.2021.785929
- Pérez-Pinedo, D., Neville, J. M., Pasinetti, G., McKean, C., Taylor, R., and McIlroy, D. (2023). Frond orientations with independent current indicators demonstrate the reclining rheotropic mode of life of several Ediacaran rangeomorph taxa. *Paleobiology*, 1–22. doi: 10.1017/pab.2023.2
- RStudio Team (2020). RStudio: integrated development for R. Available at: <http://www.rstudio.com/>
- Shostak, S. (2018). Is *Hydra* an Alarm Clock? *BJSTR* 7. doi: 10.26717/BJSTR.2018.07.001521
- Slagter, S., Hao, W., Planavsky, N. J., Konhauser, K. O., and Tarhan, L. G. (2022). Biofilms as agents of Ediacara-style fossilization. *Sci Rep* 12, 8631. doi: 10.1038/s41598-022-12473-1
- Tarhan, L. G., Hood, A. v.S., Droser, M. L., Gehling, J. G., and Briggs, D. E. G. (2016). Exceptional preservation of soft-bodied Ediacara Biota promoted by silica-rich oceans. *Geology* 44, 951–954. doi: 10.1130/G38542.1
- Taylor, R. S., Hawco, J. B., Nichols, R., and McIlroy, D. (2019). Reevaluación crítica del holotipo de *Beothukis mistakensis*, único organismo rangeomorfo excepcionalmente preservado en Mistaken Point, Terranova, Canadá. *Estud. geol.* 75, 117. doi: 10.3989/egeol.43586.572
- Taylor, R. S., Matthews, J. J., Nicholls, R., and McIlroy, D. (2021). A re-assessment of the taxonomy, palaeobiology and taphonomy of the rangeomorph organism *Hapsidophyllas flexibilis* from the Ediacaran of Newfoundland, Canada. *PalZ* 95, 187–207. doi: 10.1007/s12542-020-00537-4
- Technau, U., and Steele, R. E. (2012). Evolutionary crossroads in developmental biology: Cnidaria. *Development* 139, 4491–4491. doi: 10.1242/dev.090472

- Thiemann, M., and Ruthmann, A. (1990). Spherical forms of *Trichoplax adhaerens* (Placozoa). *Zoomorphology* 110, 37–45. doi: 10.1007/BF01632810
- Wacey, D., Kilburn, M. R., Saunders, M., Cliff, J. B., Kong, C., Liu, A. G., et al. (2015). Uncovering framboidal pyrite biogenicity using nano-scale CNorg mapping. *Geology* 43, 27–30. doi: 10.1130/G36048.1
- Waggoner, B. (2003). The Ediacaran biotas in space and time. *Integrative and Comparative Biology* 43, 104–113. doi: 10.1093/icb/43.1.104
- Zuccolotto-Arellano, J., and Cuervo-González, R. (2020). Binary fission in *Trichoplax* is orthogonal to the subsequent division plane. *Mechanisms of Development* 162, 103608. doi: 10.1016/j.mod.2020.103608

Chapter 3 : A taxonomic and palaeobiologic consideration of *Charnia* spp. from the Bonavista Peninsula of Newfoundland (CA)

Pasinetti Giovanni^{1*}, gpasinetti@mun.ca, 0000-0003-3104-9758

Fitzgerald Hayley Grace¹

Pérez-Pinedo Daniel¹, 0000-0001-5607-1164

McIlroy Duncan¹, 0000-0001-9521-499X

¹MUN Palaeobiology Group, Department of Earth Sciences, Memorial University of Newfoundland (CA)

*Corresponding author

1. Author contribution

Conceptualization: G. Pasinetti (GP), H.G. Fitzgerald (HGF), D. Pérez-Pinedo (DPP); D. McIlroy (DM);

Data Curation Management: GP, HGF;

Formal Analysis: GP, HGF, DPP;

Funding Acquisition: DM;

Investigation: GP, HGF, DPP, DM;

Methodology: GP, HGF, DPP, DM;

Project Administration: GP, DM;

Resources: DM;

Software: GP, HGF;

Supervision: DM;

Validation: GP, DPP, DM;

Visualization: GP;

Writing – Original Draft Preparation: GP;

Writing – Review & Editing: GP, DPP, DM, RST.

2. Key words

RANGEOMORPH TAXONOMY, CHARNIDA, EDIACARAN SYSTEMATICS, MORPHOMETRY, PALAEOECOLOGICAL RECONSTRUCTIONS

3. Abstract

Despite the genus *Charnia* being one of the most widely distributed rangeomorphs early late Ediacaran fossiliferous assemblages, there are currently only two valid species. Here, we describe a third species, *C. ewinoni* sp. nov., based on material from the Bonavista and Avalon Peninsulas of Newfoundland (CA). The new species has unique traits, such as the presence of a long stem, a parallel-sided outline, first-order branches ranging from sigmoidal to straight and a less zig-zagged midline. Hierarchical clustering and morphospace analyses support the creation of a new taxon, distinguishing *C. ewinoni* sp. nov. from the type material of *C. masoni* from the Charnwood Forest (UK) and also from *C. gracilis* which was recently described from the Shibantan Member of Dengying Formation, China. Taphonomic evidence, along with the peculiar orientations of the fossils on the Matthews Surface with respect to the inferred palaeocurrent, suggest the possibility of a reclining lifestyle for the new species, challenging previous reconstructions of the mode of life of the genus.

4. Introduction

The oldest evidence for complex multicellular body plans can be found in the fossil record of the oldest of the three traditional late Ediacaran assemblages, the Avalon assemblage (Waggoner, 2003). Avalonian fossil communities are dominated by the Rangeomorpha and the Arboreomorpha (Narbonne, 2004; Laflamme and Narbonne, 2008a, 2008b), which occur along with a large number of problematic macrofossils, and the first eumetazoans (Liu et al., 2010; Liu and McIlroy, 2015; Dunn et al., 2021). The Rangeomorpha and Arboreomorpha share some similarities, such as the presence of a frond-like petalodium and sometimes a stem and basal disc (**Fig. 1A**; Laflamme et al., 2007), which has led some authors to suggest that they might have metazoan-grade structures (Dunn et al., 2021). While the Arboreomorpha consistently have a frondose structure, the morphology within branches is not the self-similar fractal-like architecture characteristic of the Rangeomorpha. The fundamental bauplan of the Arboreomorpha is that of a frond attached to a stem—the frond being either planar (Laflamme et al. 2018; Dunn et al., 2019a), or curved (Pérez-Pinedo et al., 2022)—and pea-pod shaped organs on one surface which are inferred to have had a role in feeding (Dunn et al., 2019a). The Rangeomorpha, in contrast, have a large diversity of gross morphology, constructed by up to 4 orders of rangeomorph elements in a range of orientations (e.g. Jenkins, 1985; Brasier et al., 2012), but only sometimes having a stem (Narbonne, 2004; Taylor et al., 2021). The current taxonomic framework used to discriminate among rangeomorph taxa is contentious, resulting in the existence of a large number of unnamed species, problematic taxa, with some taxa being used as “waste-baskets”, which is an impediment to realistic ecological modelling (McIlroy et al., 2021).

Charnia masoni is among the most widely distributed Ediacaran taxa—both spatially and temporally—and was the first complex macrofossil to be positively identified from

Precambrian strata (Ford, 1958, 1962). The holotype (**Fig. 3.1 D**) was discovered by Tina Negus and later by Roger Mason in Charnwood Forest, Leicestershire, UK (Howe et al., 2012). The genus *Charnia* belongs to the rangeomorph clade Charnida (Laflamme and Narbonne, 2008b). *Charnia* is abundant in the Ediacaran of Newfoundland, both from the Mistaken Point Ecological Reserve (MPER) of the southern Avalon Peninsula (*Charnia* spp., Laflamme and Narbonne, 2008b) and from the Discovery UNESCO Global Geopark on the Bonavista Peninsula (*Charnia masoni* and *Charnia* sp., Hofmann et al., 2008) (**Fig. 3.1 A-B**), as well as new discoveries from Upper Island Cove (Narbonne et al., 2009) and elsewhere in Conception Bay (McKean et al., 2023; **Fig. 3.1C**). Many specimens from the Bonavista Peninsula (**Fig. 3.1 A-B**), and some from the Avalon Peninsula, differ from the type species in having a distinct stem at the end of the frondose portion, a parallel-sided petalodium and a straighter midline rather than the distinctively zigzagged midline of *C. masoni* (**Fig. 3.1 D**).

This study compares the peculiar specimens from Newfoundland (**Fig. 3.1 A-C**) with the *C. masoni* (**Fig. 3.1 D**) as well as *C. gracilis* from the Shibantan biota of South China (Wu et al., 2022), employing a statistical approach based on morphometrics. The taphonomy, species associations, and functional morphology of the Newfoundland material is assessed herein employing field and lab observations along with measurements of frond orientations from a *Charnia* rich surface known as the Matthews Surface on the Bonavista Peninsula.

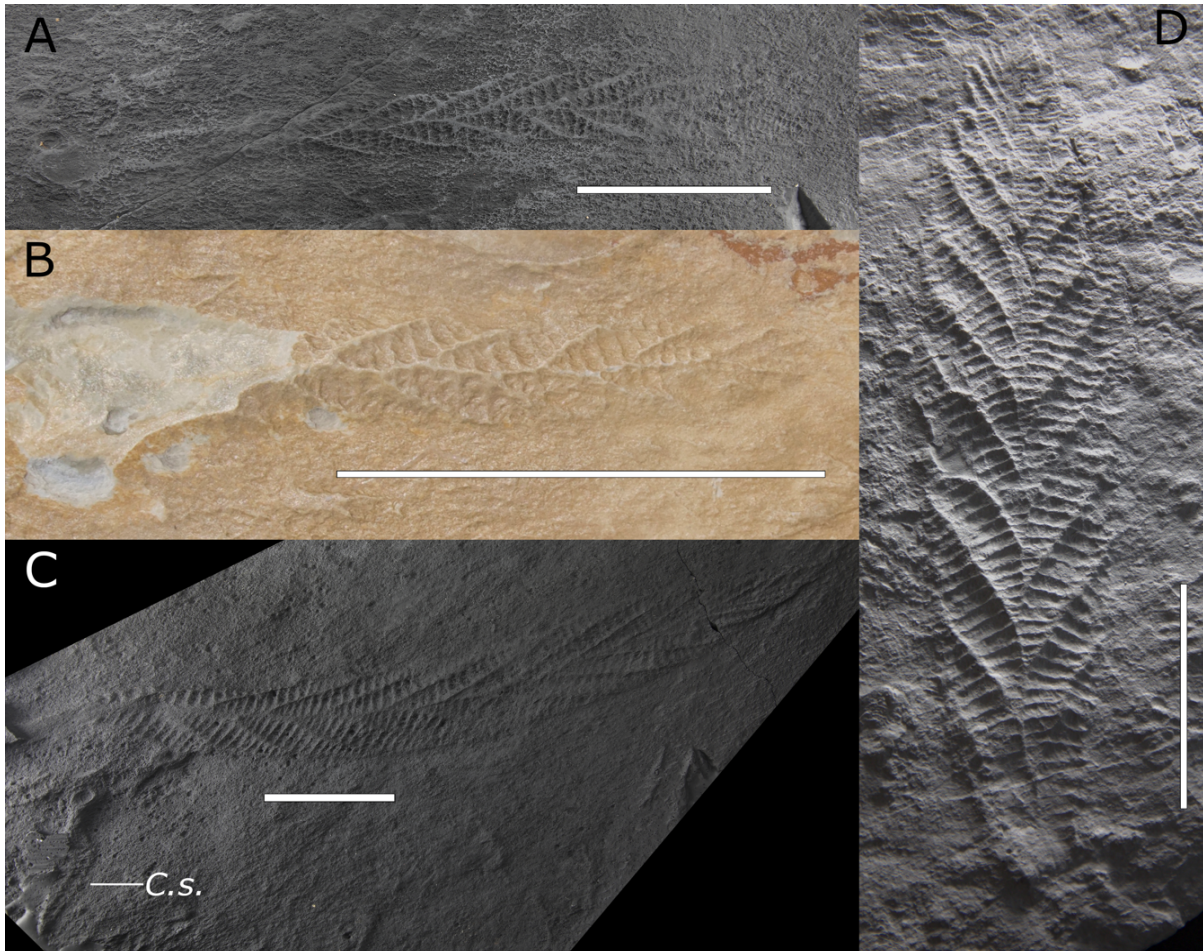


Figure 3.1: diversity of *Charnia* sp. from Newfoundland.

A) *Charnia* sp. jesmonite cast from the Bonavista Peninsula (Matthews Surface), note the straight midline and the presence of a stem with a globose structure at the end; **B)** field photograph of *Charnia* sp. from the Bonavista Peninsula (MUN surface), fossil damaged at the expected position of the stem; **C)** *Charnia* sp. jesmonite cast from Inner Meadow, Conception Bay (Newfoundland), note straight first-order branches, note a small unrelated arboreomorph (*Charniodiscus spinosus*), oriented perpendicular to the *Charnia* frond; **D)** cast of the *C. masoni* holotype from the UK, note the more accentuated zig-zagged midline, sigmoidal first-order branches, ovate outline. Scale bars = 5 cm.

5. Geological setting

Our study encompasses 40 complete specimens from Newfoundland, Canada (Fig. 3.2 A-B), the Charnwood inlier in the UK, and the Shibantan biota of South China. The North Quarry in Charnwood Forest (~562–557 Ma; Noble et al., 2015) hosts the type material of *Charnia masoni*, including several specimens that have already been subject of morphometric analysis (Dunn et al., 2018, 2019b) *Charnia* is also common in the Ediacaran strata of the Avalon and Bonavista Peninsulas in Newfoundland, including juvenile specimens (e.g. Pigeon Cove, the oldest occurrence of the genus (Liu et al., 2013); and Upper Island Cove (Narbonne et al., 2009; Brasier et al., 2013; Mckean et al., 2023) to super-mature specimens, comparable to *Charnia masoni* “*grandis*” (Boynton and Ford, 1995; Boynton, 1999; Hofmann et al., 2008; Wilby et al., 2011, later synonymized with *C. masoni*, Brasier et al., 2012).

In the Newfoundland sections, *Charnia* first appears in the Drook Formation (Liu et al., 2013), around 574.17±0.19 Ma (Matthews et al., 2020) and is found in the overlying Briscal (not present in the Bonavista Peninsula), Mistaken Point and Trepassey formations. The depositional environments of these *Charnia*-bearing Ediacaran-aged rocks range from deep basinal to mid-slope settings, particularly in association with sandstones, siltstones and tuffites which are strongly influenced by density currents (Wood et al., 2003; Ichaso et al., 2007; Matthews et al., 2020; McIlroy et al., 2022).

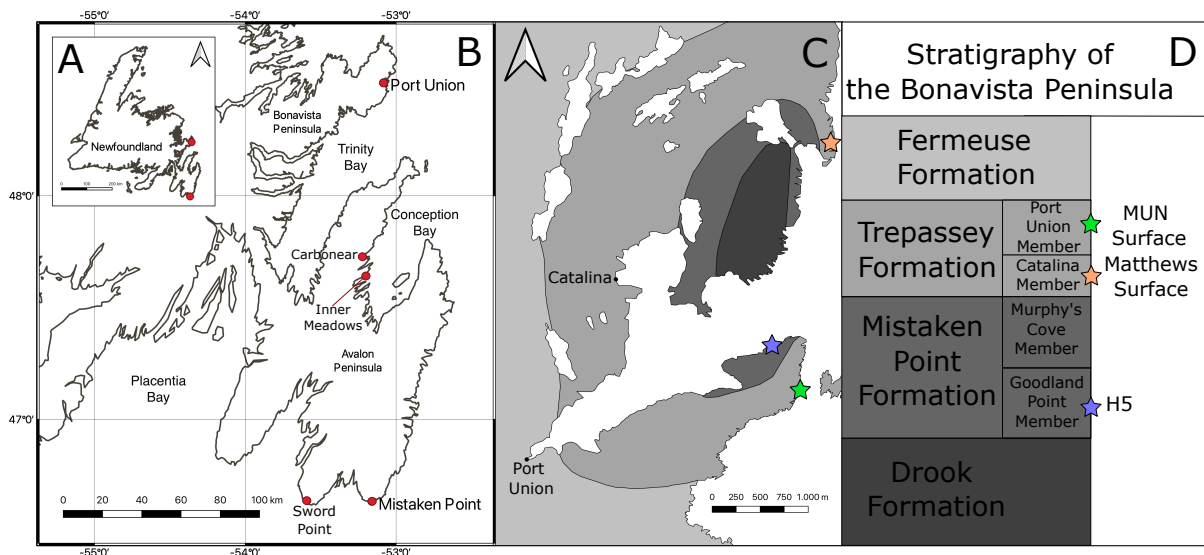


Figure 3.2: map and stratigraphy of the fossiliferous localities.

A) Map of Newfoundland, with the two main fossiliferous areas: the Mistaken Point ecological reserve and the Discovery UNESCO Global Geopark (Bonavista Peninsula) marked by red dots; **B)** detail of eastern Newfoundland, with the main fossiliferous localities in red: in the Southern Avalon Peninsula, Sword Point and the Mistaken Point Ecological Reserve, in the central Avalon Peninsula, Carbonear and Inner Meadow; in the Bonavista Peninsula, the Port Union area; **C)** detail of the main *Charnia*-bearing fossiliferous localities of the Catalina Dome: orange star: Matthews Surface, purple star: H5; green star: MUN Surface; **D)** simplified stratigraphy of the Bonavista Peninsula, lithostratigraphically correlated with the Avalon Peninsula. Stratigraphic position of the fossiliferous localities in the Discovery Geopark indicated by stars.

Our analyses require consideration of complete *Charnia* specimens, which are known from six localities in Newfoundland, four of which have only one complete specimen (H-5, **Fig. 3.2 C-D**; cf. H5 of Hofmann et al. 2008), the MUN Surface (**Fig. 3.2 C-D**; cf. Liu et al., 2016) Carbonear (McKean et al., 2023) and Sword Point (cf. Laflamme et al., 2007). The newly discovered Inner Meadow site currently has two specimens, while the Matthews Surface (**Fig. 3.2 C-D**; cf. LC6 in Dunn et al., 2019b; Liu and Dunn, 2020) has a large assemblage of twenty well-preserved specimens.

The Sword Point Surface is located on the southern Avalon Peninsula (**Fig. 3.2 A-B**) and is part of the Mistaken Point biota. Sites at Carbonear and Inner Meadow, Upper Island Cove constitute the coeval Conception Bay biota (**Fig. 3.2 B**; Narbonne 2004; Narbonne et al. 2009; Brasier et al. 2013; McKean et al. 2023). The Matthews Surface, HF5 (Liu & Dunn 2020), and the MUN Surface (Liu et al. 2016) are located in the Catalina Dome on the Bonavista Peninsula (**Fig. 3.2 A-C**; cf. Hofmann et al. 2008), which exposes strata of the Conception and St. John's Groups (**Fig. 3.2 D**; O'Brien and King, 2005). The Bonavista Peninsula biota is best known as the type locality of *Haootia quadriformis*, the oldest eumetazoan in the fossil record (Liu et al., 2014, 2015). The Matthews Surface is the most fossiliferous surface within the Catalina Member, which has been correlated with the Trepassey Formation in the St. John's Group (O'Brien and King, 2002, 2005) and has a relatively diverse biota of six different Ediacaran macrofossil species preserved in-situ. The surface lies within a turbiditic succession, and is cast by a thin tuff, and overlain by a series of 1-1.5 m thick siltstone units, alternating with thin turbiditic sandstones with ripple cross lamination with paleocurrents towards the south (190°).

Fossils on the Matthews Surface are preserved as negative impressions on the upper bedding surface of a fine siltstone, immediately overlain by a thin layer of tuff/tuffite (**Fig. 3.3 A**) that is inferred to have smothered the community in-situ as an obrution deposit (cf. Seilacher, 1999). The negative impressions left on the siltstone by the decomposed organisms were cast by collapse of the overlying tuff onto the surface. In the case of positive relief stems, the tuff is considered to have lithified before decomposition of the stem tissues, resulting in the upper surface being cast (**Fig. 3.3 A-B**). Counterparts to the impressions can sometimes be found on the bottom of the overlying tuffaceous layer (**Fig. 3.3 A-B**).

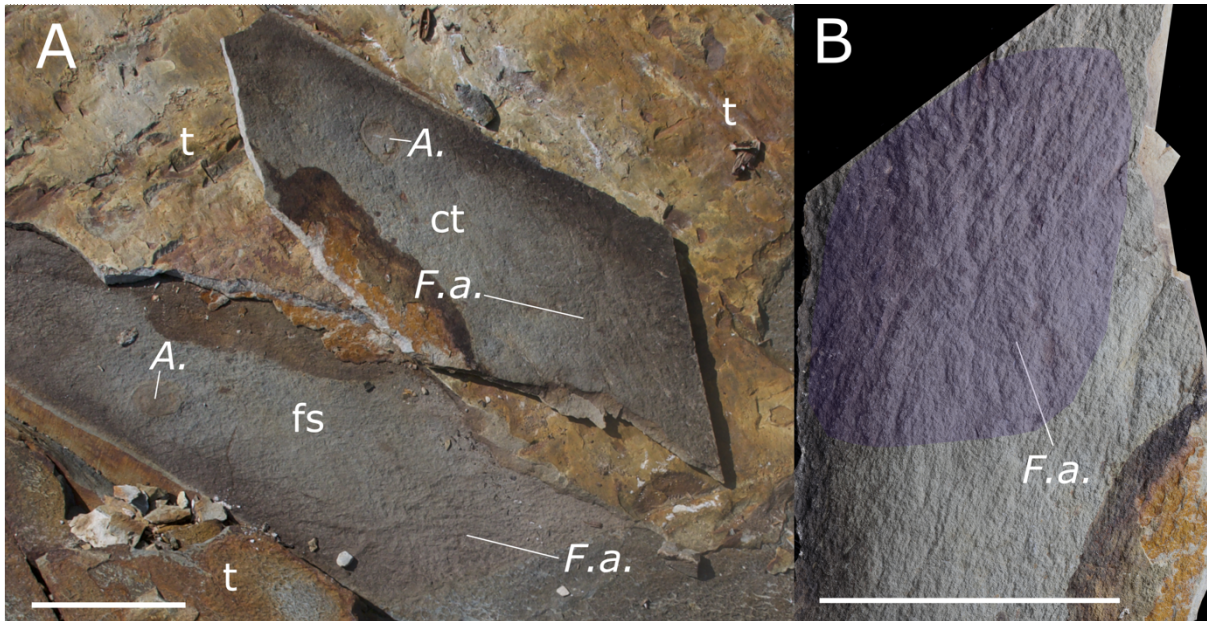


Figure 3.3: preservation on the Matthews Surface.

A) Matthews Surface: fossiliferous surface (“fs”) overlain by tuffs (“t”). On the fossiliferous surface, negative impressions of *Fractofusus andersoni* (“F.a.”) and positive relief *Aspidella* (“A.”). A counterpart to the fossiliferous surface (“ct”), reveals a positive relief *Fractofusus* and a negative relief *Aspidella* impression; **B)** detail of the counterpart, showing a positive hyporelief of a *Fractofusus*. Scale bars = 5 cm.

5. Materials and methods

5.1. Data collection

Measurements of seven variables were digitized with the software ImageJ from forty complete specimens of *Charnia* from the Charnian Supergroup of the UK (n=11), the Conception and St. John's groups of Newfoundland (n=26), and from three of the published photographs of the Shibantan biota of South China (Wu et al. 2022). The Newfoundland material was photographed directly in the field from 6 different localities. All of the Newfoundland specimens are preserved in-situ with jesmonite replicas of key specimens deposited at The Rooms (the Provincial Museum of Newfoundland and Labrador). Measurements were also taken from one additional specimen, the rangeomorph *Culmofrons plumosa* from the MUN Surface (Pasinetti & McIlroy 2023), for use as an outlier. The measured variables are listed in **Table 3.1**. Five untransformed continuous variables were measured in each specimen (**Fig. 3.4 A-B**):

[V1]: length of the petalodium (**Fig. 3.4 A**);

[V2]: width of the petalodium (**Fig. 3.4 A**);

[V3]: length of the stem (**Fig. 3.4 A**);

[V4]: marginal length of the longest first-order branch (**Fig. 3.4 B**);

[V5]: width of the longest first-order branch (**Fig. 3.4 B**).

Additionally, three variables pertaining the angles for the first-order branches were measured to quantify differences in first-order branches shapes and their relative positions in the petalodium (**Fig. 3.4 B**):

[V6]: degree of sigmoidal curvature of the first-order branches, described by the morphological descriptor X, proposed by Wu et al. (2022), which has been shown to effectively

discriminate sigmoidal ($X \geq 0,3$) from straight ($X \leq 0,3$) branches by measuring angles tangent to the branches: $X = |(a-b)/(a+b)|$ (**Fig. 3.4 B**).

[V7]: distal angle of first-order branch (cf. “divergence angle” in Wu et al. 2022), which relates to the shape of the petalodium, ovate ($V7 \geq 30^\circ$) or parallel sided ($V7 \leq 30^\circ$): $V7 = (a+b)$ (**Fig. 3.4 B**).

[V8]: proximal branching angle of first-order branches, which discriminates between zig-zagged ($V8 \geq 20^\circ$) and straight midlines ($V8 \leq 20^\circ$) (**Fig. 3.4 B**).

Four additional variables are ratios of the above variables:

[V9] = [V2]/[V1] petalodium width/length of petalodium

[V10] = [V3]/[V1] length of stem/length of petalodium

[V11] = [V4]/[V1] marginal length of longest first-order branch/length of petalodium

[V12] = [V5]/[V1] width of longest first-order branch/length of petalodium

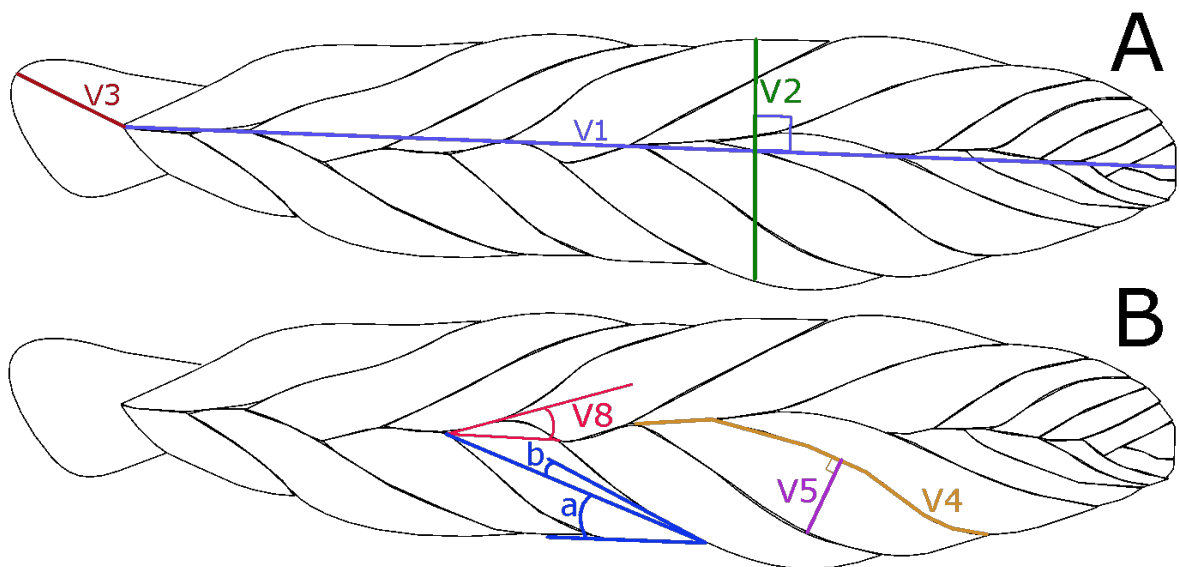


Figure 3.4: idealized *Charnia masoni* from the UK explaining how the different variables were collected.

A) Continuous variables V1, V2, V3. V2 is measured as the longest segment perpendicular to V1 that connect both sides of the specimens; V3 is the longest segment connecting the basal-

most first-order branch to the margin of the “connective tissue/stem”; **B**) continuous variables V4 and V5: V4 is measured as a segmented line best approximating the marginal length of the longest branch, V5 is the longest segment connecting the two sides of the first-order branch that’s perpendicular to V4. V6: $X=|(a-b)/(a+b)$; V7: $a+b$; V8: proximal divergence angle.

A logarithmic transformation was applied to the five continuous variables, generating the transformed variables [tV1]; [tV2]; [tV3]; [tV4]; [tV5] (**Tab. 3.1**). Transformed variables have been shown to produce more accurate representations of population structure (Bak and Meesters, 1998; Meesters et al., 2001) and have been previously used in Ediacaran population analysis (Darroch et al., 2013; Pérez-Pinedo et al., 2023).

Non-equidistant semi-landmarks coordinates were collected using imageJ from the best preserved first-order branch of complete specimens from the Charnian, UK (n=8), Newfoundland, Canada (n=16) and Shibantan, South China (n=3). Measurements were relative to a homologous point at the basal point (closest to the axis) of the largest first-order branch of the petalodium of *Charnia*, by analogy with the methodology of Olsen (2017). The non-equidistant semi-landmarks were transformed into 100 equally spaced landmarks with the package “Stereomorphs” (Olsen and Westneat, 2015) and are arranged in an array of matrices to be used in backtransform morphospace analysis.

Table 3.1: list of measured variables used in this study.

List of measured variables				
Name	Variable	Dimensions	Transformed	NAs
V1	Length of the petalodium	numeric, cm	tV1: logarithmic transformation	0
V2	Width of the petalodium	numeric, cm	tV2: logarithmic transformation	0
V3	Length of the stem	numeric, cm	tV3: logarithmic transformation	MUN: 1
V4	Marginal length of the longest FOB	numeric, cm	tV4: logarithmic transformation	0

V5	Width of the longest FOB	numeric, cm	tV5: logarithmic transformation	0
V6	Morphological descriptor X	numeric, ND	NA	0
V7	Distal divergence angle	angle, degrees	NA	0
V8	Proximal divergence angle	angle, degrees	NA	0
V9	Ratio V2/V1	numeric, ND	NA	0
V10	Ratio V3/V1	numeric, ND	NA	MUN: 1
V11	Ratio V4/V1	numeric, ND	NA	0
V12	Ratio V5/V1	numeric, ND	NA	0

This list includes the names used for each variable used in this manuscript, a description of the variable, the type of variable and the dimensions measured (ND=Non-Dimensional), whether a normalizing transformation was applied and if transformation was not applicable (NA).
 FOB=First-order rangeomorph Branch

5.2. Linear models

To analyze the morphometric distinctions between *Charnia masoni* and the stemmed Newfoundland species, we treated assemblages of specimens from the North Quarry (Charnian, UK; including the type material of *C. masoni*) and the Matthews Surface (Newfoundland, Canada) as two distinct dataset subsets. We initially conducted a two-sample Welch T-Test on each of the continuous variables for the two assemblages, in order to test their statistical dissimilarity and validate our assumptions. Additionally, we performed Shapiro-Wilko tests on the transformed and untransformed variables for each of the two assemblages to test for normality. Size-frequency distribution graphs were also generated for each of the untransformed and transformed continuous variables (V1 to V5; tV1 to tV5).

Further in-depth exploration of the dataset involved computing linear models for pairs of transformed and untransformed continuous variables from the North Quarry and Matthews Surface assemblages of *Charnia* spp. Linear models for each of the two assemblages were subsequently plotted together, with data collected from all other specimens. Assumptions of linearity of the data, normality of the residuals, homoscedasticity and independence of residuals errors were tested for each of the computed linear models.

5.3. Backtransform morphospace

Morphospace plots are compiled using ordination algorithms based on homologous coordinates to represent shape variability in biological populations and can be useful to tackle taphonomic and taxonomic problems in Ediacaran palaeontology (Laflamme et al., 2007; Pasinetti and McIlroy, 2023). The backtransform morphospace analysis algorithm proposed by Olsen (2017) produces a morphospace plot with idealized shapes in the background, allowing easy identification of morphological variations within the plot along with a qualitative visual assessment. The analyses are performed in RStudio with the packages StereoMorph (Olsen and Westneat, 2015) and Geomorph (Baken et al., 2021). The coordinates of equidistant semilandmarks representing the outline of the biggest first-order branches of each specimen were transformed into Procrustes coordinates by performing Generalized Procrustes Analyses (GPA). The GPA algorithm scale shapes and aligns coordinates based on homologous points such that the shape variation can be analyzed with a Principal Component Analysis (PCA).

The function `btShapes` of the StereoMorph package allows plotting of PCA results on a backtransformed morphospace, allowing visualization of the major variation trends in the shape of the first-order branches. Backtransform morphospace analyses were performed on two different sets of data:

- 1) only specimens from the UK and Newfoundland (excluding Inner Meadow) were included, in order to assess and characterize morphological differences between the Newfoundland specimens and *Charnia masoni*.

- 2) data from Newfoundland and the Shibantan biota (South China) were subsequently added to the analysis to determine their taxonomic affiliation.

5.4. PCA and HCPC

Hierarchical clustering based on principal components analyses (HCPC) can be used to tackle taxonomic problems and has been used to define Ediacaran species (Kenchington and Wilby, 2014; Taylor et al., 2019; Hawco et al., 2020), with the RStudio package Factormine (Lê et al., 2008). Our analyses were performed on the whole dataset (specimens from Newfoundland, UK and South China) on a selected number of variables. The HCPC algorithm first computes a PCA from the selected variables. At this step, the number of principal components to be retained in the HCPC is chosen based on visual assessment of the percentage of variation explained by each principal component (Peres-Neto et al., 2005). Hierarchical clustering is subsequently performed on the selected principal component using Ward's Clustering Criterion (Ward, 1963). Since we assume smaller variance within clusters than between clusters (Dillon and Goldstein, 1984), the optimal number of clusters is selected based on the biggest decrease of variance within clusters (cf. the inertia-gain method of Husson et al., 2010). A dendrogram can be produced by projecting the clusters over the first principal component and the final computed clustering is visualized within an ordination with axes PC1 and PC2. Keiser-Meyer-Olkin (KMO) tests (Kaiser, 1970), performed in RStudio with the package Psych (Revelle, 2021) can help identify and select variables suitable for factor analyses. The results of KMO tests, coupled with qualitative assessment of trial principal component analyses, allow determination of the three groups of variables that would explain the highest amount of variability in the dataset, and therefore those that would produce the most reliable clusters. To account for the absence of a stem in many of the Charnian specimens, HCPC.1 and HCPC.3 were performed without including variables that pertain to stem length. Since it has been proposed that one major difference between the UK and the Newfoundland material—a straight versus zig-zagged midline—could potentially be taphonomic (Laflamme

et al. 2007; Hofmann et al. 2008), only analyses HCPC.3 and HCPC.4 included the variable V8, which accounts for differences in midline morphology.

The four HCPC clustering analyses are based on the following variables:

HCPC.1: V6 (descriptor X), V7 (distal divergence angle), V9 (petalodium width/length);

HCPC.2: V6, V7, V9, V10 (stem length/petalodium length);

HCPC.3: V6, V7, V8 (proximal divergence angle), V9;

HCPC.4: V6, V7, V8, V9, V10.

6. Results

6.1. Statistical analyses

Two-sample Welch T-Tests reveal that *Charnia* specimens from the Matthews Surface are significantly different from *Charnia masoni* from the Charnian, UK with respect to both the untransformed variables V2 to V5 and the transformed variables tV2 to tV5 (Fig. 5B-E), but not for V1 and tV1 (Fig. 5A).

Published studies of size-frequency distribution in Ediacaran assemblages are typically right-skewed and assume a gaussian bell distribution shape when a logarithmic transformation is applied (Darroch et al., 2013; Pérez-Pinedo et al., 2023). Size-frequency distribution graphs for the whole dataset, the Charnian subset and the Newfoundland subset, were plotted for both transformed and untransformed variables (Fig. 3.4). The resulting distributions show peaks in the Charnian dataset at higher values of petalodium width (V2 and tV2, Fig. 3.6 B), longest branch length (V4 and tV4, Fig. 3.6 D) and longest branch width (V5 and tV5, Fig. 3.6 E) relative to both the assemblage from the Matthews Surface, Newfoundland, and the entire dataset (including material from the Shibantan biota, China), while all of the subsets show similar distribution peaks of the petalodium length (V1 and tV1). This is consistent with the Welch T-Test results for this variable.

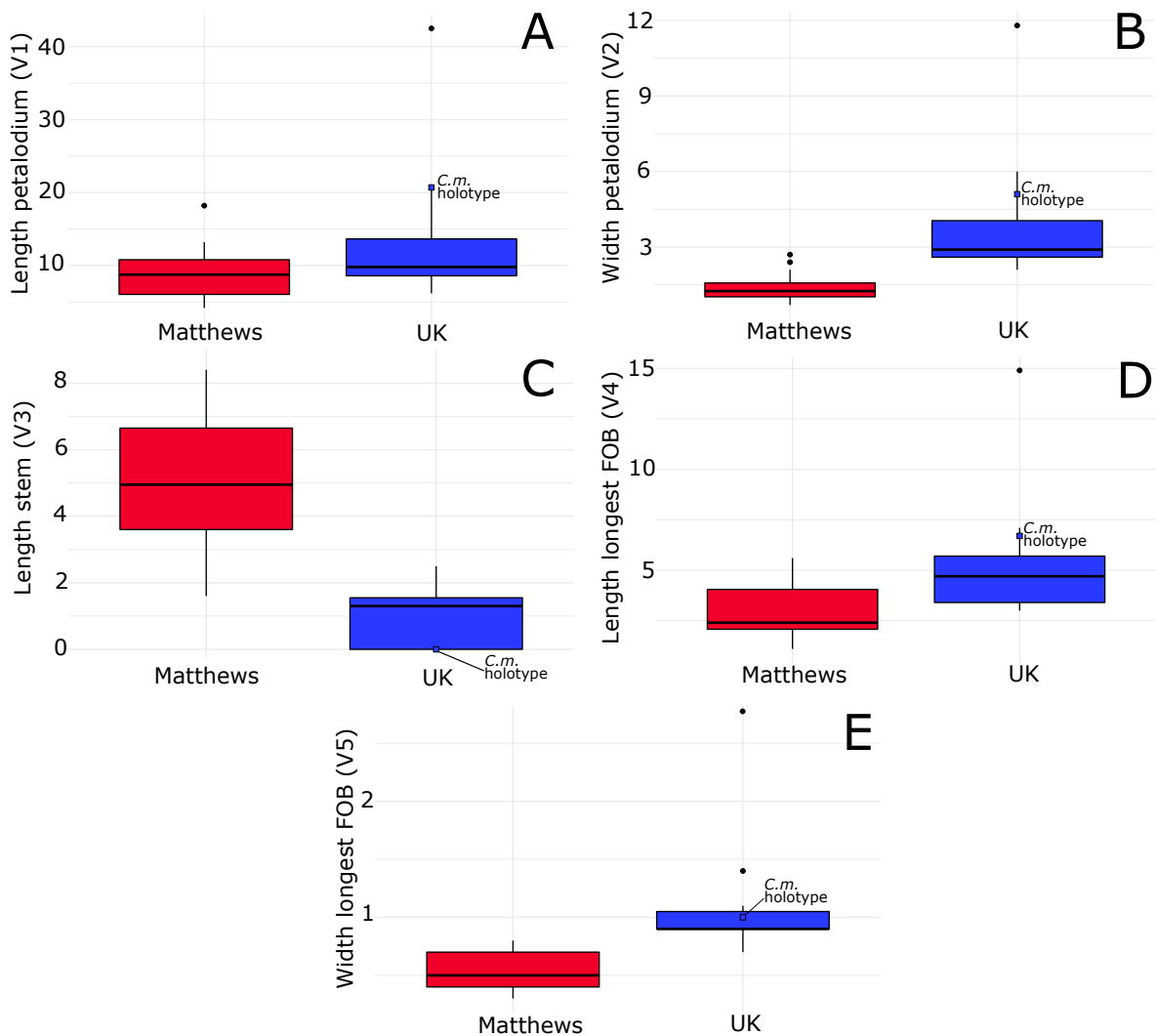


Figure 3.5: box plots showing statistical differences for each of the 5 continuous variables between the two main specimen groups.

Main specimen groups: Matthews Surface (red) and Charnwood Forest (blue). Black dots represent outliers; blue boxes represent the holotype of *C. masoni*. All variables (V1-V5) expressed in centimeters. **A)** V1 length of the petalodium, not significantly different in Matthews Surface vs Charnwood, UK; **B)** V2 width of the petalodium, significantly different in Matthews Surface vs Charnwood, UK; **C)** V3 length of the stem, significantly different in Matthews Surface vs Charnwood, UK; **D)** V4 length of the longest first-order branch, significantly different in Matthews Surface vs Charnwood; **E)** V5 width of the longest first-order branch, significantly different in Matthews surface specimens vs Charnwood, UK.

Distribution peaks of the Matthews Surface assemblage are at higher values of stem length (V3 and tV3) compared to the Charnian material, while *C. gracilis* typically does not have a stem (**Fig. 3.6 C**). The transformed values for the width of the petalodium (tV2) for *C. gracilis* are intermediate between the wide-bodied, ovate, Charnian specimens and the narrow-bodied Newfoundland assemblages (**Fig. 3.6 B**), and have high values of tV4 (longest branch length, **Fig. 3.6 D**), which is most comparable to the Charnian specimens (including the type material of *C. masoni*), but with lower values of tV5 (longest branch width, **Fig. 3.6 E**), while the Newfoundland material show shorter, but relatively wide, longest first-order branches. Descriptor V6 (sinusoidal descriptor X of Wu et al., 2022) effectively discriminates between the sigmoidal first-order branches of *C. masoni* ($X > 0.3$) and the more blade-shaped branches of *C. gracilis* ($0 < X < 0.3$). The nature of the sigmoidal shape, along with first-order branch divergence angles — which are consistently lower in *C. gracilis* (Wu et al., 2022) — enable discrimination between the two species. Our findings confirm these results, with the Charnian material (*C. masoni*) consistently showing higher distribution peaks for V6 (**Fig. 3.6 F**) and V7 (**Fig. 3.6 G**) compared to *C. gracilis*, as well as for V8 (**Fig. 3.6 H**), which appear to effectively discriminate between the zig-zagged midlines of *C. masoni* and the straight midlines of *C. gracilis* and specimens from Newfoundland.

Morphometric characterization of the majority of specimens from Newfoundland demonstrate that the morphology is, to some degree, intermediate between the morphometry of *C. masoni* and *C. gracilis*, with $0.2 < X_{(p2)} < 0.59$. The average first-order branch distal divergence angle (V7) in the Matthews Surface assemblage is 30° which is greater than the range of 18° - 20° reported for *C. gracilis* (Wu et al., 2022) and on the lower end of the 26° - 44° range reported herein for *C. masoni*. The proximal divergence angle of first-order branches (V8) discriminates between straight (low V8) and zig-zagged (high V8) midlines, since the appearance of the midline depends on how much the distal portion of each first-order branch

crosses to the opposite side of the organism (**Fig. 3.4 B**). The typically zig-zagged axis of *C. masoni* from the Charnian of the UK show higher distribution peaks of V8, around 25°, which is distinct from the lower distribution peaks of the Matthews Surface *Charnia* (approx. 12°) and the *C. gracilis* material (approx. 8°), which both have essentially straight midlines. By comparing ratios of the continuous variables, we show that the Charnian material has petalodia with first-order branches that are relatively broad (V9, **Fig. 3.7 A**), long (V11, **Fig. 3.7 C**) and wide (V12, **Fig. 3.7 D**) relative to the Newfoundland material, but with comparatively shorter stems (V10, **Fig. 3.7 B**).

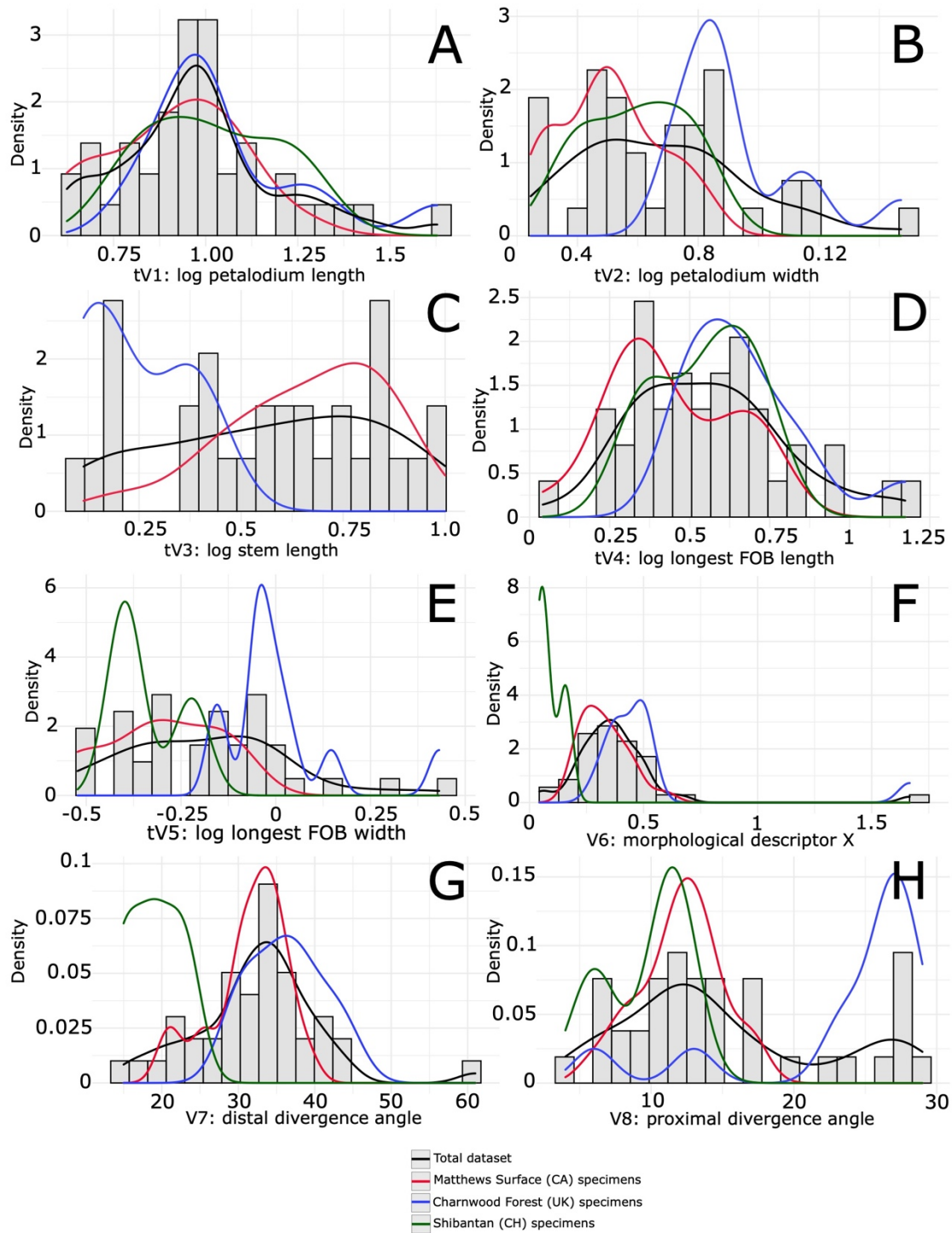


Figure 3.6: size frequency distribution graphs for the first 8 variables.

A) distribution of tV1 (natural logarithm of the petalodium length (cm)); **B)** distribution of tV2 (natural logarithm of the petalodium width (cm)); **d)** distribution of tV3 (natural logarithm of the stem length (cm)), *C. gracilis* does not have a stem and it is not included ; **C)** distribution of tV4 (natural logarithm of the longest first-order branch length (cm)); **E)** distribution of tV5 (natural logarithm of the longest first-order branch width (cm)); **F)** distribution of V6

(morphological descriptor X measured on the longest first-order branch, discriminating between straight ($X < 0.3$) and sigmoidal ($X > 0.3$) first-order branches); **G**) distribution of $V7$ (distal divergence angle of the longest first-order branch); **H**) distribution of $V8$ (proximal divergence angle of the longest first-order branch, discriminating between straight (low $V8$) and zig-zagged midlines (higher $V8$)).

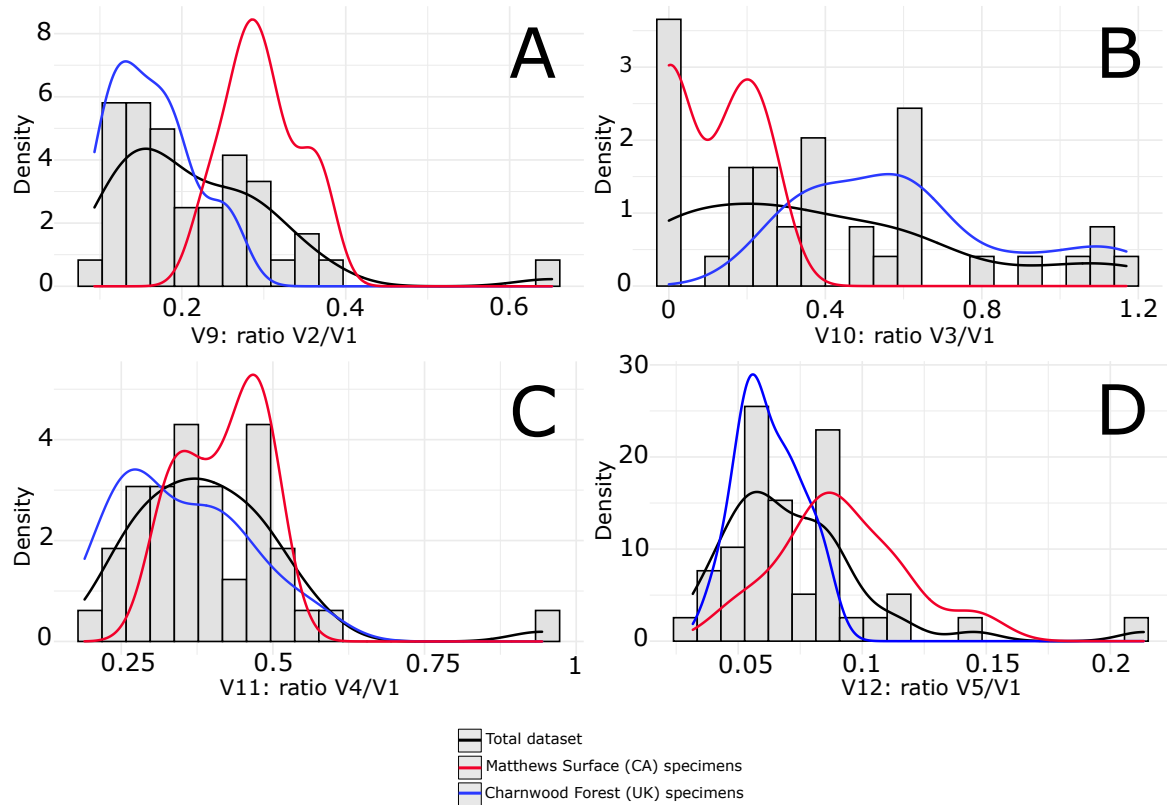


Figure 3.7: size frequency distribution graphs of the ratios of the continuous variables (cm) over the length of the petalodium ($V1$; cm).

A) distribution of the ratio of $V2$ (width of the petalodium) over $V1$; **B)** distribution of the ratio of $V3$ (length of the stem) over $V1$; **C)** distribution of the ratio of $V4$ (length of the longest first-order branch) over $V1$; **D)** distribution of the ratio of $V5$ (width of the longest first-order branch) over $V1$.

Linear models computed for each of the two assemblages found some similar trends as well as several important differences. A strong linear relationship was found between the length

of the petalodium (tV1) and its width (tV2) for *C. masoni* from the UK and the Matthews Surface material from Newfoundland (**Fig. 3.8 A**). No significant correlations are found between the ratio width/length of the petalodium (V9) and the length of the petalodium (V1) for the Matthews Surface assemblage, while the *C. masoni* from the Charnian of the UK does not meet the assumptions for linear models (**Fig. 3.8 D**).

The Charnian *C. masoni* do not show any significant correlation between the length of the stem (tV3) (if they present one) and the length of the petalodium (tV1), while the Matthews Surface specimens have a strongly positive linear relationship (**Fig. 3.8 B**). The correlation between the ratio (V10) of the length of the stem (V3) divided by the length of the petalodium (V1) and the length of the petalodium is negative for the Matthews Surface material, but not significant for *C. masoni* from the Charnian. The marginal length (tV4) and the width (tV5) of the longest branch show positive correlation with the length (tV1) and the width (tV2) of the petalodium in both the Charnian *C. masoni* and Matthews Surface assemblages (tV4 vs tV1, **Fig. 3.8 C**). Specimen UK10 from the Charnian assemblage, as well as the arbitrarily chosen outlier *Culmofrons plumosa*, are found to be outliers in all of the significant linear models.

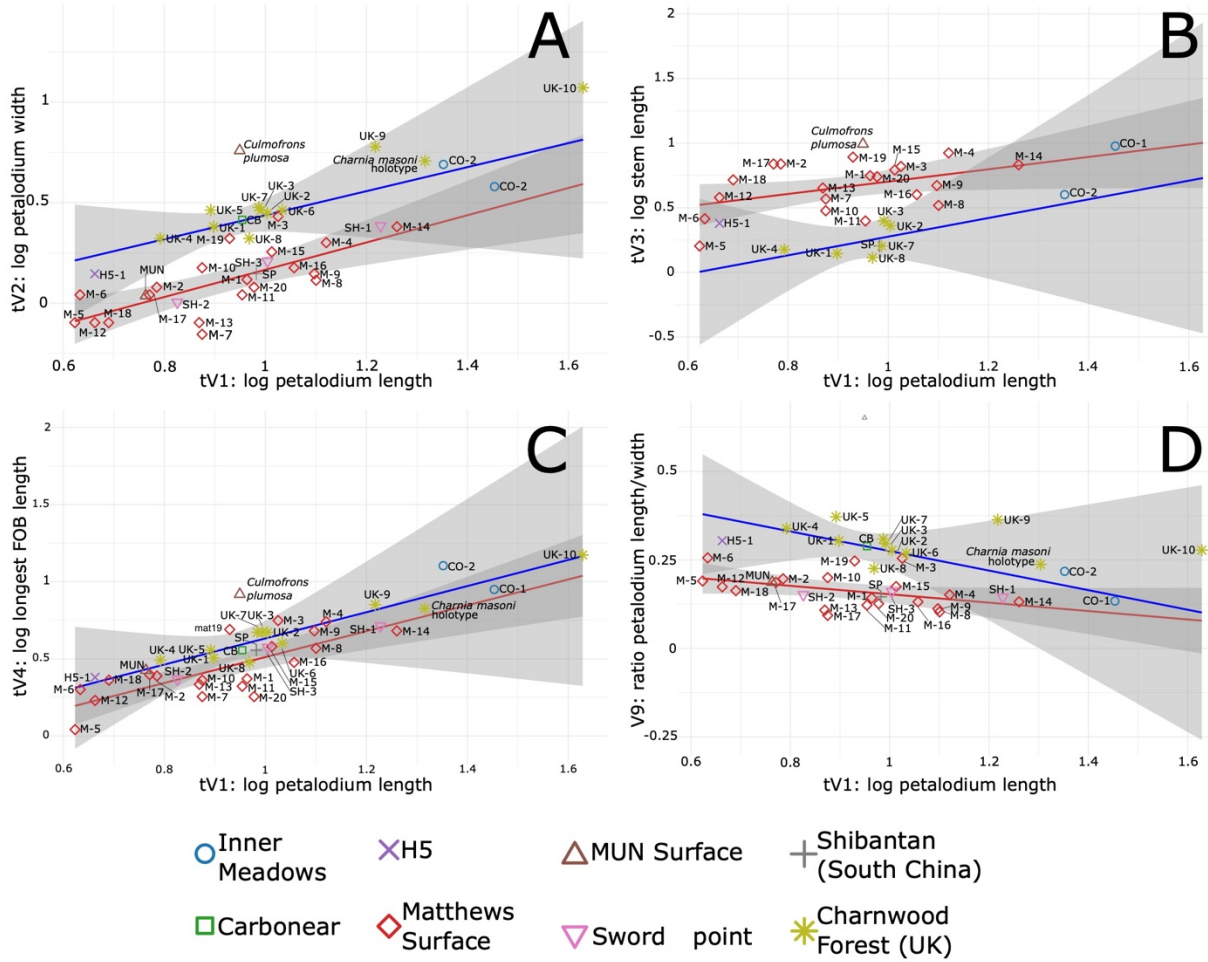


Figure 3.8: linear models for different transformed and untransformed variables.

The Matthews (red line) and the Charnian (blue line) populations are treated independently. Additional *Charnia* sp. specimens from Newfoundland, *Charnia gracilis* specimens and *Culmofrons plumosa* are plotted for comparison but not included in the linear models. **A)** linear model between the natural logarithm of the length of the petalodium vs natural logarithm of the petalodium width; **B)** linear model between the natural logarithm of the length of the petalodium vs natural logarithm of the stem length (specimens without a stem are excluded); **C)** linear model between the natural logarithm of the length of the petalodium vs natural logarithm of the longest first-order branch marginal length; **D)** linear model between the untransformed length of the petalodium vs the ratio petalodium width/petalodium length.

6.2. Backtransform morphospace

Two set of backtransform morphospace analyses were performed, first on well-preserved specimens from P1, P2, MUN Surface and H5, and then with the inclusion of two *Charnia gracilis* specimens from the Shibantan biota, and the Inner Meadow material.

The first backtransform morphospace ordination (**Fig. 3.9 A-B**) found that the first two principal components (PC1 and PC2) explain the large majority of the shape variability (respectively 45% and 23%), with PC3 dropping to only 11%. PC1 broadly describes the shape of first-order branches, with elongated and increased sigmoidal curvature to the left of the graph, and straighter branches towards the right of the graph (**Fig. 3.9 A**). PC2 appears to be correlated with width of the first-order branches and their proximal insertion angles. Wider and shorter branches with higher insertion angles are at lower values of PC2, and slimmer branches are at higher values of PC2. PC3 broadly correlates with branches that are either more proximally inflated (higher PC3 values) or less proximally inflated (lower PC3 values). Both the Charnian and Matthews Surface specimens occupy a large morphospace, even though the Charnian material has greater variability and some specimens that plot far apart. This is consistent with the Charnian material having large morphological variation. The relative dimensions of the wider first-order branches is also large. The assemblage includes: small (presumably juvenile) specimens; e.g. UK-4; **Fig. 3.9 A-B**); to adult specimens (e.g. UK-8; **Fig. 3.9 A-B**); and specimens that have been considered to be super-mature (e.g. the holotype of *C. masoni* and UK-10, **Fig. 3.9 A-B**; cf. Wilby et al., 2015; Dunn et al., 2019a). In contrast, the Matthews Surface material, as well as the two other specimens from the Catalina Dome (MUN and H5), plot close together, varying mostly along the PC2 and PC3, while occupying the portion of PC1 that represents specimens with a pronounced sigmoidal curvature.

When the completely preserved *Charnia gracilis* specimens from the Shibantan biota are added to the analyses, along with the problematic specimens from the Inner Meadow locality, Newfoundland, the greater shape variability in the dataset makes it difficult to interpret the variation along the different principal components. A large portion of the variation (39%) is described by PC1 (**Fig. 3.9 C**), which encompasses variation in the ratio between width and length of widest first-order branches. PC1 is also correlated with an increase of the proximal divergence angle observable from the left to the right of the graph (**Fig. 3.9 C**). Principal Component 2 (34% of the variation) correlates with the degree of sigmoidal curvature in the first-order branches, with straighter branches having lower values within PC2, and sigmoidal branches having higher values (**Fig. 3.9 C-D**). PC3 explains only a small amount of variation in the dataset (9%) and is difficult to interpret. The Charnian *C. masoni* occupy the largest portion of the PC3 morphospace, almost entirely overlapping the morphospace occupied by the Matthews Surface material and the other Newfoundland material from Conception Bay and Sword Point.

The material of *C. gracilis* from Shibantan, China, plots away from the rest of the *Charnia* specimens, segregating in the lower left corner of the ordination in PC1 and PC2 (**Fig. 3.9 C-D**). Specimens from Inner Meadow plot along with *C. gracilis*, which they share with them the elongated, almost straight, first-order branch outline and their extremely low proximal insertion angles, even though they are much bigger than the type material of *C. gracilis*.

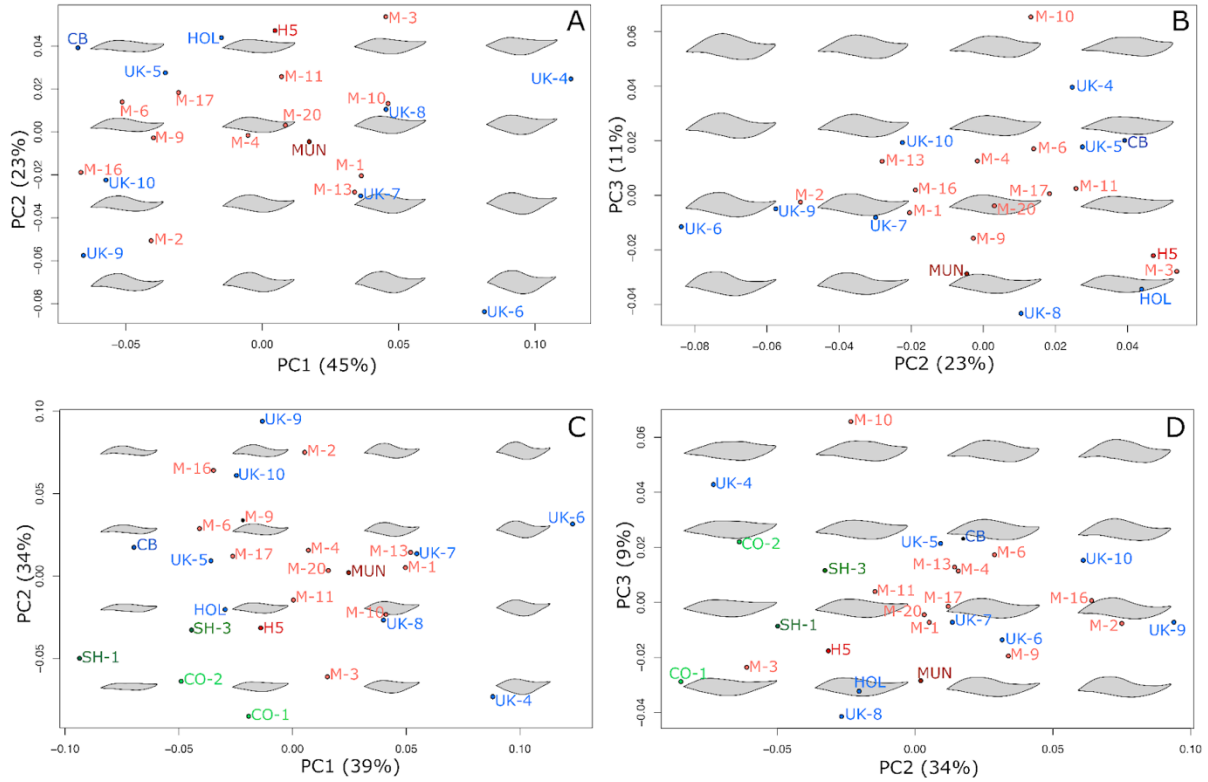


Figure 3.9: backtransform morphospace analyses of the largest first-order branch of each specimen.

A) Backtransform morphospace projection of PC1 and PC2 based on the Canadian (Red) and the British (Blue) material; **B)** backtransform morphospace projection of PC2 and PC3 based on the Canadian and the British material; **C)** backtransform morphospace projection of PC1 and PC2 based on the Bonavista, Charnian and Shibantan (Green) material; **D)** backtransform morphospace projection of PC2 and PC3 based on the Bonavista, Charnian and Shibantan material.

6.3. Hierarchical clustering based on principal components (HCPC)

The MUN surface specimen was excluded from the hierarchical clustering because the stem is not preserved (damaged by rockfall). The hierarchical clustering of principal components HCPC.1 includes variables that account for the shape of the petalodium: the ratio width/length (V9) broadly describes the shape of the petalodium, while the variables V6 and V7 describe the shape of the first-order branches and their angle of divergence from the outline of the petalodium. HCPC.1 (**Fig. 3.10 A-B**) finds 4 clusters as the most likely solution. The clustering assigns all the specimens of *C. gracilis* from the Shibantan biota, as well as four specimens from the Matthews Surface and both Inner Meadow specimens to cluster 1. Cluster 2 encompasses the majority of the Matthews Surface material, as well as the only complete Sword Point specimen. In this analysis, UK10 constitutes a cluster by itself, away from the other specimens including the other *Charnia* from the Charnwood Forest. Cluster 4 contains all of the specimens from the Charnian of the UK, except UK10, as well as some material from Newfoundland (the H5 specimen, the Carbonear specimen (CB1) and two specimens from the Matthews Surface).

The HCPC.2 (**Fig. 3.10 C-D**) analyses take into account the presence of a stem (V10) and show very similar results to HCPC.1, finding 4 similar clusters. Cluster 1 finds similarities between the *C. gracilis* material and the Inner Meadow specimens, while cluster 2 groups together the majority of the Newfoundland material. As with HCPC.1, specimen UK 10 is an outlier, while all the other Charnian material and CB1 from Carbonear, Newfoundland, group together in cluster 4. However, no Matthews Surface specimens are included in cluster 4, and the inclusion of H5-1 in either cluster 2 or cluster 4 is not well supported. Excluding UK10 yields similar results in both HPCP analyses. The HCPC.1 and auxiliary clustering analyses on other combinations of variables tend to group Shibantan material together, and close to the

Inner Meadow specimens, with which they share a low petalodium width/length ratio, first-order branches that are narrow and elongated, a very low proximal divergence angle, and the absence of a stem. The two specimens from Inner Meadow have a long and wider petalodium than the complete *C. gracilis* specimens included herein, but dimensions are consistent with those of the larger (incomplete) specimens reported by Wu et al. (2022).

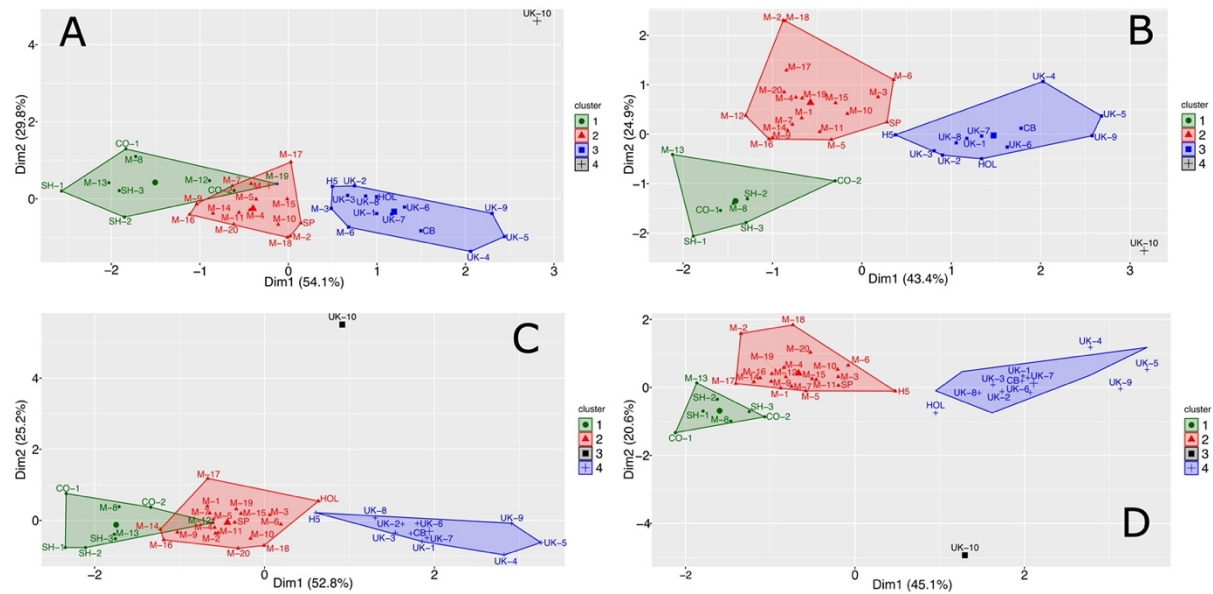


Figure 3.10: HCPC clusters solutions computed on PCA based on different variables.

A) HCPC.1 finds 4 clusters, variables: ratio width/length (V9), morphological descriptor X (V6), distal divergence angle (V7); **B)** HCPC.2 finds 4 clusters, variables: ratio width/length (V9), morphological descriptor X (V6), distal divergence angle (V7), ratio stem length/petalodium length (V10); **C)** HCPC.3 finds 4 clusters, variables: ratio width/length (V9), morphological descriptor X (V6), distal divergence angle (V7), proximal divergence angle (V8); **D)** HCPC.4 finds 4 clusters, variables: ratio width/length (V9), morphological descriptor X (V6), distal divergence angle (V7), proximal divergence angle (V8), ratio stem length/petalodium length (V10).

Both HCPC.3 (**Fig. 3.10 C**) and HCPC.4 (**Fig. 3.10 D**) consider the proximal divergence angle, a trait that encapsulates differences between specimens with straight vs zigzagged midlines. The analysis HCPC.3 does not account for the presence of a stem and

results in four groups that encompass: 1) the *C. gracilis* material from Shibantan and the Inner Meadow Surface specimen; 2) most of the *Charnia* specimens from Matthews Surface (18 out of 20); 3), most of the *Charnia* from the Charnian (9 out of 11); and 4) a single specimen of *Charnia* from the Charnian (specimen UK10), which clusters by itself (**Fig. 3.10 C**). The analysis HCPC.4 includes all of the measured variables—including the presence/absence of a stem—in the same analysis, producing clustering solutions consistent with the results of the previous HCPCs (**Fig. 3.10 D**). Cluster 1 is composed of the *C. gracilis* material, the Inner Meadow material and two of the Matthews Surface specimens. Cluster 2 contains all of the remaining specimens from Newfoundland, except for CB1 (from Carbonear), which clusters with all of the Charnian *Charnia masoni* material in cluster 4, and specimen UK10 is isolated in cluster 3 from all the other clusters as in the other HCPC analyses.

6.4. Bonavista Peninsula *Charnia* sp.

Two species of *Charnia* have previously been described from the Ediacaran of Southern Avalon Peninsula: *Charnia wardi* (Narbonne and Gehling, 2003) and *Charnia antecessens* (Laflamme et al., 2007). However, *C. wardi* was reassigned to *Trepassia* (Narbonne et al., 2009) and *C. antecessens* to *Vinlandia* (Brasier et al., 2012), leaving *Charnia masoni* as the only species of the genus reported from the Newfoundland (Narbonne, 2004; Narbonne et al., 2009; Brasier et al., 2013) and one of the only two valid species of the genus, along with *C. gracilis* (Wu et al., 2022).

Most of the *Charnia* specimens found from the Bonavista Peninsula show important morphological distinctions from both *C. masoni* and *C. gracilis*. The presence of a stem and lack of a prominent zig-zagged axis in *Charnia* from the Bonavista Peninsula material has been noted previously (Laflamme et al., 2007; Hofmann et al., 2008). The unusual parallel sided nature of the Bonavista Peninsula material has been noted previously (Laflamme et al., 2007; Dunn et al., 2019), contrasting with the more ovate *C. masoni*. Those specimens were interpreted as taphomorphs of *C. masoni* in which the distally furled first-order branches were partially excluded from the preservational plane due to lifting by a current (Laflamme et al., 2007).

The extremely well-preserved *Charnia* sp. from the Matthews Surface do not show any distal degradation in preservational quality, which is expected in the taphonomic model of Laflamme et al. (2007), having sharp lateral margins and microbial matground features that abut closely against the fossils, which argues against temporary lifting prior to casting (**Fig. 3.11 E**).

The presence of stems and holdfasts in the Bonavista material, features absent in typical *C. masoni*, was considered problematic by Hofmann et al. (2008), who did not support the

taphonomic explanation for the straight midline in some *Charnia*, preferring to invoking the possibility of dissimilar “ventral and dorsal [sic]” sides to *C. masoni*. Subsequent work, (Dunn et al., 2019) treated parallel vs curved margined *Charnia* as two morphs of the same species (“parallel-sided” and “ovate” *C. masoni*), without addressing how the taphonomic considerations of Laflamme et al. (2007) might affect their differences.

6.5. Systematic Palaeontology

Although undoubtedly assigned to the genus *Charnia*, our morphometric analyses show that the parallel-sided *Charnia* from Newfoundland have notable morphometric differences from the type material of both *C. masoni* and *C. gracilis*. We therefore propose the creation of a new species of *Charnia*, which is to the best of our knowledge only known from the Bonavista Peninsula, including the Matthews Surface assemblage, Locality H5 of Hofmann et al. (2008) and the MUN Surface near Burnt Point, Catalina Harbour.

Clade: Rangeomorpha Pflug, 1972

Genus: *Charnia* Ford, 1958

Species: *Charnia ewinoni* sp. nov.

2008 *Charnia masoni* Hofmann et al. p. 17. figs 13.1; 13.4; 13.5

2015 *Charnia masoni* Liu et al., p. 1361, fig. 2d

2019 *Charnia masoni* Dunn et al., p. 167-168, fig. 7-8

2019 *Charnia masoni* Liu & Dunn, p. 1326, fig. 4d

2023 *Charnia masoni* Pasinetti & McIlroy, p. 4, fig. 3c

Holotype: The holotype remains in-situ on the Matthews Surface, with the plastotype being deposited at the Rooms (NFM ***; **Fig. 3.11 A, E**).

Paratype: three paratypes were selected from the Matthews Surface: A (**Fig 3.11 B**); B (**Fig. 3.11 C**) and C (**Fig. 3.11 D**). The paratypes are preserved in situ, and a plastotype of paratype A is deposited to the Rooms (NFM ***). Paratype C has a partially preserved petalodium and was not included in the statistical analyses.

Etymology: The species name of *C. ewinoni* is derived from the Beothuk word "ewinon", meaning feather. We use the Beothuk language to honour and remember the original inhabitants of the island of Newfoundland at the time of European colonization.

Diagnosis: *Charnia* species characterized by an elongated, parallel-sided petalodium, tapering at the apical end and attached to at the base to an elongated stem which may end in a basal globose or discoidal structure. First-order branches vary in shape from sigmoidal (majority) to straight (uncommon), and diverge from the midline with an average proximal angle of 12° and an average distal angle of 31°. The baso-proximal portions of the first-order branches connect across the axis of the petalodium, alternating left and right of a relatively straight midline that develops baso-apically with glide-plane symmetry. First-order branches are composed of sub-rectangular second-order branches, which are divided into third-order branches that diverge distally in the basal direction. Only faint impressions of fourth-order branches can be observed.

Occurrence: Mistaken Point and Trepassey formations of the Catalina Dome on the Bonavista Peninsula of Newfoundland – Discovery UNESCO Global Geopark.

Description: *C. ewinoni* specimens from the Bonavista Peninsula have a unipolar frond, characterized by an elongated and parallel-sided petalodium, connected to an elongated stem terminating in a discoidal structure. The petalodium is preserved as negative impression of the bottom of the organism on the fossiliferous surface, sharply separated from it by a slightly raised ridge that outlines its shape, while the stem is typically preserved as a positive impression on the fossiliferous surface (cf. **Fig. 3.11 A-B**). The frond is typically straight, but four specimens, including paratype B (**Fig. 3.11 C**) are bent in proximity of the junction between the stem and the petalodium and one specimen is slightly bent (~20%) in the mid-portion of the petalodium.

The *C. ewinoni* in our study (N = 20) show petalodium lengths ranging from 4.2 cm to 18.2 cm (holotype: 7.5 cm) with an average of 8.5 cm, and petalodium widths between 0.7 cm and 2.7, with an average of 1.4 cm (holotype 0.8 cm). Average width/length ratio of the petalodium is 0.17 cm and stem lengths range from 1.6 cm to 8.4 cm (holotype: 4.5 cm), with the mean ratio between stem length and petalodium length 0.6.

The petalodium is typically composed of about 9-12 first-order branches per side, alternatingly inserting on an axis following a relatively straight midline, with low proximal divergence angles (approx. 12°) and distal divergence angles ranging from 21° to 39° with an average of 31°. The first-order branches are composed of about 10-12 sub-rectangular second-order branches, which are at approximately 90° to the axis of the first-order branches, and easily seen in the holotype (**Fig. 3.11 A**). Third-order branches, when preserved, are perpendicular to the second-order branches, but diverge distally in their basal portion, towards the sides of the organism (**Fig. 3.11 D-E**). Only faint impressions, suggesting the presence of a fourth order of branches, can be observed, especially in paratype C (**Fig. 3.11 D**).

Remarks: First-order branches have highly variable shape, ranging from blade-like and elongated (comparable to *C. gracilis*) to sigmoidal (similar to *C. masoni*). First-order branches are insert at a low angle on the midline (**Fig. 3.11 A-C**), dissimilar to the more pronounced zig-zagged midline of *C. masoni*.

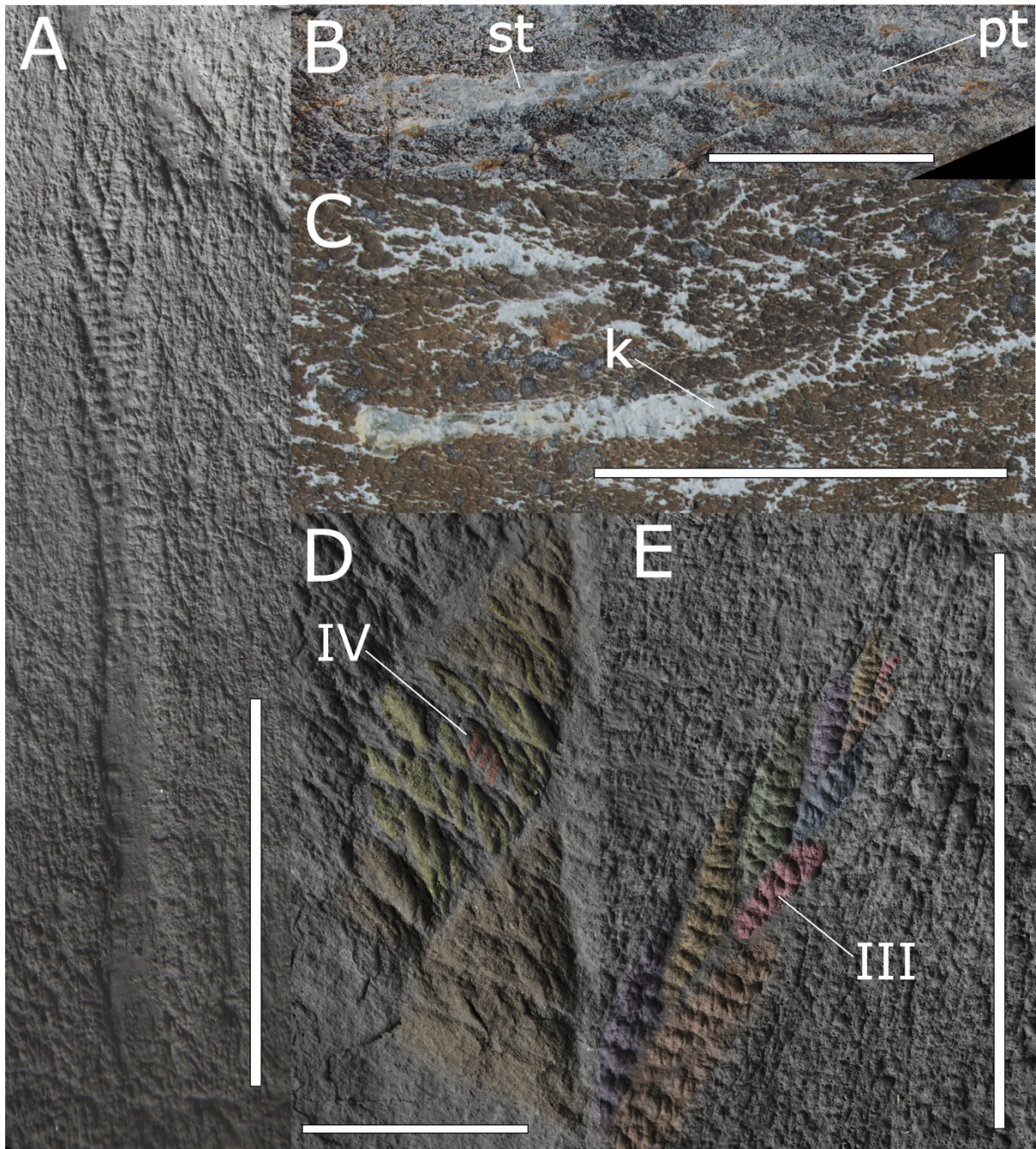


Figure 3.11: holotype and paratype of *Charnia ewinoni*.

A) Holotype of *C. ewinoni* from the Matthews surface. Note the parallel-sided petalodium, straight midline, sigmoidal first-order branches, presence of stem; B) Paratype A, note the positively preserved stem (“st”) and the negatively preserved petalodium (“pt”); C) Paratype B, kinked (“k”) between the stem and the petalodium portions D) branching in paratype C, showing branching details in orange: second-order branches, in green: third-order branches, in red: faint fourth-order impressions (“IV”); e) detail of the well preserved apical portion of the holotype, third-order branches (“III”).

7. Discussion

7.1. Bonavista Peninsula specimens

Different independent statistical analyses quantify the morphological difference between the type material of *Charnia masoni* and *C. gracilis* and support the creation of, *C. ewinoni* sp. nov., represented by specimens from both the Matthews Surface (Liu and Dunn, 2020), the MUN Surface (Liu et al., 2016), and the H5 locality of Hofmann et al. (2008).

The most notable difference between *C. masoni* and *C. ewinoni* is the presence of a stem in *C. ewinoni*, whose length is strongly correlated to the length of the petalodium, a morphological trait not preserved in the other two species of *Charnia*. The exception to this is the small “connective structures” in *C. masoni* documented by Dunn et al. (2019) and the “globose structures” associated with one specimen of *C. masoni* and one specimen of *C. gracilis* (cf. “holdfasts” of Wu et al., 2022, fig 2.1).

Size frequency distribution graphs show different distribution peaks for the three species for all of the variables pertaining to the dimensions of the petalodium, apart from the length. However, measured lengths of the petalodia range from 6.2 cm to 42.5 cm in the UK material, while they are restricted between 4.2 cm and 18.2 cm in *C. ewinoni* suggesting a lower variability in length for the taxon.

Although all branches in *C. masoni* are sigmoidal, they show higher variability in branch shape than the other two species, attested to by a larger morphospace occupied (**Fig. 3.9**), and a wider range of sigmoidal curvature (**Fig. 3.6; 3.9**). First-order branches of *C. masoni* have large variability in their length and width both within a specimen and in the species as a whole. Both *Charnia gracilis* and *C. ewinoni* have tightly constrained first-order branch shapes and occupy a substantially smaller morphospace than *C. masoni* (**Fig. 3.9**). *Charnia ewinoni* typically have narrow sigmoidal first branches, with descriptor X values around 0.3,

which is the threshold between sigmoidal and straight first-order branches (Wu et al., 2022). The sinuosity of *C. ewinoni* first-order branches is intermediate between that of *C. masoni* and *C. gracilis* (X values range from 0.2 to 0.59), and branch shapes similarly occupy an intermediate morphospace (**Fig. 3.9 B**). *Charnia gracilis* have the most tightly constrained branch shapes, with straight and elongated blade like branches consistently showing X descriptor values below the 0.3 threshold of Wu et al. (2022).

Low angles of proximal insertion of the first-order branches in *C. ewinoni* result in a straight midline that clearly discriminates it from *C. masoni*, which has a zigzagged midline. Since branch morphologies of *C. masoni* and *C. ewinoni* are similar, and their morphospaces overlap, differences in petalodium shape and midline morphology are to be attributed to the organizational differences observed in the arrangement of the first-order branches in the petalodium, rather than taphonomic differences and marginal curling as previously suggested (Laflamme et al. 2007; Hofmann et al. 2008), which would result in non-overlapping morphospaces.

The only specimen from Newfoundland with a zig-zagged midline is from Carbonear (Conception Bay, Newfoundland). When assessed using linear models and hierarchical clustering algorithms, this specimen plots consistently with *C. masoni* pertaining to length and width of the petalodium, length of the stem and shape and angles of the first-order branches and therefore we consider them to be likely conspecific.

Even though some specimens of *C. ewinoni* plot with *C. gracilis* in some HCPCs, backtransform morphospace analyses support the taxonomic segregation of *Charnia gracilis* specimens from both *C. masoni* and *C. ewinoni*. The specimens from the Inner Meadow locality consistently plot with *C. gracilis* in both HCPCs and backtransform morphospace analyses and are tentatively considered conspecific, extending the range of the species from S. China to Newfoundland.

7.2. Other specimens from Newfoundland

Charnia ewinoni appears to be endemic to the Bonavista Peninsula, while other *Charnia* specimens from the Avalon Peninsula (Carbonear, Inner Meadow and Sword Point specimens) are problematic and can only be tentatively assigned to other *Charnia* species.

The Carbonear specimen of *Charnia* (CB1, **Fig. 3.12 A**) is very similar in shape to some *C. masoni* from the Charnian of the UK and similarly has a zig-zagged midline and no stem, therefore representing a probable *C. masoni*. There are also two incomplete *C. masoni* specimens from the E Surface at Mistaken Point (**Fig. 3.12 B**). The attribution of other material from Newfoundland to *C. masoni* is not supported by our analyses (Narbonne et al., 2009, fig. 11; Liu et al., 2015, fig. 2d; Liu and Dunn, 2020, fig. 7-8).

Even though only one specimen from Sword Point was complete enough to be included in our dataset, the surface has 15 specimens, which are unsuitable for statistical analyses due to tectonic distortion and poorly preserved portions of the petalodia. Specimens from this locality have a parallel sided outlines rather similar to that of *C. ewinoni* and may have a short stem with a small circular basal disc about the thickness of the stem. The *Charnia* specimens from Sword Point also have a strongly zig-zagged midline (**Fig. 3.12 B**), similar to that of *C. masoni*, a species which also sometimes has a short stem and—tenuous—evidence for a basal disc (see Dunn et al., 2019), making the species-level identification of the Sword Point population problematic.

The Inner Meadow *Charnia* (**Fig. 3.1 C**; **3.12 D**) have several peculiarities: both specimens have a large number of first-order branches (20+ per side), which is similar to the problematic Charnian specimen UK10. The Inner Meadow material has very low proximal and distal divergence angles, as well as straight first-order branches with low morphological descriptor X values and a very subtle if not absent sigmoidal curvature. HCPCs and

backtransform morphospace ordinations both find the Inner Meadow material to be comparable to *C. gracilis* due to their straight first-order branch morphology and their low divergence angles (Fig. 3.12 D).

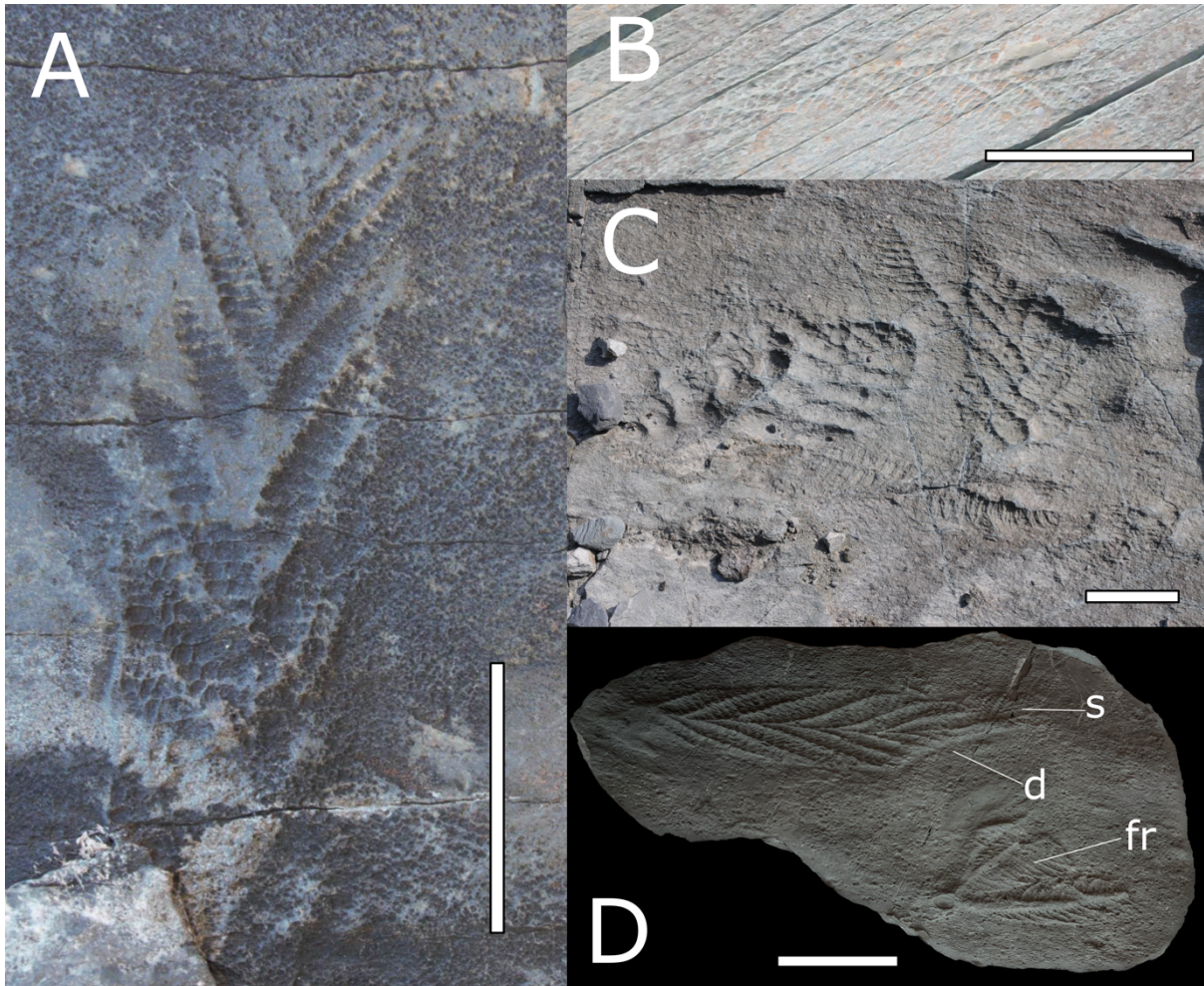


Figure 3.12: other *Charnia* specimens from Newfoundland.

A) *C. masoni* from Carbonear; **B)** problematic *Charnia* from Sword Point, note the parallel-sided petalodium and the zig-zagged midline; **C)** two *C. masoni* from the E Surface (MPER), note the accentuated zig-zagged midline and the ovate outline; **D)** *Charnia* from the EM Coombs Surface, Inner Meadow, compared to *C. gracilis*. Note the straight, elongate first-order branches, as well as damage in the petalodium (“d”) followed by two-dimensional secondary growth (“s”), which is difficult to reconcile with an erect lifestyle. An unrelated, undescribed frond (“fr”) is also present.

7.3. Orientation of the Matthews Surface specimens

Field measurements of climbing ripples within a sandstone about 1.5 m above the Matthews Surface document turbidity currents towards 190°. Other published current orientations (Mason et al. 2013) from the south of the Catalina Dome suggest palaeocurrents towards the west or south-west in the Catalina Member, becoming south to south-east direction in the Upper Port Union Member. Observations from Ichaso et al. (2007), Wood et al. (2003) and Mason et al. (2013) propose the presence of contourite currents running perpendicular to the downslope direction of the turbidites in the Bonavista and Avalon depositional basins (Ichaso et al. 2007) though there is little objective evidence for this in the Catalina Dome successions.

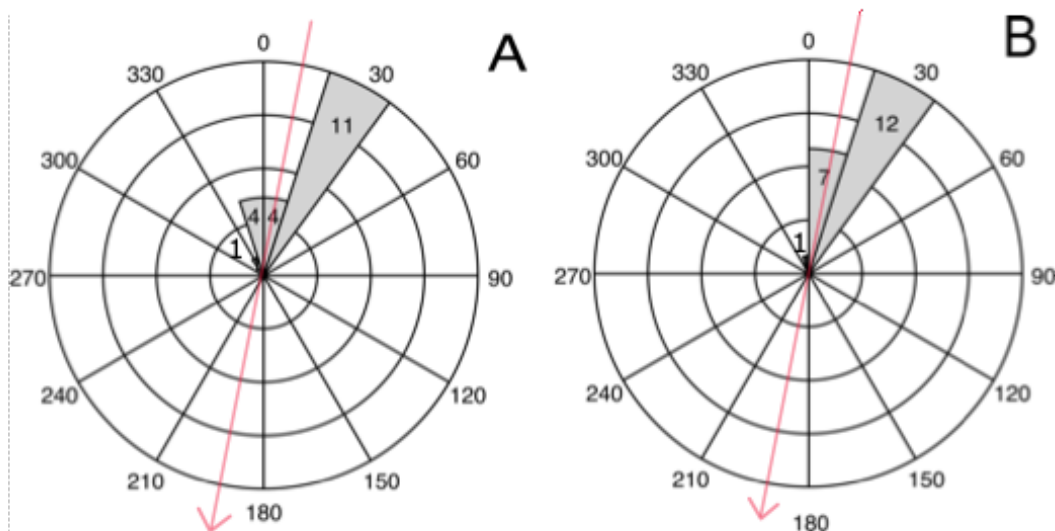


Figure 3.13: rose plots showing the orientation of the petalodia and the stems *C. ewinoni* specimens on the Matthews Surface.

Size of the bins proportional to the number of specimens in a certain orientation. **A)** orientation of the petalodia (n=20) **B)** orientation of the stems (n=20). Red arrows indicate the current direction (10°-190°).

Specimens of *Charnia ewinoni* from the Matthews Surface have a preferential orientation both for the petalodium and the stem, which can be slightly different in the same specimens, since most of them (14 out of 20) are slightly bent at the point of junction. Petalodia are mostly oriented with the apical pole pointing between 0° and 30°, with an average of 12° (**Fig. 3.13 A**), while the stems have an average orientation of 17° (**Fig. 3.13 B**) and there is an average angle of 8° between the two structures. Another frondose organism from the same surface, the arboreomorph *Arborea* sp., which is generally considered to have been erect (Vixseboxse et al. 2022; Pérez-Pinedo et al. 2023; McIlroy et al. 2023) is recorded to have an orientation towards 170°, which is almost orthogonal to that of *Charnia*. This, along with the physical sedimentary structures demonstrates that *C. ewinoni* is preferentially orientated into the current, perhaps in a rheotropic manner (cf. McIlroy et al. 2023).

7.4. *Charnia-Fractofusus* life-association

Fractofusus andersoni is the most abundant rangeomorph species in the Catalina Done, with hundreds of specimens preserved on the Johnson Discovery Surface (cf “Locality 14” of Hoffman et al., 2008; Mitchell et al., 2015). *Fractofusus andersoni* typically has a rounded oval outline, with two poles and two rows of first-order rangeomorph branches, which are inserted perpendicular to the zig-zagged midline in an alternating fashion (Gehling and Narbonne, 2007; Hofmann et al., 2008; Taylor et al., 2023). Each first-order branch has two broadly symmetrical rows of second-order branches, which are divided into third-order branches, in a typical “displayed rangeomorph structure” (*sensu* Brasier et al., 2013). The midline of *F. andersoni* is generally intact and not prone to the common bending/kinking of the congeneric *Fractofusus misrai* (cf. Taylor et al., 2023).

On the Matthews Surface, *Fractofusus andersoni* is of low abundance, but has the idiomorphic rounded ellipsoidal morphology. However, some specimens can be found in direct association with either the stem or the petalodium of *Charnia* specimens, in which instance they have less regular outlines. The outline of *F. andersoni* can be interrupted by a reduced growth of the second-order branches within the first-order branch where it is in close proximity, or in direct contact with, the stem of *Charnia ewinoni* (**Fig. 3.14 A-B**). One regular *Fractofusus* specimen has the stem of the holotype of *C. ewinoni* crossing half of its impression, perpendicular to its midline and close to one of its two poles (**Fig. 3.14 A**). Two first-order branches of *F. andersoni* lie on either side of the *Charnia* stem, with second and third-order branch impressions on the positive relief left by the stem and seemingly extending outside the elliptical outline of the *Fractofusus* (“sg” in **Fig. 3.14 A**), which shows unusual secondary growth (cf. Dunn et al., 2019). The midline of the *Fractofusus andersoni* also has a rare instance of a kinking (which is common in *F. misrai* Taylor et al., 2023), with a bent midline and the

closest pole slightly displaced in direction of the *Charnia*. High order branches are better preserved on the opposite side of the midline with respect to *Charnia* (**Fig. 3.14 A**)—and those branches on the same side as the *Charnia* stem but further away from it—while the portions of *F. andersoni* in contact with *Charnia* have a more indistinct mesh-like pattern, possibly indicative of necrosis (“sg” in **Fig. 3.14 A**).

A second specimen from the Matthews Surface has associations with two *Fractofusus*, both in proximity of the stem and of the petalodium of *C. ewinoni* (**Fig. 3.14 B**). The *Charnia*-*Fractofusus* relationship at the stem is similar to the one previously described (**Fig. 3.14 A**), with the *F. andersoni* growing around the positively preserved stem of *Charnia*, while the second *Fractofusus* overlaps the negative impression of the petalodium of *Charnia* (“o” in **Fig. 3.14 B**). This suggests that the *Fractofusus* was growing adventitiously under the petalodium of *Charnia*, leaving a thin impression on top the deeper impressions left by the latter. The same specimen is also associated with filaments, of probable microbial origin, preserved in a positive epirelief and cutting across the positively preserved stem of *Charnia* (**Fig. 3.14 B**) Even though the ecological meaning of the association is unclear (predation, parasitism or accidental association), these peculiar characteristics suggest that both the *Fractofusus* and the filament would have been in direct contact with the *Charnia* stems and petalodium for an extended period of time on the Ediacaran seafloor, possibly during the life of both taxa.

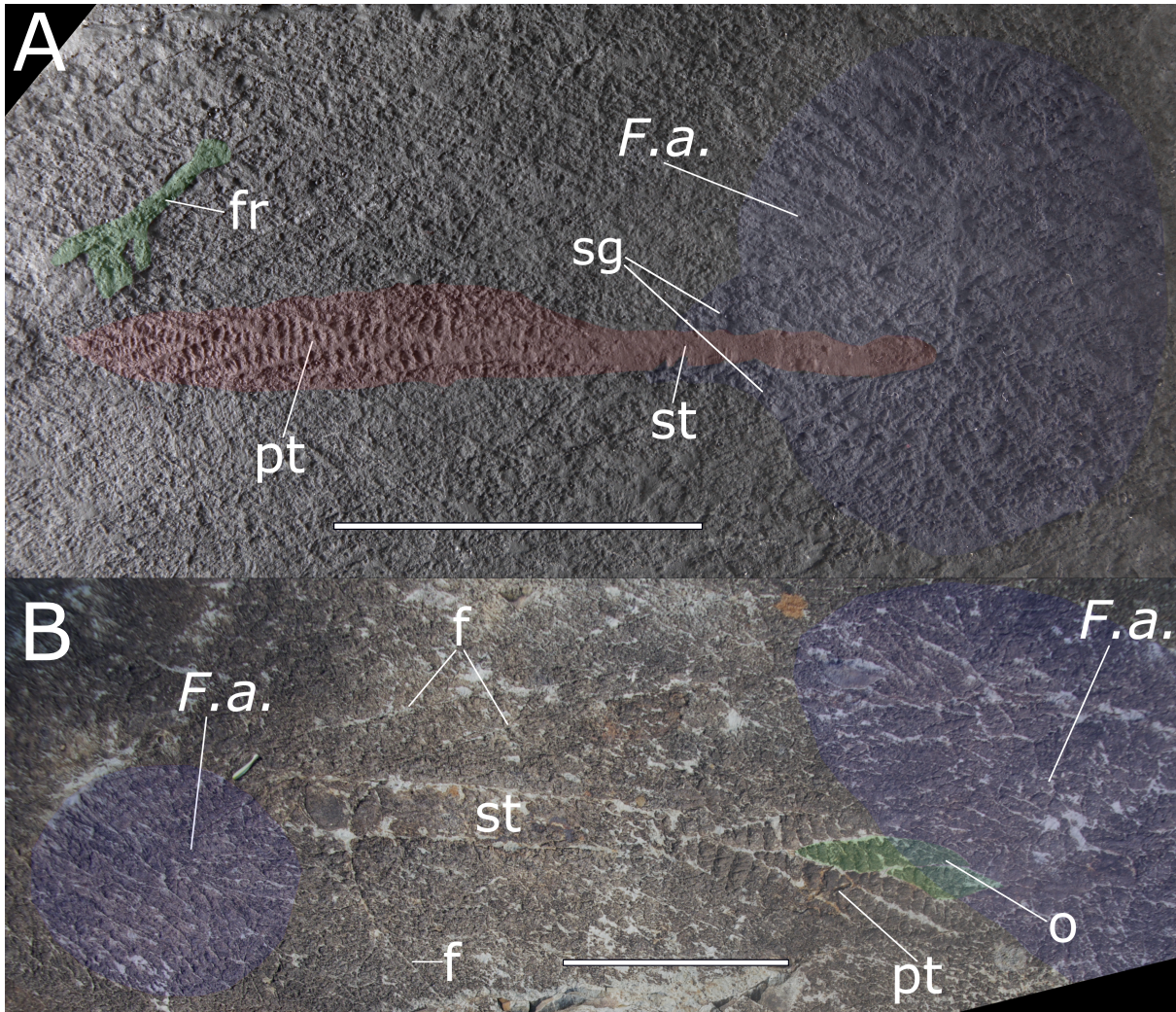


Figure 3.14: in life associations on the Matthews Surface

A) Holotype of *Charnia ewinoni* (colored in red) with the stem (“st”) in relationship with a *Fractofusus andersoni* (“F.a.”, blue), not a small unrelated frond (“fr”, green) oriented at about 60° with respect to the petalodium (“pt”) of *C. ewinoni*. Note the *F. andersoni* mesh-like secondary growth (“sg”) in proximity of the *C. ewinoni* stem; **B)** *C. ewinoni* in contact with two *F. andersoni*, in proximity of the stem and the petalodium, and 3 filaments (“f”). Note the overlapping region (“o”) of the impressions of two first-order branches of *Charnia* (green) and of one first-order branch of *Fractofusus* (blue), and one filament positively preserved on top of the positive epirelief of the stem. Scale bars = 5 cm.

7.5. Mode of Life of *Charnia* spp.

When discussing the mode of life of extinct organisms, especially those that do not have a Phanerozoic fossil record, it is important to establish rigorous hypothesis to test: in particular, since Rangeomorphs are typically preserved horizontally on fossiliferous surfaces, the most reasonable null hypothesis should be that they were preserved in their – horizontal/reclining – life position (Dufour and McIlroy, 2017; McIlroy et al., 2020, 2022). Taphonomic evidence for a reclining or infaunal lifestyle has been proposed for a number of rangeomorph species, including *Fractofusus andersoni* and *F. misrai* (Seilacher, 1992; Gehling and Narbonne, 2007); *Rangea schneiderhoehoni* (Grazhdankin, 2004; Grazhdankin and Seilacher, 2005), *Charnia masoni* (Grazhdankin, 2004; McKean et al., 2023); *Hapsidophyllas flexibilis* (Taylor et al., 2022) and *Culmofrons plumosa* (Pasinetti and McIlroy, 2023), as well as most members of the clade Petalonamae (e.g. Grazhdankin and Seilacher, 2005).

A reclining lifestyle might have been supported by a chemosymbiotic relationship with sulfur-oxidizing bacteria, since the rangeomorph elements could have evolved to maximise exchange surfaces with bacteria, under different potential ecto- and/or endo-symbiotic relationships (Dufour and McIlroy 2017; McIlroy et al., 2021). In the case of *Charnia*, direct evidence for a reclining lifestyle has been proposed by Grazhdankin (2004), who noted that three-dimensionally preserved *Charnia* specimens from Russia truncate sedimentary laminae, implying that they spent a long time on the seafloor during life. Despite this, most contemporary authors consider *Charnia* to have been an upright organism, based on taphonomic and ecological considerations (Clapham and Narbonne, 2002; Clapham et al., 2003; Laflamme et al., 2007, 2012; Laflamme and Narbonne, 2008b, 2008a; Vixseboxse et al., 2021).

The body plans of some Ediacaran organisms invite comparison with extant taxa (pennatulacean cnidarians and macroalgae), which has led several authors to assume—as a starting position—that many of the Rangeomorpha were erect in life (Clapham and Narbonne, 2002; Laflamme and Narbonne, 2008a; Laflamme et al., 2012). While there is no direct evidence for a rangeomorph living erect in the water column in life (e.g. preservation in the hypothetically erect life position; or association with *Kullingia*-like concentric drag or swing marks; cf. Jensen et al., 2002), several indirect lines of evidence have been proposed for such lifestyle and the characteristic rangeomorph “fractal” branching has been seen as the result of an adaptation to filter-feeding or osmotrophy (Laflamme et al., 2009; Narbonne et al., 2009).

Evidence taken to support an erect mode of life in many frondose rangeomorphs is the observation that many specimens have preferential orientation, sometimes this is consistent with independent paleocurrent indicators (e.g. ripples), implying tethering of the organisms or “felling” in the direction of the turbidite at the time of burial (Seilacher, 1992; Wood et al., 2003; Mason et al., 2013). The felling model is evocative though the use of the term “felled” is unfortunate as it implies something cut or broken whereas most authors are actually inferring that the frond is bent, deflated or otherwise collapsed without breakage.

However, frondose organisms can commonly be found in orientations that are not consistent with independent paleocurrent indicators (e.g. Seilacher, 1992; Wood et al., 2007). Recent attempts to explain the up-current orientation of fronds (Vixseboxse et al., 2021) invoked unrealistic fluid mechanics, which involve upslope deposition of turbidites, and are instead supportive of a reclining rheotropic mode of life (McIlroy et al., 2022; Pérez-Pinedo et al., 2023, McKean et al., 2023). Two unequivocal *Charnia* specimens from the Catalina Dome are reported growing in directly opposite orientations within centimetres of one another, and in association with independent paleocurrent indicators, further supporting a rheotropic growth response model over that of a felling model (McKean et al., 2023). On the Matthews Surface,

we record one specimen of *Arborea* sp. growing in an opposite direction with regards to *Charnia*. Most *Arborea* do seem to be oriented in the prevailing current at the time of burial (Vixseboxse et al., 2021; McIlroy et al., 2022; Pérez-Pinedo et al., 2023), suggesting by analogy that the Matthews Surface *Charnia* are likely growing into the current.

In an attempt to try to explain the incongruence between the turbidite current directions and frond orientations—such as the current-orthogonal holotype of *Beothukis* on the E surface at Mistaken Point—some authors have invoked contour currents or tidal currents (e.g., Wood et al., 2007). The presence of such background currents would imply that the fronds fell in the current direction long before final burial. This model, problematically, requires that the turbulent action of the subsequent density flow that deposited the tuffite and felled many erect taxa failed to affect those already dead specimens. We consider that unimodal orientations do not necessarily imply that an organism was tethered to the seafloor or that it was felled by a depositional event but can also be due to rheotropic growth of reclining organisms relative to a background current (McIlroy et al., 2022; Pérez-Pinedo et al., 2023; McKean et al., 2023).

Our results show that *Charnia ewinoni* on the Matthews Surface preferentially grew in the inferred upslope direction (as inferred from our measurement of ripple cross lamination in associated turbidites), and approximately 90° to the inferred contourite direction (Mason et al., 2013). We consider it unlikely that diurnally reversing tidal currents in a deep marine channel would have resulted in all of the specimens on the surface falling in the same direction, without any of them getting displaced by the turbiditic flows at the time of burial. Moreover, specimens that do have a discoidal structure at the end of the stem do not show any sign of tearing or bending in proximity of the junction between the two structures, but rather have an elongated discoidal structure that tapers in the direction of the stem and the rest of the frond. Most specimens also have a bending or a curvature in the petalodium or in proximity of its junction with the stem, which is difficult to explain under any paleocurrent conditions. This is

comparable to the commonly kinked frond of *Charniodiscus procerus* (Pérez-Pinedo et al., 2023), which was previously inferred to be due to the frond wrapping around the stem (Seilacher, 1992). The fronds of *Charniodiscus procerus* and *Charnia ewinoni* are almost always kinked to the left when viewed from base to tip.

Differential preservation quality of proximal and distal portions of some rangeomorph fossils has been presented as evidence for an erect lifestyle: under the felling model, the distal portions of the organisms would have collected sediment underneath, leaving a fainter impression (Laflamme et al., 2007; Flude and Narbonne, 2008). We do not observe any such gradient in preservation in *C. ewinoni* from the Matthews Surface (**Fig. 3.1 A; 3.12 C**) and MUN Surface, as well as in the *C. masoni* from the E Surface (**Fig. 3.12 C**) and in the two specimens from Inner Meadow (**Fig. 3.1 C**), which all appear to be preserved with sharp outlines and a high preservational resolution in both distal and proximal portion (e.g., **Fig. 3.10 E**), supporting preservation of *C. ewinoni* in reclining life position.

The functional morphology of modern organisms, such as pennatulacean Cnidaria, fungi and macroalgae, has strongly influenced the investigation of Ediacaran organisms (Clapham and Narbonne, 2002; Laflamme et al., 2007, Laflamme and Narbonne 2008). *Aspidella*-like holdfasts are fairly uncommon in all species of *Charnia*, including *C. ewinoni*, with the exception of one specimen of *C. masoni* from the Shibantan biota (Wu et al., 2022). The presence of a stem is unequivocal only in *C. ewinoni*, while the assemblages of *C. masoni* and *C. gracilis* at their type localities include stemless specimens that sometimes show poorly preserved globose structures (“holdfasts”) in their basal portions interpreted by some as holdfasts (Dunn et al., 2019). It has been suggested that the absence of an holdfast can be explained by the holdfast developing under the sediment in *C. masoni* and *C. gracilis* (Dunn et al., 2019; Wu et al., 2023), a position which would have excluded the structure from the taphonomic window. However, no direct evidence for the presence of an internal mold of a

stem or the decayed holdfast can be found in association with the frond (see also McKean et al., 2023). It is also possible that the association of *Charnia* and *Aspidella* could be accidental, or the result of predation/parasitism interactions, since *Aspidella*-like discs are most typically associated with the Arboreomorpha, a group that is architecturally quite different from the Rangeomorpha (Dececchi et al., 2017). Obvious cross-cutting juxtapositions are common, but there is a general reluctance to consider accidental association of organisms with discoidal structures at the base of their stem. Stems and holdfasts can potentially perform several functions even in reclining organisms: 1) by anchoring the frond to the microbial matground and offering structural support against the action of currents (cf. *Charniodiscus procerus*, Pérez-Pinedo et al., 2022; *Culmofrons plumosa*, Pasinetti and McIlroy, 2023); 2) playing a role in juvenile organism's settlement and development; or 3) serving functions comparable that of a trophosome or nutrient storage.

Tiering models in Ediacaran communities are regarded as indirect evidence for an erect lifestyle of some of the taxa (Clapham and Narbonne, 2002; Bamforth et al., 2008), and they might have driven ecological successions of different taxonomic groups (Clapham et al., 2002). The two studies include only a small number of surfaces (respectively n=3 and n=9) restricted in space and time around the MPER and involve several qualitative variables, driven by the null hypothesis that some taxa were erect. It has also been noted that Ediacaran taxonomy, especially of the MPER assemblage, is still severely lacking clarity and consensus and many genera have been used as “waste-bin” to group dissimilar non-conspecific problematic taxa (McIlroy et al., 2023). Tiering and ecological successions models, even though they complement the idea of “the garden of Ediacara” (cf. McMenamin, 1986), do not preclude the possibility of other ecological interpretations, since models including reclining frondose rangeomorphs have not yet been tested and therefore are not falsifiable.

The evidence here discussed, as well as the *Charnia-Fractofusus* and *Charnia*-filaments associations from the Matthews Surface, might suggest that *Charnia* spp. were reclining epibenthic organisms, and ecological and tiering models including erect-growing members of the Charnida should be revisited.

8. Conclusion

The study supports the creation of a new species of *Charnia ewinoni* sp. nov., which is hitherto only known from the Bonavista Peninsula. Statistical analyses and morphometric descriptions consistently differentiate *C. ewinoni* from *Charnia masoni* and *C. gracilis*. Our new species, *C. ewinoni* sp. nov. is characterized by an elongated, parallel-sided petalodium, connected to an elongated stem sometimes terminating in a proportionally small discoidal structure. The stem, which is a distinctive feature of this new taxon, shows correlations with the length of the petalodium, providing a morphological trait not observed in other *Charnia* species.

Field measurements of ripple cross lamination, and detailed analyses of specimen orientation on the Matthews Surface indicate a preferential growth direction that opposes the turbidite downslope. In contrast with earlier interpretations, this finding challenges the notion of *Charnia* as a strictly erect organism (see also McKean et al., 2023). The observed orientation, approximately 90° from the inferred contourite direction, suggests that other factors, such as tidal currents or complex sedimentological conditions, may have influenced the positioning of these organisms in life.

While it remains unclear whether the nature of the association between *Fractofusus andersoni* and *Charnia ewinoni* specimens on the Matthews Surface represent a functional strategy for one or both species or is only accidental, secondary growth and suggest a prolonged interaction between the two organisms and therefore a reclining lifestyle for *C. ewinoni*.

Contrary to earlier interpretations that classified *Charnia* as strictly erect, our findings challenge this hypothesis. Evidence of unimodal orientations, the absence of a gradient in preservation between proximal and distal portions, and the discovery of *Charnia* specimens

with opposing growth orientations on the same surface collectively suggest the revision of previous ecological interpretations.

9. Acknowledgements

Fossil surfaces in the Bonavista Peninsula are protected under Reg. 67/11, of the Historic Resources Act 2011 and their access is only allowed under permission from the Government of Newfoundland and Labrador. Fieldwork near Port Union was conducted under permit from the Government of Newfoundland and Labrador. Thanks are due to: Edith and Neville Samson for their kind support; Mike Steele for help collecting field data; Jack Matthews for his discovery of the Matthews Surface; and Natural Sciences and Engineering Research Council of Canada (NSERC) for Discovery Grant (individual) and DAG funding to DM.

10. References

- Bak, R., and Meesters, E. (1998). Coral population structure: the hidden information of colony size-frequency distributions. *Mar. Ecol. Prog. Ser.* 162, 301–306. doi: 10.3354/meps162301
- Baken, E. K., Collyer, M. L., Kaliontzopoulou, A., and Adams, D. C. (2021). geomorph v4.0 and gmShiny: Enhanced analytics and a new graphical interface for a comprehensive morphometric experience. *Methods Ecol Evol* 12, 2355–2363. doi: 10.1111/2041-210X.13723
- Bamforth, E. L., Narbonne, G. M., and Anderson, M. M. (2008). Growth and ecology of a multi-branched Ediacaran rangeomorph from the Mistaken Point assemblage, Newfoundland. *Journal of Paleontology* 82, 763–777. doi: 10.1666/07-112.1
- Boynton, H. E. (1999). New fossils in the Precambrian of Charnwood Forest, Leicestershire, England. *Mercian Geologist* 14, 4.
- Boynton, H. E., and Ford, T. D. (1995). Ediacaran fossils from the Precambrian (Charnian Supergroup) of Charnwood Forest, Leicestershire, England. *Mercian Geologist* 13, 156–182.
- Brasier, M. D., Antcliffe, J. B., and Liu, A. G. (2012). The architecture of Ediacaran fronds. *Palaeontology* 55, 1105–1124. doi: 10.1111/j.1475-4983.2012.01164.x
- Brasier, M. D., Liu, A. G., Menon, L., Matthews, J. J., McIlroy, D., and Wacey, D. (2013). Explaining the exceptional preservation of Ediacaran rangeomorphs from Spaniard's Bay, Newfoundland: A hydraulic model. *Precambrian Research* 231, 122–135. doi: 10.1016/j.precamres.2013.03.013
- Clapham, M. E., and Narbonne, G. M. (2002). Ediacaran epifaunal tiering. *Geology* 30, 627–630. doi: 10.1130/0091-7613(2002)030<0627:EET>2.0.CO;2
- Clapham, M. E., Narbonne, G. M., and Gehling, J. G. (2003). Paleoecology of the oldest known animal communities: Ediacaran assemblages at Mistaken Point, Newfoundland. *Paleobiology* 29, 527–544. doi: 10.1666/0094-8373(2003)029<0527:POTOKA>2.0.CO;2
- Darroch, S. A. F., Laflamme, M., and Clapham, M. E. (2013). Population structure of the oldest known macroscopic communities from Mistaken Point, Newfoundland. *Paleobiology* 39, 591–608. doi: 10.1666/12051
- Dillon, W., and Goldstein, M. (1984). *Multivariate analysis: methods and applications*. Wiley. New York: Wiley.

- Dufour, S. C., and McIlroy, D. (2017). Ediacaran pre-placozoan diploblasts in the Avalonian biota: the role of chemosynthesis in the evolution of early animal life. *Geological Society, London, Special Publications* 448, 211–219. doi: 10.1144/SP448.5
- Dunn, F. S., Grazhdankin, D. V., Liu, A. G., and Wilby, P. R. (2021). The developmental biology of *Charnia* and the eumetazoan affinity of the Ediacaran rangeomorphs. *Science Advances*, 14.
- Dunn, F. S., Liu, A. G., and Donoghue, P. C. J. (2018). Ediacaran developmental biology: Ediacaran developmental biology. *Biol Rev* 93, 914–932. doi: 10.1111/brv.12379
- Dunn, F. S., Liu, A. G., and Gehling, J. G. (2019a). Anatomical and ontogenetic reassessment of the Ediacaran frond *Arborea arborea* and its placement within total group Eumetazoa. *Palaeontology* 62, 851–865. doi: 10.1111/pala.12431
- Dunn, F. S., Wilby, P. R., Kenchington, C. G., Grazhdankin, D. V., Donoghue, P. C. J., and Liu, A. G. (2019b). Anatomy of the Ediacaran rangeomorph *Charnia masoni*. *Pap Palaeontol* 5, 157–176. doi: 10.1002/spp2.1234
- Flude, L. I., and Narbonne, G. M. (2008). Taphonomy and ontogeny of a multibranching Ediacaran fossil: *Bradgatia* from the Avalon Peninsula of Newfoundland. *Can. J. Earth Sci.* 45, 1095–1109. doi: 10.1139/E08-057
- Ford, T. D. (1958). Pre-Cambrian fossils from Charnwood Forest. *Proceedings of the Yorkshire Geological Society* 31, 211–217. doi: 10.1144/pygs.31.3.211
- Ford, T. D. (1962). The Pre-Cambrian fossils of Charnwood Forest. *Transactions of the Leicester Literary and Philosophical Society* 56, 57–62.
- Gehling, J. G., and Narbonne, G. M. (2007). Spindle-shaped Ediacara fossils from the Mistaken Point assemblage, Avalon Zone, Newfoundland. *Can. J. Earth Sci.* 44, 367–387. doi: 10.1139/e07-003
- Grazhdankin, D. (2004). Patterns of Distribution in the Ediacaran Biotas: Facies versus Biogeography and Evolution. *Paleobiology* 30, 203–221.
- Grazhdankin, D., and Seilacher, A. (2005). A re-examination of the Nama-type Vendian organism *Rangea schneiderhoehni*. *Geol. Mag.* 142, 571–582. doi: 10.1017/S0016756805000920
- Hawco, J. B., Kenchington, C. G., Taylor, R. S., and Mcilroy, D. (2020). A multivariate statistical analysis of the Ediacaran rangeomorph taxa *Beothukis* and *Culmofrons*. *PALAIOS* 35, 495–511. doi: 10.2110/palo.2020.049
- Hofmann, H. J., O'Brien, S. J., and King, A. F. (2008). Ediacaran biota on Bonavista Peninsula, Newfoundland, Canada. *J. Paleontol.* 82, 1–36. doi: 10.1666/06-087.1
- Howe, M. P. A., Evans, M., Carney, J. N., and Wilby, P. R. (2012). New perspectives on the globally important Ediacaran fossil discoveries in Charnwood Forest, UK: Harley's 1848 prequel to Ford (1958). *Proceedings of the Yorkshire Geological Society* 59, 137–144.

- Husson, F., Josse, J., and Pages, J. (2010). Principal component methods - hierarchical clustering - partitional clustering: why would we need to choose for visualizing data? *Technical Report - Agrocampus*.
- Ichaso, A. A., Dalrymple, R. W., and Narbonne, G. M. (2007). Paleoenvironmental and basin analysis of the late Neoproterozoic (Ediacaran) upper Conception and St. John's groups, west Conception Bay, Newfoundland. *Can. J. Earth Sci.* 44, 25–41. doi: 10.1139/e06-098
- Jenkins, R. J. F. (1985). The enigmatic Ediacaran (late Precambrian) genus *Rangea* and related forms. *Paleobiology* 11, 336–355. doi: 10.1017/S0094837300011635
- Jensen, S., Gehling, J. G., Droser, M. L., and Grant, S. W. F. (2002). A scratch circle origin for the medusoid fossil *Kullingia*. *LET* 35, 291–299. doi: 10.1111/j.1502-3931.2002.tb00089.x
- Kaiser, H. F. (1970). A second generation little jiffy. *Psychometrika* 35, 401–415. doi: 10.1007/BF02291817
- Kenchington, C. G., and Wilby, P. R. (2014). Of time and taphonomy: preservation in the Ediacaran. *The Paleontological Society Papers* 20, 23. doi: <https://doi.org/10.1017/S1089332600002825>
- Laflamme, M., Flude, L. I., and Narbonne, G. M. (2012). Ecological tiering and the evolution of a stem: the oldest stemmed frond from the Ediacaran of Newfoundland, Canada. *J. Paleontol.* 86, 193–200. doi: 10.1666/11-044.1
- Laflamme, M., and Narbonne, G. M. (2008a). Competition in a Precambrian world: palaeoecology of Ediacaran fronds. *Geology Today* 24, 182–187. doi: 10.1111/j.1365-2451.2008.00685.x
- Laflamme, M., and Narbonne, G. M. (2008b). Ediacaran fronds. *Palaeogeography, Palaeoclimatology, Palaeoecology* 258, 162–179. doi: 10.1016/j.palaeo.2007.05.020
- Laflamme, M., Narbonne, G. M., Greentree, C., and Anderson, M. M. (2007). Morphology and taphonomy of an Ediacaran frond: *Charnia* from the Avalon Peninsula of Newfoundland. *SP* 286, 237–257. doi: 10.1144/SP286.17
- Laflamme, M., Xiao, S., and Kowalewski, M. (2009). Osmotrophy in modular Ediacara organisms. *Proceedings of the National Academy of Sciences* 106, 14438–14443. doi: 10.1073/pnas.0904836106
- Lê, S., Josse, J., and Husson, F. (2008). FactoMineR : An R Package for Multivariate Analysis. *J. Stat. Soft.* 25. doi: 10.18637/jss.v025.i01
- Liu, A. G., and Dunn, F. S. (2020). Filamentous Connections between Ediacaran Fronds. *Current Biology* 30, 1322–1328.e3. doi: 10.1016/j.cub.2020.01.052

- Liu, A. G., Matthews, J. J., and McIlroy, D. (2016). The *Beothukis* / *Culmofrons* problem and its bearing on Ediacaran macrofossil taxonomy: evidence from an exceptional new fossil locality. *Palaeontology* 59, 45–58. doi: 10.1111/pala.12206
- Liu, A. G., Matthews, J. J., Menon, L. R., McIlroy, D., and Brasier, M. D. (2014). *Haootia quadriformis* n. gen., n. sp., interpreted as a muscular cnidarian impression from the Late Ediacaran period (approx. 560 Ma). *Proc. R. Soc. B.* 281, 20141202. doi: 10.1098/rspb.2014.1202
- Liu, A. G., and McIlroy, D. (2015). Horizontal surface traces from the Fermeuse Formation, Ferryland (Newfoundland, Canada), and their place within the Late Ediacaran ichnological revolution. *Geological Association of Canada, Miscellaneous Publication* 9, 141–156.
- Liu, A. G., McIlroy, D., Matthews, J. J., and Brasier, M. D. (2013). Exploring an Ediacaran ‘nursery’: growth, ecology and evolution in a rangeomorph palaeocommunity. *Geology Today* 29, 23–26. doi: 10.1111/j.1365-2451.2013.00860.x
- Liu, A. G., McIlroy, D., and Brasier, M. D. (2010). First evidence for locomotion in the Ediacara biota from the 565 Ma Mistaken Point Formation, Newfoundland. *Geology* 38, 123–126. doi: 10.1130/G30368.1
- Mason, S. J., Narbonne, G. M., Dalrymple, R. W., and O’Brien, S. J. (2013). Paleoenvironmental analysis of Ediacaran strata in the Catalina Dome, Bonavista Peninsula, Newfoundland. *Can. J. Earth Sci.* 50, 197–212. doi: 10.1139/cjes-2012-0099
- Matthews, J. J., Liu, A. G., Yang, C., McIlroy, D., Levell, B., and Condon, D. J. (2020). A chronostratigraphic framework for the rise of the Ediacaran macrobiota: New constraints from Mistaken Point Ecological Reserve, Newfoundland. *Geological Society of America Bulletin* 133, 13. doi: 10.1130/B35646.1
- McIlroy, D., Hawco, J., McKean, C., Nicholls, R., Pasinetti, G., and Taylor, R. (2020). Palaeobiology of the reclining rangeomorph *Beothukis* from the Ediacaran Mistaken Point Formation of southeastern Newfoundland. *Geol. Mag.*, 1–15. doi: 10.1017/S0016756820000941
- McIlroy, D., Pérez-Pinedo, D., Pasinetti, G., McKean, C., Taylor, R. S., and Hiscott, R. N. (2022). Rheotropic epifaunal growth, not felling by density currents, is responsible for many Ediacaran fossil orientations at Mistaken Point. *Front. Earth Sci.* 10, 849194. doi: 10.3389/feart.2022.849194
- McKean, C., Taylor, R. S., and McIlroy, D. (2023). New taphonomic and sedimentological insights into the preservation of high-relief Ediacaran fossils at Upper Island Cove, Newfoundland. *LET* 56, 1–17. doi: 10.18261/let.56.4.2
- McMenamin, M. A. S. (1986). The Garden of Ediacara. *PALAIOS* 1, 178. doi: 10.2307/3514512
- Meesters, E., Hilterman, M., Kardinaal, E., Keetman, M., De Vries, M., and Bak, R. (2001). Colony size-frequency distributions of scleractinian coral populations: spatial and interspecific variation. *Mar. Ecol. Prog. Ser.* 209, 43–54. doi: 10.3354/meps209043

- Mitchell, E. G., Kenchington, C. G., Liu, A. G., Matthews, J. J., and Butterfield, N. J. (2015). Reconstructing the reproductive mode of an Ediacaran macro-organism. *Nature* 524, 343–346. doi: 10.1038/nature14646
- Narbonne, G. M. (2004). Modular construction of Early Ediacaran complex life forms. *Science* 305, 1141–1144. doi: 10.1126/science.1099727
- Narbonne, G. M., and Gehling, J. G. (2003). Life after snowball: The oldest complex Ediacaran fossils. *Geology* 31. doi: 10.1130/0091-7613(2003)031<0027:LASTOC>2.0.CO;2
- Narbonne, G. M., Laflamme, M., Greentree, C., and Trusler, P. (2009). Reconstructing a lost world: Ediacaran rangeomorphs from Spaniard's Bay, Newfoundland. *J. Paleontol.* 83, 503–523. doi: 10.1666/08-072R1.1
- Noble, S. R., Condon, D. J., Carney, J. N., Wilby, P. R., Pharaoh, T. C., and Ford, T. D. (2015). U-Pb geochronology and global context of the Charnian Supergroup, UK: Constraints on the age of key Ediacaran fossil assemblages. *Geological Society of America Bulletin* 127, 250–265. doi: 10.1130/B31013.1
- O'Brien, S. J., and King, A. F. (2002). Neoproterozoic Stratigraphy of the Bonavista Peninsula: preliminary results, regional correlations and implication for sediment-hosted stratiform copper exploration in the Newfoundland Avalon Zone. *Geological Survey* 02, 229–244.
- O'Brien, S. J., and King, A. F. (2005). Late Neoproterozoic (Ediacaran) stratigraphy of Avalon Zone sedimentary rocks, Bonavista Peninsula, Newfoundland. *Geological Survey* 05, 13.
- Olsen, A. M. (2017). Feeding ecology is the primary driver of beak shape diversification in waterfowl. *Funct Ecol* 31, 1985–1995. doi: 10.1111/1365-2435.12890
- Olsen, A. M., and Westneat, M. W. (2015). StereoMorph: an R package for the collection of 3D landmarks and curves using a stereo camera set-up. *Methods Ecol Evol* 6, 351–356. doi: 10.1111/2041-210X.12326
- Pasinetti, G., and McIlroy, D. (2023). Palaeobiology and taphonomy of the rangeomorph *Culmofrons plumosa*. *Palaeontology* 66, e12671. doi: 10.1111/pala.12671
- Peres-Neto, P. R., Jackson, D. A., and Somers, K. M. (2005). How many principal components? stopping rules for determining the number of non-trivial axes revisited. *Computational Statistics & Data Analysis* 49, 974–997. doi: 10.1016/j.csda.2004.06.015
- Pérez-Pinedo, D., McKean, C., Taylor, R., Nicholls, R., and McIlroy, D. (2022). *Charniodiscus* and *Arborea* are separate genera within the Arboreomorpha: Using the holotype of *C. concentricus* to resolve a taphonomic/taxonomic tangle. *Front. Earth Sci.* 9, 785929. doi: 10.3389/feart.2021.785929
- Pérez-Pinedo, D., Neville, J. M., Pasinetti, G., McKean, C., Taylor, R., and McIlroy, D. (2023). Frond orientations with independent current indicators demonstrate the reclining

- rheotropic mode of life of several Ediacaran rangeomorph taxa. *Paleobiology*, 1–22. doi: 10.1017/pab.2023.2
- Revelle, W. (2021). psych: Procedures for Personality and Psychological Research. Available at: <https://CRAN.R-project.org/package=psych>
- Seilacher, A. (1992). Vendobionta and Psammocorallia: lost constructions of Precambrian evolution. *Journal of the Geological Society* 149, 607–613. doi: 10.1144/gsjgs.149.4.0607
- Seilacher, A. (1999). Biomat-Related Lifestyles in the Precambrian. *PALAIOS* 14, 86. doi: 10.2307/3515363
- Taylor, R. S., Hawco, J. B., Nichols, R., and McIlroy, D. (2019). Reevaluación crítica del holotipo de *Beothukis mistakensis*, único organismo rangeomorfo excepcionalmente preservado en Mistaken Point, Terranova, Canadá. *Estud. geol.* 75, 117. doi: 10.3989/egeol.43586.572
- Taylor, R. S., Matthews, J. J., Nicholls, R., and McIlroy, D. (2021). A re-assessment of the taxonomy, palaeobiology and taphonomy of the rangeomorph organism *Hapsidophyllas flexibilis* from the Ediacaran of Newfoundland, Canada. *PalZ* 95, 187–207. doi: 10.1007/s12542-020-00537-4
- Taylor, R. S., Nicholls, R., Neville, J. M., and McIlroy, D. (2023). Morphological variation in the rangeomorph organism *Fractofusus misrai* from the Ediacaran of Newfoundland, Canada. *Geol. Mag.* 160, 146–166. doi: 10.1017/S0016756822000723
- Vixseboxse, P. B., Kenchington, C. G., Dunn, F. S., and Mitchell, E. G. (2021). Orientations of Mistaken Point fronds indicate morphology impacted ability to survive turbulence. *Front. Earth Sci.* 9, 762824. doi: 10.3389/feart.2021.762824
- Waggoner, B. (2003). The Ediacaran biotas in space and time. *Integrative and Comparative Biology* 43, 104–113. doi: 10.1093/icb/43.1.104
- Ward, J. H. (1963). Hierarchical Grouping to Optimize an Objective Function. *Journal of the American Statistical Association* 58, 236–244. doi: 10.1080/01621459.1963.10500845
- Wilby, P. R., Carney, J. N., and Howe, M. P. A. (2011). A rich Ediacaran assemblage from eastern Avalonia: Evidence of early widespread diversity in the deep ocean. *Geology* 39, 655–658. doi: 10.1130/G31890.1
- Wood, D. A., Dalrymple, R. W., Narbonne, G. M., Gehling, J. G., and Clapham, M. E. (2003). Paleoenvironmental analysis of the late Neoproterozoic Mistaken Point and Trepassy formations, southeastern Newfoundland. *Can. J. Earth Sci.* 40, 1375–1391. doi: 10.1139/e03-048
- Wu, C., Pang, K., Chen, Z., Wang, X., Zhou, C., Wan, B., et al. (2022). The rangeomorph fossil *Charnia* from the Ediacaran Shibantan biota in the Yangtze Gorges area, South China. *J. Paleontol.*, 1–17. doi: 10.1017/jpa.2022.97

Chapter 4 : The macrofossil *Lydonia jiggamintia* gen. et sp. nov. from the Ediacaran of Newfoundland: from pseudofossil to metazoan-grade epibiont

Pasinetti Giovanni^{1*}, gpasinetti@mun.ca, 0000-0003-3104-9758

Menon Latha², 0000-0002-8805-7903

Chida Nagi¹, 0009-0001-0216-7440

McKean Christopher¹, 0009-0004-4007-4458

Olschewski Pascal¹, 0000-0002-2472-7138

Pérez-Pinedo Daniel¹, 0000-0001-5607-1164

Taylor Rod³, 0000-0003-3072-6040

McIlroy Duncan¹, 0000-0001-9521-499X

¹MUN Palaeobiology Group, Department of Earth Sciences, Memorial University of Newfoundland (CA)

² Department of Earth Sciences, University of Oxford (UK)

³Johnson Geo Centre, Newfoundland (CA)

*Corresponding author

1. Author contributions

Conceptualization: G. Pasinetti (GP); D. McIlroy (DM);

Data Curation Management: GP;

Formal Analysis: GP;

Funding Acquisition: DM;

Investigation: GP, DM;

Methodology: GP;

Project Administration: GP, DM;

Resources: DM;

Software: GP;

Supervision: DM;

Validation: GP, D. Pérez-Pinedo (DPP), DM;

Visualization: GP, N. Chida (NG), C. McKean (CM), P. Olschewski (PO), DPP;

Writing – Original Draft Preparation: GP, DM;

Writing – Review & Editing: GP, LM, DPP, DM, RST.

3. Key Words

EDIACARAN, EARLY ANIMALS EVOLUTION, IVESHEADIOMORPH, PORIFERA EVOLUTION, PALAEOECOLOGY.

4. Abstract

The Ediacaran rocks from Discovery UNESCO Global Geopark, Newfoundland, contain a rich fossil record, with remarkable preservation and unusually great abundance of Ediacaran organisms. This study focuses on the large, enigmatic taxon, previously described as “*Blackbrookia*”, that is particularly common on the Johnson Discovery Surface along with the super-abundant rangeomorph *Fractofusus andersoni*. Unlike the pseudofossil *Blackbrookia*, the form under consideration is considered a body fossil and given a new name herein (*Lydonia jiggamintia* gen et sp. nov.). *Lydonia* is characterized by infilled pores on its upper surface, which we consider to be related to the presence of an aquiferous system. We thus suggest that *Lydonia* might be analogous to modern encrusting porifera in its body plan. Statistical analyses of *Lydonia* populations allow us to reconstruct the morphospace occupied by the species, as well as to consider aspects of ontogeny and population structure. If accepted as a sponge, *Lydonia* would constitute further evidence for metazoan life in the Ediacaran, with important implications for our understanding of the record of Porifera and evidence for a lengthening of the Ediacaran food chain.

5. Introduction

The Ediacaran strata of the Catalina Dome, Bonavista Peninsula (**Fig. 4.1 A-B**) have yielded a diverse biota of rangeomorphs, arboreomorphs and *incertae sedis* (Hofmann et al., 2008), belonging to the Avalon Assemblage, the oldest of the Ediacaran macrofossil assemblages (Waggoner, 2003). The biota is similar to the classic Mistaken Point biota (Liu et al. 2016), but with taxa having notably different stratigraphic ranges (Hofmann et al., 2008; Matthews et al., 2020; Pérez-Pinedo et al., 2022). The biota of the Catalina Dome was probably preserved in a shallower—perhaps offshore shelf—depositional environment than the classic Mistaken Point assemblage of the Avalon Peninsula (Hofmann et al., 2008). The most notable difference between the two biotas is the superabundance of *Fractofusus andersoni* in the Catalina Dome, whereas *Fractofusus misrai* is the numerically dominant taxon at Mistaken Point. One of the largest organisms in the Catalina Dome assemblage is the form referred to as “*Blackbrookia*” by Hofmann et al. (2008), a large obovate to ovate fossil, which commonly has a folded/wrinkled axial region. The material of *Blackbrookia* from Charnwood Forest, UK (Boynton and Ford, 1995) has subsequently been considered to be an ivesheadiomorph pseudofossil (Liu et al., 2011). When referring to the type material of *Blackbrookia*, and other related pseudofossils, the genus name is not italicized according to modern convention (cf. Arumberia, McIlroy and Walter, 1997; Kinneyia, Jensen et al., 2002, Porada et al., 2008).

The collective term “ivesheadiomorphs” for these effaced forms is a catch-all intended to aid communication of a range of taphomorphs rather than define a taxonomically coherent grouping (Liu et al., 2011). The group is an important component of marine Ediacaran ecosystems of Avalonia and have been variously called by the informal names “pizza discs”, “lobate discs” and “bubble discs” (Narbonne et al., 2009; Laflamme et al., 2012; Kenchington and Wilby, 2014; Mitchell and Butterfield, 2018), as well as by the Latin binomials “*Ivesheadia*

lobata”, “*Blackbrookia oaksi*” and “*Shepshedia palmata*” (cf. Boynton and Ford, 1995: respectively, fig. 12, 17, 16). Ivesheadia, Blackbrookia and Shepshedia in the strict sense (not the “*Blackbrookia*” of Hofmann et al., 2008) are considered pseudofossils formed by post-mortem processes involving microbial degradation, matground overgrowth and sedimentation, which resulted in effacement of the original fossils (Liu et al., 2011).

While the ivesheadiomorphs are not body fossils *sensu stricto* — rather they represent microbially mediated sedimentation associated with the carcasses of macroscopic organisms such as the Rangeomorpha and Arboreomorpha — their importance stems from their being a record of necromass on the unbioturbated, ungrazed deep marine seafloors of Avalonia (Liu et al., 2011). It has been suggested that they can be taphomorphs in morphological continuum with well-known taxa (Liu et al., 2011; Antcliffe et al., 2015; Mitchell and Butterfield, 2018). More significantly however, this evidence for microbial nutrient recycling demonstrates a significant change in the carbon cycle in which buried organisms are used by microbes and subsequently possible chemosymbiotic organisms such as *Fractofusus* (Dufour and McIlroy, 2017; McIlroy et al., 2021, 2022).

The large fossils described as “*Blackbrookia*” by Hofmann et al. (2008) from the Johnson Discovery Surface (JDS hereafter) of the Ediacaran of the Catalina Dome (also previously known as “Hofmann Locality 14” in Hofmann et al. 2008; and the “Discovery Surface”; (Fig. 4.1 B-C) are the focus of this study. The forms described by Hofmann et al. (2008) do not closely conform to the British type material and present sharp boundaries and distinct morphologies, more fossil-like than any of the ivesheadiomorphs. While they do have a broadly ivesheadiomorph morphology (i.e. ovate and wrinkled), they often differ in having a porose surface morphology (Hofmann et al., 2008), which has led to comparisons with the Cambrian sponge genus *Crumillospongia* (McIlroy et al., 2021). Blackbrookia does not show evidence for a single exhalating opening (“osculum”, in Porifera anatomy), but rather their

porose body surface suggests the presence of an aquiferous system that is analogous to that of modern encrusting demosponges. This is in contrast to early Cambrian sponges, which are thought to have evolved from a primitive “ascon” bodyplan, with a single osculum (Botting and Muir, 2018). Some large Blackbrookia-shaped fossils from the JDS have a gross morphology strongly resembling the porose Blackbrookia, except they have a smooth surface texture and are thus more similar to the ivesheadiomorph pseudofossils. None of the ivesheadiomorph pseudofossils from the Charnian of the UK (described as Ivesheadia, Shepshedia and Blackbrookia; Boynton and Ford, 1995) have porose surface textures. Since the Catalina Dome forms are more complex than the British ivesheadiomorphs (including Blackbrookia)—and since the name Blackbrookia was applied to a pseudofossil (Liu et al., 2011)—the more fossil-like porose forms from the Catalina Dome warrant further attention and require re-naming, especially in the context of the new discoveries presented herein.

6. Geological setting

Fossil specimens originally considered to be “*Blackbrookia*” have been reported in Newfoundland only from two localities in the Catalina Dome of the Bonavista Peninsula (the Johnson Discovery Surface and Locality 13 in Hofmann et al., 2008) (**Fig. 4.1 A**). The two surfaces have very similar fossil communities, dominated by super-abundant *Fractofusus andersoni*, but otherwise have low species diversity: Hofmann et al. (2008) report only three taxa from the JDS and six from Hoffman Locality 13. Both surfaces lie stratigraphically close to each other within the Catalina Member (Hofmann et al., 2008) (**Fig. 4.1 B**), which has been lithostratigraphically correlated with the Trepassey Formation of the St. John’s Group on the eastern Avalon Peninsula (O’Brien and King, 2005; Mason et al., 2013) (**Fig. 4.1 C**). The *Blackbrookia*-bearing surfaces lie within a mudstone-rich succession with some thickly bedded turbidites (1-2 m) characterized by normal grading, interbedded with thin cross-bedded sandstones (2-3 cm thick). Fossils are preserved on the JDS both as negative epireliefs (rangeomorphs) and positive epireliefs (the “*Blackbrookia*”) on a red-brown silty surface and overlain by a 0.5 mm thick layer of tuff.

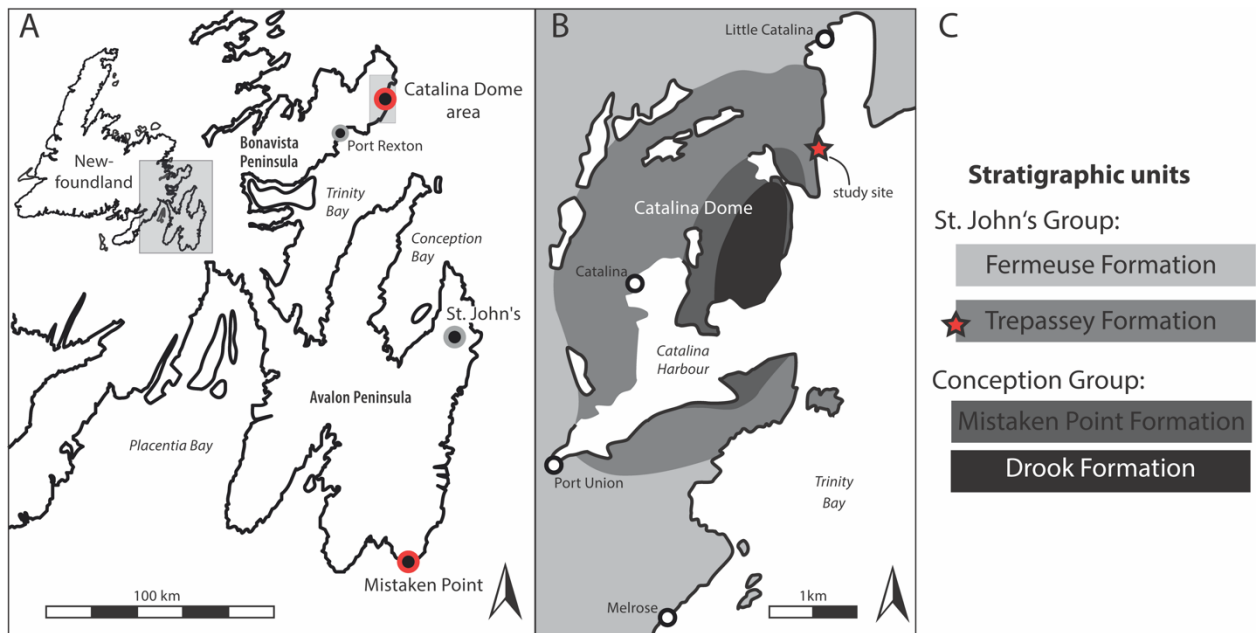


Figure 4.1: map and stratigraphy of the fossiliferous localities.

A) Map of Newfoundland and detail of the Avalon and Bonavista peninsulas, red dots indicate the two main fossiliferous localities: the Mistaken Point Ecological Reserve and the Catalina Dome area in the Discovery Global UNESCO Geopark; **B)** detail of the Catalina Dome area, surrounding the communities of Little Catalina, Catalina, Port Union and Melrose. Study site (JDS) in the Trepassey Formation of Little Catalina indicated by a red star; **C)** simplified stratigraphy of the Catalina Dome.

The surface is a classic example of Conception-style preservation (Narbonne, 2005) which involves the casting of the specimens in-situ by a layer of tuff that preserves either the upper or lower surfaces of the organisms, depending on the rigidity of the original tissues. Other, previously undescribed, specimens of “*Blackbrookia*” come from the D and E surfaces of the Mistaken Point Formation of the Conception Group in the Mistaken Point Ecological Reserve (MPER) in the southern Avalon Peninsula, Newfoundland (**Fig. 4.1 A**).

7. Materials and Methods

For the morphometric analyses that form part of this study, 38 specimens previously assigned to “*Blackbrookia*” (assigned to *Lydonia* gen. nov. below) from the Johnson Discovery Surface have been photographed and measured. In order to morphometrically characterize the new genus, a dataset was collected with the software imageJ and analyzed in R studio (R Core Team, 2022). After identifying the major axis of the specimens, the longest measurable length perpendicular to the major axis was considered as the minor axis. Length of the major (V1) and the minor (V2) axes and their major/minor axial ratio (V3) were measured for each specimen and treated as continuous variables (Tab. 4.1), along with the qualitative variables “presence/absence of papillate texture” (V4, Tab. 4.1) and regularity of the profile of the organism (V5: sub-elliptical/irregular Tab. 4.1). Specimens are recorded in our dataset by an identification code composed of the letters “r” and “i” (representing regular and irregular specimens, respectively), followed by an identification number.

Table 4.1: variables used in this study.

	Number of specimens	V1: Length of major axis	V2: Length of minor axis	V3: Ratio V1/V2	V4: Pores
V5: Regular (“r”)	18	Mean: 35.48 cm	Mean: 15.10 cm	Mean: 1.99	Yes: 17 No: 1
V5: Irregular (“i”)	20	Mean: 23.31 cm	Mean: 15.21 cm	Mean: 1.57 cm	Yes: 10 No: 10
Total	38	Mean: 28.93 cm	Mean: 15.16 cm	Mean: 1.51 cm	Yes: 27 No: 11

Table indicating mean values for V1 (length of the major axis), V2 (length of the minor axis), V3 (Ratio V1/V2) and presence or absence of pores (V4) for the two population subsets (regular/irregular) and the total.

Normality of the continuous variables (V1, V2, V3) was assessed by Shapiro-Wilk tests and only V1 was found to be normally distributed (Shapiro-Wilk test: $\alpha = 0.05$; p -value[V1] = 0.057, p -value[V2] = 0.004, p -value[V3] = 0.020). Logarithmic (natural logarithm) transformation was therefore applied to the data, producing the transformed variables tV1, tV2 and tV3, which are all revealed to be normally distributed by Shapiro-Wilk tests (Shapiro-Wilk test: $\alpha=0.05$; p -value[tV1] = 0.341, p -value[tV2] = 0.463, p -value[tV3] = 0.419). Even though approaches using non-transformed data have been attempted (e.g. Mitchell et al., 2015), transformed data are typically preferred as they usually produce a more precise representation of population structure (Bak and Meesters, 1998; Meesters et al., 2001; Darroch et al., 2013; Pérez-Pinedo et al., 2023).

Assumptions of linearity, homoscedasticity, and normality of the residuals and independence of residual error terms were satisfied for the transformed variables and therefore relationships between continuous variables were initially explored using linear models.

A Welch Two Sample t-test was applied to test whether the means of the two subsets of the population “r” and “i” are statistically different.

To investigate the morphospace occupied by the specimens of the Catalina Dome population, backtransform morphospace analyses were used. The method, developed by Olsen and Westneat (2015) and Olsen (2017) — used previously in taxonomic studies of the Ediacaran biota (Laflamme et al., 2007; Pasinetti and McIlroy, 2023) — employs equidistant semi-landmarks, computed from digitized pictures of the 33 most complete specimens using the R package Stereomorph, version 1.6.4 (Olsen and Westneat, 2015; Olsen, 2017), from which generalized coordinates for each specimen were generated using Procrustes analyses. The generalized coordinates were analysed with a Principal Component Analysis (PCA) and were replotted in a backtransform morphospace in order to visually represent the variability in

shape of the population (see Olsen (2017) for methodology). The resulting ordination was then compared with the qualitative assessment of the organism profile.

Size–frequency distribution histograms can be used to infer age classes and population structure within a monospecific population (Darroch et al., 2013; Pérez-Pinedo et al., 2023). The Gaussian finite mixture model-based clustering algorithms of the package MCLUST allows the identification of the most likely number of size modes (and therefore age/size classes) within a single population (Scrucca et al., 2016). A likelihood-based model selection criterion, BIC (Bayesian Information Criterion), was used to select the best model. Both univariate and bivariate size–frequency distribution analyses were performed in order to produce a model for the population structure of the assemblage and to infer the history of colonization and development on the JDS (see Darroch et al., 2013 and Pérez-Pinedo et al., 2023 for methodology).

8. Results

8.1. Morphology of the Catalina Dome “*Blackbrookia*”

The gross morphology of “*Blackbrookia*” in the Catalina Dome is highly variable, typically broadly sub-oval with one pointed end and one rounded end, sometimes with longitudinal Ivesheadia-like ridges (Fig. 4.2 A-B).

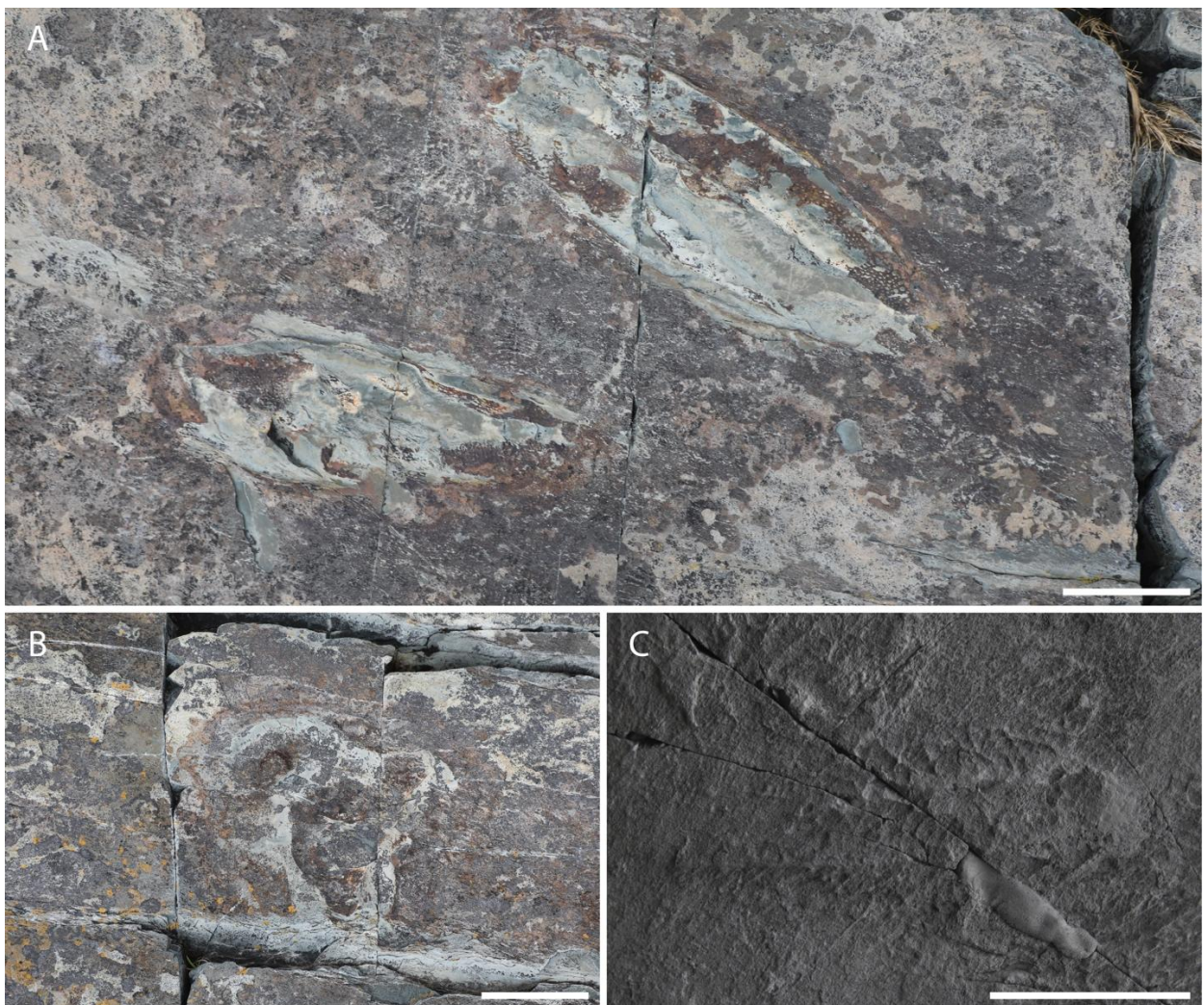


Figure 4.2: diversity of specimens from the JDS.

A) Two regular specimens in situ. Top: holotype of *Lydonia* gen. nov. (specimen id: r8); bottom: specimen id: r9. The two specimens have been previously figured by Hofmann et al. 2008 (fig.

25.4); **B**) irregular, trilobate specimen; **C**) obovate rangeomorph with a central ridge. Scale bars = 5 cm.

The outlines of the JDS specimens show continuous variation from those with a smooth sub-oval profile (**Fig. 4.2 A**), to more irregular ones (**Fig. 4.2 B**). We qualitatively recognize two main morphogroups in the field (recorded in our dataset as the qualitative variable V5, regulars/irregulars) based on the aspect of their outline. Regular specimens have a neat elliptical profile characterized by a marginal ridge separating the body of the organism from the fossiliferous surface and elevating the upper surface of the fossil above the preservational plane (**Fig. 4.2 A**). Irregular specimens may include additional lobes or can deviate from the sub-elliptical shape towards being more sub-triangular (**Fig. 4.2 B**). We note here that there is, however, an undescribed rangeomorph with a central ridge (**Fig. 4.2 C**) from the JDS that is comparable to the common obovate form of “*Blackbrookia*” from the same locality.

8.1.1. Statistical results: Linear regressions

A linear regression (p -value = 0.00065) between the logarithms of the lengths of the major axes (tV1) and those of the minor axes (tV2) of the specimens in the JDS population shows a positive relationship between the two variables ($y = 0.4914x + 1.0306$), albeit it has a low R^2 value (0.2855) (**Fig. 4.3 A**).

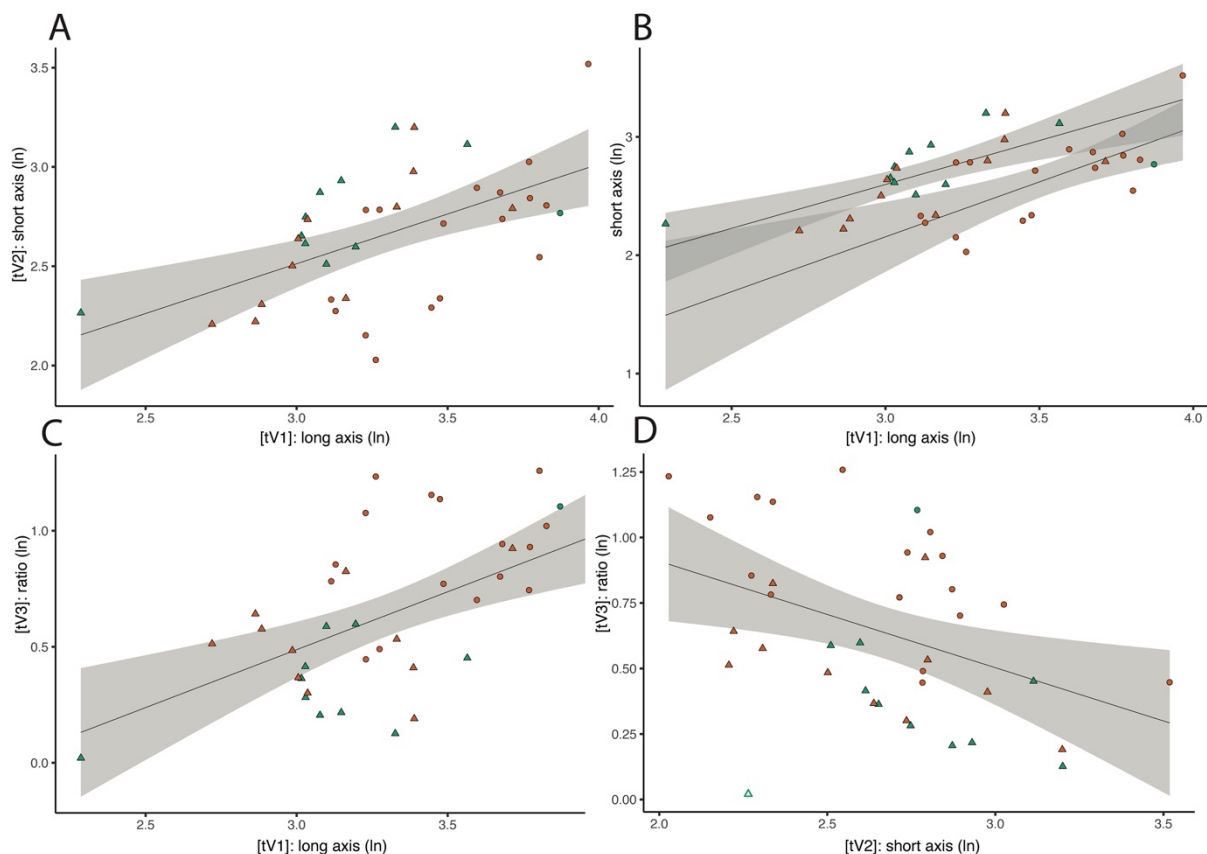


Figure 4.3: linear models between different variables in the JDS population.

A) Linear model between tV1 and tV2; **B)** linear model between tV1 and tV2, treating regular and irregular specimens separately; **C)** linear model between tV1 and tV3; **D)** linear model between tV2 and tV3. Circles represent regular specimens and triangles represent irregular specimens.

A linear regression between tV3 (log of ratio) and tV1 (log of long axis) shows a positive correlation ($y=0.4988x-1.0088$, $R^2=0.2955$, $p\text{-value}=0.00034$) (**Fig. 4.3 C**). A similar trend is found when computing the same linear regression in the two subsets of the JDS population: regulars and irregulars (**Fig. 4.3 B**). However, when comparing the ratio (tV3) with the short axis (tV2), a negative correlation is found ($y=-0.4064x+1.7223$, $R^2=0.1656$, $p\text{-value}=0.01013$) (**Fig. 4.3 D**). This negative correlation also stands true for the “regulars” subset of the JDS population, while for the “irregulars” subset the correlation is not statistically significant ($\alpha\text{-value}\gg 0.05$).

8.1.2. Statistical results: backtransform morphospace analyses and orientations

A backtransform morphospace analysis shows the range of variability within the population of the JDS. This methodology allows us to visually represent the morphospace occupied by a dataset by ordinating the specimens on two principal components (PC1 and PC2; **Fig. 4.4**) computed on generalized coordinates to capture the shape variability of the specimens. PC1 (which explains 67% of variance) captures the eccentricity of the shape of the organisms, which range from sub-circular to sub-elliptical, and PC2 (explaining 21% of variance) appears to capture other shape irregularities, especially along the minor axis, such as the presence of a third lobe in the profile.

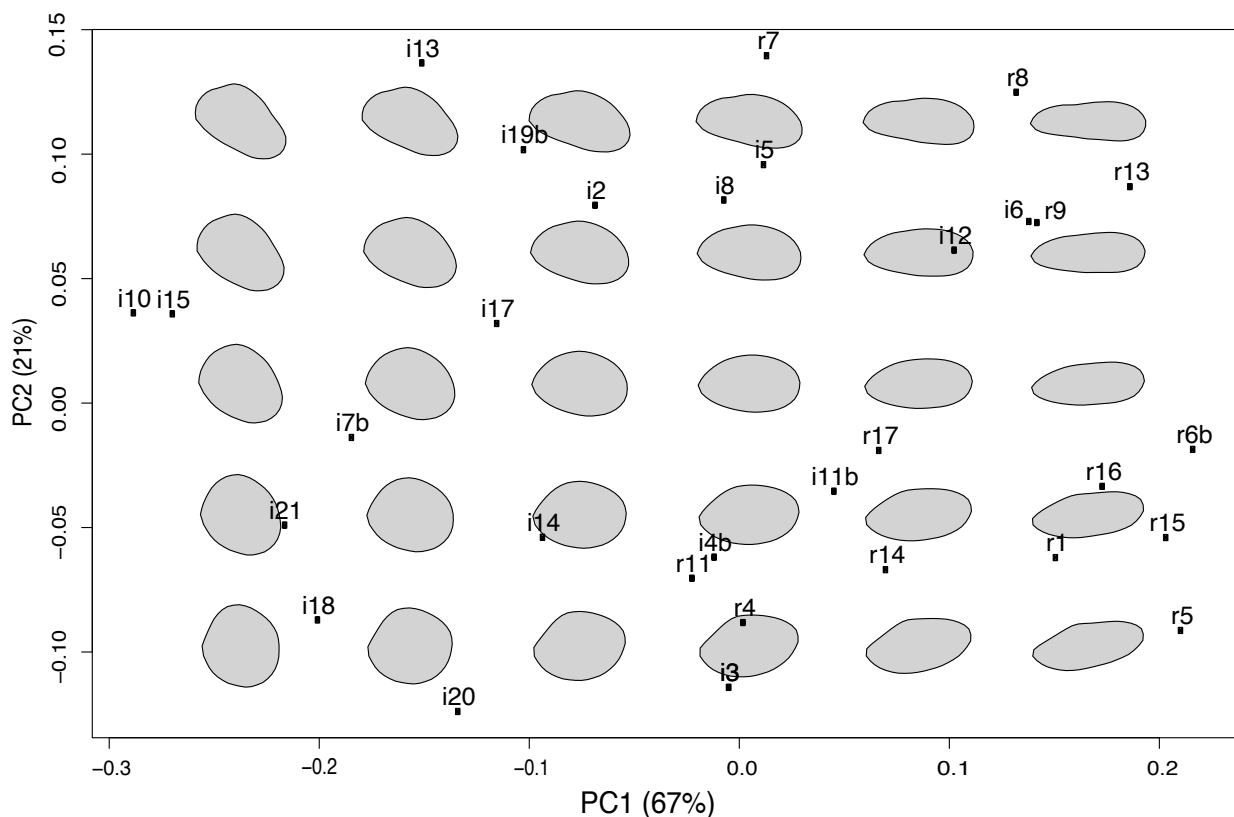


Figure 4.4: backtransform morphospace analyses of part of the JDS population (N=33).

Specimens are identified by the letter “r” (regular) and “i” (irregular) and by an identification number.

The specimens distribute in the ordination without any evident pattern of aggregation. Regular specimens appear to be restricted to the right side of the ordination (as expected, as they were selected partly because of their higher eccentricity), but irregular specimens appear to occupy the entire morphospace (**Fig. 4.4**).

Most specimens (23 of the 30 measured, 76%) on the JDS are oriented with their long axis parallel to the regional S-SW directed paleocurrent (15° - 195° , **Fig. 4.5 A**) as determined from current ripple foresets (**Fig. 4.5 B**) and consistent with regional basin reconstructions of Mason et al. (2013) while some specimens (7 out of 31, 2 regulars and 5 irregulars) are oriented broadly orthogonal to the paleocurrent. The observed wavy ripples may be indicative of internal waves in the basin, as the surfaces was deposited below the lowest wave base, suggesting that the organisms were subject to periodic inversion of the direction of current. Observations in the field suggest that some strings of regular specimens appear to be arranged in a line at a low angle with respect to the paleocurrent, with a few meters between each specimen.

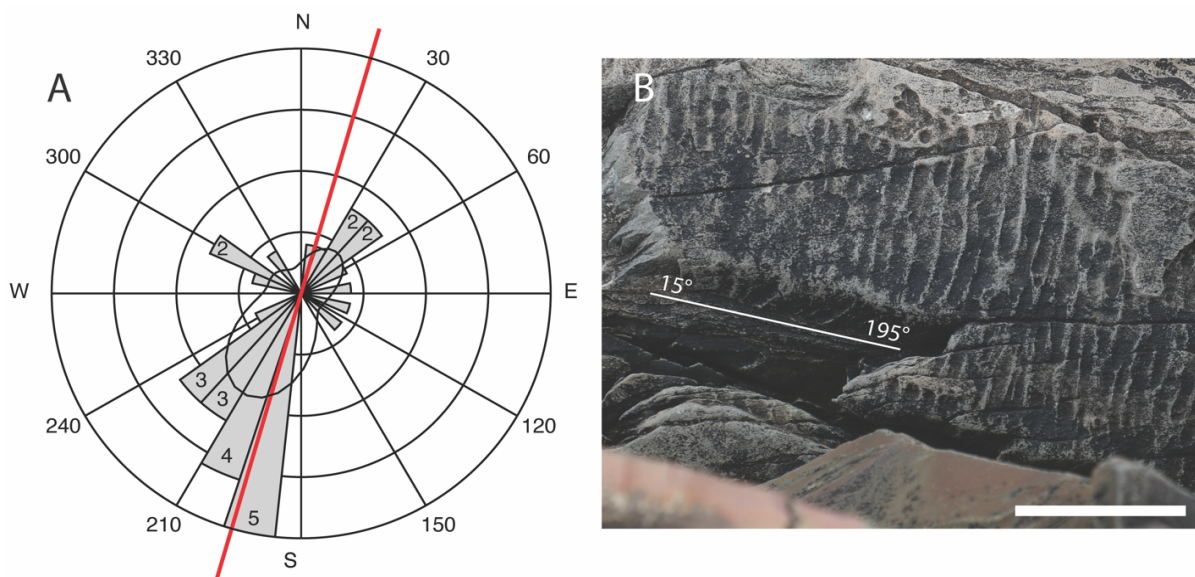


Figure 4.5: rose plot of fossil orientations (grey) relative to the palaeocurrent.

A) Rose plot with orientations of part of the JDS population (N=31) and kernel distribution. Number in the bins is the number of specimens, bins without numbers have count of 1. The red line is the direction of the inferred palaeocurrent (about 15° - 195°); **B)** roughly symmetrical

sharp crested ripples recording the palaeocurrent direction of 15-195°, stratigraphically underlying the fossiliferous horizon..

8.1.3. Upper Surface Morphology

It has been noted that the upper surfaces of many of the Catalina Dome “*Blackbrookia*” have millimetric circular structures, which have been described as pores (Hofmann et al., 2008; Dufour and McIlroy, 2017; McIlroy et al., 2021). An extensive ferruginous mesh-like layer covers both the upper surface of the fossils, as well as the rest of the fossiliferous surface (**Fig. 4.6 A**), with the pores representing an interruption of this layer as features of the upper surface of the “*Blackbrookia*” organism. The pores are filled by unconsolidated silty sediment. Pyritic replacement of soft tissues is not otherwise known in the Ediacaran of Avalonia but is the common mode of preservation of some lightly biomineralized Ediacaran taxa (e.g. *Cloudina*, Smith et al., 2016). The ferruginous layer extends uninterruptedly above the “*Blackbrookia*” specimens and beyond their margins, covering the entire surface and corresponding to the layer upon which *Fractofusus* specimens leave their impression. Such layers are typically interpreted as the oxidative pyritic replacement of an extensive microbial matground (Gehling, 1999; Liu, 2016; Pasinetti and McIlroy, 2023), suggesting that “*Blackbrookia*” was reclining on the seafloor, possibly covered by the microbial matground, piercing through it, and accessing the water column with structures whose positions correspond to the pores on the upper surface of the fossil. Other Ediacaran taxa are considered to have been preserved due to the presence of a pyritic death mask associated with a microbial matground (Gehling, 1999; Mapstone and McIlroy, 2006; Liu, 2016; Pasinetti and McIlroy, 2023) or even a pyritic envelope, in the case of more three dimensionally preserved fossils (McKean et al., 2023).

The specimens considered herein commonly have a folded or torn upper surface (**Fig. 4.6 B**), consistent with the post-mortem collapse of an organism that was somewhat convex in life.

Our studies have revealed, for the first time, short subconical projections in association with a single specimen of “*Blackbrookia*” (**Fig. 4.6 C**) from the JDS. These suggest the

presence of short papillae on the upper surface of the large ovate morph. The projections are filled with the same siltstone that underlies the ferruginous layer and can be interpreted to be internal moulds of tubular papillae (**Fig. 4.6 D**). The mouldic preservation of papillae has previously been suggested for the common porose morphology (McIlroy et al., 2021).

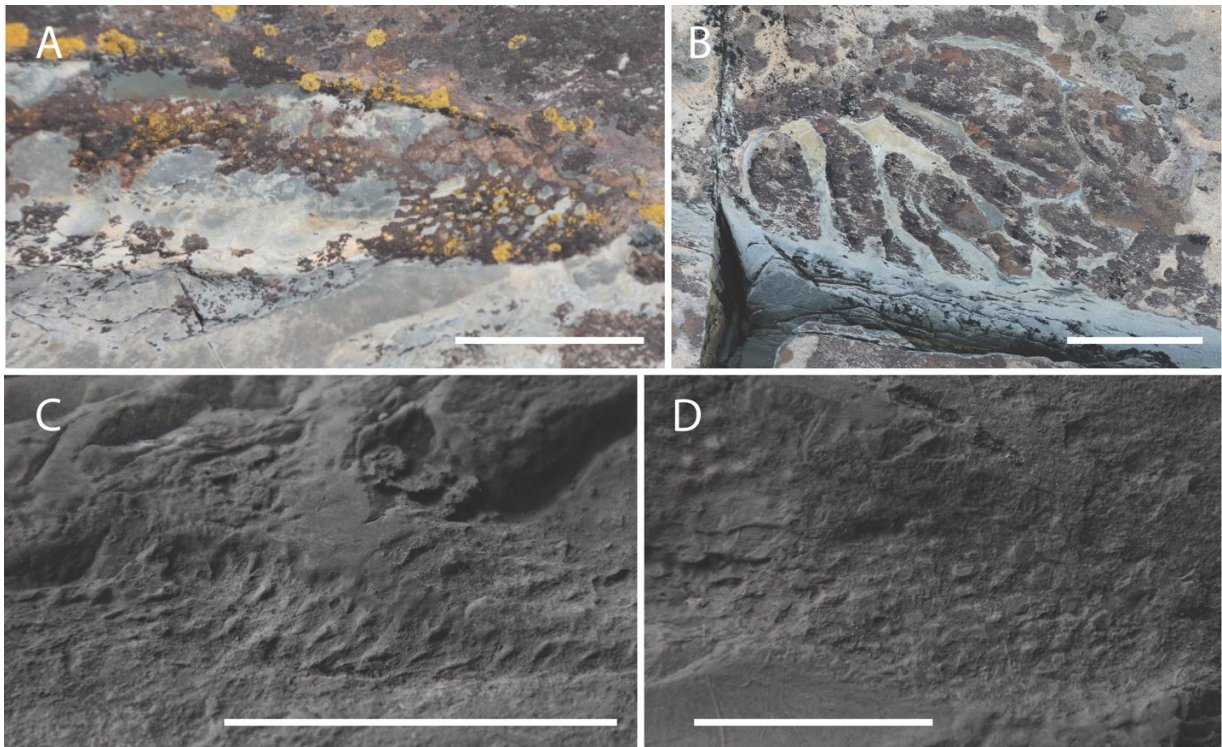


Figure 4.6: *Lydonia* upper surface patterns.

A) Detail of ferruginous mesh-like pattern on the surface of a regular specimen (r8). Scale bar = 5 cm; **B)** irregular specimen (i4) showing a folded upper surface, specimen previously figured in Hofmann et al. 2008 (fig. 25.2). Scale bar = 5 cm; **C)** detail of the subconical projections observed in a single specimen (r9). Scale bar = 5 cm.; **D)** detail of pores morphology in specimen r8. Scale bar = 5 cm.

The size and spacing of pores on the upper surface of “*Blackbrookia*” from the Catalina Dome is uneven both within, and also between, specimens (**Fig. 4.7 A-B**). Subjectively, there is no relationship between “pore” size and specimen length, which is perhaps to be expected if

the pores are preserved internal moulds of the bases of tubular papillae, although some of the smaller specimens do have larger pores (**Fig. 4.7 B**).

Irregular specimens are also often associated with less prominent pores on the upper surface (**Fig. 4.2 B**), which may be a taphonomic artefact, perhaps resulting from decay and microbial overgrowth of “*Blackbrookia*” or related taxon (47% of irregular specimens but only 6% of the regular specimens do not have pores).

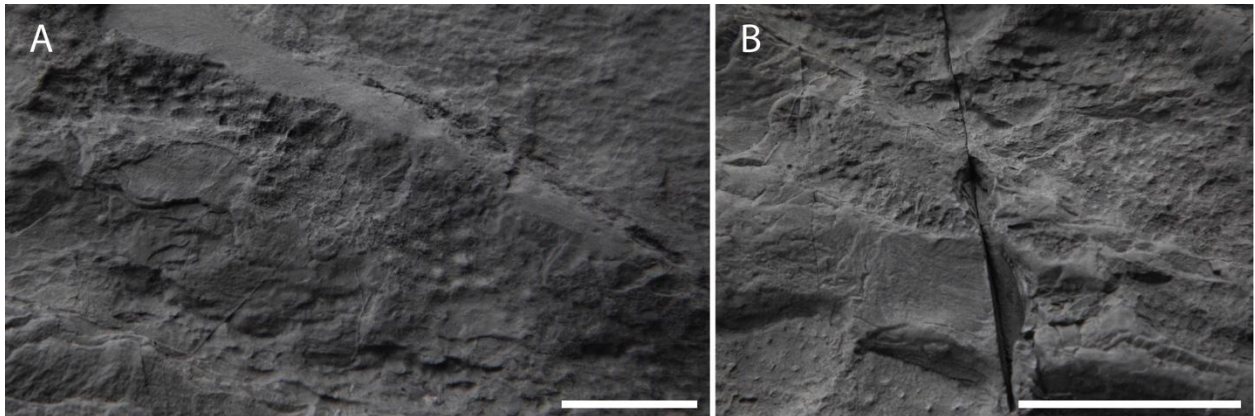


Figure 4.7: pores morphology in ‘*Blackbrookia*’.

A) Variability of pores morphology within a single specimen (r8); **B)** detail of size variation of the pores within a single specimen (r8). Scale bars = 5 cm.

The upper surface of reclining rangeomorph fossils is generally not preserved in the Ediacaran biotas of Avalonia. Several rangeomorphs from the Upper Island Cove biota (Narbonne, 2004) do have well preserved upper surfaces (Brasier et al., 2013; Mckean et al., 2023), none of which resemble the porose upper surface of the Catalina Dome “*Blackbrookia*”. However, the upper surface of a specimen of *Charnia* sp. has been documented from the Ediacaran of the White Sea (Butterfield, 2020) showing rangeomorph-type architecture and pores on the upper surface, which are regularly spaced and cannot be compared with “*Blackbrookia*”.

8.1.4. Lower Surface Morphology

The most surprising component of our revisiting of the Catalina Dome “*Blackbrookia*” has been the discovery of two specimens with rangeomorph-type branching structures preserved on the lower surface of the organism. Most specimens from the JDS do not preserve the lower surface. Both specimens with preserved rangeomorph branching are the obovate morph (**Fig. 4.8 A, C-D**), which is comparable to the gross morphology of an undescribed rangeomorph (**Fig. 4.2 C**).

The clearest example of a “*Blackbrookia*” overlying a rangeomorph has large cm-wide displayed rangeomorph units with second-order branching (**Fig. 4.8 C**) morphologically comparable to that of *Fractofusus andersoni* (**Fig. 4.8 B**), which is super-abundant on the same surface (Hofmann et al., 2008: fig. 25.3). The branches are however anomalously long and wide for *F. andersoni* and the gross morphology of the obovate “*Blackbrookia*” is unlike the typical ovate morphology of *F. andersoni* (Gehling and Narbonne, 2007). Some broken/truncated specimens of *F. andersoni* are known from the surface, which would create a more obovate shape, but all of those are an order of magnitude smaller than the figured “*Blackbrookia*” (**Fig. 4.8 C**).

The second obovate “*Blackbrookia*”-topped rangeomorph is better preserved in that finer details of the rangeomorph branching are evident, though these are longer and narrower than in the other specimen described above and the branching is poorly ordered, with some resemblance to beothukid or *Bradgatia*-like branching (cf. Brasier et al., 2012; **Fig. 4.8 A, D**). The “*Blackbrookia*” expression on this specimen is the perforated-pinacoderm-type preservation, which is best preserved towards the pointed end of the fossil.

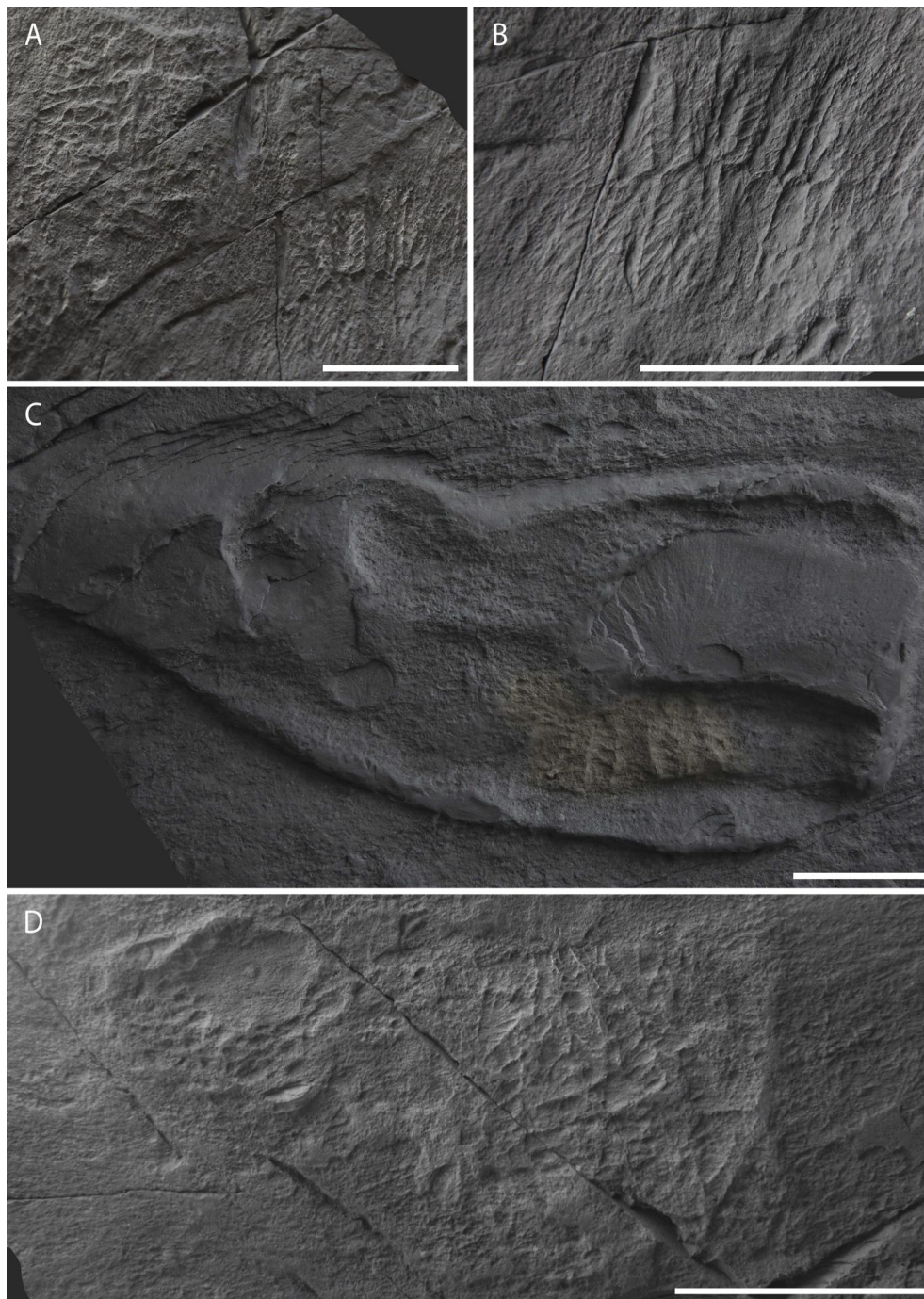


Figure 4.8: rangeomorph-‘*Blackbrookia*’ associations.

A) “*Blackbrookia*” specimen showing *Bradgatia*-like branching. Scale bar = 5 cm; **B)** *Fractofusus andersoni* from the JDS. Scale bar = 5 cm; **C)** fusiform specimen (i11) showing *Fractofusus*-like branching (in yellow). Specimen previously figured in Hofmann et al. 2008 (cf. fig. 25.3). Scale bar = 5 cm; **D)** detail of the “*Blackbrookia*” specimen with *Bradgatia*-like branching, showing porose morphology at the pointed end of the fossil. Scale bar = 5 cm.

8.2. Population structure of the Johnson Discovery Surface

Untransformed length and width frequency distributions were right-skewed and moderately depart from normality. Log-transformed quantitative variables (tV1, tV2, tV3 in **Fig. 4.9 A, C, E**; following Darroch et al., 2013) and ratio of major axis/minor axis (V3) were normally distributed.

When normality of the two subsets (regular and irregular) is tested separately, Shapiro-Wilk tests always find a normal distribution of all the variables, non-transformed and transformed.

Size–frequency distributions graphs (**Fig. 4.9 A, C, E**) can be helpful in reconstructing population structure and can be used to suggest reproductive and growth models within a population (Meesters et al., 2001; Darroch et al., 2013; Pérez-Pinedo et al., 2023). Irregular specimens show distribution peaks at lower values of tV1 (**Fig. 4.9 A**), at similar values of tV2 (**Fig. 4.9 C**) and at higher values of tV3 (**Fig. 4.9 E**) compared to regular specimens (**Fig. 4.9 A, C, E**). A Welch Two Sample t-test indicates that the means of all the variables, untransformed and transformed, are statistically different for the two subsets of “regular” and “irregular” specimens, with regular specimens showing greater mean values for the variables V1, tV1, V3 and tV3 and smaller values for V2 and tV2 (**Tab. 4.1**). The lower V3 and tV3 values measured in the irregular specimens are consistent with the lower eccentricity shown by backtransform morphospace analyses (**Fig. 4.4**).

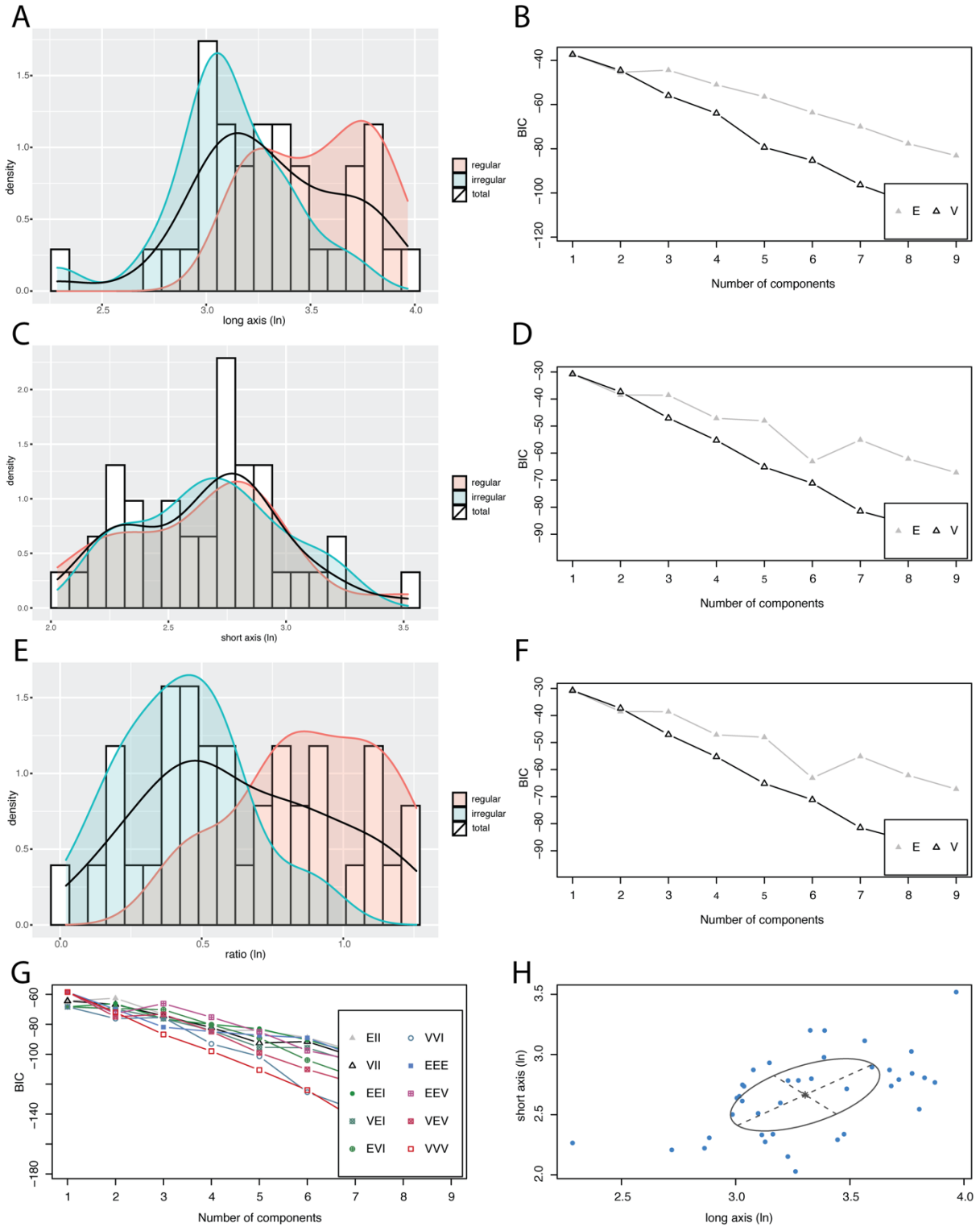


Figure 4.9: size frequency distribution graphs and BIC.

A) Size frequency distribution of tV1; **B)** Bayesian Inference Criterion (BIC) results for univariate data [tV1]; **C)** size frequency distribution of tV2; **D)** Bayesian Inference Criterion (BIC) results for univariate data [tV2]; **E)** size frequency distribution of tV3; **F)** Bayesian

Inference Criterion (BIC) results for univariate data [tV3]); **G**) Bayesian Inference Criterion (BIC) results for bivariate data [tV1+tV2]; **H**) classification of the data point according to the best model (EEE, ellipsoidal, equal volume, shape and orientation) for bivariate [tV1+tV2] BIC. (**B; D; F**): E and V correspond to models that assume equal and unequal variance. (**G**): A three letter code is associated to each model, which correspond to shape, volume and orientation, respectively and can be constrained (“E”) or unconstrained (“V”).

To find the most likely number of modes, and therefore possible age classes within the population, a likelihood-based model selection criterion (BIC) was used to choose the most probable clustering solutions produced by Gaussian finite mixture model-based clustering algorithms (Scrucca et al. 2016). Univariate analyses on the transformed variables tV1 (**Fig. 4.9 B**), tV2 (**Fig. 4.9 D**) and tV3 (**Fig. 4.9 F**) resulted in a single mode as the best fitting model, assuming both equal and unequal variance. When conducting multivariate analyses, Mclust generates best-fitting models that assume ellipsoidal, diagonal, and spherical distributions. Models that assume ellipsoidal distributions are the most biologically realistic, as they allow unequal variances on two axes. The single mode found by the univariate analyses is confirmed from bivariate [tV1+tV2] clustering solutions (**Fig. 4.9 G-H**), which also finds a single mode ellipsoidal distribution as the most likely grouping solution for the analysed specimens.

8.3. Other porose-textured taxa from the Mistaken Point biota

Mistaken Point on the southeast coast of Newfoundland's Avalon Peninsula is well known for its abundant deep marine Ediacaran biotas (Narbonne, 2005), with most work having focused on fossils from the taxonomically diverse E Surface (Seilacher, 1992; Narbonne, 2005; Darroch et al., 2013; Taylor et al., 2021, 2023; Vixseboxse et al., 2021; McIlroy et al., 2022). The underlying D Surface is however under-studied and includes examples of recently described arboreomorphs (Pérez-Pinedo et al., 2022) and the abundant rangeomorphs *Fractofusus* (Taylor et al., 2023), *Bradgatia* (Flude and Narbonne, 2008) and *Pectinifrons* (Bamforth et al., 2008), as well as rare *Hapsidophyllas flexibilis* (Taylor et al., 2021). Previously overlooked on the D and parts of the E surface are surface textures comparable to those of “*Blackbrookia*”, except preserved as internal moulds of the pores (**Fig. 4.10 A-C**). In some cases, the low relief porose texture pseudomorphs another—possibly arboreomorph—taxon (**Fig. 4.10 A**), but it also exists as small circular positive epirelief features with no associated branching structures preserved (**Fig. 4.10 C**) or as a less pronounced low-relief obovate shape (**Fig. 4.10 B**). When wet, these fossils are distinguished by their slightly lighter colour, suggesting that there may be some biomineral present or there is a differential fill of a leuconoid-like aquiferous cavity (**Fig. 4.10 A-C**).

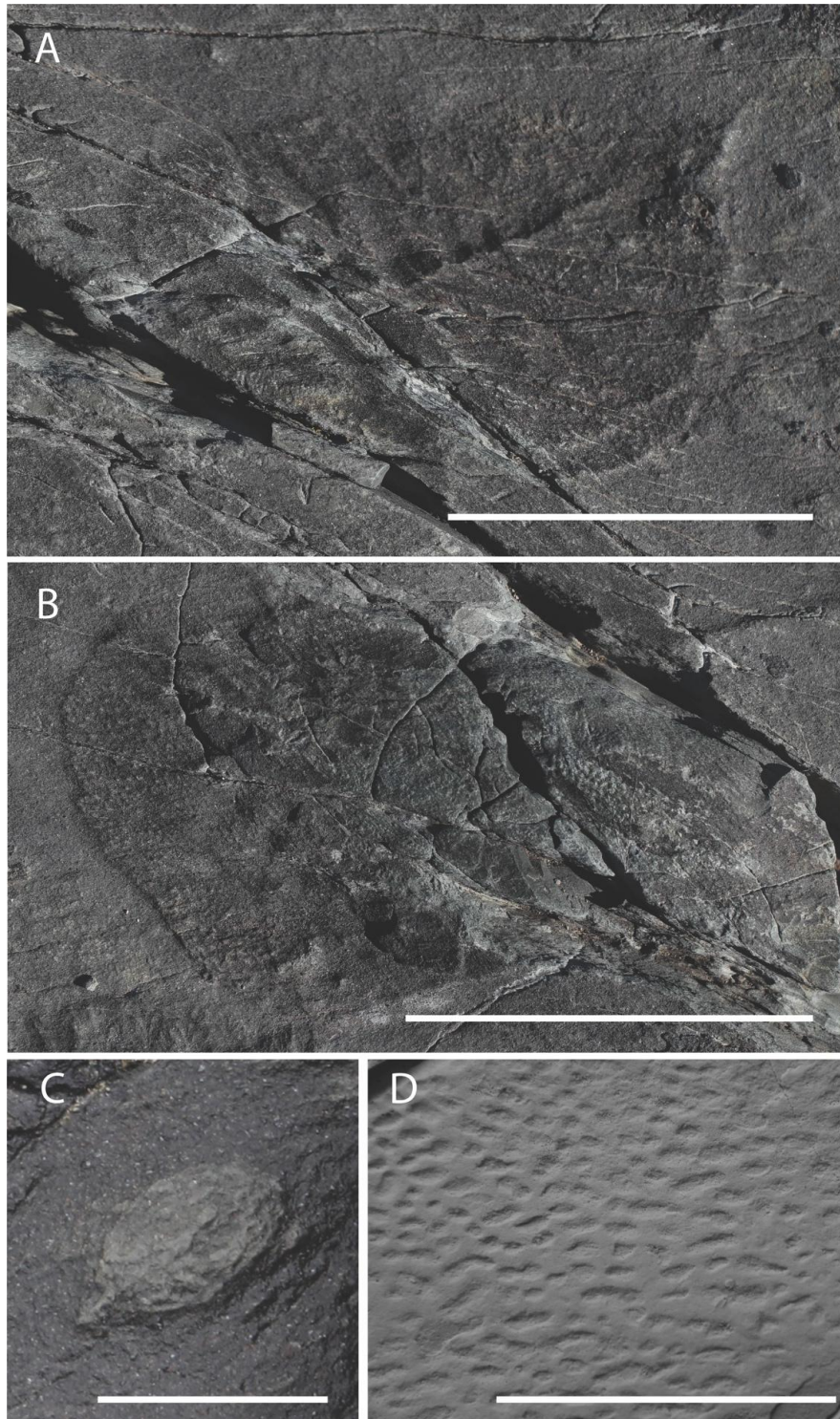


Figure 4.10: other porose-textured taxa.

A) Specimen encrusting a possible arboreomorph from the D Surface at MPER, scale bar = 5 cm; B) obovate specimen from the D Surface at MPER, scale bar = 5 cm; C) Small circular specimen showing pores but no recognizable branching morphology from the E surface at MPER. Scale bar = 1 cm; D) fossil matground *Kinneyia* from the Cambrian of South Africa. Scale bar = 5 cm.

8.4. Competing models for “*Blackbrookia*” morphology

8.4.1. Association with underlying frondose organisms

Competing models for the “*Blackbrookia*”–rangeomorph association are explored, as well as possible systematic interpretations of the taxon. Any viable model should account for all the observations and such models compared to determine whether there is a likely best fit.

The association of rangeomorph branching at low topographic levels in some “*Blackbrookia*”, makes it tempting to suggest that the Rangeomorpha might have had a leuconoid-like aquiferous system with ostia and oscula. In such a model, rangeomorphs might be reclining organisms with a high surface area lower surface, possibly for harbouring chemosymbionts (cf. Dufour and McIlroy, 2017; McIlroy et al., 2021; Pasinetti and McIlroy, 2023), in which case the upper sponge-like surface might be used for feeding and respiration, with an aquiferous system in the intervening cavity.

The upper surface of some rangeomorph taxa are known from rare examples of three-dimensional preservation, including: the Upper Island Cove biota in Newfoundland (Narbonne, 2004; Narbonne et al., 2009; Brasier et al., 2013; McIlroy et al., 2020; McKean et al., 2023); rangeomorphs from the Flinders Ranges, Australia (Gehling, 1999); and two specimens of *Charnia* from the White Sea (Butterfield, 2020). Of these, only the White Sea *Charnia* have pores (compared to the Cnidaria by Butterfield, 2022) and those specimens have rangeomorph-type architecture on the upper surface. None of these examples are similar to the morphology of the Catalina Dome “*Blackbrookia*”, which is considered highly unlikely to be a rangeomorph and alternate hypotheses must be sought. The preservational style seen might reflect the lower surface of reclining rangeomorphs being rather firm (Dufour and McIlroy, 2017), potentially being further cast by the basal tissues of the “*Blackbrookia*”.

Associations between necromass (ivesheadiomorphs) and subsequent rangeomorphs (especially *Fractofusus*) resulting from community succession is common in the Ediacaran of Newfoundland (Liu et al., 2011; Dufour and McIlroy, 2017), giving cause for caution in interpreting the Catalina Dome “*Blackbrookia*” as the top of a rangeomorph. The association of pustulate surfaces with an arboreomorph on the D surface at Mistaken Point (**Fig. 4.10 A**) and other taxa such as a strap-like form on the E surface suggest that the morphology is not restricted to the Rangeomorpha, which are a clade distinct from the Arboreomorpha (Dececchi et al., 2017; Pérez-Pinedo et al., 2022). As such, the hypothesis that the “*Blackbrookia*” of the JDS are the tops of rangeomorphs is rejected.

8.4.2. *If not rangeomorph then what?*

Many possibilities have been proposed for the affinities of different elements of the classic frondose members of the Ediacaran biota, with authors suggesting that some taxa might be ancestors of modern taxonomic groups, including fungi, metazoans, protists and algae (Retallack, 1994; Boynton and Ford, 1995; Dunn et al., 2021) extinct “stem” groups of modern clades (Xiao and Laflamme, 2009) or, in some cases, even extinct kingdoms (Seilacher, 1992). It is clear however that the Ediacaran biota include a large diversity of taxa, often superficially similar to each other but with substantially different Bauplans (for example, frondose rangeomorphs and arboreomorphs; Dececchi et al., 2017), suggesting that the diversity of Ediacaran ecosystem has been largely underestimated and the taxonomic position of each fossil should be considered separately.

The appearance of the proposed perforate upper surface of the “*Blackbrookia*” component does resemble some end members of Kinneyia-type microbial matground surfaces (Noffke et al., 2021), though the expression of matground pustules is often trigonous rather than circular (**Fig. 4.10 D**) and the porose structures in “*Blackbrookia*” are limited to the top portion of the fossil and are not observed in the surrounding matground. The porose and particularly the papillate textures of the Catalina Dome “*Blackbrookia*” are difficult to reconcile with a microbial matground model and are better explained as infilled structures that represented raised openings in the body of the organisms in life. While it seems evident that “*Blackbrookia*” is the body fossil of a collapsed macro-organism, determining its systematic nature remains, as for many other Ediacaran taxa, problematic.

It is unlikely that “*Blackbrookia*” is an algal taxon or any other photosynthetic group, as the Ediacaran successions of the Catalina Dome have been inferred to have been deposited at substantial depth, often at the bottom of the continental slope (O’Brien and King, 2004, 2005; Mason et al., 2013). Similarly, we can reject the hypothesis that “*Blackbrookia*” was

fungal, as most marine fungi are microscopic, and no marine mushrooms are known (Cunliffe, 2023) . Instead, the size of the organisms, as well as their complex morphology, suggest that they could be investigated as candidate metazoans. The discovery of *Haootia quadriformis* (Liu et al., 2014), a stem cnidarian, in nearby strata of similar age, confirms that eumetazoans had already evolved and differentiated during the Ediacaran. However, there is sparse evidence for bilaterians in the Avalon Assemblage (Liu and McIlroy, 2015) and “*Blackbrookia*” does not have any characteristic eumetazoan traits.

The porose morphology of the best-preserved example leads us to suggest that “*Blackbrookia*”, from the Catalina Dome in particular, are candidates for being considered sponges. The pores in “*Blackbrookia*” resemble “oscula” (i.e. the exhalant openings) of modern encrusting demosponges. However, encrusting demosponges are typically amorphous in outline (in contrast with the regular outlines of “*Blackbrookia*”). Additionally, early sponges are believed to have evolved from thin-bodied taxa with only one exhalant opening (Botting and Muir, 2018). Moreover, Botting and Muir (2018) refute the presence of Ediacaran sponges, including specimens with articulated spicules (Li et al., 1998; Wörheide et al., 2012; Dohrmann and Wörheide, 2017) in favour of Early Cambrian evolution and diversification. This hypothesis is supported by some molecular evidence, which determine Ctenophora as sister group of all other animals rather than the Porifera, which have traditionally been considered the most basal of all metazoans (Jákely et al., 2015; Ryan and Chiodin, 2015; Schultz et al., 2023).

Even if molecular analyses were to positively identify the Ctenophora as sister group of all other Metazoa, this would make the Porifera a sister group of the Eumetazoa, which have also been confirmed to be present in the Avalon Assemblage (Liu et al., 2014; 2015). Therefore, even though there is not enough evidence to positively assess “*Blackbrookia*” as a poriferan, it is also not possible to reject this hypothesis yet on stratigraphic grounds.

Lastly, the possibility remains that “*Blackbrookia*” is an extinct Porifera-like clade, with no Phanerozoic record, as has been proposed for almost all Ediacaran groups at some stage (e.g., Seilacher, 1992). This possibility should be taken into consideration, even though it is not possible to falsify it.

9. Discussion

The macrofossils of the Ediacaran biota are difficult to treat systematically, partly because of the difficulties in preserving soft-bodied Ediacaran organisms (Gehling, 1999; McIlroy et al., 2009); their complex morphology (Brasier and Antcliffe, 2004, 2009; Narbonne, 2004); and the fact that we know little about their life cycles (Brasier and Antcliffe, 2004; Mitchell et al., 2015; Liu and Dunn, 2020) and especially affinities (Ford, 1958; Jenkins, 1985; Seilacher, 1992, 1999; Retallack, 1994; Sperling et al., 2007; Sperling and Vinther, 2010; Butterfield, 2020; Dunn et al., 2021). There is also a lack of clarity over whether many Ediacaran taxa should be covered by the International Code of Zoological Nomenclature (ICZN) or the International Code of Nomenclature for algae, fungi and plants (ICN; formerly the International Code of Botanical Nomenclature). Many Ediacaran macrofossils are known primarily from their morphologically simple basal disks that have few diagnostic characters (e.g., *Aspidella s.l.*; *Hiemalora*). Some discoidal taxa have even been found in association with more than one frondose taxon. For example, both *Primocandelabrum hiemaloranum* (Hofmann et al., 2008) and *Arborea* sp. (Wang et al., 2020) have both been observed with a *Hiemalora* base, despite apparently belonging to two unrelated clades of frondose taxa (the Rangeomorpha and Arboreomorpha respectively; see Dececchi et al., 2018; Pérez-Pinedo et al., 2022). Additionally, many occurrences of *Hiemalora* do not have any associated frond (Fedonkin, 1982). For this reason, organ taxa—which are accepted in the ICN but not the ICZN—have been invoked (Hofmann et al., 2008), despite recent suggestions that the Rangeomorpha and Arboreomorpha belong in the Eumetazoa (Dunn et al., 2019, 2021).

The discussion above suggests that the taxa referred to by the obsolete name “*Blackbrookia*” from the Catalina Dome (**Fig. 4.1**) are distinct from the pseudofossil

Blackbrookia from the UK (Liu et al., 2011). As such the material requires formal taxonomic treatment.

9.1. Systematic Palaeontology

Genus *Lydonia* gen. nov.

2008 *Blackbrookia* sp., Hofmann et al., fig. 25, 1-5.

2015 ‘Blackbrookia’, Liu et al., fig. 5g.

2017 *Blackbrookia*, Dufour and McIlroy, fig. 2a-c.

2017 ‘*Blackbrookia*’, Liu et al., fig. 14f.

2021 cf. *Crumillospongia*, McIlroy et al., fig. 5a.

Etymology: Named for the punk rock legend John Lydon, with whom this taxon is considered to have shared a spiky “hairstyle”.

Diagnosis: Ovate to vase shaped fossils commonly preserved in positive relief and covered in small pores, or an iron-rich mesh-like reticulate structure. Upper surface is typically longitudinally folded, sometimes with a positive relief rim. Shape is very variable, and the size of pores is similarly variable within and between specimens. Typical size range is from 15-40 cm in the longest dimension.

Type Species: *Lydonia jiggamintia* by monotypy.

Etymology: Jiggamint is latinized from the Beothuk word for gooseberry (a spiky current). We use the Beothuk word to honour the original inhabitants of the island of Newfoundland who were extirpated by European colonizers. Isolated words were recorded from captured Beothuk in the early 1800’s (especially from Oubee, Desmasduwit and Shawnadithit).

Diagnosis: as for the genus.

Holotype: Specimen remains *in situ* on the Johnson Discovery Surface (**Fig. 4.2 A**; **Fig. 4.11**), from the Trepassey Formation of the Catalina Dome, Bonavista Peninsula, Newfoundland, CA (**Fig. 4.1 B-C**).

Plastotype: a cast of the holotype has previously been accessioned to the Rooms Corporation of Newfoundland and Labrador (St. John's, NL) with the accession number NFM F-534 (Hofmann et al., 2008).

Paratype: paratype A: regular specimen, in situ on the Discovery Surface (**Fig. 4.2 A**, bottom); paratype B: irregular specimen, in situ on the Discovery Surface (**Fig. 4.2 B**).

Description: the holotype is an obovate specimen with a smooth profile and a clear polarity along the longest axis from a rounded end to a pointed end and is preserved as a positive epirelief on the fossiliferous surface, from which it is separated by an abrupt positive rim. The long axis is 32.3 cm long and the short axis is 10.4 cm long, with a ratio of 3.11. The holotype is symmetrical with respect to the long axis. The holotype has a longitudinal fold in its central portion that runs all the way from the rounded pole to the pointed one. Both sides of the ridge have an extensive mesh-like pattern of small pores of regular size, with a diameter of about 0.5 cm. Two main morphologies are present: regular specimens, such as Paratype A, which strongly resemble the obovate shape of the holotype, and irregular specimens, such as Paratype B, which has a lobate profile but a similar porose surface and raised rim.



Figure 4.11: holotype of *Lydonia*.

Jesmonite cast of the holotype of *Lydonia jiggamintia*. Scale bar = 10 cm.

Discussion: *Lydonia* are variable in shape, with ovate, circular, sock-shaped, semi-circular and almost square forms known. The upper surface may be covered in small pores, which might have been openings in life, possibly with raised rims or papillae extruding, or alternatively there may be a ferruginous mesh-like covering to the upper surface; or a combination of the two modes of preservation. The size distribution of pores or mesh size is not systematic but spacing in-between is typically less than 0.5cm. Common gross outlines of *Lydonia* are obovate and ovate (cf. Holotype, Paratype A), but many specimens have an irregular profile that diverge from a regular ovoid with lobes and convex curves in their profile (cf. Paratype B). Both ovoid and irregular forms may have one or more folded ridges and a positive relief rim.

9.2. Morphological Reconstruction

The mode of life of *Lydonia* is considered to be that of a sessile epibenthic or semi-infaunal organism, which potentially colonized other macro-organisms. To date, *Lydonia* is only documented from surfaces with abundant *Fractofusus*, though the two are not thought to be related. The wrinkled upper surface of *Lydonia* resembles that of a collapsed upper surface that was originally slightly inflated in life (**Fig. 4.6 B**). The distribution of pores and the presence of papillae is based on direct morphological evidence from the holotype in the form of short silty internal moulds of papillae, and by comparison with modern papillate sponges such as the demosponge *Polymastia*.

Other pustulate taxa from Mistaken Point in south-eastern Newfoundland (**Fig. 4.10 A-C**) are likely to have had similar morphologies; they are found overgrowing other organisms (arboreomorphs) or as discrete colonies. The Mistaken Point fossils extend laterally beyond the underlying organism to grow in contact with the seafloor and its matground. The lack of wrinkling in those Mistaken Point *Lydonia* suggests that they had a thinner body than the *Lydonia* from the Catalina Dome, potentially analogous to that of modern encrusting demosponges (Goodwin et al., 2021). A single specimen has bulging 3D textures near the presumed centre of the body, suggesting that the middle of the organism was thicker than nearer the margins (**Fig. 4.10 C**).

9.3. Palaeobiology and development of the Catalina Dome specimens

The population of *Lydonia* from the JDS have highly variable outlines, from circular to elliptical and irregular, and maximum dimensions ranging from 9.8 cm to 52.7 cm in length. Regular specimens have long/short axial ratios (V3) from 1.35 to 3.52, with an average of 1.99 (**Tab. 4.1**), while irregular specimens have a lower eccentricity and V3 values that range from 1.02 and 2.51, with an average of 1.57. Most specimens on the surface (76%) are broadly oriented with the long axis in the direction of the inferred palaeocurrent, either with the pointed or the blunt end upstream, with V3 ranging from 1.02 to 3.52, with an average of 2.10. The remaining specimens are oriented broadly perpendicular to the palaeocurrent, with the pointy end on either side of it: such specimens have a low long/short axial ratio (1.12 to 1.66, with one outlier at 2.23 and an average of 1.50), which a Welch Two Sample t-test confirms to be significantly lower than the average V3 of oriented specimens. Both regular and irregular specimens can be found in both orientation groups.

Linear regressions between tV2 (short axis) and tV3 (ratio) show a negative correlation (**Fig. 4.3 D**), indicating that the species was likely subject to allometric growth. In an isometric growth model, we would expect tV3 to remain constant through the life of the specimen, but it appears that the long axis was subject to faster growth than the short, possibly to increase the surface exposed to the current without too much increase in drag. Under the assumption of allometric growth, V3 and tV3 can be interpreted to be loosely correlated to the age of the organism. This would create a fast flow of current on top of the specimen along its long axis, increasing its access to particulate and dissolved organic matter and enabling improved gas exchange with the water column. This is also consistent with the lower long/short axis ratio characteristic of specimens oriented perpendicular to the current: an increase of the short axis relative to the long axis would have elongated the specimen in the direction parallel to the

current. Similar allometric growth was described by Darroch et al. (2013) for several taxa from the Mistaken Point E and D surfaces, including *Thectardis avalonensis* and *Fractofusus misrai*.

Backtransform morphospace analyses suggest that differences in the profile shape of the specimens on the JDS do not represent taxonomic differences. Regular and irregular comprise a continuum, with differences probably arising from developmental and palaeobiological factors or, in some cases, such as the Ivesheadia-like specimens, post-mortem processes. This would also be consistent with the large percentage of irregular specimens lacking pores, possibly due to necrosis and/or microbial overgrowth (cf. Liu et al. ,2011). We observe that regular specimens are typically longer than irregular specimens (**Fig. 9A**), suggesting that they might have either 1) colonized the surface earlier, 2) have a micro-environmental advantage or 3) have a rheotropic advantage.

As there is supporting evidence for the organisms being reclining on the seafloor or semi-infaunal, possibly covered in microbial matground, it is possible that the obovate shape of the strongly parallel-oriented end members of the population represents an advantageous adaptation to the inferred directional paleocurrents, by increasing the exposed surface without increasing drag or lift.

If we interpret *Lydonia* as an epibenthic organism which potentially settled by encrusting and overgrowing other organisms, it is possible that the differences in shape could also be attributed to the characteristics of the host organism. *Lydonia* encrusting small organisms or highly decomposed organisms might have soon run out of space (or nutrients if they performed saprotrophy in some way and might also exhibit secondary growth (**Fig. 4.2 B**). These findings are consistent with the proposed interpretation of the population of *Lydonia* from the JDS being a poriferan or an organism with a poriferan-like morphology.

9.4. Population Models

Our analyses suggest that the specimens on the JDS all belong to the same species and that there are no distinctive size modes or age classes. Darroch et al. (2013) gives three possible explanations to the absence of size modes within Ediacaran benthic communities: 1) the *all for one* model, where all of the specimens belong to the same age class and are the result of a single colonization/recruitment event; 2) the *slow and steady* model, in which growth rates are slower relative to the seasonal reproductive rates and 3) the *continuous* reproduction model, in which the absence of age classes is the result of continuous aseasonal reproduction. All the three models have been documented in benthic marine invertebrate communities. The *all for one* model typically results in organisms of very similar sizes (e.g., holothurians Billett and Hansen, 1982) and it would require invoking local environmental differences to explain the high size variability observed in the JDS community. Ediacaran seafloors are typically interpreted as being rather homogeneous (Butterfield, 1997; Darroch et al., 2013), in terms of spatial distribution of nutrients and for this reason the “all for one” model was deemed unlikely to explain the single size modes in several Ediacaran communities in Newfoundland (Darroch et al., 2013). Moreover, we observe a large variability for the V3 and tV3 variables in the JDS population, which has been interpreted as a possible proxy for age. In a “slow and steady” model, age classes resulting from seasonal reproductive events are present, but slow growth rates of the organisms result in a continuous size-frequency distribution and a single size mode, while in a continuous reproduction model the absence of different size modes is the result of aseasonal reproduction.

Support for a “slow and steady” model in Ediacaran communities can be found in modern deep-marine benthic communities, which are characterized by slower growth rates than similar taxa in shallow waters (e.g., bivalves, Turekian et al., 1975; and octocorals Cordes et

al., 2001). Modern sponges have been found to reproduce seasonally in both deep and shallow water settings (Witte, 1996; Shaffer et al., 2020); this is coupled with slow growth rates and great longevity (Leys and Lauzon, 1998; Baquiran et al., 2020). In some cases, growth rates might also be correlated with seasonality (Leys and Lauzon, 1998). When growth rates are fast, as in the case of the giant barrel sponge, seasonal reproduction could result in distinct size modes within a population (McMurray et al., 2010).

Since we were not able to recognize seasonal or aseasonal reproductive patterns in the *Lydonia* assemblage of the JDS, it is not possible to distinguish between the two hypotheses and a combination of the two (aseasonal reproduction and slow growth rates) is also possible.

9.5. Candidate sponges of Ediacaran age from Newfoundland

Candidate sponges among the Ediacaran biota are generally contentious but of significant importance for the calibration of molecular clocks (e.g. Cummings et al. 2017). The Ediacaran taxon that is most widely attributed to the Porifera or pre-sponges is the inferred infundibuliform *Thectardis avalonensis* (Clapham et al., 2004; Sperling et al., 2007; Dufour and McIlroy, 2017; Aragonés Suarez and Leys, 2022), which likely lived in a reclined position commonly with the open end of the cone either orientated directly into or away from a weak current at least at Mistaken Point (McIlroy et al., 2022b), and is also present on the Johnson Discovery Surface. Specimens of *Thectardis* do not preserve spicules and as such do not meet the high bar that has been set for confirming a fossil poriferan by Antcliffe et al. (2014). While the fossil record of the Porifera might be contentious, there is also scope for the preservation of Cavalier-Smith (2017) “pre-sponge” grade of organization (Dufour and McIlroy, 2017, 2018). It is perhaps possible that *Thectardis* meets the criteria for this pre-sponge grade of organization. Other porose taxa without spicules that could be considered as possible sponges include *Kuckaraukia* sp. and *Gibbavasis kushkii* from what may be the latest Ediacaran of Iran (Razumovskiy et al., 2015; Vaziri et al., 2018).

10. Conclusions

Determining the clade to which Ediacaran macrofossils belong is challenging. An unequivocal sponge fossil would need evidence for an aquiferous system including ostia/oscula, along with evidence for a spiculate skeleton. The latter is not yet recognized for *Lydonia* or the other sponge-like taxa in the offshore shelf to deep-marine Ediacaran strata of Avalonian Newfoundland and therefore does not meet Antcliffe's bar for determining a fossil as poriferan (Antcliffe et al., 2014). The presence of an aquiferous system is evinced by the inferred originally inflated morphology of *Lydonia* and the evidence for numerous openings (similar to demosponge osculae) of the upper surface, which were possibly raised into the water column on short papillae. The presence of pores in the upper surface of *Lydonia* is likely correlated with a filter-feeding mode of life, possibly similar to that of modern encrusting sponges.

The presence of *Lydonia* on top of rangeomorph and arboreomorph fossils is unlikely to be accidental. Having excluded *Lydonia* as being part of the underlying organism, we are left with the possibility that the dead bodies of other organisms would have offered a settling substrate for larval or juvenile *Lydonia*, and it could be possibly correlated with a saprotrophic secondary feeding strategy. The population structure of a *Lydonia*-rich assemblage in the Ediacaran of Avalonia reveals a single size mode, similar to that of other Ediacaran assemblages (Darroch et al., 2013) and consistent with modern poriferan population structure (Baquiran et al., 2020), but not unequivocally so.

The poriferan-like morphology of *Lydonia* suggests that other evidence of sponges—such as spicules—might yet be found in the Ediacaran of Avalonia. Such evidence would then meet the high bar set by Antcliffe et al. (2014) for conclusive demonstration of Ediacaran sponges that could then be used to help unravel the early history of animal life.

11. Acknowledgements

Fossil surfaces in the Bonavista Peninsula are protected under Reg. 67/11, of the Historic Resources Act 2011 and their access is only allowed under permission from the Government of Newfoundland and Labrador. Fieldwork near Port Union was conducted under permit from the Government of Newfoundland and Labrador. Thanks are due to: Edith and Neville Samson for their kind support; Mike Steele for help collecting field data; Don Johnson for his discovery of the Johnson Discovery Surface; and Natural Sciences and Engineering Research Council of Canada (NSERC) for Discovery Grant (individual) and DAG funding to DM.

12. References

- Antcliffe, J. B., Callow, R. H. T., and Brasier, M. D. (2014). Giving the early fossil record of sponges a squeeze. *Biological Reviews* 89, 972–1004. doi: 10.1111/brv.12090
- Antcliffe, J. B., Hancy, A. D., and Brasier, M. D. (2015). A new ecological model for the ~565Ma Ediacaran biota of Mistaken Point, Newfoundland. *Precambrian Research* 268, 227–242. doi: 10.1016/j.precamres.2015.06.015
- Aragonés Suarez, P., and Leys, S. P. (2022). The sponge pump as a morphological character in the fossil record. *Paleobiology* 48, 446–461. doi: 10.1017/pab.2021.43
- Bak, R., and Meesters, E. (1998). Coral population structure: the hidden information of colony size-frequency distributions. *Mar. Ecol. Prog. Ser.* 162, 301–306. doi: 10.3354/meps162301
- Bamforth, E. L., Narbonne, G. M., and Anderson, M. M. (2008). Growth and ecology of a multi-branched Ediacaran rangeomorph from the Mistaken Point assemblage, Newfoundland. *Journal of Paleontology* 82, 763–777. doi: 10.1666/07-112.1
- Baquiran, J. I. P., Nada, M. A. L., Posadas, N., Manogan, D. P., Cabaitan, P. C., and Conaco, C. (2020). Population structure and microbial community diversity of two common tetillid sponges in a tropical reef lagoon. *PeerJ* 8, e9017. doi: 10.7717/peerj.9017
- Billett, D. S. M., and Hansen, B. (1982). Abyssal aggregations of *Kolga hyalina* Danielssen and Koren (Echinodermata: Hoiothurioidea) in the northeast Atlantic Ocean: a preliminary report. *Deep-Sea Research* 29, 799–818. doi: 10.1016/0198-0149(82)90799-9
- Botting, J. P., and Muir, L. A. (2018). Early sponge evolution: A review and phylogenetic framework. *Palaeoworld* 27, 1–29. doi: 10.1016/j.palwor.2017.07.001
- Boynton, H. E., and Ford, T. D. (1995). Ediacaran fossils from the Precambrian (Charnian Supergroup) of Charnwood Forest, Leicestershire, England. *Mercian Geologist* 13, 156–182.
- Brasier, M., and Antcliffe, J. B. (2004). Decoding the Ediacaran Enigma. *Science* 305, 1115–1117. doi: 10.1126/science.1102673
- Brasier, M. D., and Antcliffe, J. B. (2009). Evolutionary relationships within the Avalonian Ediacara biota: new insights from laser analysis. *Journal of the Geological Society* 166, 363–384. doi: 10.1144/0016-76492008-011
- Brasier, M. D., Liu, A. G., Menon, L., Matthews, J. J., McIlroy, D., and Wacey, D. (2013). Explaining the exceptional preservation of Ediacaran rangeomorphs from Spaniard's Bay, Newfoundland: A hydraulic model. *Precambrian Research* 231, 122–135. doi: 10.1016/j.precamres.2013.03.013

- Butterfield, N. J. (1997). Plankton ecology and the Proterozoic-Phanerozoic transition. *Paleobiology* 23, 247–262. doi: 10.1017/S009483730001681X
- Butterfield, N. J. (2020). Constructional and functional anatomy of Ediacaran rangeomorphs. *Geol. Mag.*, 1–12. doi: 10.1017/S0016756820000734
- Cavalier-Smith, T. (2017). Origin of animal multicellularity: precursors, causes, consequences—the choanoflagellate/sponge transition, neurogenesis and the Cambrian explosion. *Phil. Trans. R. Soc. B* 372, 20150476. doi: 10.1098/rstb.2015.0476
- Clapham, M. E., Narbonne, G. M., Gehling, J. G., Greentree, C., and Anderson, M. M. (2004). *Thectardis avalonensis*: A new Ediacaran fossil from the Mistaken Point biota, Newfoundland. *Journal of Paleontology* 78, 1031–1036. doi: 10.1666/0022-3360(2004)078<1031:taanf>2.0.co;2
- Cordes, E. E., Nybakken, J. W., and VanDykhuisen, G. (2001). Reproduction and growth of *Anthomastus ritteri* (Octocorallia: Alcyonacea) from Monterey Bay, California, USA. *Marine Biology* 138, 491–501. doi: 10.1007/s002270000470
- Cunliffe, M. (2023). Who are the marine fungi? *Environmental Microbiology* 25, 131–134. doi: 10.1111/1462-2920.16240
- Darroch, S. A. F., Laflamme, M., and Clapham, M. E. (2013). Population structure of the oldest known macroscopic communities from Mistaken Point, Newfoundland. *Paleobiology* 39, 591–608. doi: 10.1666/12051
- Decechi, T. A., Narbonne, G. M., Greentree, C., and Laflamme, M. (2017). Relating Ediacaran Fronds. *Paleobiology* 43, 171–180. doi: 10.1017/pab.2016.54
- Dohrmann, M., and Wörheide, G. (2017). Dating early animal evolution using phylogenomic data. *Sci Rep* 7, 3599. doi: 10.1038/s41598-017-03791-w
- Dufour, S. C., and McIlroy, D. (2017). Ediacaran pre-placozoan diploblasts in the Avalonian biota: the role of chemosynthesis in the evolution of early animal life. *Geological Society, London, Special Publications* 448, 211–219. doi: 10.1144/SP448.5
- Dufour, S. C., and McIlroy, D. (2018). An Ediacaran pre-placozoan alternative to the pre-sponge route towards the Cambrian explosion of animal life: a comment on Cavalier-Smith 2017. *Phil. Trans. R. Soc. B* 373, 20170148. doi: 10.1098/rstb.2017.0148
- Dunn, F. S., Grazhdankin, D. V., Liu, A. G., and Wilby, P. R. (2021). The developmental biology of *Charnia* and the eumetazoan affinity of the Ediacaran rangeomorphs. *Science Advances*, 14.
- Fedonkin, M. A. (1982). A new generic name for some Precambrian Coelenterates. *Paleontologicheskij Zhurnal* 2.
- Flude, L. I., and Narbonne, G. M. (2008). Taphonomy and ontogeny of a multibranch Ediacaran fossil: *Bradgatia* from the Avalon Peninsula of Newfoundland. *Can. J. Earth Sci.* 45, 1095–1109. doi: 10.1139/E08-057

- Ford, T. D. (1958). Pre-Cambrian fossils from Charnwood Forest. *Proceedings of the Yorkshire Geological Society* 31, 211–217. doi: 10.1144/pygs.31.3.211
- Gehling, J. G. (1999). Microbial mats in terminal Proterozoic siliciclastics: Ediacaran death masks. *PALAIOS* 14, 40. doi: 10.2307/3515360
- Gehling, J. G., and Narbonne, G. M. (2007). Spindle-shaped Ediacara fossils from the Mistaken Point assemblage, Avalon Zone, Newfoundland. *Can. J. Earth Sci.* 44, 367–387. doi: 10.1139/e07-003
- Goodwin, C., Dinn, C., Nefedova, E., Nijhof, F., Murillo, F. J., and Nozères, C. (2021). Two new species of encrusting sponge (Porifera, family Crellidae) from eastern Canada. *Can. J. Zool.* 99, 760–772. doi: 10.1139/cjz-2021-0041
- Hofmann, H. J., O'Brien, S. J., and King, A. F. (2008). Ediacaran biota on Bonavista Peninsula, Newfoundland, Canada. *J. Paleontol.* 82, 1–36. doi: 10.1666/06-087.1
- Jákely, G., Paps, J., and Nielsen, C. (2015). The phylogenetic position of ctenophores and the origin(s) of nervous systems. *EvoDevo* 6, 1. doi: 10.1186/2041-9139-6-1
- Jenkins, R. J. F. (1985). The enigmatic Ediacaran (late Precambrian) genus *Rangea* and related forms. *Paleobiology* 11, 336–355. doi: 10.1017/S0094837300011635
- Kenchington, C. G., and Wilby, P. R. (2014). Of time and taphonomy: preservation in the Ediacaran. *The Paleontological Society Papers* 20, 23. doi: <https://doi.org/10.1017/S1089332600002825>
- Laflamme, M., Flude, L. I., and Narbonne, G. M. (2012). Ecological tiering and the evolution of a stem: the oldest stemmed frond from the Ediacaran of Newfoundland, Canada. *J. Paleontol.* 86, 193–200. doi: 10.1666/11-044.1
- Laflamme, M., Narbonne, G. M., Greentree, C., and Anderson, M. M. (2007). Morphology and taphonomy of an Ediacaran frond: *Charnia* from the Avalon Peninsula of Newfoundland. *SP* 286, 237–257. doi: 10.1144/SP286.17
- Leys, S. P., and Lauzon, N. R. J. (1998). Hexactinellid sponge ecology: growth rates and seasonality in deep water sponges. *Journal of Experimental Marine Biology and Ecology* 230, 111–129. doi: 10.1016/S0022-0981(98)00088-4
- Li, C.-W., Chen, J.-Y., and Hua, T.-E. (1998). Precambrian Sponges with Cellular Structures. *Science* 279, 879–882. doi: 10.1126/science.279.5352.879
- Liu, A. G. (2016). Framboidal pyrite shroud confirms the “Death Mask” model for moldic preservation of Ediacaran soft-bodied organism. *PALAIOS* 31, 259–274. doi: 10.2110/palo.2015.095
- Liu, A. G., and Dunn, F. S. (2020). Filamentous Connections between Ediacaran Fronds. *Current Biology* 30, 1322-1328.e3. doi: 10.1016/j.cub.2020.01.052

- Liu, A. G., Matthews, J. J., Menon, L. R., McIlroy, D., and Brasier, M. D. (2014). *Haootia quadriformis* n. gen., n. sp., interpreted as a muscular cnidarian impression from the Late Ediacaran period (approx. 560 Ma). *Proc. R. Soc. B.* 281, 20141202. doi: 10.1098/rspb.2014.1202
- Liu, A. G., and McIlroy, D. (2015). Horizontal surface traces from the Fermeuse Formation, Ferryland (Newfoundland, Canada), and their place within the Late Ediacaran ichnological revolution. *Geological Association of Canada, Miscellaneous Publication* 9, 141–156.
- Liu, A. G., Mcilroy, D., Antcliffe, J. B., and Brasier, M. D. (2011). Effaced preservation in the Ediacara biota and its implications for the early macrofossil record: Ediacaran Taphomorph. *Palaeontology* 54, 607–630. doi: 10.1111/j.1475-4983.2010.01024.x
- Mapstone, N. B., and McIlroy, D. (2006). Ediacaran fossil preservation: Taphonomy and diagenesis of a discoid biota from the Amadeus Basin, central Australia. *Precambrian Research* 149, 126–148. doi: 10.1016/j.precamres.2006.05.007
- Mason, S. J., Narbonne, G. M., Dalrymple, R. W., and O'Brien, S. J. (2013). Paleoenvironmental analysis of Ediacaran strata in the Catalina Dome, Bonavista Peninsula, Newfoundland. *Can. J. Earth Sci.* 50, 197–212. doi: 10.1139/cjes-2012-0099
- Matthews, J. J., Liu, A. G., Yang, C., McIlroy, D., Levell, B., and Condon, D. J. (2020). A chronostratigraphic framework for the rise of the Ediacaran macrobiota: New constraints from Mistaken Point Ecological Reserve, Newfoundland. *Geological Society of America Bulletin* 133, 13. doi: 10.1130/B35646.1
- McIlroy, D., Brasier, M. D., and Lang, A. S. (2009). Smothering of microbial mats by macrobiota: implications for the Ediacara biota. *Journal of the Geological Society* 166, 1117–1121. doi: 10.1144/0016-76492009-073
- McIlroy, D., Dufour, S. C., Taylor, R., and Nicholls, R. (2021). The role of symbiosis in the first colonization of the seafloor by macrobiota: Insights from the oldest Ediacaran biota (Newfoundland, Canada). *Biosystems* 205, 104413. doi: 10.1016/j.biosystems.2021.104413
- McIlroy, D., Pérez-Pinedo, D., Pasinetti, G., McKean, C., Taylor, R. S., and Hiscott, R. N. (2022). Rheotropic epifaunal growth, not felling by density currents, is responsible for many Ediacaran fossil orientations at Mistaken Point. *Front. Earth Sci.* 10, 849194. doi: 10.3389/feart.2022.849194
- McIlroy, D., and Walter, M. R. (1997). A reconsideration of the biogenicity of *Arumberia banksi* Glaessner & Walter. *Alcheringa: An Australasian Journal of Palaeontology* 21, 79–80. doi: 10.1080/03115519708619187
- McKean, C., Taylor, R. S., and Mcilroy, D. (2023). New taphonomic and sedimentological insights into the preservation of high-relief Ediacaran fossils at Upper Island Cove, Newfoundland. *LET* 56, 1–17. doi: 10.18261/let.56.4.2

- McMurray, S. E., Henkel, T. P., and Pawlik, J. R. (2010). Demographics of increasing populations of the giant barrel sponge *Xestospongia muta* in the Florida Keys. *Ecology* 91, 560–570. doi: 10.1890/08-2060.1
- Meesters, E., Hilterman, M., Kardinaal, E., Keetman, M., De Vries, M., and Bak, R. (2001). Colony size-frequency distributions of scleractinian coral populations: spatial and interspecific variation. *Mar. Ecol. Prog. Ser.* 209, 43–54. doi: 10.3354/meps209043
- Mitchell, E. G., and Butterfield, N. J. (2018). Spatial analyses of Ediacaran communities at Mistaken Point. *Paleobiology* 44, 40–57. doi: 10.1017/pab.2017.35
- Mitchell, E. G., Kenchington, C. G., Liu, A. G., Matthews, J. J., and Butterfield, N. J. (2015). Reconstructing the reproductive mode of an Ediacaran macro-organism. *Nature* 524, 343–346. doi: 10.1038/nature14646
- Narbonne, G. M. (2004). Modular construction of Early Ediacaran complex life forms. *Science* 305, 1141–1144. doi: 10.1126/science.1099727
- Narbonne, G. M. (2005). The Ediacara biota: Neoproterozoic origin of animals and their ecosystems. *Annu. Rev. Earth Planet. Sci.* 33, 421–442. doi: 10.1146/annurev.earth.33.092203.122519
- Narbonne, G. M., Laflamme, M., Greentree, C., and Trusler, P. (2009). Reconstructing a lost world: Ediacaran rangeomorphs from Spaniard’s Bay, Newfoundland. *J. Paleontol.* 83, 503–523. doi: 10.1666/08-072R1.1
- Noffke, N., Beraldi-Campesi, H., Callefo, F., Carmona, N. B., Cuadrado, D. G., Hickman-Lewis, K., et al. (2021). “Microbially induced sedimentary structures (MISS),” in *Encyclopedia of Geology* (Elsevier), 545–554. doi: 10.1016/B978-0-08-102908-4.00109-0
- O’Brien, S. J., and King, A. F. (2005). Late Neoproterozoic (Ediacaran) stratigraphy of Avalon Zone sedimentary rocks, Bonavista Peninsula, Newfoundland. *Geological Survey* 05, 13.
- Olsen, A. M. (2017). Feeding ecology is the primary driver of beak shape diversification in waterfowl. *Funct Ecol* 31, 1985–1995. doi: 10.1111/1365-2435.12890
- Olsen, A. M., and Westneat, M. W. (2015). StereoMorph: an R package for the collection of 3D landmarks and curves using a stereo camera set-up. *Methods Ecol Evol* 6, 351–356. doi: 10.1111/2041-210X.12326
- Pasinetti, G., and McIlroy, D. (2023). Palaeobiology and taphonomy of the rangeomorph *Culmofrons plumosa*. *Palaeontology* 66, e12671. doi: 10.1111/pala.12671
- Pérez-Pinedo, D., McKean, C., Taylor, R., Nicholls, R., and McIlroy, D. (2022). *Charniodiscus* and *Arborea* are separate genera within the Arboreomorpha: Using the holotype of *C. concentricus* to resolve a taphonomic/taxonomic tangle. *Front. Earth Sci.* 9, 785929. doi: 10.3389/feart.2021.785929

- Pérez-Pinedo, D., Neville, J. M., Pasinetti, G., McKean, C., Taylor, R., and McIlroy, D. (2023). Frond orientations with independent current indicators demonstrate the reclining rheotropic mode of life of several Ediacaran rangeomorph taxa. *Paleobiology*, 1–22. doi: 10.1017/pab.2023.2
- Porada, H., Ghergut, J., and Bouougri, E. H. (2008). Kinneyia-type wrinkle structures--critical review and model of formation. *PALAIOS* 23, 65–77. doi: 10.2110/palo.2006.p06-095r
- Razumovskiy, A. A., Ivantsov, A. Yu., Novikov, I. A., and Korochantsev, A. V. (2015). Kuckaraukia multituberculata: A new Vendian fossil from the basa formation of the Asha Group in the South Urals. *Paleontol. J.* 49, 449–456. doi: 10.1134/S0031030115050111
- Retallack, G. J. (1994). Were the Ediacaran fossils lichens? *Paleobiology* 20, 523–544. doi: 10.1017/S0094837300012975
- Ryan, J. F., and Chiodin, M. (2015). Where is my mind? How sponges and placozoans may have lost neural cell types. *Phil. Trans. R. Soc. B* 370, 20150059. doi: 10.1098/rstb.2015.0059
- Schultz, D. T., Haddock, S. H. D., Bredeson, J. V., Green, R. E., Simakov, O., and Rokhsar, D. S. (2023). Ancient gene linkages support ctenophores as sister to other animals. *Nature* 618, 110–117. doi: 10.1038/s41586-023-05936-6
- Scrucca, L., Fop, M., Murphy, T., Brendan, and Raftery, A., E. (2016). mclust 5: Clustering, Classification and Density Estimation Using Gaussian Finite Mixture Models. *The R Journal* 8, 289. doi: 10.32614/RJ-2016-021
- Seilacher, A. (1992). Vendobionta and Psammocorallia: lost constructions of Precambrian evolution. *Journal of the Geological Society* 149, 607–613. doi: 10.1144/gsjgs.149.4.0607
- Seilacher, A. (1999). Biomat-Related Lifestyles in the Precambrian. *PALAIOS* 14, 86. doi: 10.2307/3515363
- Shaffer, M. R., Davy, S. K., Maldonado, M., and Bell, J. J. (2020). Seasonally driven sexual and asexual reproduction in temperate *Tethya* species. *The Biological Bulletin* 238, 89–105. doi: 10.1086/708624
- Smith, E. F., Nelson, L. L., Strange, M. A., Eyster, A. E., Rowland, S. M., Schrag, D. P., et al. (2016). The end of the Ediacaran: Two new exceptionally preserved body fossil assemblages from Mount Dunfee, Nevada, USA. *Geology* 44, 911–914. doi: 10.1130/G38157.1
- Sperling, E. A., Pisani, D., and Peterson, K. J. (2007). Poriferan paraphyly and its implications for Precambrian palaeobiology. *SP* 286, 355–368. doi: 10.1144/SP286.25
- Sperling, E. A., and Vinther, J. (2010). A placozoan affinity for *Dickinsonia* and the evolution of late Proterozoic metazoan feeding modes: Placozoan affinity for *Dickinsonia*. *Evolution & Development* 12, 201–209. doi: 10.1111/j.1525-142X.2010.00404.x

- Taylor, R. S., Matthews, J. J., Nicholls, R., and McIlroy, D. (2021). A re-assessment of the taxonomy, palaeobiology and taphonomy of the rangeomorph organism *Hapsidophyllas flexibilis* from the Ediacaran of Newfoundland, Canada. *PalZ* 95, 187–207. doi: 10.1007/s12542-020-00537-4
- Taylor, R. S., Nicholls, R., Neville, J. M., and McIlroy, D. (2023). Morphological variation in the rangeomorph organism *Fractofusus misrai* from the Ediacaran of Newfoundland, Canada. *Geol. Mag.* 160, 146–166. doi: 10.1017/S0016756822000723
- Turekian, K. K., Cochran, J. K., Kharkar, D. P., Cerrato, R. M., Vaisnys, J. R., Sanders, H. L., et al. (1975). Slow growth rate of a deep-sea clam determined by ²²⁸Ra chronology. *Proc. Natl. Acad. Sci. U.S.A.* 72, 2829–2832. doi: 10.1073/pnas.72.7.2829
- Vaziri, S. H., Majidifard, M. R., and Laflamme, M. (2018). Diverse Assemblage of Ediacaran fossils from Central Iran. *Sci Rep* 8, 5060. doi: 10.1038/s41598-018-23442-y
- Vixseboxse, P. B., Kenchington, C. G., Dunn, F. S., and Mitchell, E. G. (2021). Orientations of Mistaken Point fronds indicate morphology impacted ability to survive turbulence. *Front. Earth Sci.* 9, 762824. doi: 10.3389/feart.2021.762824
- Waggoner, B. (2003). The Ediacaran biotas in space and time. *Integrative and Comparative Biology* 43, 104–113. doi: 10.1093/icb/43.1.104
- Wang, X., Pang, K., Chen, Z., Wan, B., Xiao, S., Zhou, C., et al. (2020). The Ediacaran frondose fossil *Arborea* from the Shibantan limestone of South China. *J. Paleontol.* 94, 1034–1050. doi: 10.1017/jpa.2020.43
- Witte, U. (1996). Seasonal reproduction in deep-sea sponges-triggered by vertical particle flux? *Marine Biology* 124, 571–581. doi: 10.1007/BF00351038
- Wörheide, G., Dohrmann, M., Erpenbeck, D., Larroux, C., Maldonado, M., Voigt, O., et al. (2012). “Deep phylogeny and evolution of sponges (Phylum Porifera),” in *Advances in Marine Biology* (Elsevier), 1–78. doi: 10.1016/B978-0-12-387787-1.00007-6
- Xiao, S., and Laflamme, M. (2009). On the eve of animal radiation: phylogeny, ecology and evolution of the Ediacara biota. *Trends in Ecology & Evolution* 24, 31–40. doi: 10.1016/j.tree.2008.07.015

Summary

This thesis tackles different interdisciplinary problems related to the late Ediacaran fossil assemblages of the Avalon and Bonavista peninsulas of Newfoundland, focusing in particular on three main species: the two rangeomorph *Culmofrons plumosa* and *Charnia ewinoni* and the putative metazoan *Lydonia jiggamintia*.

Culmofrons plumosa specimens from the MUN Surface in the Bonavista Peninsula are exceptionally preserved, allowing us to draw conclusions about their modes of life and taphonomy. The close interaction of the species with the microbial matground that was pervasive of Ediacaran seafloors is indicative of a reclining lifestyle, possibly in combination with microbial symbionts. At the same time, the matground plays a crucial role in the preservation of an impression of the organism, resulting in a combination of positive and negative features that could have only been achieved if *C. plumosa* was reclining in life. The exceptional preservation of the specimens also allows us to produce developmental models for the species, by considering the rate and order of new branches insertions. We also observe the presence of propagules involved in a secondary reproductive strategy, which would have been useful in the event of burial of the organism. The resulting reconstruction is that of a reclining organism, living partially buried under the microbial matground, that grew by addition of new branches at the apical portion and a subsequent inflation of the structures.

Charnia specimens from the Bonavista Peninsula present several morphological differences from the British type material and other Avalonian specimens. In particular, our material presents a parallel-sided frond, sigmoidal branches, a straight midline and the presence of a stem, in contrast with the more obovate profiles of *C. masoni*, which typically have a zig-zagged midline and rarely present a stem. Through the use of morphometric analyses (linear models), backtransform morphospace analyses and hierarchical clustering algorithms based on

computed principal components, we were able to separate the Bonavista material from other *Charnia*, suggesting the creation of a new co-generic taxon, *Charnia ewinoni* sp. nov..

C. ewinoni is particularly abundant on the Matthews Surface ($N > 20$), where most of the specimens are oriented broadly perpendicularly to the inferred palaeocurrent. As the palaeocurrent direction likely coincided with the downslope direction, we can infer that the specimens were not felled by the turbidite from an upright position, as it was previously hypothesized for *Charnia*, but rather they were likely living reclining on the seafloor.

Specimens of a non-frondose fusiform macrofossil from the Bonavista Peninsula, previously described as *Blackbrookia oaksi* are here described as the new genus and species *Lydonia jiggamintia*, on the basis of morphometry and the presence of a specialized structures. Morphometric and backtransform morphospace analyses support the identity of the Bonavista populations as a single taxon, which presented evidence for porose openings, possibly correlated with raised papillae, likely indicative of a complex aquiferous system of metazoan-grade. As the JD Surface hosts a snapshot of a large population of *L. jiggamintia* all buried at the same time, it is possible to use a Bayesian Inference Criterion (BIC) algorithm to identify age cohorts and model the population dynamics of the species. The resulting model support the identification of *L. jiggamintia* as a metazoan, as it shows a slow growing population with continuous aseasonal reproduction, akin to that of modern Porifera.

List of References

- Amthor, J. E., Grotzinger, J. P., Schröder, S., Bowring, S. A., Ramezani, J., Martin, M. W., et al. (2003). Extinction of *Cloudina* and *Namacalathus* at the Precambrian-Cambrian boundary in Oman. *Geol* 31, 431. doi: 10.1130/0091-7613(2003)031<0431:EOCANA>2.0.CO;2
- Anderson, M. M., and Misra, S. B. (1968). Fossils found in the Pre-Cambrian Conception Group of South-eastern Newfoundland. *Nature* 220, 680–681. doi: 10.1038/220680a0
- Antcliffe, J. B., Callow, R. H. T., and Brasier, M. D. (2014). Giving the early fossil record of sponges a squeeze. *Biological Reviews* 89, 972–1004. doi: 10.1111/brv.12090
- Antcliffe, J. B., Hancy, A. D., and Brasier, M. D. (2015). A new ecological model for the ~565Ma Ediacaran biota of Mistaken Point, Newfoundland. *Precambrian Research* 268, 227–242. doi: 10.1016/j.precamres.2015.06.015
- Aragonés Suarez, P., and Leys, S. P. (2022). The sponge pump as a morphological character in the fossil record. *Paleobiology* 48, 446–461. doi: 10.1017/pab.2021.43
- Bak, R., and Meesters, E. (1998). Coral population structure: the hidden information of colony size-frequency distributions. *Mar. Ecol. Prog. Ser.* 162, 301–306. doi: 10.3354/meps162301
- Baken, E. K., Collyer, M. L., Kaliontzopoulou, A., and Adams, D. C. (2021). geomorph v4.0 and gmShiny: Enhanced analytics and a new graphical interface for a comprehensive morphometric experience. *Methods Ecol Evol* 12, 2355–2363. doi: 10.1111/2041-2
- Bamforth, E. L., Narbonne, G. M., and Anderson, M. M. (2008). Growth and ecology of a multi-branched Ediacaran rangeomorph from the Mistaken Point assemblage, Newfoundland. *Journal of Paleontology* 82, 763–777. doi: 10.1666/07-112.1
- Baquiran, J. I. P., Nada, M. A. L., Posadas, N., Manogan, D. P., Cabaitan, P. C., and Conaco, C. (2020). Population structure and microbial community diversity of two common tetillid sponges in a tropical reef lagoon. *PeerJ* 8, e9017. doi: 10.7717/peerj.9017
- Billett, D. S. M., and Hansen, B. (1982). Abyssal aggregations of *Kolga hyalina* Danielssen and Koren (Echinodermata: Hoiothurioidea) in the northeast Atlantic Ocean: a preliminary report. *Deep-Sea Research* 29, 799–818. doi: 10.1016/0198-0149(82)90799-9
- Bobrovskiy, I., Hope, J. M., Ivantsov, A., Nettersheim, B. J., Hallmann, C., and Brocks, J. J. (2018). Ancient steroids establish the Ediacaran fossil *Dickinsonia* as one of the earliest animals. *Science* 361, 1246–1249. doi: 10.1126/science.aat7228
- Boddy, C. E., Mitchell, E. G., Merdith, A., and Liu, A. G. (2022). Palaeolatitudinal distribution of the Ediacaran macrobiota. *JGS* 179, jgs2021-030. doi: 10.1144/jgs2021-030

- Bode, H., Berking, S., David, C. N., Gierer, A., Schaller, H., and Trenkner, E. (1973). Quantitative analysis of cell types during growth and morphogenesis in *Hydra*. *W. Roux' Archiv f. Entwicklungsmechanik* 171, 269–285. doi: 10.1007/BF00577725
- Botting, J. P., and Muir, L. A. (2018). Early sponge evolution: A review and phylogenetic framework. *Palaeoworld* 27, 1–29. doi: 10.1016/j.palwor.2017.07.001
- Bottjer, D. J. (2010). The Cambrian substrate revolution and early evolution of the phyla. *J. Earth Sci.* 21, 21–24. doi: 10.1007/s12583-010-0160-7
- Bottjer, D. J., Hagadorn, J. W., and Dornbos, S. Q. (2000). The Cambrian substrate revolution. *GSA Today* 10, 32.
- Boynton, H. E. (1999). New fossils in the Precambrian of Charnwood Forest, Leicestershire, England. *Mercian Geologist* 14, 4.
- Boynton, H. E., and Ford, T. D. (1995). Ediacaran fossils from the Precambrian (Charnian Supergroup) of Charnwood Forest, Leicestershire, England. *Mercian Geologist* 13, 1
- Brasier, M., Cowie, J., and Taylor, M. (1994). Decision on the Precambrian-Cambrian boundary stratotype. *Episodes* 17, 3–8. doi: 10.18814/epiiugs/1994/v17i1.2/002
- Brasier, M., and Antcliffe, J. B. (2004). Decoding the Ediacaran enigma. *Science* 305, 1115–1117. doi: 10.1126/science.1102673
- Brasier, M. D., and Antcliffe, J. B. (2009). Evolutionary relationships within the Avalonian Ediacara biota: new insights from laser analysis. *Journal of the Geological Society* 166, 363–384. doi: 10.1144/0016-76492008-011
- Brasier, M. D., Antcliffe, J. B., and Liu, A. G. (2012). The architecture of Ediacaran fronds. *Palaeontology* 55, 1105–1124. doi: 10.1111/j.1475-4983.2012.01164.x
- Briggs, D. E. G. (2003). The Role of Decay and Mineralization in the Preservation of Soft-Bodied Fossils. *Annu. Rev. Earth Planet. Sci.* 31, 275–301. doi: 10.1146/annurev.earth.31.100901.144746
- Budd, G. E., and Jensen, S. (2017). The origin of the animals and a ‘Savannah’ hypothesis for early bilaterian evolution: Early evolution of the animals. *Biol Rev* 92, 446–473. doi: 10.1111/brv.12239
- Butterfield, N. J. (1997). Plankton ecology and the Proterozoic-Phanerozoic transition. *Paleobiology* 23, 247–262. doi: 10.1017/S009483730001681X
- Butterfield, N. J. (2020). Constructional and functional anatomy of Ediacaran rangeomorphs. *Geol. Mag.*, 1–12. doi: 10.1017/S0016756820000734
- Cavalier-Smith, T. (2017). Origin of animal multicellularity: precursors, causes, consequences—the choanoflagellate/sponge transition, neurogenesis and the Cambrian explosion. *Phil. Trans. R. Soc. B* 372, 20150476. doi: 10.1098/rstb.2015.0476

- Clapham, M. E., and Narbonne, G. M. (2002). Ediacaran epifaunal tiering. *Geology* 30, 627–630. doi: 10.1130/0091-7613(2002)030<0627:EET>2.0.CO;2
- Clapham, M. E., Narbonne, G. M., and Gehling, J. G. (2003). Paleoecology of the oldest known animal communities: Ediacaran assemblages at Mistaken Point, Newfoundland. *Paleobiology* 29, 527–544. doi: 10.1666/0094-8373(2003)029<0527:POTOKA>2.0.CO;2
- Clapham, M. E., Narbonne, G. M., Gehling, J. G., Greentree, C., and Anderson, M. M. (2004). *Thectardis avalonensis*: A new Ediacaran fossil from the Mistaken Point biota, Newfoundland. *Journal of Paleontology* 78, 1031–1036. doi: 10.1666/0022-3360(2004)078<1031:taanef>2.0.co;2
- Cordes, E. E., Nybakken, J. W., and VanDykhuisen, G. (2001). Reproduction and growth of *Anthomastus ritteri* (Octocorallia: Alcyonacea) from Monterey Bay, California, USA. *Marine Biology* 138, 491–501. doi: 10.1007/s002270000470
- Cunliffe, M. (2023). Who are the marine fungi? *Environmental Microbiology* 25, 131–134. doi: 10.1111/1462-2920.16240
- Darroch, S. A. F., Laflamme, M., and Clapham, M. E. (2013). Population structure of the oldest known macroscopic communities from Mistaken Point, Newfoundland. *Paleobiology* 39, 591–608. doi: 10.1666/12051
- Darroch, S. A. F., Laflamme, M., Schiffbauer, J. D., and Briggs, D. E. G. (2012). Experimental formation of a microbial death mask. *PALAIOS* 27, 293–303. doi: 10.2110/palo.2011.p11-059r
- Darroch, S. A. F., Laflamme, M., and Wagner, P. J. (2018). High ecological complexity in benthic Ediacaran communities. *Nat Ecol Evol* 2, 1541–1547. doi: 10.1038/s41559-018-0663-7
- Darwin, C. (1859). *On the origin of species by means of natural selection, or, The preservation of favoured races in the struggle for life*. 6th ed. London: John Murray.
- Dec, T., O'Brien, S. J., and Knight, I. (1992). Late precambrian volcanoclastic deposits of the avalonian eastport basin (newfoundland appalachians): petrofacies, detrital clinopyroxene geochemistry and palaeotectonic implications. *Precambrian Research* 59, 243–262. doi: 10.1016/0301-9268(92)90059-W
- Decechi, T. A., Narbonne, G. M., Greentree, C., and Laflamme, M. (2017). Relating Ediacaran Fronds. *Paleobiology* 43, 171–180. doi: 10.1017/pab.2016.54
- Dillon, W., and Goldstein, M. (1984). *Multivariate analysis: methods and applications*. Wiley. New York: Wiley.
- Dohrmann, M., and Wörheide, G. (2017). Dating early animal evolution using phylogenomic data. *Sci Rep* 7, 3599. doi: 10.1038/s41598-017-03791-w

- Dufour, S. C., and McIlroy, D. (2017). Ediacaran pre-placozoan diploblasts in the Avalonian biota: the role of chemosynthesis in the evolution of early animal life. *Geological Society, London, Special Publications* 448, 211–219. doi: 10.1144/SP448.5
- Dufour, S. C., and McIlroy, D. (2018). An Ediacaran pre-placozoan alternative to the pre-sponge route towards the Cambrian explosion of animal life: a comment on Cavalier-Smith 2017. *Phil. Trans. R. Soc. B* 373, 20170148. doi: 10.1098/rstb.2017.0148
- Dunn, F. S., Grazhdankin, D. V., Liu, A. G., and Wilby, P. R. (2021). The developmental biology of *Charnia* and the eumetazoan affinity of the Ediacaran rangeomorphs. *Science Advances*, 14.
- Dunn, F. S., Liu, A. G., and Donoghue, P. C. J. (2018). Ediacaran developmental biology: Ediacaran developmental biology. *Biol Rev* 93, 914–932. doi: 10.1111/brv.12379
- Dunn, F. S., Liu, A. G., and Gehling, J. G. (2019a). Anatomical and ontogenetic reassessment of the Ediacaran frond *Arborea arborea* and its placement within total group Eumetazoa. *Palaeontology* 62, 851–865. doi: 10.1111/pala.12431
- Dunn, F. S., Wilby, P. R., Kenchington, C. G., Grazhdankin, D. V., Donoghue, P. C. J., and Liu, A. G. (2019b). Anatomy of the Ediacaran rangeomorph *Charnia masoni*. *Pap Palaeontol* 5, 157–176. doi: 10.1002/spp2.1234
- Evans, S. D., Hughes, I. V., Gehling, J. G., and Droser, M. L. (2020). Discovery of the oldest bilaterian from the Ediacaran of South Australia. *Proc Natl Acad Sci USA* 117, 7845–7850. doi: 10.1073/pnas.2001045117
- Fedonkin, M. A. (1982). A new generic name for some Precambrian Coelenterates. *Paleontologicheskii Zhurnal* 2.
- Flude, L. I., and Narbonne, G. M. (2008). Taphonomy and ontogeny of a multibranching Ediacaran fossil: *Bradgatia* from the Avalon Peninsula of Newfoundland. *Can. J. Earth S* 45, 1095–1109, <https://doi.org/10.1139/E08-057>
- Ford, T. D. (1958). Pre-Cambrian fossils from Charnwood Forest. *Proceedings of the Yorkshire Geological Society* 31, 211–217. doi: 10.1144/pygs.31.3.211
- Ford, T. D. (1962). The Pre-Cambrian fossils of Charnwood Forest. *Transactions of the Leicester Literary and Philosophical Society* 56, 57–62.
- Gehling, J. G. (1999). Microbial mats in terminal Proterozoic siliciclastics: Ediacaran death masks. *PALAIOS* 14, 40. doi: 10.2307/3515360
- Gehling, J. G., and Narbonne, G. M. (2007). Spindle-shaped Ediacara fossils from the Mistaken Point assemblage, Avalon Zone, Newfoundland. *Can. J. Earth Sci.* 44, 367–387. doi: 10.1139/e07-003
- Goodwin, C., Dinn, C., Nefedova, E., Nijhof, F., Murillo, F. J., and Nozères, C. (2021). Two new species of encrusting sponge (Porifera, family Crellidae) from eastern Canada. *Can. J. Zool.* 99, 760–772. doi: 10.1139/cjz-2021-0041

- Grazhdankin, D. (2004). Patterns of Distribution in the Ediacaran Biotas: Facies versus Biogeography and Evolution. *Paleobiology* 30, 203–221.
- Grazhdankin, D., and Seilacher, A. (2005). A re-examination of the Nama-type Vendian organism *Rangea schneiderhoehni*. *Geol. Mag.* 142, 571–582. doi: 10.1017/S0016756805000920
- Grazhdankin, D. V., Balthasar, U., Nagovitsin, K. E., and Kochnev, B. B. (2008). Carbonate-hosted Avalon-type fossils in arctic Siberia. *Geol* 36, 803. doi: 10.1130/G24946A.1
- Gruber-Vodicka, H. R., Leisch, N., Kleiner, M., Hinzke, T., Liebeke, M., McFall-Ngai, M., et al. (2019). Two intracellular and cell type-specific bacterial symbionts in the placozoan *Trichoplax* H2. *Nat Microbiol* 4, 1465–1474. doi: 10.1038/s41564-019-0475-9
- Gürich, G. (1929). Die ältesten fossilien Südafrikas. *Zeitschrift für Praktische Geologie* 37.
- Gürich, G. (1933). Die kuibis-fossilien der Namaformation von Südwestafrika. *Paläontologische Zeithschrift* 15, 137–145.
- Hall, J. G., Smith, E. F., Tamura, N., Fakra, S. C., and Bosak, T. (2020). Preservation of erniettomorph fossils in clay-rich siliciclastic deposits from the Ediacaran Wood Canyon Formation, Nevada. *Interface Focus*. 10, 20200012. doi: 10.1098/rsfs.2020.0012
- Hawco, J. B., Kenchington, C. G., Taylor, R. S., and Mcilroy, D. (2020). A multivariate statistical analysis of the Ediacaran rangeomorph taxa *Beothukis* and *Culmofrons*. *PALAIOS* 35, 495–511. doi: 10.2110/palo.2020.049
- Hofmann, H. J., O'Brien, S. J., and King, A. F. (2008). Ediacaran biota on Bonavista Peninsula, Newfoundland, Canada. *J. Paleontol.* 82, 1–36. doi: 10.1666/06-087.1
- Howe, M. P. A., Evans, M., Carney, J. N., and Wilby, P. R. (2012). New perspectives on the globally important Ediacaran fossil discoveries in Charnwood Forest, UK: Harley's 1848 prequel to Ford (1958). *Proceedings of the Yorkshire Geological Society* 59, 137–144.
- Hoyal Cuthill, J. F., and Conway Morris, S. (2017). Nutrient-dependent growth underpinned the Ediacaran transition to large body size. *Nat Ecol Evol* 1, 1201–1204. doi: 10.1038/s41559-017-0222-7
- Husson, F., Josse, J., and Pages, J. (2010). Principal component methods - hierarchical clustering - partitional clustering: why would we need to choose for visualizing data? *Technical Report - Agrocampus*.
- Ichaso, A. A., Dalrymple, R. W., and Narbonne, G. M. (2007). Paleoenvironmental and basin analysis of the late Neoproterozoic (Ediacaran) upper Conception and St. John's groups, west Conception Bay, Newfoundland. *Can. J. Earth Sci.* 44, 25–41. doi: 10.1139/e06-098

- Ivantsov, A., Nagovitsyn, A., and Zakrevskaya, M. (2019). Traces of locomotion of Ediacaran macroorganisms. *Geosciences* 9, 395. doi: 10.3390/geosciences9090395
- Ivantsov, A. Yu. (2009). New reconstruction of *Kimberella*, problematic Vendian metazoan. *Paleontol. J.* 43, 601–611. doi: 10.1134/S003103010906001X
- Ivantsov, A. Yu. (2010). Paleontological evidence for the supposed Precambrian occurrence of Mollusks. *Paleontol. J.* 44, 1552–1559. doi: 10.1134/S0031030110120105
- Ivantsov, A. Yu. (2011). Feeding traces of Proarticulata—the Vendian metazoa. *Paleontol. J.* 45, 237–248. doi: 10.1134/S0031030111030063
- Ivantsov, A. Yu. (2013). Trace fossils of Precambrian metazoans “Vendobionta” and “Mollusks.” *Stratigr. Geol. Correl.* 21, 252–264. doi: 10.1134/S0869593813030039
- Ivantsov, A., Zakrevskaya, M., Nagovitsyn, A., Krasnova, A., Bobrovskiy, I., and Luzhnaya (Serezhnikova), E. (2020). Intravital damage to the body of *Dickinsonia* (Metazoa of the late Ediacaran). *J. Paleontol.* 94, 1019–1033. doi: 10.1017/jpa.2020.65
- Jenkins, R. J. F. (1985). The enigmatic Ediacaran (late Precambrian) genus *Rangea* and related forms. *Paleobiology* 11, 336–355. doi: 10.1017/S0094837300011635
- Jensen, S., Gehling, J. G., Droser, M. L., and Grant, S. W. F. (2002). A scratch circle origin for the medusoid fossil Kullingia. *LET* 35, 291–299. doi: 10.1111/j.1502-3931.2002.tb00089.x
- Kaiser, H. F. (1970). A second generation little jiffy. *Psychometrika* 35, 401–415. doi: 10.1007/BF02291817
- Kenchington, C. G., Dunn, F. S., and Wilby, P. R. (2018). Modularity and Overcompensatory Growth in Ediacaran Rangeomorphs Demonstrate Early Adaptations for Coping with Environmental Pressures. *Current Biology* 28, 3330-3336.e2. doi: 10.1016/j.cub.2018.08.036
- Kenchington, C. G., and Wilby, P. R. (2014). Of time and taphonomy: preservation in the Ediacaran. *The Paleontological Society Papers* 20, 23. doi: <https://doi.org/10.1017/S1089332600002825>
- Knoll, A. H., Walter, M. R., Narbonne, G. M., and Christie-Blick, N. (2006). The Ediacaran Period: a new addition to the geologic time scale. *LET* 39, 13–30. doi: 10.1080/00241160500409223
- Laflamme, M., Darroch, S. A. F., Tweedt, S. M., Peterson, K. J., and Erwin, D. H. (2013). The end of the Ediacara biota: Extinction, biotic replacement, or Cheshire Cat? *Gondwana Research* 23, 558–573. doi: 10.1016/j.gr.2012.11.004
- Laflamme, M., Flude, L. I., and Narbonne, G. M. (2012). Ecological tiering and the evolution of a stem: the oldest stemmed frond from the Ediacaran of Newfoundland, Canada. *J. Paleontol.* 86, 193–200. doi: 10.1666/11-044.1

- Laflamme, M., and Narbonne, G. M. (2008a). Competition in a Precambrian world: palaeoecology of Ediacaran fronds. *Geology Today* 24, 182–187. doi: 10.1111/j.1365-2451.2008.00685.x
- Laflamme, M., and Narbonne, G. M. (2008b). Ediacaran fronds. *Palaeogeography, Palaeoclimatology, Palaeoecology* 258, 162–179. doi: 10.1016/j.palaeo.2007.05.020
- Laflamme, M., Narbonne, G. M., Greentree, C., and Anderson, M. M. (2007). Morphology and taphonomy of an Ediacaran frond: *Charnia* from the Avalon Peninsula of Newfoundland. *SP* 286, 237–257. doi: 10.1144/SP286.17
- Laflamme, M., Schiffbauer, J. D., Narbonne, G. M., and Briggs, D. E. G. (2011). Microbial biofilms and the preservation of the Ediacara biota: Ediacaran preservation. *Lethaia* 44, 203–213. doi: 10.1111/j.1502-3931.2010.00235.x
- Laflamme, M., Xiao, S., and Kowalewski, M. (2009). Osmotrophy in modular Ediacara organisms. *Proceedings of the National Academy of Sciences* 106, 14438–14443. doi: 10.1073/pnas.0904836106
- Lê, S., Josse, J., and Husson, F. (2008). FactoMineR : An R Package for Multivariate Analysis. *J. Stat. Soft.* 25. doi: 10.18637/jss.v025.i01
- Leys, S. P., and Lauzon, N. R. J. (1998). Hexactinellid sponge ecology: growth rates and seasonality in deep water sponges. *Journal of Experimental Marine Biology and Ecology* 230, 111–129. doi: 10.1016/S0022-0981(98)00088-4
- Li, C.-W., Chen, J.-Y., and Hua, T.-E. (1998). Precambrian Sponges with Cellular Structures. *Science* 279, 879–882. doi: 10.1126/science.279.5352.879
- Liu, A. G. (2016). Framboidal pyrite shroud confirms the “Death Mask” model for moldic preservation of Ediacaran soft-bodied organism. *PALAIOS* 31, 259–274. doi: 10.2110/palo.2015.095
- Liu, A. G., and Dunn, F. S. (2020). Filamentous Connections between Ediacaran Fronds. *Current Biology* 30, 1322-1328.e3. doi: 10.1016/j.cub.2020.01.052
- Liu, A. G., Kenchington, C. G., and Mitchell, E. G. (2015). Remarkable insights into the paleoecology of the Avalonian Ediacaran macrobiota. *Gondwana Research* 27, 1355–1380. doi: 10.1016/j.gr.2014.11.002
- Liu, A. G., Matthews, J. J., and McIlroy, D. (2016). The *Beothukis* / *Culmofrons* problem and its bearing on Ediacaran macrofossil taxonomy: evidence from an exceptional new fossil locality. *Palaeontology* 59, 45–58. doi: 10.1111/pala.12206
- Liu, A. G., Matthews, J. J., Menon, L. R., McIlroy, D., and Brasier, M. D. (2014). *Haootia quadriformis* n. gen., n. sp., interpreted as a muscular cnidarian impression from the Late Ediacaran period (approx. 560 Ma). *Proc. R. Soc. B.* 281, 20141202. doi: 10.
- Liu, A. G., and McIlroy, D. (2015). Horizontal surface traces from the Fermeuse Formation, Ferryland (Newfoundland, Canada), and their place within the Late Ediacaran

- ichnological revolution. *Geological Association of Canada, Miscellaneous Publication* 9, 141–156.
- Liu, A. G., McIlroy, D., Antcliffe, J. B., and Brasier, M. D. (2011). Effaced preservation in the Ediacara biota and its implications for the early macrofossil record: Ediacaran Taphomorph. *Palaeontology* 54, 607–630. doi: 10.1111/j.1475-4983.2010.01024.x
- Liu, A. G., McIlroy, D., Matthews, J. J., and Brasier, M. D. (2013). Exploring an Ediacaran ‘nursery’: growth, ecology and evolution in a rangeomorph palaeocommunity. *Geology Today* 29, 23–26. doi: 10.1111/j.1365-2451.2013.00860.x
- Liu, A. G., Mcilroy, D., Matthews, J. J., and Brasier, M. D. (2014). Confirming the metazoan character of a 565 Ma trace-fossil from Mistaken Point, Newfoundland. *PALAIOS* 29, 420–430. doi: 10.2110/palo.2014.011
- Mangano, G. M., and Buatois, L. A. (2017). The Cambrian revolutions: Trace-fossil record, timing, links and geobiological impact. *Earth-Science Reviews* 173, 96–108. doi: 10.1016/j.earscirev.2017.08.009
- Mapstone, N. B., and McIlroy, D. (2006). Ediacaran fossil preservation: Taphonomy and diagenesis of a discoid biota from the Amadeus Basin, central Australia. *Precambrian Research* 149, 126–148. doi: 10.1016/j.precamres.2006.05.007
- Mason, S. J., Narbonne, G. M., Dalrymple, R. W., and O’Brien, S. J. (2013). Paleoenvironmental analysis of Ediacaran strata in the Catalina Dome, Bonavista Peninsula, Newfoundland. *Can. J. Earth Sci.* 50, 197–212. doi: 10.1139/cjes-2012-0099
- Matthews, J. J., Liu, A. G., Yang, C., McIlroy, D., Levell, B., and Condon, D. J. (2020). A chronostratigraphic framework for the rise of the Ediacaran macrobiota: New constraints from Mistaken Point Ecological Reserve, Newfoundland. *Geological Society of America Bulletin* 133, 13. doi: 10.1130/B35646.1
- McIlroy, D., Brasier, M. D., and Lang, A. S. (2009). Smothering of microbial mats by macrobiota: implications for the Ediacara biota. *Journal of the Geological Society* 166, 1
- McIlroy, D., Dufour, S. C., Taylor, R., and Nicholls, R. (2021). The role of symbiosis in the first colonization of the seafloor by macrobiota: Insights from the oldest Ediacaran biota (Newfoundland, Canada). *Biosystems* 205, 104413. doi: 10.1016/j.biosystems.2021.104413
- McIlroy, D., Hawco, J., McKean, C., Nicholls, R., Pasinetti, G., and Taylor, R. (2020). Palaeobiology of the reclining rangeomorph *Beothukis* from the Ediacaran Mistaken Point Formation of southeastern Newfoundland. *Geol. Mag.*, 1–15. doi: 10.1017/S0016756820000941
- McIlroy, D., and Horak, J. M. (2006). “Neoproterozoic: the late Precambrian terranes that formed Eastern Avalonia,” in *The Geology of England and Wales*, eds. P. J. Brenchley and P. F. Rawson (The Geological Society of London), 9–23. doi: 10.1144/GOEWP.2

- McIlroy, D., and Logan, G. A. (1999). The impact of bioturbation on infaunal ecology and evolution during the Proterozoic-Cambrian transition. *PALAIOS* 14, 58. doi: 10.2307/3515361
- McIlroy, D., Pérez-Pinedo, D., Pasinetti, G., McKean, C., Taylor, R. S., and Hiscott, R. N. (2022). Rheotropic epifaunal growth, not felling by density currents, is responsible for many Ediacaran fossil orientations at Mistaken Point. *Front. Earth Sci.* 10, 849194. doi: 10.3389/feart.2022.849194
- McKean, C., Taylor, R. S., and McIlroy, D. (2023). New taphonomic and sedimentological insights into the preservation of high-relief Ediacaran fossils at Upper Island Cove, Newfoundland. *LET* 56, 1–17. doi: 10.18261/let.56.4.2
- McMenamin, M. A. S. (1986). The Garden of Ediacara. *PALAIOS* 1, 178. doi: 10.2307/3514512
- Menon, L. R., McIlroy, D., and Brasier, M. D. (2013). Evidence for Cnidaria-like behavior in ca. 560 Ma Ediacaran *Aspidella*. *Geology* 41, 895–898. doi: 10.1130/G34424.1
- Meesters, E., Hilterman, M., Kardinaal, E., Keetman, M., De Vries, M., and Bak, R. (2001). Colony size-frequency distributions of scleractinian coral populations: spatial and interspecific variation. *Mar. Ecol. Prog. Ser.* 209, 43–54. doi: 10.3354/meps209043
- Misra, S. B. (1969). Late Precambrian (?) Fossils from Southeastern Newfoundland. *Geol Soc America Bull* 80, 2133. doi: 10.1130/0016-7606(1969)80[2133:LPPFSN]2.0.CO;2
- Mitchell, E. G., and Butterfield, N. J. (2018). Spatial analyses of Ediacaran communities at M
- Mitchell, E. G., and Kenchington, C. G. (2018). The utility of height for the Ediacaran organisms of Mistaken Point. *Nat Ecol Evol* 2, 1218–1222. doi: 10.1038/s41559-018-0591-6
- Mitchell, E. G., Kenchington, C. G., Liu, A. G., Matthews, J. J., and Butterfield, N. J. (2015). Reconstructing the reproductive mode of an Ediacaran macro-organism. *Nature* 524, 343–346. doi: 10.1038/nature14646
- Murphy, J. B., Keppie, J. D., Dostal, J., and Nance, R. D. (1999). “Neoproterozoic-early Paleozoic evolution of Avalonia,” in *Laurentia-Gondwana connections before Pangea* (Geological Society of America). doi: 10.1130/0-8137-2336-1.253
- Nance, R. D., Murphy, J. B., and Keppie, J. D. (2002). A Cordilleran model for the evolution of Avalonia. *Tectonophysics* 352, 11–31. doi: 10.1016/S0040-1951(02)00187-7
- Nance, R. D., Murphy, J. B., Strachan, R. A., D’Lemos, R. S., and Taylor, G. K. (1991). Late Proterozoic tectonostratigraphic evolution of the Avalonian and Cadomian terranes. *Pr*
- Narbonne, G. M. (2004). Modular construction of Early Ediacaran complex life forms. *Science* 305, 1141–1144. doi: 10.1126/science.1099727

- Narbonne, G. M. (2005). The Ediacara biota: Neoproterozoic origin of animals and their ecosystems. *Annu. Rev. Earth Planet. Sci.* 33, 421–442. doi: 10.1146/annurev.earth.33.092203.122519
- Narbonne, G. M., Laflamme, M., Greentree, C., and Trusler, P. (2009). Reconstructing a lost world: Ediacaran rangeomorphs from Spaniard’s Bay, Newfoundland. *J. Paleontol.* 83, 503–523. doi: 10.1666/08-072R1.1
- Noble, S. R., Condon, D. J., Carney, J. N., Wilby, P. R., Pharaoh, T. C., and Ford, T. D. (2015). U-Pb geochronology and global context of the Charnian Supergroup, UK: Constraints on the age of key Ediacaran fossil assemblages. *Geological Society of America Bulletin* 127, 250–265. doi: 10.1130/B31013.1
- Noffke, N., Beraldi-Campesi, H., Callefo, F., Carmona, N. B., Cuadrado, D. G., Hickman-Lewis, K., et al. (2021). “Microbially induced sedimentary structures (MISS),” in *Encyclopedia of Geology* (Elsevier), 545–554. doi: 10.1016/B978-0-08-102908-4.00109-0
- O’Brien, S. J., and King, A. F. (2002). Neoproterozoic Stratigraphy of the Bonavista Peninsula: preliminary results, regional correlations and implication for sediment-hosted stratiform copper exploration in the Newfoundland Avalon Zone. *Geological Survey* 02, 229–244.
- O’Brien, S. J., and King, A. F. (2005). Late Neoproterozoic (Ediacaran) stratigraphy of Avalon Zone sedimentary rocks, Bonavista Peninsula, Newfoundland. *Geological Survey* 05, 13.
- Olsen, A. M. (2017). Feeding ecology is the primary driver of beak shape diversification in waterfowl. *Funct Ecol* 31, 1985–1995. doi: 10.1111/1365-2435.12890
- Olsen, A. M., and Westneat, M. W. (2015). StereoMorph: an R package for the collection of 3D landmarks and curves using a stereo camera set-up. *Methods Ecol Evol* 6, 351–356. doi: 10.1111/2041-210X.12326
- Parry, L. A., Boggiani, P. C., Condon, D. J., Garwood, R. J., Leme, J. de M., McIlroy, D., et al. (2017). Ichnological evidence for meiofaunal bilaterians from the terminal Ediacaran and earliest Cambrian of Brazil. *Nat Ecol Evol* 1, 1455–1464. doi: 10.1038/s41559-0
- Pasinetti, G., and McIlroy, D. (2023). Palaeobiology and taphonomy of the rangeomorph *Culmofrons plumosa*. *Palaeontology* 66, e12671. doi: 10.1111/pala.12671
- Pasinetti, G., and McIlroy, D. (2023). Data from: Palaeobiology and taphonomy of the rangeomorph *Culmofrons plumosa*. *Dryad Digital Repository*. doi: 10.5061/dryad.ksn02v785
- Pearse, V. B. (1989). Growth and Behavior of *Trichoplax adhaerens*: First Record of the Phylum Placozoa in Hawaii. *Pacific Science* 43, 5.

- Peres-Neto, P. R., Jackson, D. A., and Somers, K. M. (2005). How many principal components? stopping rules for determining the number of non-trivial axes revisited. *Computational Statistics & Data Analysis* 49, 974–997. doi: 10.1016/j.csda.2004.06.015
- Pérez-Pinedo, D., McKean, C., Taylor, R., Nicholls, R., and McIlroy, D. (2022). *Charniodiscus* and *Arborea* are separate genera within the Arboreomorpha: Using the holotype of *C. concentricus* to resolve a taphonomic/taxonomic tangle. *Front. Earth Sci.* 9, 785929. doi: 10.3389/feart.2021.785929
- Pérez-Pinedo, D., Neville, J. M., Pasinetti, G., McKean, C., Taylor, R., and McIlroy, D. (2023). Frond orientations with independent current indicators demonstrate the reclining rheotropic mode of life of several Ediacaran rangeomorph taxa. *Paleobiology*, 1–22. doi: 10.1017/pab.2023.2
- Pfluger, F. (1999). Matground structures and redox facies. *PALAIOS* 14, 25. doi: 10.
- Porada, H., Ghergut, J., and Bouougri, E. H. (2008). Kinneyia-type wrinkle structures--critical review and model of formation. *PALAIOS* 23, 65–77. doi: 10.2110/palo.2006.p06-095r
- Pu, J. P., Bowring, S. A., Ramezani, J., Myrow, P., Raub, T. D., Landing, E., et al. (2016). Dodging snowballs: Geochronology of the Gaskiers glaciation and the first appearance of the Ediacaran biota. *Geology* 44, 955–958. doi: 10.1130/G38284.1
- Razumovskiy, A. A., Ivantsov, A. Yu., Novikov, I. A., and Korochantsev, A. V. (2015). *Kuckaraukia multituberculata*: A new Vendian fossil from the basa formation of the Asha Group in the South Urals. *Paleontol. J.* 49, 449–456. doi: 10.1134/S0031030115050111
- Retallack, G. J. (1994). Were the Ediacaran fossils lichens? *Paleobiology* 20, 523–544. doi: 10.1017/S0094837300012975
- Revelle, W. (2021). psych: Procedures for Personality and Psychological Research. Available at: <https://CRAN.R-project.org/package=psych>
- RStudio Team (2020). RStudio: integrated development for R. Available at: <http://www.rstudio.com/>
- Ryan, J. F., and Chiodin, M. (2015). Where is my mind? How sponges and placozoans may have lost neural cell types. *Phil. Trans. R. Soc. B* 370, 20150059. doi: 10.1098/rstb.2015.0059
- Schopf, J. W. (2000). Solution to Darwin's dilemma: Discovery of the missing Precambrian record of life. *PNAS* 97, 6947–6953.
- Schultz, D. T., Haddock, S. H. D., Bredeson, J. V., Green, R. E., Simakov, O., and Rokhsar, D. S. (2023). Ancient gene linkages support ctenophores as sister to other animals. *Nature* 618, 110–117. doi: 10.1038/s41586-023-05936-6

- Scrucca, L., Fop, M., Murphy, T., Brendan, and Raftery, A., E. (2016). mclust 5: Clustering, Classification and Density Estimation Using Gaussian Finite Mixture Models. *The R Journal* 8, 289. doi: 10.32614/RJ-2016-021
- Seilacher, A. (1989). Vendozoa: Organismic construction in the Proterozoic biosphere. *LET* 22, 229–239. doi: 10.1111/j.1502-3931.1989.tb01332.x
- Seilacher, A. (1992). Vendobionta and Psammocorallia: lost constructions of Precambrian evolution. *Journal of the Geological Society* 149, 607–613. doi: 10.1144/gsjgs.149.4.0607
- Seilacher, A., and Pflüger, F. (1994). “From biomats to benthic agriculture: A biohistoric revolution,” in *Biostabilization of Sediments*, eds. W. E. Krumbein, D. M. Paterson, and L. J. Stal (Bibliotheks Und Infomationssystem Der Carl Von Ossietzky Universität), 97
- Shaffer, M. R., Davy, S. K., Maldonado, M., and Bell, J. J. (2020). Seasonally driven sexual and asexual reproduction in temperate *Tethya* species. *The Biological Bulletin* 238, 89–105. doi: 10.1086/708624
- Shostak, S. (2018). Is *Hydra* an Alarm Clock? *BJSTR* 7. doi: 10.26717/BJSTR.2018.07.001521
- Slagter, S., Hao, W., Planavsky, N. J., Konhauser, K. O., and Tarhan, L. G. (2022). Biofilms as agents of Ediacara-style fossilization. *Sci Rep* 12, 8631. doi: 10.1038/s41598-022-12473-1
- Smith, E. F., Nelson, L. L., Strange, M. A., Eyster, A. E., Rowland, S. M., Schrag, D. P., et al. (2016). The end of the Ediacaran: Two new exceptionally preserved body fossil assemblages from Mount Dunfee, Nevada, USA. *Geology* 44, 911–914. doi: 10.1130/G38157.1
- Sperling, E. A., Pisani, D., and Peterson, K. J. (2007). Poriferan paraphyly and its implications for Precambrian palaeobiology. *SP* 286, 355–368. doi: 10.1144/SP286.25
- Sperling, E. A., and Vinther, J. (2010). A placozoan affinity for *Dickinsonia* and the evolution of late Proterozoic metazoan feeding modes: Placozoan affinity for *Dickinsonia*. *Evolution & Development* 12, 201–209. doi: 10.1111/j.1525-142X.2010.00404.x
- Tarhan, L. G., Hood, A. v.S., Droser, M. L., Gehling, J. G., and Briggs, D. E. G. (2016). Exceptional preservation of soft-bodied Ediacara Biota promoted by silica-rich oceans. *Geology* 44, 951–954. doi: 10.1130/G38542.1
- Taylor, R. S., Hawco, J. B., Nichols, R., and McIlroy, D. (2019). Reevaluación crítica del holotipo de *Beothukis mistakensis*, único organismo rangeomorfo excepcionalmente preservado en Mistaken Point, Terranova, Canadá. *Estud. geol.* 75, 117. doi: 10.3989/egeol.43586.572
- Taylor, R. S., Matthews, J. J., Nicholls, R., and McIlroy, D. (2021). A re-assessment of the taxonomy, palaeobiology and taphonomy of the rangeomorph organism *Hapsidophyllas flexibilis* from the Ediacaran of Newfoundland, Canada. *PalZ* 95, 187–207. doi: 10.1007/s12542-020-00537-4

- Taylor, R. S., Nicholls, R., Neville, J. M., and McIlroy, D. (2023). Morphological variation in the rangeomorph organism *Fractofusus misrai* from the Ediacaran of Newfoundland, Canada. *Geol. Mag.* 160, 146–166. doi: 10.1017/S0016756822000723
- Technau, U., and Steele, R. E. (2012). Evolutionary crossroads in developmental biology: Cnidaria. *Development* 139, 4491–4491. doi: 10.1242/dev.090472
- Thiemann, M., and Ruthmann, A. (1990). Spherical forms of *Trichoplax adhaerens* (Placozoa). *Zoomorphology* 110, 37–45. doi: 10.1007/BF01632810
- Turekian, K. K., Cochran, J. K., Kharkar, D. P., Cerrato, R. M., Vaisnys, J. R., Sanders, H. L., et al. (1975). Slow growth rate of a deep-sea clam determined by ²²⁸Ra chronology. *Proc. Natl. Acad. Sci. U.S.A.* 72, 2829–2832. doi: 10.1073/pnas.72.7.2829
- Turner, S., and Vickers-Rich, P. (2007). Sprigg, Glaessner and Wade and the discovery and international recognition of the Ediacaran fauna. *SP* 286, 443–445. doi: 10.1144/SP286.37
- Vaziri, S. H., Majidifard, M. R., and Laflamme, M. (2018). Diverse Assemblage of Ediacaran fossils from Central Iran. *Sci Rep* 8, 5060. doi: 10.1038/s41598-018-23442-y
- Vixseboxse, P. B., Kenchington, C. G., Dunn, F. S., and Mitchell, E. G. (2021). Orientations of Mistaken Point Fronds Indicate Morphology Impacted Ability to Survive Turbulence. *Front. Earth Sci.* 9, 762824. doi: 10.3389/feart.2021.762824
- Wacey, D., Kilburn, M. R., Saunders, M., Cliff, J. B., Kong, C., Liu, A. G., et al. (2015). Uncovering framboidal pyrite biogenicity using nano-scale CNorg mapping. *Geology* 43, 27–30. doi: 10.1130/G36048.1
- Waggoner, B. (2003). The Ediacaran biotas in space and time. *Integrative and Comparative Biology* 43, 104–113. doi: 10.1093/icb/43.1.104
- Wang, X., Pang, K., Chen, Z., Wan, B., Xiao, S., Zhou, C., et al. (2020). The Ediacaran frondose fossil *Arborea* from the Shibantan limestone of South China. *J. Paleontol.* 94, 1034–1050. doi: 10.1017/jpa.2020.43
- Ward, J. H. (1963). Hierarchical Grouping to Optimize an Objective Function. *Journal of the American Statistical Association* 58, 236–244. doi: 10.1080/01621459.1963.10500845
- Wilby, P. R., Carney, J. N., and Howe, M. P. A. (2011). A rich Ediacaran assemblage from eastern Avalonia: Evidence of early widespread diversity in the deep ocean. *Geology* 39, 655–658. doi: 10.1130/G31890.1
- Witte, U. (1996). Seasonal reproduction in deep-sea sponges-triggered by vertical particle flux? *Marine Biology* 124, 571–581. doi: 10.1007/BF00351038
- Wörheide, G., Dohrmann, M., Erpenbeck, D., Larroux, C., Maldonado, M., Voigt, O., et al. (2012). “Deep phylogeny and evolution of sponges (Phylum Porifera),” in *Advances in Marine Biology* (Elsevier), 1–78. doi: 10.1016/B978-0-12-387787-1.00007-6

- Wood, D. A., Dalrymple, R. W., Narbonne, G. M., Gehling, J. G., and Clapham, M. E. (2003). Paleoenvironmental analysis of the late Neoproterozoic Mistaken Point and Trepassy formations, southeastern Newfoundland. *Can. J. Earth Sci.* 40, 1375–1391. doi: 10.1139/e03-048
- Wu, C., Pang, K., Chen, Z., Wang, X., Zhou, C., Wan, B., et al. (2022). The rangeomorph fossil *Charnia* from the Ediacaran Shibantan biota in the Yangtze Gorges area, South China. *J. Paleontol.*, 1–17. doi: 10.1017/jpa.2022.97
- Zuccolotto-Arellano, J., and Cuervo-González, R. (2020). Binary fission in *Trichoplax* is orthogonal to the subsequent division plane. *Mechanisms of Development* 162, 103608. doi: 10.1016/j.mod.2020.103608